BIODIESEL-BIODIESEL MIXTURES TO UPGRADE FUEL PROPERTIES AND LOWER EXHAUST GAS EMISSIONS

KEMAL MASERA

Doctor of Philosophy

ASTON UNIVERSITY

July 2019

Aston University

BIODIESEL-BIODIESEL MIXTURES TO UPGRADE FUEL PROPERTIES AND LOWER EXHAUST GAS EMISSIONS

Kemal Masera

Doctor of Philosophy

2019

Abstract

Biodiesels are considered as promising alternatives to fossil diesel. Biodiesels produced from various resources can have different fuel properties; hence they do not always comply with the BS EN 14214 standard. This could lead to engine operation and emission challenges. This thesis aims to optimise fuel properties by biodiesel-biodiesel blending in order to improve the fuel properties, combustion and emission characteristics. In this study, biodiesels were produced from different resources such as sheep fat, chicken fat and waste cooking oils; it was found that they do not comply with the BS EN 14214 biodiesel standard. Waste cooking oil-sheep fat biodiesels and cottonseed-chicken fat biodiesels were blended separately at varying proportions and observed that blends of animal fat biodiesels with waste cooking oil or inedible vegetable biodiesels gave promising fuel properties. Waste cooking oil biodiesel-sheep fat biodiesel at 60/40 and 50/50 volume fractions meet the BS EN 14214 standard. Waste cooking oil biodiesel, sheep fat biodiesel and their blends at 60/40, 50/50 and 30/70 ratios were tested in a three cylinder diesel engine and results were compared to fossil diesel. Moreover, effect of degree of unsaturation was also investigated. It was found that decreasing degree of unsaturation resulted in shortened combustion duration, higher heat release at the pre-mix combustion phase, reduced CO and increased NOx emissions. Moreover, 50/50 blend gave the highest in-cylinder pressure around 5% higher than respective neat biodiesels. The 50/50 waste cooking oil biodiesel-sheep fat biodiesel blend gave 3.3% lower CO_2, 74% lower CO and 2.5% higher NOx than fossil diesel. The engine tests were also conducted using the cottonseed biodiesel, chicken fat biodiesel and their blends at 60/40, 50/50 and 30/70 ratios. Cottonseed biodiesel-chicken fat biodiesel blends at 60/40 and 50/50 ratios gave 4.2% higher in-cylinder pressure than diesel; furthermore, the CO_2, CO and NO emissions were reduced by 5.8%, 15% and 6.5% compared to fossil diesel respectively. In order to further improve the emission characteristics of the biomixture fuels, 2-Butoxyethanol was tested as a novel biodiesel additive. Both 50/50 biomixtures doped with the additive (15% by volume) led to further increase in in-cylinder pressure and slight decrease in combustion duration by 5% and 2° CA, respectively when compared to the same without additive. A 5% increase in the brake specific fuel consumption and 2.6% decrease in brake thermal efficiency were observed when additive was used. However, 5% reduction in NO gas emission was achieved. In addition, the biomixtures were tested in a novel SNCR after-treatment design which reduced the NO emissions of the 50/50 biomixtures by 6% with distilled water injection and 15% with urea-water solution injection. The research study concluded that waste cooking oil biodiesel-sheep fat biodiesel and cottonseed biodiesel-chicken fat biodiesel blends at 50/50 ratios are recommended for compression ignition engine application.

Acknowledgements

List of Publications

1. Masera, K., & Hossain, A. K. (2019). Combustion characteristics of cottonseed biodiesel and chicken fat biodiesel mixture in a multi-cylinder compression ignition engine. *SAE Technical Paper 2019-01-0015, 1*, pp. 1-14. doi: 10.4271/2019-01-0015.

2. Masera, K., & Hossain, A. K. (2019). Biofuels and thermal barrier: A review on compression ignition engine performance, combustion and exhaust gas emission. *Journal of the Energy Institute*. Elsevier Ltd, 92(3), pp. 783–801. doi: 10.1016/j.joei.2018.02.005.

3. Masera, K., & Hossain, A. K. (2017). Production, characterisation and assessment of biomixture fuels for compression ignition engine application. *International Journal of Mechanical, Aerospace, Industrial, Mechatronic and Manufacturing Engineering*, 11(12), pp. 1857 - 1863. doi: scholar.waset.org/1307-6892/10008317.

List of submitted papers

4. Masera, K., Hossain, A. K., Davies, P. A., & Doudin, K. (2019). Experimental investigation of the 2-butoxyethanol as a biodiesel additive. *Energy (submitted)*,

5. Masera, K., Hossain, A. K., Griffiths, G., & Safdar, S. (2019). Understanding the effect of degree of unsaturation by blending waste cooking oil biodiesel and sheep fat biodiesel. *Fuel (to be submitted)*,

6. Masera, K., & Hossain, A. K. (2020). Injection of urea-water solution through a modified selective non-catalytic reduction (SNCR) after-treatment system to reduce NOx emission. *4th South East European Conference on Sustainable Development of Energy, Water and Environment Systems,* Sarajevo, Bosnia and Herzegovina, *(abstract submitted)*,

Table of Contents

List of Abbreviations

1G	First generation
2G	Second generation
3G	Third generation
Θ	Crank angle ($^\circ$)
ρ	Air density
a	Crank shaft length (m)
A100	Sheep fat biodiesel
A/F	Air fuel ratio
b	Bore diameter (m)
bdc	Bottom dead centre
bmep	Brake mean effective pressure
BSEC	Brake specific energy consumption (MJ/kWh)
BSFC	Brake specific fuel consumption (kg/kWh)
BTE	Brake thermal efficiency (%)
CD	Combustion duration ($^\circ$CA)
CFPP	Cold filter plugging point ($^\circ$C)
CI	Compression ignition
CN	Cetane number
CO	Carbon monoxide
CO100	Cottonseed oil biodiesel
CO80CH20	Cottonseed oil biodiesel 80% + Chicken fat biodiesel 20%
CO60CH40	Cottonseed oil biodiesel l 60% + Chicken fat biodiesel l 40%
CO50CH50	Cottonseed oil biodiesel 50% + Chicken fat biodiesel 50%
CO42.5CH42.5B15	Cottonseed oil biodiesel 42.5% + Chicken fat biodiesel 42.5% + 2-Butoxyethanol 15%
CO30CH70	Cottonseed oil biodiesel 30% + Chicken fat biodiesel 70%
CO10CH90	Cottonseed oil biodiesel 10% + Chicken fat biodiesel 90%
CO_2	Carbon dioxide
CH100	Chicken fat biodiesel
DAG	Diglycerides
DECC	Department of Energy and Climate Change (UK)
DEF	Diesel exhaust fluid
defra	Department for Environment Food and Rural Affairs (UK)
Dft	Department for Transport (UK)
DI	Direct injection
DOC	Diesel oxidation catalysts
DPF	Diesel particulate filter
DU	Degree of unsaturation (%weight)
EOC	End of combustion ($^\circ$CA)
FAME	Fatty acid methyl ester
FFA	Free fatty acid
FTIR	Fourier transform infrared spectroscopy
GC-MS	Gas chromatography – mass spectrum
GHG	Greenhouse gas
HCCI	Homogeneous charge compression ignition
HC	Unburned hydrocarbon emissions
HHV	Higher heating value (MJ/kg)
HLB	Hydrophilic-lipophilic balance

HR	Heat release (J)
HRR	Heat release rate (J/^{o}CA)
i	Number of cylinders
ID	Ignition delay (^{o}CA)
IDI	Indirect injection
imep	Indicated mean effective pressure
IV	Iodine value
j	Number of strokes
l	Connecting rod length (m)
LHR	Low heat rejection
LHV	Lower heating value (MJ/kg)
LTC	Low temperature combustion
m	Mass
MAG	Monoglycerides
M_f	Mass flow rate of fuel (kg/s)
M_h	Molecular weight of hydrophilic
M_i	Molecular weight of lipophilic
N	Engine speed (rpm)
ND	Not detected
NO	Nitrogen oxide
NO_2	Nitrogen dioxide
NOx	Nitrogen oxides
O_2	Oxygen
P_b	Brake power (kW)
PAHs	Polycyclic aromatic hydrocarbons
PCDD/Fs	polychlorinated dibenzo-p-dioxins/dibenzofurans
PM	Particulate matter
R100	Rapeseed biodiesel
R85	Rapeseed biodiesel 85% + 2-Butoxyethanol 15%
RCCI	Reactivity controlled compression ignition
s	Stroke distance (m)
SCR	Selective catalytic reduction
SI	Spark ignition
SNCR	Selective non-catalytic reduction
SOC	Start of combustion (^{o}CA)
SOI	Start of injection (^{o}CA)
T	Torque (Nm)
TAG	Triglycerides
TBC	Thermal barrier coating
TDC	Top dead centre
Tstd	Standard atmosphere temperature
ULSD	Ultra-low sulphur diesel
Vc	Clearance volume
Vd	Displacement volume
Vtitre	Volume of titre
W100	Waste cooking oil biodiesel
W85	Waste cooking oil biodiesel 85% + 2-Butoxyethanol 15%
W80A20	Waste cooking oil biodiesel 80% + Sheep biodiesel 20%
W60A40	Waste cooking oil biodiesel 60% + Sheep biodiesel 40%
W50A50	Waste cooking oil biodiesel 50% + Sheep biodiesel 50%

W42.5A42.5B15	Waste cooking oil biodiesel 42.5% + Sheep biodiesel 42.5% + 2-Butoxyethanol 15%
W30A70	Waste cooking oil biodiesel 30% + Sheep biodiesel 70%
W10A90	Waste cooking oil biodiesel 10% + Sheep biodiesel 90%
WCO	Waste cooking oil

List of Tables

List of Figures

XV

Chapter 1

1. INTRODUCTION

1.1. Fossil fuel challenges

The Earth is suffering from climate change. The gradual increase in its surface temperature is causing serious problems such as melting polar ice, rising sea levels, drought and climate change (Wang *et al.*, 2017). Global warming is caused by emissions of greenhouse gases (GHG). Combustion of fossil fuels is one of the main sources of GHG emission (Davis *et al.*, 2018). Despite that, petroleum products are the commonly used energy source. The World Bank (2017) report that 80.7% of the world's energy was supplied by fossil fuels in 2017. The distribution of sources such as natural gas, crude oil and coal was studied by Ritchie and Max, (2019) and given in Figure 1.1. The annual global CO_2 emissions from fossil fuels were studied by the US Department of Energy and given in Figure 1.2 (Boden *et al.*, 2015). The total annual CO_2 emission was recorded as 9776 million metric tons for overall fossil fuel usage in 2013 (Boden *et al.*, 2015).
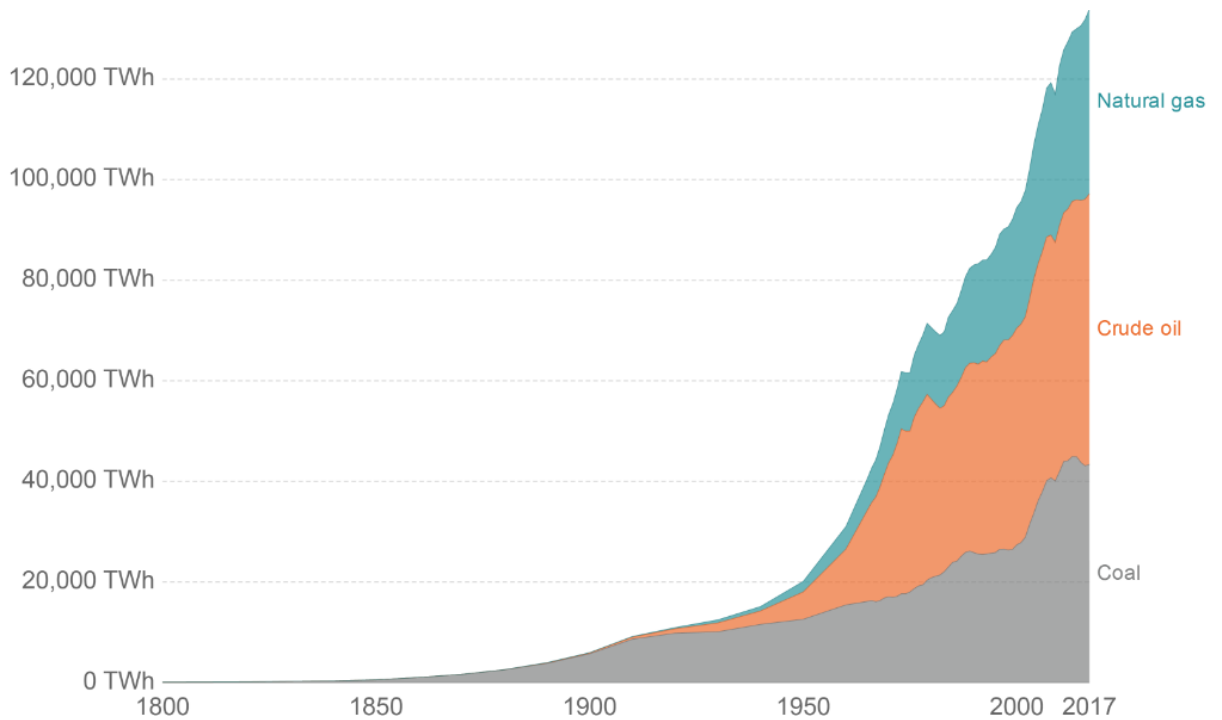
Figure 1.1: Global primary energy consumption by fossil fuel source, taken from (Ritchie and Max, 2019).
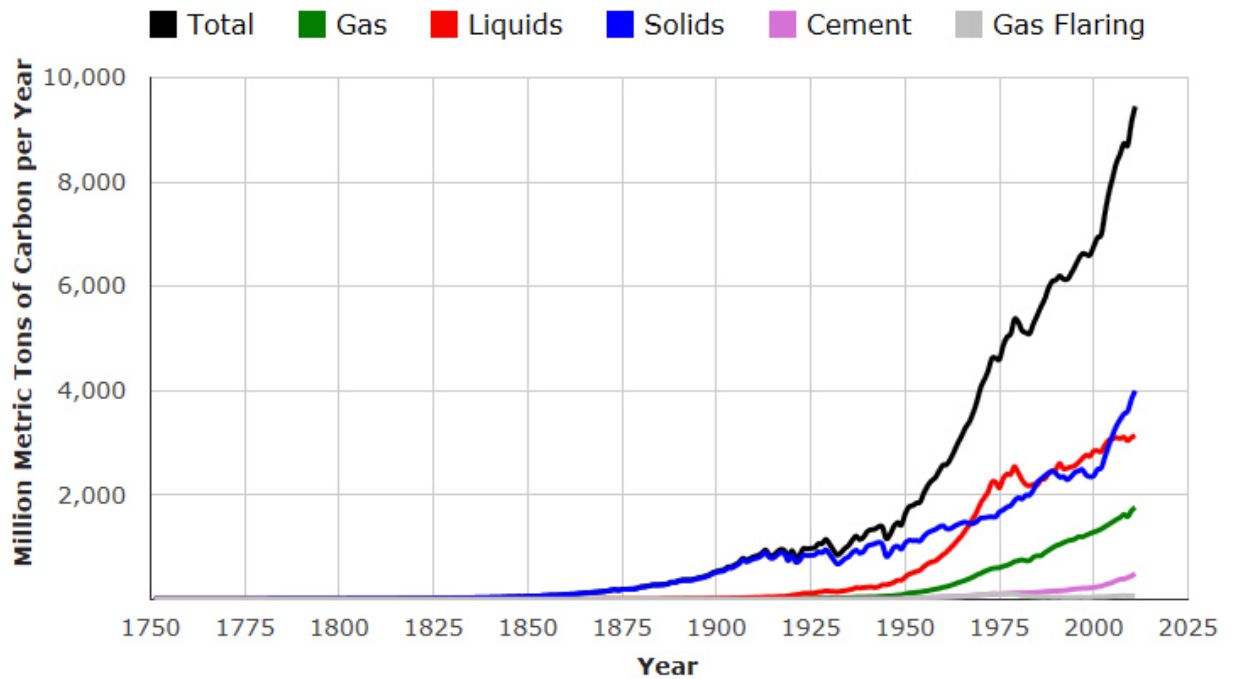
Figure 1.2: Total and individual contributors of annual global fossil fuel carbon emissions, taken from (Boden *et al.*, 2015).

Although there is a slightly decreasing trend on fossil fuel consumption, UK still heavily depends on fossil fuels as shown in Figure 1.3. The overall fossil fuel consumption of the UK was recorded as around 84% in 2016 (The UK Department for Business Energy and Industrial Strategy, 2017).
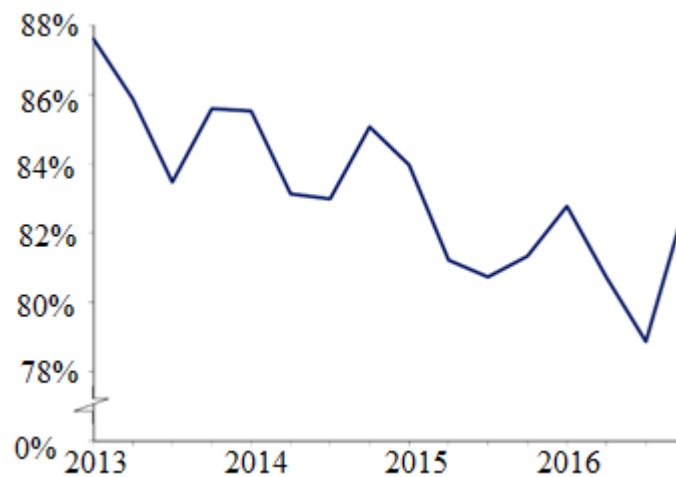
Figure 1.3: Fossil fuel consumption of the UK, taken from (The UK Department for Business Energy and Industrial Strategy, 2017).

Fossil fuels pose additional problems such as the depletion of petroleum resources and security of supply (Gumus *et al.*, 2012). The literature warns about the limited lifetime of the fossil fuel reserves. For example, a study conducted in 2017 predicts depletion duration of crude oil, natural gas and coal within around 35, 37 and 107 year time, respectively (Senthur Prabu *et al.*, 2017). Although dates are just estimates, this type of study highlights the fossil fuel depletion problem.

Finally, yet importantly, usage of fossil-based petroleum fuels poses danger directly to human health (Chen and Lippmann, 2009; Anderson *et al.*, 2012; Ristovski *et al.*, 2012). Fossil fuel combustion in diesel engines is identified as one of the greatest contributors to GHG emissions, hence to human health (Campbell-Lendrum and Prüss-Ustün, 2019). Lloyd and Cackette (2001) reported the direct effect of exhaust gas emissions such as soot and NOx on cancer, cardiovascular and respiratory effects on human health. The carbon soot from diesel engine constitutes 73-83% of particulate matter (PM) (Tsai *et al.*, 2014). The other pollutants in soot are soluble organic fractions, ash content, trace metals, sulphur compounds, and other substances like polycyclic aromatic hydrocarbons (PAHs), and polychlorinated dibenzo-p-dioxins/dibenzofurans (PCDD/Fs) (Lin *et al.*, 2005, Lin *et al.*, 2008; Chuang *et al.*, 2010; Tsai *et al.*, 2014). The risk of respiratory, cardiovascular and lung cancer diseases are increased when humans are exposed to PM and NOx emissions (Lloyd and Cackette, 2001). The Health Protection Agency in the UK declared 11900 premature deaths caused by the presence of GHG gasses in the breathing atmosphere (Vardoulakis and Heaviside, 2012). To sum up, it is widely accepted that alternative solutions should gain more importance to overcome fossil fuel challenges.

1.2. Sustainable energy sources

The European Union set targets to reduce harmful exhaust gas emissions by 24% and 32% lower than the 1990 level with the utilisation of alternative energy sources by 2020 and 2030 respectively (European Parliament, 2009, 2015; European Commision, 2014). More specifically, 10% biodiesel requirement for transport fuels by 2020 was imposed on member countries (Forte *et al.*, 2018). The Department for Transport UK also sets a minimum target of 12.4% biofuel volume fraction in transport fuels by 2032 (Norman, 2018). Overall, bioenergy demand is also estimated to increase in accordance with the restricted emission regulations and targets (Department of Energy and Climate Change, 2012). According to the International Renewable Energy Agency (2017), renewables are the best way of CO_2 reduction as they can reduce the global CO_2 prediction for 2050 by 44% Figure 1.4. Therefore, some countries also encourage the renewable energy utilisation (by means of tax benefits, incentives and grants) to meet the emission targets (Igobo, 2015).
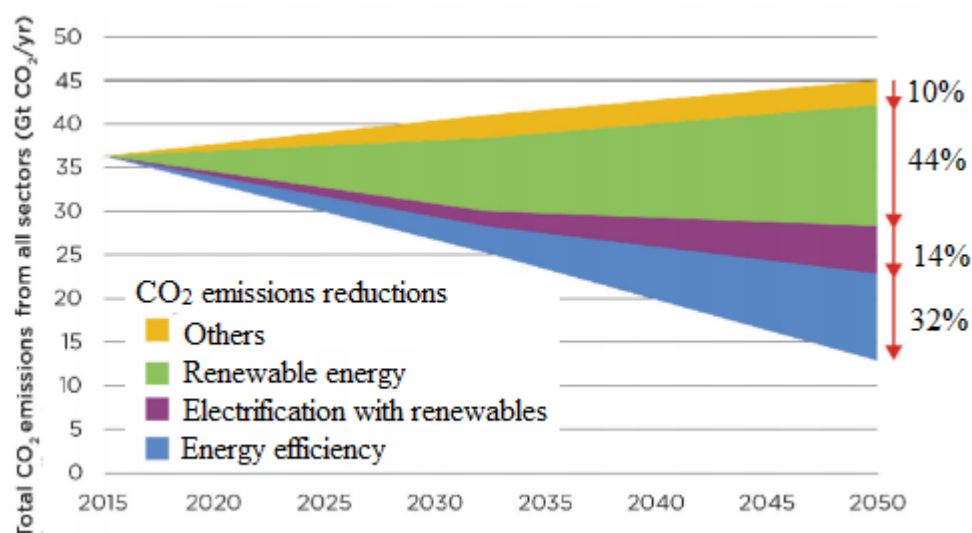
Figure 1.4: Primary CO_2 emission reduction potentials by technology, adapted from (©International Renewable Energy Agency, 2017).

According to the latest data provided by the International Energy Agency (2019), renewables contribute 25% and 32% of the total electricity production of the world and UK, respectively. Bioenergy, hydro, wind, geothermal and solar were the main renewable energy sources reported worldwide with contributions of 2%, 16%, 4%, 0.04% and 2% respectively. According to Kumar and Sharma (2011), biofuel production will increase significantly in the future, thus various feedstock shall be investigated to replace fossil fuels in the long term.

1.3. Biodiesel produced from waste resources

Biofuels are a promising source of alternative energy for replacing fossil fuels because of several advantages. They; (i) are biodegradable, (ii) are sustainable, (iii) produced from any organic substances including wastes, (iv) reduce exhaust gases such as HC, CO and smoke, (v) have the potential to help in waste disposal, (vi) are used in different applications like vehicle fuel, heating, electricity production, etc. Moreover, The presence of oxygen content of biofuels typically yields more efficient combustion than diesel (Baskar and Senthilkumar, 2016). Biofuels can be found in all three phases referring to liquid, solid and gas. The liquid phase attracts the most attention due to several advantages, such as high energy content per unit volume, and better storage and distribution opportunities. These resources are generally obtained from vegetables, animals and waste components. By nature, oils are in the liquid phase and this property makes them the easiest candidates for the chemical processes like transesterification and water emulsion. Solid fats are typically exposed to the

4

rendering process to convert into the liquid phase. Similarly, solid waste resources can be converted into a liquid by pyrolysis technique (Hossain and Davies, 2013).

Edible/non-edible vegetable oils, waste cooking oils (WCO), animal fats and algae oils are the most popular biofuel examples. Although neat oils of the mentioned feedstock can be utilised directly (i.e. in a diesel engine), their fuel properties can also be upgraded by some applications. To illustrate, feedstock can be transesterified to produce biodiesel and/or emulsified with water. Bio-alcohols such as bio-ethanol and bio-butanol are also utilised as bioenergy sources. They are typically produced from sugar cane, grains and corn. Bioethanol mainly finds application in spark ignition engines for replacing gasoline (Escobar *et al.*, 2009). For example, bioethanol has a high self-ignition temperature and latent heat of vaporisation, low calorific value and cetane number (Escobar *et al.*, 2009). In contrast, biodiesel and neat oils (and their blends with Alcohols to some extent) are all applicable for compression ignition engines (Escobar *et al.*, 2009).

Land usage problems and food challenges have fostered a growing interest in waste-derived biofuels such as animal fats, waste cooking oils and inedible vegetable oils (Sander *et al.*, 2018). Animal fats and used cooking oil are considered as wastes and disposal of those substances is subject to certain procedures in the EU and UK (Environment Agency, 2015). According to the Quality Protocol, which is a joint initiative between the Environment Agency and, Waste and Resources Action Programme (applies to England, Wales, and Northern Ireland), animal waste and waste cooking oil feedstock can be regarded as fully recovered if they are converted into biodiesel in a suitable way (Environment Agency, 2015). This makes the mentioned feedstock interesting for biodiesel production.

Oil and fat feedstock (triglycerides) can be converted into biodiesel (fatty acid methyl ester) by transesterification technique to improve the fuel properties (Meher *et al.*, 2006). Pyrolysis (thermal cracking) and emulsification are the other ways to upgrade fuel properties (Ma and Hanna, 1999; Melo-Espinosa *et al.*, 2015). By far, biodiesel is considered the most promising technique in terms of energy efficiency and overall enhancement of fuel properties (Salamanca *et al.*, 2012). By converting organic feedstock (triglycerides) into biodiesel (methyl esters) (see Figure 1.5), it is also expected to observe better performance and fewer emissions from the engine operation (Öner and Altun, 2009; Behçet, 2011). Accordingly, biodiesel occupies the bigger portion of the renewable energy supply among the mentioned techniques. According to the UK Department for Transport (2018), biodiesel shared 47% of the renewable fuel supply in 2018. Its inherent properties, biodegradability, carbon neutrality, environmental attributes and applicability to diesel engines (without any major modifications) make waste derived biodiesels viable alternative fuels (Özener *et al.*, 2014). The literature agrees that waste biodiesels can be one of the sustainable alternatives of fossil diesel and reduce major GHG emissions (Sakthivel *et al.*, 2018).
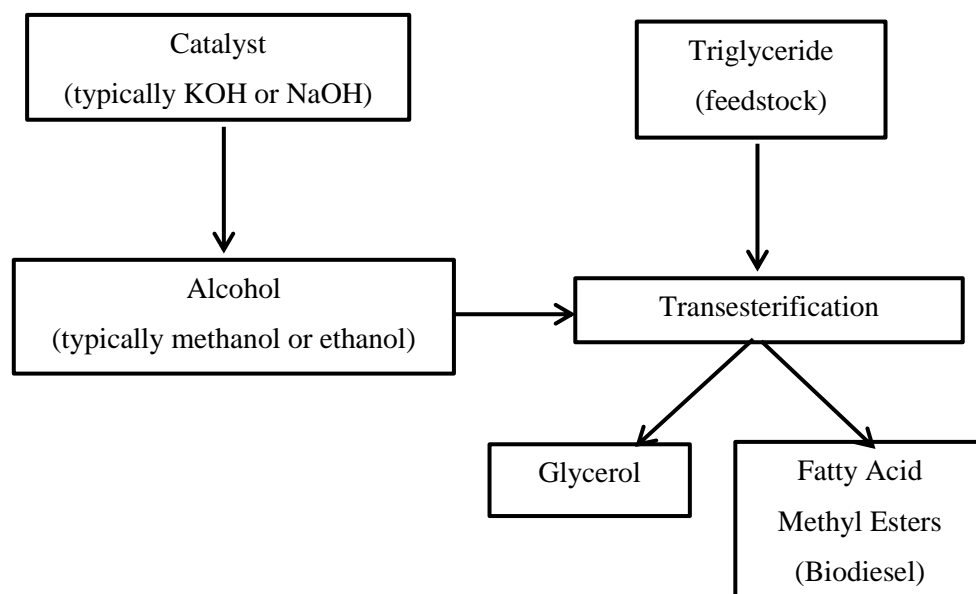
Figure 1.5: Transesterification process i.e. converting feedstock into biodiesel.

Although biodiesel has promising properties, the chemical structures of biodiesel and petroleum diesel are different. Biodiesel is composed of various Fatty Acid Methyl Esters (FAME) which are long carbon chains, whereas fossil diesel has aromatics compounds. This difference creates variations on fuel properties and engine operation i.e. engine performance, combustion characteristics and exhaust gas emissions. Thus, any biodiesel to be used in the diesel engine has to fulfil the British and European standard BS EN 14214. However, it is not easy to produce biodiesel which satisfies this norm. Note that biodiesel properties highly depend on the feedstock. Hence, fulfilling the standard could be harder for specific feedstock. For example, biodiesels derived from WCO could have high unsaturation which reduces resistance to oxidation and cause early degradation (Refaat, 2009). Another drawback of biodiesels is increased NOx emissions as a result of increased combustion temperature due to better combustion (Thangaraja *et al.*, 2016). Although PM, HC, CO and CO_2 emissions can be significantly reduced by biodiesel, numerous studies addressed increased NOx emission for the 100% biodiesel application on unmodified diesel engines (Hoekman and Robbins, 2012; Mofijur *et al.*, 2013; Palash *et al.*, 2013). Other technical issues associated with the neat biodiesel could be: (i) starting the engine in cold weather, (ii) sticking and clogging of fuel injector holes, fuel filters, and inlet/exhaust valves, and (iii) compatibility of fuel supply pipe materials with the biodiesel (Bhale *et al.*, 2009; Verma *et al.*, 2016; Datta and Mandal, 2017).

The broad aim of this research is to obtain high-quality biodiesel-biodiesel blends from waste and/or inedible vegetable oil feedstock. By this means, waste disposal can be supported, biodiesel challenges can be minimised and lower exhaust gas emissions can be achieved. Pros and cons of biodiesel candidates will be determined in terms of fuel properties. Next, biodiesels will be blended with each

other in a way that poor fuel properties of a particular biodiesel will be upgraded. Ultimately, biodiesel-biodiesel blends (biomixtures) will be produced with optimised fuel properties to improve fuel combustion and reduce exhaust gas emissions. In addition, further exhaust emission reduction (especially the NOx) will be examined with fuel additive and after-treatment system.

1.4. Thesis outline and structure

This PhD thesis is composed of 8 chapters. Brief outlines of each chapter are given below:

Chapter 1: The first chapter describes the world's fossil fuel utilisation and associated negative aspects such as fossil fuel depletion, environmental issues and health problems. The potential renewable energy sources were also outlined with emphasis on bioenergy. Waste-derived biodiesels are outlined as promising energy sources to replace fossil diesel. Some challenges with biodiesel utilisation, are briefly explained and the broad aim of the thesis is introduced.

Chapter 2: A critical literature review summarises the current knowledge and outcomes in the research field of various biodiesel feedstock. Literature is reviewed in detail regarding fuel properties of biodiesel obtained from waste resources (i.e. animal fats, waste cooking oil) and inedible vegetable oils. The engine test results of the mentioned biodiesels are also reviewed to understand the pros and cons of animal fat biodiesel compared to waste cooking oil and inedible vegetable biodiesels. Articles about biodiesel-biodiesel blending are also reviewed. Moreover, engine modifications and aftertreatment systems are outlined with an emphasis on engine performance improvement and/or NOx reduction. Finally, the promising research gaps are defined and the aims and objectives are introduced.

Chapter 3: The methodology of the study is introduced in this chapter. The biodiesel production principle and procedure used for this study are explained. Fuel characterisation methods are explained with reference to British and European standard, BS EN 14214. The experimental facilities used to conduct this research are described. The analytical methods used to convert measured raw data into significant results are also described.

Chapter 4: The fuel property optimisation of waste biodiesels is studied by the blending technique. Sheep fat biodiesel and waste cooking oil biodiesel are blended at different fractions to investigate any improvements in fuel properties, engine performance, combustion and exhaust emission. In addition, the effects of biodiesel degree of unsaturation are investigated in the biomixture engine results.

Chapter 5: Poor fuel properties of chicken biodiesel were upgraded by the blending technique. The fuel properties of chicken biodiesel-cottonseed biodiesel biomixtures are analysed at different volume

fractions; and tested in a diesel engine for the scope of improved combustion and reduced CO-CO_2 emissions.

Chapter 6: 2-Butoxyethanol is investigated as a biodiesel additive. The popular biodiesels in the UK (waste cooking oil biodiesel and rapeseed biodiesels) and the 50/50 fractions of the biomixtures investigated in chapters 4 and 5 are doped with the 2-Butoxyethanol additive and tested. NO emission reductions of biodiesels are investigated in the presence of the additive which had an ether structure with an alcohol branch.

Chapter 7: An after-treatment system, a combination of Selective Catalytic Reduction (SCR) and Selective Non-Catalytic Reduction (SNCR) technique, is investigated with the biomixtures. Three after-treatment designs are compared through CFD software in terms of turbulence intensity and particle residence time. Then the selected design manufactured and tested for reducing the NOx penalty of biodiesels.

Chapter 8: The final chapter summarises the important results of the research and the extent to which the main aims and objectives are met. The recommendations from the research and future work potentials are also addressed.

1.5. Aims and objectives of this thesis

The overall aim of this thesis is to blend two different biodiesels in accordance with their fuel properties for enhancing the engine performance, combustion characteristics and exhaust emissions. Biodiesels should comply with the BS EN 14214 standard, and must reduce harmful exhaust gas emissions when compared to fossil diesel. One emerging option being pursued is blending of highly chemically-saturated biodiesels with relatively chemically-unsaturated biodiesels to optimise the overall fuel properties. Additionally, novel fuel additive and exhaust aftertreatment design are examined with an emphasis on biodiesel NOx penalty.

The objectives of the study are:

1. To understand feedstock of biodiesel-biodiesel blends by a detailed literature review in terms of biodiesel fuel properties, and their combustion and emission characteristics results in the compression ignition engines.
2. To produce biodiesel-biodiesel blends (biomixtures) in order to identify promising volume ratios which meets BS EN 14214 biodiesel standard. Moreover, to understand the effect of biodiesel degree of unsaturation on engine test results.

3. To assess the combustion and emission characteristics of the produced biomixtures in a CI engine and determine promising biodiesel-biodiesel blends (biomixtures) which improves combustion characteristics and reduces harmful exhaust emissions.

4. To assess the effectiveness of the 2-Butoxyethanol as biomixture and neat biodiesels additive in terms of fuel properties, engine performance, combustion characteristics and exhaust emissions characteristics.

5. To design a new SNCR aftertreatment system for minimising the NOx penalty of biofuels by injections of distilled water and urea-water solution separately at the exhaust system.

6. Recommend on biodiesel-biodiesel mixture(s) for CI engine application with additive or with after-treatment system.

Chapter 2

2. LITERATURE REVIEW

2.1. Introduction

This chapter presents a review of waste and inedible plant oil feedstock for biodiesel production. Fuel properties and engine test results of various biodiesels are also reviewed from the literature. Various feedstock and their compression ignition (CI) engine applications are summarised to select the best matching feedstock for biodiesel-biodiesel blending. In addition, various engine modifications and NOx reduction techniques are also reviewed to optimise the engine performance, combustion characteristics and exhaust emissions of CI engines when operated on biodiesel.

2.2. Feedstock for biodiesel production

Biodiesel is a sustainable, environmentally-friendly, energy efficient and biodegradable fuel (Salamanca *et al.*, 2012; Masera and Hossain, 2017). The most popular feedstock types found in the literature are vegetable oils, waste animal products, waste cooking oils and algae oil. According to the type of feedstock, biodiesels can be categorised under three sections which are: first generation (1G), second generation (2G) and third generation (3G). The first generation biodiesels are produced from edible vegetable oils (Sakthivel *et al.*, 2018) such as sunflower oil (Saba *et al.*, 2016), rapeseed oil (Mazanov *et al.*, 2016), rice bran oil (Chhabra *et al.*, 2017), soybean oil (Torres-Rodríguez *et al.*, 2016) etc. Even though 1G biodiesels are widely available and have a relatively easier conversion process, their utilisation as a fuel may affect the food industry and cause an increase in food prices (Sakthivel *et al.*, 2018). On the other hand, non-edible oils are categorised as 2G biodiesels (Sakthivel *et al.*, 2018). The final category is 3G biodiesels which are mainly produced from algal biomass. Apart from the above mentioned feedstock, there are some waste feedstock such as waste animal fats and waste cooking oil, which can be used for biodiesel production. Regarding the categorisation of waste cooking oils and waste animal fats, there is no consensus in the literature. Some studies categorise them as second generation biodiesels (Lee and Lavoie, 2013) and some categorise as third generation biodiesels (Sakthivel *et al.*, 2018). No matter which category they are, waste derived biodiesels are very important as the sustainable disposal of the converted wastes have achieved along with fuel production.

2.2.1. Waste animal fats

Animal fats have been used for different purposes such as heating and lighting since prehistoric times (Piaszyk, 2012). Increasing environmental problems like global worming led researchers to investigate animal fats as alternative fuel source. Waste animal fats are generally by-products of butchers, abattoirs and industrial meat processing companies. Figure 2.1 presents the process of typical animal fat feedstock i.e. sheep tallow for biodiesel production. As no edible agents of animal take place in the rendering process, it is a sustainable and waste feedstock. Waste animal fats can be obtained from a wide variety of sources. For example, tallow can be derived from sheep/lamb (Bhatti *et al.,* 2008), beef (Ashraf *et al.,* 2017) and lard (Sander *et al.*, 2018); poultry fat from turkey (Emiroğlu *et al.*, 2018), chicken (Ashraf *et al.*, 2017), goose (Sander *et al.*, 2018) and duck (Chung *et al.*, 2009); and oils from various fish species (Behçet, 2011).
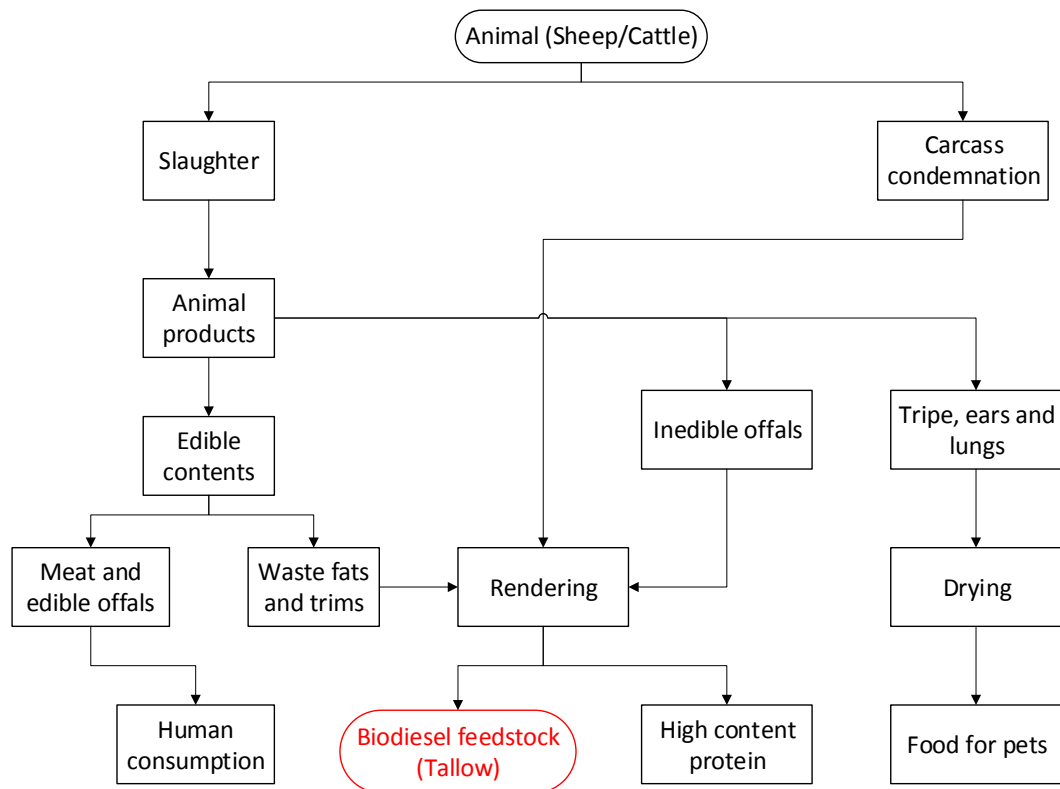
Figure 2.1: Production of animal fat feedstock, adapted from (Adewale *et al.,* 2015).

As shown in Figure 2.1, waste animal fats, trims, and inedible contents of the animals are used for tallow production. In the rendering process, animal wastes are cut into small pieces (crushed) with the help of crushing equipment. Then smaller materials are heated. Finally, animal fats are squeezed to

separate the liquid. Consequently, tallow and remaining meat and bone meal parts are obtained at the end of the rendering process (Figure 2.2) (Şen *et al.*, 2018). According to UK Department for Transport, (2018), tallow biodiesel accounts for around 2.5% of the UK origin biofuels.

Aston University

Illustration removed for copyright restrictions

Figure 2.2: Industrial facilities for rendering processes (© Mavitec B.V., 2015).

2.2.2. Waste cooking oils

The utilisation of waste cooking oils does not conflict with food or land usage as they are wastes. This type of feedstock can be categorised into two different subgroups. The first subgroup is the remaining oils after cooking purpose, also known as yellow grease (Adewale *et al.*, 2015). Depending on the use, waste cooking oils may contain some food residuals which may include some meat grease, fish or chicken oils. Typically, these feedstock are produced at industrial food suppliers and restaurants. Being a waste product along with high availability makes yellow grease waste cooking oil (WCO) a cost-effective feedstock for biodiesel production (Mohammadshirazi *et al.*, 2014; Khang *et al.*, 2017). The second subgroup, which is also known as brown grease, is the food grease which is collected via grease traps (Adewale *et al.*, 2015). Grease traps are placed on the sewer system i.e. after the sink. Design of the grease trap separates the grease/oil and water. Brown grease feedstock have free fatty acid (FFA) value higher than 15% (Adewale *et al.*, 2015). The relatively high FFA content of brown grease make the biodiesel production process more difficult compared to yellow grease feedstock.

Waste cooking oils from industrial companies are stored at special stations designed to have minimum contact with air, moisture and light. This is to prevent oxidation of feedstock (Predojević, 2008). Figure 2.3 shows a typical waste cooking oil collection station. According to literature, waste cooking

oil made up the largest share at 42% of total biodiesel supply to the UK (UK Department for Transport, 2018).

Figure 2.3: A typical waste cooking oil collection station (Geograph, 2009).

2.2.3. Inedible vegetable oils

Some vegetables are not suitable as a food source for both human and animal due to the existence of toxic substances and their FFA contents (Adewale *et al.*, 2015). Researchers have investigated the feasibility of inedible vegetable oils as biodiesel fuel. Some popular inedible vegetable oils are Karanja (Pongamia pinnata pierre) (Hossain and Davies, 2012), Physic nut (Jatropha curcas) (Tiwari *et al.*, 2007), Cottonseed (Gossypium hirsutum) (Eevera *et al.*, 2009), Mahua (Madhuca indica) (Shameer and Ramesh, 2017), Rubber seed (Hevea brasileinsis) (Ramadhas *et al.*, 2005), Castor bean (Ricinus communis) (da Silva César *et al.*, 2010), Yellow oleander (Thevetia peruviana) (Deka and Basumatary, 2011), Tobacco (Nicotiana tabacum) (García-Martínez *et al.*, 2017), Sea mango (Cerbera odollam) (Ang *et al.*, 2015), Euphorbiaceae, Oleaginous, Brassicacease and Leguminosae (Adewale *et al.*, 2015). The utilisation of the mentioned feedstock can be cost-effective especially at the local places where the plants grow by themselves due to their availability. Figure 2.4 illustrates pictures of some popular inedible vegetables.

2.3. Transesterification of triglycerides

Although neat oils (triglycerides) can be used in CI engines, transesterification of triglycerides enhances the fuel properties such as viscosity and volatility, which in turn results in better performance and fewer emissions on the engine operation (Öner and Altun, 2009; Behçet, 2011). Transesterification is a well-known method to produce biodiesel from any organic feedstock. The process found in early 1940 for simplyfting the glycerol extracting during soap production (Van Gerpen, 2005), later it has been used for biodiesel production. This reversible reaction occurs between the triglycerides and alcohol agents in the presence of a catalyst. Methanol and ethanol are the commonly used alcohols for the transesterification process (Carvalho *et al.*, 2017; Shu *et al.*, 2018). If the transesterification is carried out with the methanol then the product is called Fatty Acid Methyl Ester (FAME), similarly, it is called Fatty Acid Ethyl Ester (FAEE) if the alcohol is ethanol. According to transesterification stoichiometry, three moles of alcohol react with one mole of triglyceride and produce one mole of glycerine and three moles of fatty acid esters in the presence of a catalyst Figure 2.5. At the end of the transesterification process, phase separation occurs and two liquids are obtained which are fatty acid esters (biodiesel) at the top and glycerine at the bottom.
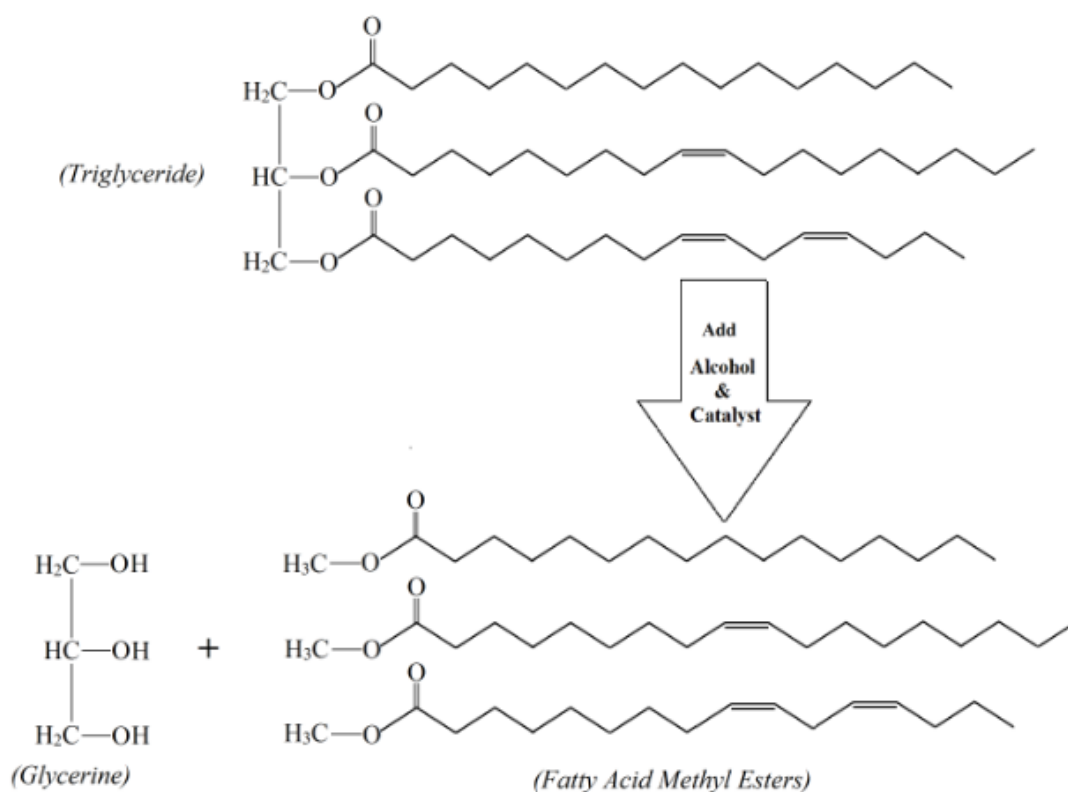
Figure 2.4: Biodiesel (methyl ester) production via transesterification.

2.3.1. Pre-treatment

According to the acid value of a feedstock, pre-treatment of oil might be necessary before the transesterification. Literature suggests applying pre-treatment for feedstock having free fatty acid content above 2% (Felizardo *et al.*, 2006). Because, the high acidity (FFA content) may lower the biodiesel yield and cause soap formation due to the presence of alkali catalyst (Dorado *et al.*, 2002; Lam, *et al.*, 2010). Ghadge and Raheman (2005) studied a biodiesel production from madhuca indica oil which has high FFA value as 19%. Pre-treatment of the feedstock was conducted using an acid catalyst (H_2SO_4 1% volume/volume) before the transesterification process to reduce the acid value below 2 mg KOH/g. Similarly, Ouachab and Tsoutsos (2013) used acid pre-treatment for producing biodiesel from olive pomace oil had FFA value as 27%. In their study, pre-treatment process was undertaken with the presence of H_2SO_4. Acid value (AV) and acidity parameters can be calculated by using equations 2.1 and 2.2 respectively (Ouachab and Tsoutsos, 2013).

$$\text{AV (mg KOH/g)} = \frac{V_{titre} \ Mo \ N_{KOH}}{m} \quad (2.1)$$

$$\text{Acidity (\%)} = \frac{V_{titre} \ Mo \ N_{KOH}}{m} \ 0.1 \quad (2.2)$$

Where V_{titre} is the volume of titre in millilitre, Mo is the molar mass of the oleic acid (28.2 mg/mole), m is the mass of oil in grams and N_{KOH} is the concentration of KOH solution in mole/millilitre.

2.3.2. Catalyst

Catalyst is an important parameter which directly affects the transesterification. Felizardo *et al.* (2006) investigated the effect of methanol to waste frying oil (WFO) ratio on biodiesel production rate at different catalyst amounts. According to their study, the best yield of biodiesel observed at 4.2 ratio of methanol/WFO with the presence of 0.6 wt% of KOH catalyst. Regarding catalyst types, Leung and Guo (2006) examined and compared three different alkaline catalysts, which are namely sodium methoxide (CH_3ONa), sodium hydroxide (NaOH) and potassium hydroxide (KOH). Taher and Al-Zuhair (2016) also addressed these three catalyst as most popular catalysts due to their contribution in high yield of biodiesel, cost, and relatively low reaction time and temperatures. Although the best product yield was obtained with sodium methoxide (CH_3ONa), this catalyst was not preferred due to the difficulties in the separation process. Use of KOH led to ease of separation and was recommended by the authors (Leung and Guo, 2006). The effect of reaction temperature and reaction time on transesterification was also investigated (Leung and Guo, 2006). The authors reported that during the transesterification of neat canola oil, the best temperature for the highest biodiesel yield of 93 weight%

was obtained at 45ºC in 60 minutes. On the other hand, the highest yield of 90 weight% was observed at 60ºC in 20 minutes for the WFO (Leung and Guo, 2006).

KOH and NaOH are the main conventional catalysts which are used in order to increase the reaction speed (Alptekin and Canakci, 2011). However, investigation of new catalysts started with the increasing demand for the alternative fuel sector. Moreover, soap formation challenge of KOH and NAOH during the transesterification of high FFA triglycerides also encouraged researchers to study various catalysts (Marwaha *et al.*, 2018). Mardhiah *et al.*, (2017) derived the heterogeneous catalysts under four sub groups as (i) Acid catalyst, (ii) Base catalyst, (iii) Acid-base catalyst and (iv) Biocatalysts. For example, Carvalho *et al.* (2017) conducted the biodiesel production from mucor circinelloides biomass by catalysing 12-molybdophosphoric support on alumina (H_3PMo/Al_2O_3) and recorded 97% yield. In another study, Marinković *et al.* (2017) studied the influence of CaO loading onto γ-Al_2O_3 as a catalyst for the transesterification process and obtained 94.3% yield. In addition, some enzymes were also used as a catalyst in transesterification. To illustrate, Amini *et al.* (2017) used lipase as a catalyst for the conversion of sweet basil (Ocimum basilicum) into biodiesel with 94.58% conversion rate at 47°C. Similarly, Andrade *et al.* (2017) catalysed the transesterification of 6.1% FFA castor oil by Eversa liquid enzyme and obtained 94% yield. Reviewed studies revealed that main advantages of the advanced catalysts were to increase the biodiesel production yield (of especially high FFA feedstock), to lower the transesterification temperature and time.

2.3.3. Alcohol to oil ratio

Experimental studies showed that separation time, biodiesel quality and yield changes with alcohol to triglyceride ratio. Taher and Al-Zuhair (2016) stated that the best methanol to oil molar ratio ranges between 3:1 and 4:1. Ghadge and Raheman (2005) produced biodiesel from Mahua oil which has high Free Fatty Acids (FFA) at 6:1 (0.25 v/v) methanol to oil molar ratio. The study also investigates the effect of different methanol to oil ratios at the pre-treatment (esterification) stage. According to results, higher methanol to oil ratios resulted in less acid value of oil (Ghadge and Raheman, 2005). Figure 2.6 shows the relationship between the alcohol to oil molar ratio and product yield. The yield of the sunflower biodiesel was increasing with the increasing alcohol to oil molar ratio and the maximum yield was achieved at 6:1 ratio (Gerpen, 2005). Similarly, Meher *et al.* (2006) recorded a 97% yield at the 6:1 alcohol to oil ratio in 3 hours. The study even also tested higher ratios such as 9:1, 12:1, 18:1 and 24:1 but no yield higher than 97% was reported. However, they also noted that higher ratios made the transesterification faster i.e. 97% yield was obtained in 30 min with the 24:1 ratio (Meher *et al.*, 2006).
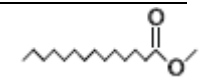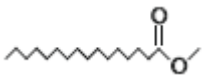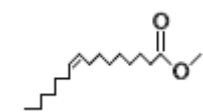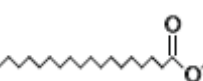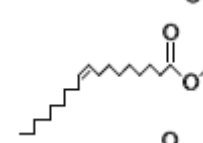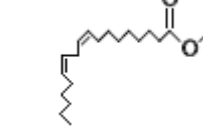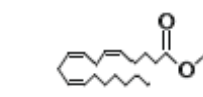
Figure 2.5: Influence of the alcohol to oil ratio on biodiesel yield in transesterification (Gerpen, 2005).

Overall, there is no solid consensus in the literature regarding the alcohol to oil ratio. This can be due to different FFA contents and chemistry of feedstock. In the literature, the main importance of the alcohol to oil ratio was pointed as the yield of triglyceride conversion into biodiesel.

2.4. Fuel properties of biodiesels

The type of feedstock (triglyceride) has a huge influence on the produced biodiesel. This is because triglycerides can be formed of different carbon chains in terms of their length and number of double bonds exists in each chain (Schönborn *et al.*, 2009). Therefore, each fatty acid methyl ester (FAME) has different fuel properties (Table 2.1). Table 2.1 shows some fuel properties of the commonly found FAMEs in biodiesel compositions. Percentages of the FAME compounds in any biodiesel influence the overall fuel quality. Hence, GC-MS analysis can be done to determine the types of FAMEs which form the biodiesel along with their percentages.

Table 2.1: Properties of some fatty acid methyl esters (Schönborn, 2009; British Standard Institution, 2010; Ramírez-Verduzco *et al.*, 2012).

| FAME | Name of FAME | Formula | (Ramírez-Verduzco *et al.*, 2012) | | | | (Schönborn, 2009) | | | | | (British Standard Institution, 2010) | Molecular structure |
			Cetane Number	Viscosity at 40 °C (mm²/s)	density at 20 °C (g/cm³)	HHV (MJ/kg)	LHV (MJ/kg)	Carbon Content (m/m %)	Hydrogen Content (m/m %)	Oxygen Content (m/m %)	Melting Point (°C)	Iodine Value (g/100g)	
C14:0	Myristic acid	$C_{15}H_{30}O_2$	65.4	3.33	0.8665	38.79	36.20	74.35	12.44	13.21	18	0	
C16:0	Palmitic acid	$C_{17}H_{34}O_2$	73.9	4.37	0.8644	39.56	36.44	n/a	12.56	n/a	32-35	0	
C16:1	Palmitoleic acid	$C_{17}H_{32}O_2$	53.3	3.59	0.8764	39.3	n/a	n/a	n/a	n/a	n/a	95	
C18:0	Stearic acid	$C_{19}H_{38}O_2$	82.3	5.59	0.8627	40.18	37.50	n/a	12.73	n/a	37-41	0	
C18:1	Oleic acid	$C_{19}H_{36}O_2$	61.7	4.6	0.8746	39.93	37.44	76.99	12.2	10.8	-20	86	
C18:2	Linoleic acid	$C_{19}H_{34}O_2$	41.1	3.79	0.8865	39.68	37.15	77.43	11.58	10.99	-35	173.2	
C18:3	Linolenic acid	$C_{19}H_{32}O_2$	20.5	3.11	0.8985	39.43	n/a	n/a	n/a	n/a	n/a	261.6	
C20:0	Arachidic acid	$C_{21}H_{42}O_2$	90.8	7	0.8613	40.7	n/a	n/a	n/a	n/a	n/a	0	

Reviews provided in Table 2.1 showed that longer carbon chain lengths result in higher cetane number, viscosity, higher heating value (HHV), lower heating value (LHV), carbon content, hydrogen content, melting point and iodine number of FAMEs. For example, cetane numbers of C14:0, C16:0, C18:0 and C20:0 were provided as 65.4, 73.9, 82.3 and 90.8 respectively (Table 2.1). Moreover, LHV values of the C14:0, C16:0 and C18:0 FAMEs were given as 36.2, 36.4 and 37.5 MJ/kg respectively (Table 2.1). Oxygen content was the only decreasing fuel property reported with respect to increasing carbon chain length. The number of double bonds in the content of FAMEs was another important factor as it directly affects the degree of unsaturation. Almost all fuel properties decreased with the presence of double bonds. To illustrate, cetane number and viscosity of C18:0 was reduced from 82.3 to 61.7 and 5.59 mm2/s to 4.6 mm2/s when there was a double bond existing in its structure, C18:1 Table 2.1. However, higher degree of unsaturation increases oxidation susceptibility of biodiesel (Gray, 1978; Sanders, 2003).

Table 2.2 demonstrated the FAME compositions of some famous animal fat, vegetable oil and waste cooking oil feedstock. Note that FAME compositions of the same feedstock, analysed by different researchers, can be different due to many reasons such as species/origin of the feedstock, biodiesel production procedure, biodiesel storage and measurement techniques.

Table 2.2: FAME compositions of some animal waste and vegetable oil biodiesels.

	Feedstock	C14:0	C16:0	C16:1	C18:0	C18:1	C18:2	C18:3	Others	Reference
Animal Waste	Chicken fat	0.7	20.9	5.4	5.6	40.9	20.5	0.0	6.0	(Supriya et al. 2017)
	Chicken fat	1.3	23.0	5.4	7.0	38.0	27.6	1.7	0.0	(Ashraf *et al.*, 2017)
	Duck fat	0.8	24.2	0.3	n/a	72.5	2.2	n/a	0.0	(Chung *et al.*, 2009)
	Duck fat	0.5	23.4	n/a	5.0	29.4	34.0	3.2	4.5	(Hamdan *et al.*, 2017)
	Goose	0.3	20.5	2.6	5.6	46.4	13.6	0.7	10.3	(Sander *et al.*, 2018)
	Sheep fat	3.0	27.0	2.0	24.1	40.7	2.0	n/a	1.2	(Banković-Ilić *et al.*, 2014)
	Sheep fat	0.8	28.1	0.4	27.2	31.3	1.6	0.6	10.0	(Bhatti *et al.*, 2008)
	Pork lard	n/a	28.1	n/a	11.6	38.1	18.8	3.4	0.0	(Mata *et al.*, 2011)
	Pork lard	1.1	19.8	2.0	11.8	44.7	10.9	1.0	8.7	(Sander *et al.*, 2018)
	Sardine Fish oil	7.4	18.7	7.7	2.5	11.5	0.0	3.1	49.1	(Mata *et al.*, 2014)
	Sardine Fish oil	6.8	20.3	6.5	4.3	19.8	2.6	1.6	38.1	(Sakthivel *et al.*, 2014)
	Beef tallow	2.7	25.3	2.0	34.7	29.9	0.8	n/a	4.6	(da Cunha *et al.*, 2009)
	Beef tallow	6.3	28.0	4.7	18.0	41.0	3.3	0.8	0.0	(Ashraf *et al.*, 2017)
	Veal tallow	5.8	23.2	3.2	13.0	37.8	6.3	0.6	10.2	(Sander *et al.*, 2018)
	Turkey fat	0.5	17.9	n/a	6.1	30.1	41.1	3.2	1.1	(Emiroğlu *et al.*, 2018)
Vegetable oil	Cottonseed oil	0.8	22.9	0.0	3.1	18.5	54.2	0.5	0.0	(Ramírez-Verduzco *et al.*, 2012)
	Cottonseed oil	23.4	n/a	n/a	n/a	22.6	n/a	52.4	1.6	(Alhassan *et al.*, 2014)
	Sunflower	0.1	6.0	0.0	5.9	16.0	71.4	0.6	0.0	(Ramírez-Verduzco *et al.*, 2012)
	Sunflower	n/a	6.3	n/a	4.3	80.4	7.7	0.3	1.0	(Moser, 2014)
	Waste cooking oil	n/a	10.9	0.6	4.0	38.1	40.5	4.7	1.2	(Moser, 2014)
	Waste cooking oil	1.1	11.5	0.6	4.2	35.2	39.7	6.2	1.4	(Man *et al.*, 2016)
	Waste cooking oil	0.3	7.7	0.5	3.5	32.3	53.3	0.3	2.1	(Ranjan *et al.*, 2018)

According to Table 2.2, C18:1 (Oleic acid) and C16:0 (Palmitic acid) were the two main FAME's found in animal fat derived biodiesels with average percentages of 37 and 23 respectively. On the other hand, C18:2 (Linoleic acid) and C18:1 (Oleic acid) were found to be the two main FAME's in the content of waste cooking oil biodiesels as 45% and 35% in average respectively. Vegetable oil biodiesels were mainly composed of unsaturated FAMEs, thus their iodine values were higher than that of animal fat biodiesels.

Fuel properties of some popular biodiesels derived from animal fats, cottonseed oil and WCO are presented in Table 2.3. Literature addresses that HHV of the animal fat based biodiesels are higher than vegetable oil and WCO derived biodiesels (Table 2.3). This is because of the higher saturation level of the animal fat based biodiesels, meaning a relatively lower amount of polyunsaturated FAMEs. Similarly, viscosities and cetane numbers of animal fat based biodiesels are observed higher than that of vegetable oils and WCO for the same reason. The literature clearly pointed out high percentages of the polyunsaturated FAMEs such as C18:2 and C18:3 in the compositions of vegetable oils (Senthur Prabu *et al.*, 2017). This also provides high iodine values for vegetable oil and WCO biodiesels. Can (2014) studied waste cooking oils collected from different resources like food factories and restaurants. The study reported that biodiesels produced from WCOs have iodine values around 125 which is higher than the 120 g/ 100g limit declared in BS EN 14214 standard. On the other hand, iodine values of animal fat derived biodiesel are reported well below the BS EN 14214 limit. For example, Wyatt *et al.* (2005) stated iodine values of tallow, lard and chicken as 54, 63 and 77 g/ 100g, respectively.

Table 2.3: Fuel properties of some biodiesels obtained from waste animal fats and vegetable oils including waste cooking oil.

Feedstock	HHV (MJ/kg)	Viscosity at 40 °C (mm²/s)	Density at 15 °C (g/cm³)	Cetane Number (-)	Iodine Value (g/100g)	Flash Point (°C)	Pour Point (°C)	Acid Value (mg KOH/g)	Reference
Beef tallow	41	5.29	0.859	58.2	44	161	14	0.2	(Ashraf *et al.*, 2017)
Chicken	41.5	5.56	0.887	57.4	38	176	12	0.8	(Ashraf *et al.*, 2017)
Duck fat	n/a	4.363	0.8785	n/a	n/a	n/a	n/a	n/a	(Hamdan *et al.*, 2017)
Fish oil	40.1	4.741	0.885	52.6	n/a	114	n/a	n/a	(Sakthivel *et al.*, 2014)
Sheep fat	n/a	5.98	0.856	59	126	n/a	-5	0.65	(Bhatti *et al.*, 2008)
Turkey fat	n/a	4.49	0.886	52.4	91.67	178	4	0.49	(Emiroğlu *et al.*, 2018)
Cottonseed	37.5	3.75	0.885	52.8	n/a	128	n/a	n/a	(Venkatesan *et al.*, 2017)
Cottonseed	41.2	4.07	0.875	54	104.7	455	n/a	0.16	(Talebian-Kiakalaieh *et al.*, 2013)
Waste cooking oil	n/a	4.6	0.871 at 20°C	51	n/a	n/a	n/a	n/a	(Man *et al.*, 2016)
Waste cooking oil	25.8	3.23	0.874 at 27°C	n/a	n/a	150	n/a	n/a	(Ranjan *et al.*, 2018)

Literature review showed that waste animal fat biodiesels and vegetable oil (including WCO) derived biodiesels are very different from each other in terms of their FAME components. This also causes significant differences in the crucial fuel properties such as viscosity, HHV, cetane number and iodine value. Vegetable oil and WCO biodiesels are typically superior to animal fat biodiesels in terms of viscosity and acid value, whereas animal fat biodiesels are better in terms of HHV, cetane number and iodine value.

2.5. Diesel engine operation using animal fat based biodiesels and blends

Engine performance and exhaust gas emissions characteristics of the compression ignition operated with animal fat biodiesels have been reviewed in this section. Studies on biodiesels produced from waste fish oils, chicken fat, beef tallow, sheep tallow and skin are reviewed.

2.5.1. Engine performance characteristics

According to the results of Lin and Li (2009), the exhaust gas temperature of fish oil biodiesel (F100) was $18^{\circ}C$ (4.7%) lower than diesel at the highest engine speed. Similarly, Behcet et al (2015) stated that exhaust gas temperatures of biodiesel blends were comparable to each other i.e. Temperatures of C20 and F20 can be assumed as the same and approximately $10^{\circ}C$ higher than diesel at almost all engine speeds. Furthermore, Godiganur et al (2010) read increased exhaust gas temperatures for F100 and F20 by $125^{\circ}C$ and $32^{\circ}C$, respectively. Table 2.4 and Figure 2.7 summarised the engine performance and exhaust emissions of the reviewed animal fat based biodiesels and blends. Note that operating conditions were different for each study reviewed in Table 2.4 and Figure 2.7. In this regard, although each study can be evaluated individually, care should be taken when making comparisons among studies.

Table 2.4: Engine performance and exhaust emissions characteristics of animal fat biodiesels compared to diesel.

Reference	Test fuel	BTE (%)	Brake Torque (%)	Brake Power (%)	BSFC (%)	CO₂ (%)	CO (%)	HC (%)	NOₓ (%)	Smoke (%)	Exhaust gas Temperature (ºC)
(Behçet *et al.*, 2015)	F20		-3.2	-4.33	8.3	-7.87	-24.4	-53.5	13.77	-16	10
(Behçet *et al.*, 2015)	C20		-1.9	-2.4	5.2	-7.87	-19.8	-20	13.77	-10	10
(Öner and Altun, 2009)	T5	-3		-2.3	6		-14		-20	-16	12
(Öner and Altun, 2009)	T20	-4		-2.3	12		-16		-40	-27	30
(Öner and Altun, 2009)	T50	-5		-4.33	18		-5		-12	-45	-10
(Öner and Altun, 2009)	T100	-7		-9	25		-15		-39	-57	5
(Lin and Li, 2009)	F100	-3			13		-9		14.3	-10	-18
(Godiganur *et al.*, 2010)	F100	-5			20.7		-59	-40	14.3		125
(Godiganur *et al.*, 2010)	F20	1			0		-22	-13.3	4.4		32
(Şen *et al.*, 2018)	C20	1.3	1.4		-3.8	-1	-55	-24	2.7	-8.9	
(Şen *et al.*, 2018)	C50	0.8	1.5		1.9	-3.9	-50	-12	3.3	-6.7	
(Srinivasan *et al.*, 2017)	S30	0			5		-25		12		
(Sakthivel *et al.*, 2014)	F100	-12				13	-33.7	-26.2	-5.2		
(Jayaprabakar *et al.*, 2019)	SS20	-6.7		4	8.3	33	-30		12.5	-71.4	

F100: fish oil methyl ester, C20: Chicken biodiesel 20% + diesel 80%, T100: Tallow biodiesel, S30: Sheep biodiesel 30% + diesel 70%, SS20: Sheep skin biodiesel 20% + diesel 80%
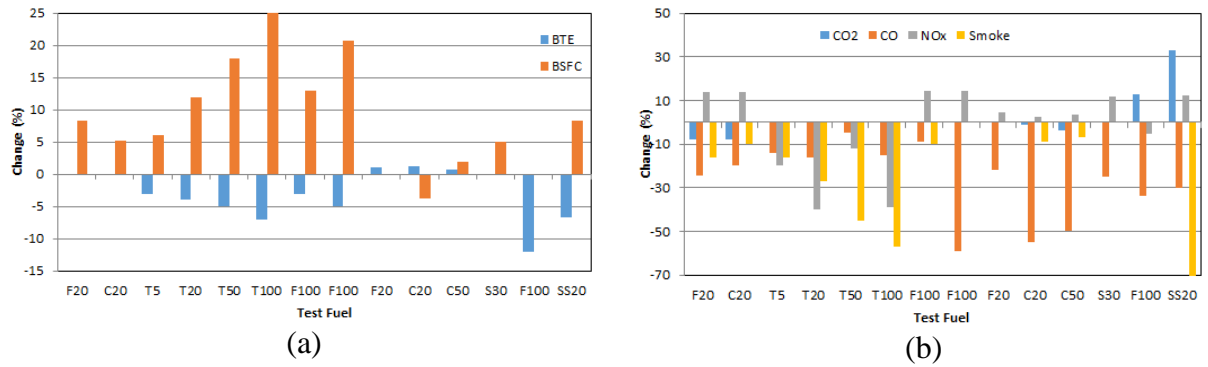
Figure 2.6: Changes in (a) engine performance and (b) exhaust emissions characteristics of animal fat biodiesels compared to diesel.

In Lin and Li's study (2009), brake specific fuel consumption (BSFC) of fish biodiesel (F100) was recorded 12.9% higher than the diesel and 3% lower than W100 (not presented in Table 2.4). Likely, Godiganur et al (2010) stated that BSFC for F100 was 20.7% higher than the diesel at full load. Similarly, Behcet et al (2015) found 8.3% increased BSFC for F20. The increase in BSFC can be related to the energy content of the fish biodiesel, which requires higher fuel to be burned to produce the same power output with diesel (Emiroğlu *et al.*, 2018). This fact also negatively influences the Brake Thermal Efficiency (BTE). Literature tabulated in Table 2.4 also stated reduced BTE in the range of 3- 12% with biodiesels. In contrast, Godiganur (2010) reported an increasing BTE for one of tested biofuel blend which was B20. It was 1 % higher than the diesel whereas other blends having higher biodiesel ratio provided lower BTE than diesel. This increasing BTE can be attributed to 80% diesel in the blend. Likely, Sen et al (2018) reported slightly improved BTE by 1.3% and 0.8% for

C20 and C50 biodiesels. However, these results were also contradicting with their BSFC value for C50 as reported 1.9% higher than diesel. This may be due to the operating condition of the particular experiments.

2.5.2. Exhaust gas emissions characteristics

2.5.2.1. *NOx emissions of animal fat based biodiesels*

NO_x gases are very harmful both to the environment and human health. In the human body, lungs are the organs affected by the NO_x. The NO_x combines with the water vapour they form nitric acids in the human lungs which cause respiratory disease (Behçet *et al.*, 2015).

Literature showed that fish biodiesel and its diesel blend increased the NOx emission in the range of 4% to 14.3% (Table 2.4 and Figure 2.7). Behçet *et al.* (2015) also concurred with the increased NOx emission with the chicken biodiesel operation as C20 had around 14% increased NO_x emission than diesel on average. This shows that the majority of the literature reports increased NOx emission for biodiesels, but there are also some studies showing reduced NOx emission with biodiesel operation (Table 2.4). Tallow biodiesel and its diesel blends gave reduced NO_x emissions by 20%, 40%, 12% and 39% for T5, T20, T50 and T100, respectively. Similarly, Sakthivel *et al.* (2014) also reported a 5.2% decrease in the NO_x emission of F100 (not shown in Table 2.4). This was probably due to varying operating conditions such as feedstock property, additive usage, engine modifications or aftertreatment conditions. Masera and Hossain (2019) stated that different parameters influence NO_x formation which might cause contradictory results. Residence time of the fuel-air mixture, spray characteristics, ambient conditions, exhaust gas recirculation (EGR) or other aftertreatment applications, physical condition of the experimental equipment, oxygen content and measurement fluctuations were all linked to NOx emissions (Omari *et al.*, 2017; Ramalingam and Rajendran, 2017; Ulusoy *et al.*, 2018).

2.5.2.2. *Smoke opacity of animal fat based biodiesels*

Particulate matter (PM) is another exhaust gas which is highly pollutant and harmful for human health. This parameter corresponds to the smoke opacity of the exhaust gas (Sakthivel *et al.*, 2014). This emission can even be experienced by the naked human eye when it is at the high concentrations.

Lin and Li (2009) stated a 4% reduction in smoke opacity for F100 compared to diesel. In general, smoke opacity followed a decreasing trend as the engine speed decreased. In the study of Behcet et al. (2015), the decreasing trend of smoke opacity contributed to improved combustion and homogeneous mixing of the substances under the effect of enhanced turbulence, swirl and jet movement of injected air with respect to increased engine speed. It was also noted that biodiesel blends of F20 and C20

emitted 16% and 10% lower smoke than diesel on average, respectively. Similarly, Oner and Altun (2009) measured a significant reduction in smoke opacity for T100 by 57% lower than diesel. Biodiesels produced from sheep biodiesels were also reported to have reduced smoke emissions (up to 71% lower than diesel) by various studies presented in Table 2.4. The main reason for the significantly reduced smoke emission with biofuels is the presence of the oxygen content (Baskar and Senthilkumar, 2016). These oxygen molecules fill sudden local oxygen vacancies and prevent smoke formation (Ozsezen *et al.*, 2009). Another reason for the smoke reduction with biodiesel is the chemical structures of FAMEs which are free of aromatic compounds (Williams *et al.*, 1986).

2.5.2.3. *CO_2 emissions of animal fat based biodiesels*

According to Sakthivel et al. (2014), CO_2 emission in the diesel engine is highly related to the efficiency of combustion. All carbon atoms in the fuel content convert into CO_2 in the case of complete combustion. Behcet et al. (2015) reported 7.87% reduction in CO_2 emission with the biodiesel usage. In contrast, Sakthivel et al. (2014) observed an 6.7% increase in CO_2 gas emission for F100. Similarly, Jayaprabakar et al. (2019) reported 33% increased CO_2 emission with SS20 biodiesel. These increased CO_2 emissions can be linked to the oxygen content of the esters that leads more efficient burning of the fuel which in turn converts more carbon into carbon dioxide rather than carbon monoxide (Sakthivel *et al.*, 2014).

2.5.2.4. *CO emission of animal fat based biodiesels*

In the absence of sufficient oxygen, CO gas may be released as a combustion product. Gürü *et al.* (2010) stated that the presence of CO emission represents incomplete combustion as full oxidation did not take place to form CO_2. According to Table 2.4, all reviewed studies reported mitigated CO emissions with animal fat derived biodiesels compared to diesel. Behçet *et al.* (2015) stated that F20 and C20 emitted respectively 24.4% and 19.8% lower CO emissions than diesel on average. Lin and Li (2009) observed 9% reduced CO emission for F100 compared to diesel. In addition, in the same study, it was noted that CO reduction for fish oil biodiesel was almost 2% lower than waste cooking oil biodiesel. Godiganur et al. (2010), also used biodiesel formed from fish oil and obtained the highest reduction in CO emission of 59% less than diesel. Like other research articles, Sakthivel (2014) also observed 33.7% decrease in CO emissions for B100. Öner and Altun (2009) reported 14%, 16%, 5%, and 15% reduced CO emissions for T5, T20, T50 and T100 compared to diesel. This review demonstrates that biodiesels reduce CO emission compared to diesel. This can be attributed to improved combustion of fuel.

2.5.2.5. HC emissions of animal fat based biodiesels

Unburned hydro carbons (HC) are the result of incomplete combustion (Komninos, 2009). All reviewed studies reported decreased HC emissions in biodiesel applications Table 2.4. This shows that biodiesels had improved combustion compared to diesel which results in better burning of fuel. This also agrees with the reduced CO emissions result in the previous section. Godiganur et al. (2010) stated that HC emissions of F20 and F100 were 13.3% and 40% lower than diesel. Likely, Sakthivel et al. (2014) also reported 26% decreased HC emission with F100. Similar to previous studies, Behçet *et al.*, (2015) also observed 53.5% and 20% reductions in HC emissions for F20 and C20 respectively. Biodiesel obtained from sheep biodiesel (S20) had a 24% lower HC emission than diesel (Şen *et al.*, 2018).

2.6. Diesel engine operation using waste cooking oil and inedible vegetable oil based biodiesels

Vegetable oils have attracted the interest of many researchers as they provide a significant energy source. Similarly, after the cooking process, waste cooking oils (WCO) can be used as an alternative fuel in their 'second life'. There is a significant number of studies on the use of vegetable oils and WCO as alternative fuels (Kumar and Sharma, 2011; Atabani *et al.*, 2013). This section reviews studies about engine testing of biodiesels derived from inedible vegetable oils or WCO. More specifically, biodiesels obtained from various waste cooking oils, waste cooking olive oil, cottonseed, Karanja and Jatropha are reviewed in this section as summarised in Table 2.5 and Figure 2.8.

Table 2.5: Changes in engine performance and exhaust emissions of the waste cooking oil and inedible vegetable oil biodiesels relative to diesel.

| Reference | Test Fuel | BTE (%) | BSFC (%) | Exhaust gas emissions | | | | | Exhaust gas Temperature (^{o}C) |
				CO_2 (%)	CO (%)	HC (%)	NO_x (%)	Smoke (%)	
(Hossain and Davies, 2012b)	W100	5	2.5	3	-90	n/a	-4	-18	-25
(An *et al.*, 2012)	W100	3	13	-20	-70	-40	-10	n/a	-70
(Lin and Li, 2009)	W100	-5	16	n/a	-7.3	n/a	13	-21	n/a
(Dorado *et al.*, 2003)	WO100	n/a	8.5	-8.6	-59	n/a	-40	n/a	n/a
(Aydin and Bayindir, 2010)	CO100	n/a	30	n/a	-52	n/a	-38	n/a	-3
(Karabektas *et al.,* 2008)	CO100	4	n/a	n/a	-38	n/a	-22	n/a	n/a
(Yucesu and Ilkilic, 2006)	CO100	n/a	10	-33	-20	n/a	-23	n/a	-70
(Raheman and Phadatare, 2004)	K100	-20	30	n/a	-92	n/a	-38	-50	0
(Ganapathy *et al.,* 2011)	J100	-7	15	n/a	-40	-33	10	-36	n/a
(Chauhan *et al.* 2011a)	J100	-8	13	40	-33	-60	52	-37	-100

W100= waste cooking oil biodiesel, CO= Cottonseed biodiesel, WO100= waste olive cooking oil biodiesel, K100= Karanja biodiesel, J100=Jatropha biodiesel, SO= Soybean biodiesel
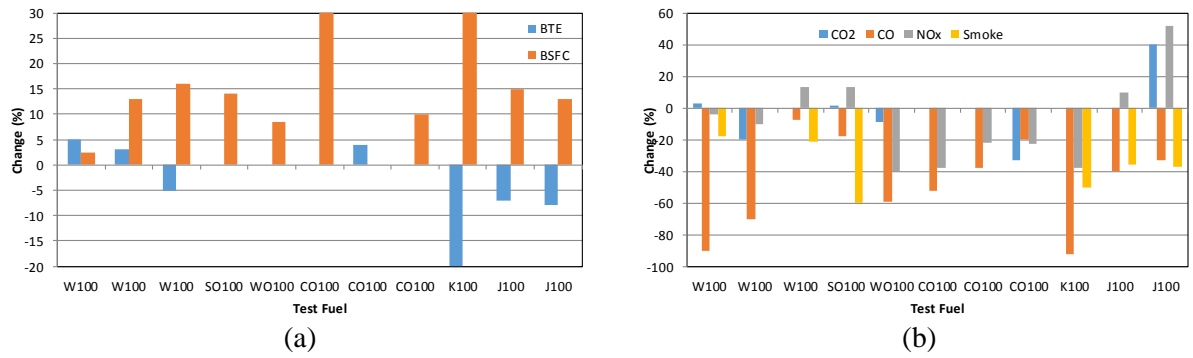
Figure 2.7: Changes in (a) engine performance and (b) exhaust emissions of the reviewed vegetable oil and waste cooking oil biodiesels relative to diesel.

Hossain and Davies (2012) tested waste cooking oil biodiesel in a three-cylinder indirect injection CI engine. According to the study, W100 had 5% and 2.5% higher BTE and BSFC than diesel at full load respectively. In-cylinder peak pressure of W100 was 9.7% and 6.7% lower than that of diesel at low and mid-range engine loads and W100 had 16% shorter combustion duration in total. Similarly, An et al (2012) reported shorter combustion duration for W100 than diesel at all engine loads. The main drawback of biodiesel was reported in CO_2 emission which was 3% greater than diesel (Hossain and Davies, 2012). On the other hand, biodiesel released 4% and 90% lower NO_x and CO emissions than diesel.

In another study, An et al. (2012) investigated the use of W10, W20, W50 and W100 biodiesels in a four-cylinder DI diesel engine. They found that W100 produced the lowest in-cylinder peak pressure (2% lower than diesel) and this was attributed to the lower calorific value of the biodiesel. Although all fuels showed comparable BSFC trends, W100 had almost 13% higher BSFC than the others under full load. However, W100 gave 3% improvement in BTE over diesel at full load. The exhaust gas temperature reduced in accordance with increased biodiesel content in the blend. Around 100°C difference between diesel and B100 was recorded for all engine speeds. Even though they reported higher CO emissions with the biodiesel operation at low engine loads, W100 released 70% lower CO than diesel at maximum engine speed. Moreover, 20% and 40% reduced CO_2 and HC emissions were measured for W100 relative to diesel. NO_x emissions at almost all loads were found comparable. The major difference between diesel and W100 of 10% in favour of W100 was reported at full load and maximum engine speed. Very similar results were also measured in the study of Lin and Li (2009) for W100 except for BTE and NOx. Unlike other W100 studies reviewed, Lin and Li found 5% improved BTE and 13% increased NOx emission for the W100 operation at full load. This is probably due to the type of W100 biodiesel used, which was described as commercial biodiesel and may have contained performance improver additives.

Dorado et al (2003) studied waste cooking olive oil biodiesel (WO100) in a three-cylinder CI engine. According to the study, WO100 gave a maximum of 58.9% reduction in CO emission, up to 8.6% reduction in CO_2 emission, 37.5% reduction in NO emission and up to 57.7% reduction in SO_2 emission compared to diesel. Whereas, NO_2 emission increased drastically as a maximum of 81% observed with the usage of biodiesel. Another bad performance feature of biodiesel is the increase of (less than 8.5%) brake specific fuel consumption. In terms of combustion efficiency, biodiesel and diesel have comparable results (Dorado *et al.*, 2003).

Aydin and Bayindir (2010) studied cottonseed biodiesel CO100 and its blends with diesel at fractions of CO5, CO20, CO50 and CO75 in a direct-injection single-cylinder diesel engine. They reported a 20% reduction in engine power and 17% decrease in engine torque with CO100 at the full load. In parallel, a 30% increase in BSFC was reported with CO100 compared to fossil diesel. However, significant reductions in the CO and NOx emissions were observed; these were 52% and 38% lower than diesel respectively. In addition, almost 100% reduction in SO_2 emission was observed again at full load. Similarly, Dorado et al. (2003) reported a significant reduction in SO_2 emission by 58% with waste frying olive oil biodiesel operation in a direct-injection diesel engine.

Like Aydin and Bayindir (2010), Karabektas et al. (2008), Yucesu and Ilkilic (2006) also reported reduction in NOx emission around 23% for cottonseed biodiesel CO100 operation. The other exhaust gas emissions like CO and CO_2 were measured lower than diesel up to 38% and 33% respectively (Table 2.5). Furthermore, BTE of the CO100 was reported 4% higher than diesel (Karabektas *et al.*, 2008). However, BSFC was reported 10% higher than diesel in the study of Yucesu and Ilkilic (2006).

Raheman and Phadatare (2004) tested Karanja biodiesel K100 and compared the results against diesel. They reported a 20% reduction in BTE and 30% increase in BSFC. Moreover, engine torque was reported 19% lower than diesel operation for K100. These results showed that K100 could not improve engine performance. This may have been due to poor fuel properties such as relatively high viscosity of 9.60 mm^2/s (compared to BS EN 14214 standard) and HHV of 36.12 MJ/kg. However, exhaust gas emissions of K100 were reported lower than diesel i.e. 92%, 38% and 50% lower CO, NOx and smoke emissions were measured for K100.

Ganapathy et al. (2011) and Chauhan et al. (2011) both studied Jatropha biodiesel J100 and reported very similar results in terms of engine performance and exhaust emissions, Table 2.5. Both studies were conducted on one-cylinder diesel engines. According to these studies, J100 had around 8% reduction in BTE and 15% increase in BSFC. Reductions in CO, HC and smoke emissions were measured up to 40%, 60% and 37% relative to diesel respectively, Table 2.5. However, CO_2 and NOx emissions of J100 were found to be 40% and 52% higher than diesel at the full engine load Table 2.5. Similarly, Ganapathy et al. (2011) also reported 10% increase in NOx emission for J100 at full load and high engine speed conditions (15 Nm and 3200 rpm).

To sum up, engine test results from biodiesels produced from waste cooking oils, cottonseed oil, Karanja oil and Jatropha oil were summarised and reviewed in this section. Among the investigated biodiesels, WCO biodiesels were found as a good candidate especially in terms of BTE, NOx and consistency of the results from different studies. Moreover, CO100 was also superior to other biodiesels especially in terms of its relatively low viscosity, higher BTE and reduced NOx emissions Table 2.5.

2.7. Diesel engine operation using biodiesel-biodiesel mixtures

Biodiesel-diesel blends are very common in the literature. However, relatively few studies have been done on biodiesel-biodiesel blends. Previous studies on biodiesel-biodiesel blending are reviewed from different perspectives in this section.

Benjumea et al (2011) conducted an experimental study on a 4-cylinder turbocharged direct-injection diesel engine to observe the effects of degree of unsaturation (DU) of palm oil and linseed oil biodiesels. According to the study, no significant effect of degree of unsaturation was reported on engine performance. However, the combustion start time of linseed oil biodiesel with an iodine value of 185.4 was 2°CA later than the palm oil biodiesel which had an iodine value of 52. Moreover, peak heat release rate (HRR) of the linseed oil biodiesel was 40% higher than the palm oil biodiesel. In terms of the exhaust emissions, higher iodine value biodiesel released approximately 40% higher NO_x and slightly higher smoke opacity compared to low iodine value biodiesel. The palm and linseed biodiesel blends reported to have a linear relationship between the base fuels for all test parameters.

Rajkumar and Thangaraja (2019) tested the karanja and coconut biodiesels in the fractions of K100, K80C20, K60C40, K40C60, K20C80 and C100. The effect of retarding Start of Injection (SOI) as a result of different fuel properties such as bulk modulus of compressibility and degree of unsaturation was investigated in a four-cylinder turbocharged diesel engine equipped with a mechanically operated injection system. The results of the study showed an increasing trend in the peak pressure with the increasing fraction of the karanja biodiesel, which had a higher degree of unsaturation and bulk modulus compared to coconut biodiesel. The trend was similar in terms of the NO emission i.e. K100, K80C20, K60C40, K40C60, K20C80 and C100 fuels had NO emissions of 765, 732, 695, 672, 628, and 590 ppm at 2500 rpm, 80% load, respectively. However, more studies are required to support these results as the karanja biodiesel used in the study was not neat but hydrogenated. The 200 ml of karanja biodiesel was diluted in 800 ml of methanol in the presence of 1 gram palladium catalyst.

Sanjid et al. (2016) blended kapok and moringa biodiesels with diesel and tested them in a 4-cylinder diesel engine. Not only the 10% and 20% biodiesels blended with diesel (i.e. KB10, KB20, MB10 and

MB20), but also 5% and 10% of neat biodiesels blended with each other along with 90% and 80% diesel (i.e. KB5MB5 and KB10MB10) and analysed. According to the authors, biodiesel-biodiesel-diesel blends had comparable engine performance with neat biodiesels and diesel. KB5MB5 and KB10MB10 biodiesel-biodiesel-diesel blends had between 14% and 17% increased NO emissions compared to diesel. Moreover, the same blends gave 1% and 2% higher CO_2 emission compared to diesel respectively. However, significant reductions on HC and CO emissions were reported as 38% and 31% for the KB10MB10 blend, respectively.

Dos Santos et al (2018) studied the traceability of biodiesel-biodiesel mixtures collected from different regions of Brazil. Fourier Transform Infrared Spectroscopy (FTIR) was used to analyse the various ratios of biodiesels obtained from soybean, tallow, palm and cotton. This preliminary study showed that biodiesels produced from different regions of Brazil can have different properties. The authors stated that biodiesel-biodiesel blending can improve fuel properties and they also recommend future works in multiple feedstock biodiesel blending.

Usta et al. (2005) highlighted the importance of soapstock feedstock, which is a side product of edible oil extraction process, as they are cheap, highly available and sustainable. However, these products may have high free acid values which make biodiesel production from soapstock more difficult compared to vegetable oils. Hence, in their study, hazelnut soapstock was blended with waste sunflower oil in 50/50 ratio to reduce the overall fatty acid content of the feedstock. The viscosity of the biodiesel obtained was very high at 25 mm^2/s; thus the biodiesel was blended with the diesel. According to results, 17.5% biodiesel blend gave the best engine performance. Similarly, in another study, Can (2014) reduced the high free fatty acid content (10%) of the WCO collected from fast food restaurants by blending them with the WCO obtained from cooking factories. The results of the study showed that 10% blend of the obtained biodiesel with diesel provided; 4% increase in BSFC, 2.8% reduction in BTE, 8.7% increase in NOx emission, 29 % decrease in HC and 51% reduction in CO emission compared to diesel.

Sharma and Ganesh (2019) analysed two different biodiesel blends produced from linseed, karanja, palm and sunflower biodiesels in a one-cylinder diesel engine. The first blend was composed of 25% of all the four biodiesels; whereas the second blend contained 37.5% of palm and karanja biodiesels and 12.5% of linseed and sunflower biodiesels. They reported that the first blend decreased the NO_x emission by 20% but increased the smoke intensity by 30%. In addition, CO_2 emission was reported 35% lower compared to diesel. The study pointed to the importance of biodiesel-biodiesel blending technique which can solve NO_x emission disadvantage of biodiesels. Similary, Mehta and Jeyaseelan (2014) reported 14% reduction in NO emission with the 80% palm biodiesel - 20% karanja biodiesel blend in a 4-cylinder turbocharged direct-injection CI engine.

Fadhil et al (2017) blended castor seed oil and waste fish oil feedstock at the ratios of 90/10, 80/20, 70/30, 60/40 and 50/50 to improve the transesterification process. They reported that 50/50 oils blend was found optimal blend for transesterification and best conditions were provided as 0.5 weight% KOH, 1:8 molar ratio of methanol, 32°C temperature and 30 minutes of stirring at 600 rpm. Although the biodiesels were not tested in any engine, this study proved that feedstock blending is a promising technique to improve the transesterification process as maximum yield was obtained at lower reaction temperature.

Summarising the biodiesel-biodiesel blending studies, it is clear that this technique is really promising for the future research. According to literature, one of the main advantageous of biodiesel-biodiesel blending could be enhancing the utilisation of cheap, highly available but low fuel quality feedstock such as soapstocks and high free acid content waste cooking oils. No study was found about the effects of using a waste cooking oil and animal fat biodiesel-biodiesel blend in a diesel engine.

2.8. Engine modifications – combined and individual effects of thermal barrier coating, injection timing, injection pressure and fuel preheating

Compression ignition engines are designed for diesel application, but physico-chemical properties of biofuels are not the same with diesel. This section reviews the engine modifications to upgrade biofuel operation in terms of engine performance, fuel combustion and exhaust emissions. Both individual and combined effects of Thermal Barrier Coating (TBC), injection timing, injection pressure and fuel preheating were reviewed in detail.

Thermal barrier coating also known as Low Heat Rejection (LHR) technique was first reported in 1978 for the purpose of increasing performance and durability of diesel engine (Kamo and Bryzik, 1978). Coating layers are typically applied via plasma spray technology which has a volume fracture of 10-20% voids and cracks (Samadi and Coyle, 2009). This minimises the heat transfer from the combustion chamber to the surroundings; thus heat rejection through the cooling system is reduced which in turn improves the thermal efficiency, mechanical power output, fuel consumption and exhaust emissions (Masera and Hossain, 2019).

Generally, two different layers are applied to form TBC; namely the primary and bond coating layers (Kumar *et al.*, 2013; Mittal *et al.*, 2013; Iscan, 2016). The thermal insulation is provided by the primary layer and bond layer is applied for the adherence between the primary layer and the substrate (Figure 2.9). The bond layer minimises the unwanted oxidation or corrosion on the surface of substrate (Saint-Ramond, 2001; Yilmaz *et al.*, 2010).

The TBC details from various biofuel studies were summarised and tabulated in Table 2.6 explicitly. The majority of the studies reviewed preferred to use Zirconium products (ZrOx) for the primary layer and NiCrAl alloy in the bond layer (Table 2.6). The Piston crown, cylinder liner, exhaust and inlet valves and cylinder head were the main surfaces coated by the researchers.
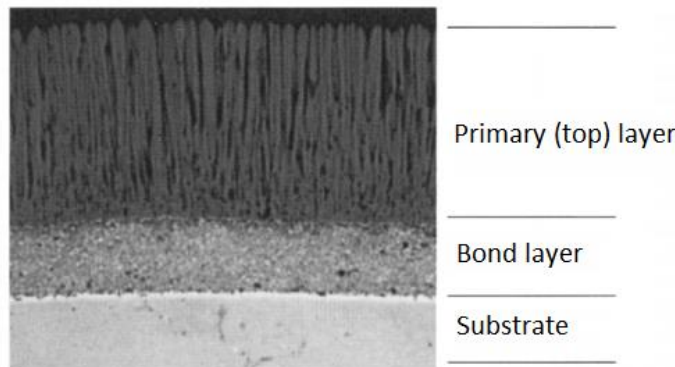
Figure 2.8: Thermal barrier coating layers (Masera and Hossain, 2019).

Table 2.6: Biofuels and thermal barrier coating details from the literature, adapted from the author's published paper (Masera and Hossain, 2019).

Ref	Fuel	COATING				Engine Components	Air Intake
		Primary Layer Material	Thickness (µm)	Bond Layer Material	Thickness (µm)		
(Aydin and Sayin, 2014)	WCOB	ZrO_2 (88%) + Al_2O_3 (8%) + MgO (4%)	400	NiCrAl	100	PC, V	Naturally aspired
(Aydin, 2013)	CSO35	ZrO_2	200			CH, PC, V	n/a
(Aydin, 2013)	SFO35	ZrO_2	200			CH, PC, V	n/a
(Hazar and Ozturk, 2010)	COB	Al_2O_3 +TiO_2	250	NiAl	50	CH, PC, V	Naturally aspired
(Iscan, 2016)	CSO65	ZrO_2	400	NiCrAl	100	PC, CL, V	Naturally aspired
(Kumar et al., 2013)	PPOB	$La_2Zr_2O_7$	350	NiCrAlY	150	PC, CH, V	Naturally aspired
(Mittal et al., 2013)	GNB15	ZrO_2+ Y_2O_3 (8% by weight)	200	NiCrAl	100	CH, V	Naturally aspired
(MohamedMusthafa et al., 2011)	RME	Fly Ash	200	No bond layer	0	CH, CL, PC, V	Naturally aspired
(MohamedMusthafa et al., 2011)	PME	Fly Ash	200	No bond layer	0	CH, CL, PC, V	Naturally aspired
(Palaniswamy and Manoharan, 2008)	Diesel	ZrO_3	250			PC, CH	n/a
(Prabhahar and Rajan, 2013)	PME	TiO_2	500			PC	Naturally aspired
(Rajan and Kumar, 2011)	JOB	ZrO_3	350	NiCrAl	150	PC	n/a
(Srikanth et al., 2013)	ECSO	PSZ	500			CH	Naturally aspired
(Taymaz et al., 2003)	n/a	$CaZrO_3$ (CH and V), $MgZrO_3$ (PC)	350	NiCrAl	150	CH, PC, V	Turbocharged
(Reddy et al., 2012)	MO	PSZ	500			CH	Naturally aspired
(Reddy et al., 2012)	MOB	PSZ	500			CH	Naturally aspired
(Rao et al., 2013)	TOB	PSZ	500			CH	Naturally aspired
(Parlak et al., 2005)	Diesel	MgO-ZrO_2 (PC), CaO-ZrO_2 (CH and V)	350	NiCrAl	150	CH, PC, V	Turbocharged
(Hasimuglu et al., 2008)	SOB	ZrO_3	n/a	NiCrAl	n/a	CH, CL, PC, V	Turbocharged
(Hazar, 2010)	CME40	Mo	n/a			CH, PC, V	n/a
(Janardhan et al., 2013)	JO	PSZ	500	supreni-90	n/a	CH, CL	Naturally aspired
(Janardhan et al., 2013)	JOB	PSZ	500	supreni-90	n/a	CH, CL	Naturally aspired
(Murthy, 2013)	RBO	PSZ	500	supreni-90	n/a	CH, CL	Naturally aspired
(Prasath et al., 2010)	JOB20	PSZ	500			CH, CL, PC, V	Turbocharged
(Sathiyagnanam et al., 2010)	ISO10	ZrO_2+Al_2O_3	150 + 150	NiCrALY	150	CH, CL, PC, V	Naturally aspired

WCO: Waste Cooking Oil Biodiesel;CSO35: Cottonseed Oil (35%), Biodiesel + Diesel (65%); SFO35: Sunflower Oil (35%), Biodiesel + Diesel (65%); COB: Corn Oil Biodiesel; CSO65: Cottonseed Oil (65%) + Diesel (35%); PPOB: Pongamia Pinnata Oil Biodiesel; GNB15: n-butanol (15%) + Gasoline (85%); RME: Rice Bran Biodiesel; PME: Pongamia Oil Biodiesel; ECSO: Cottonseed Oil Biodiesel; MO: Mohr Oil; MOB: Mohr Oil Biodiesel; TOB: Tobacco Seed Oil Biodiesel; SOB: Sunflower Oil Biodiesel; CME40: Cottonseed Oil (40%), biodiesel + Diesel (60%); JO: Jatropha Oil; JOB: Jatropha Oil Biodiesel; RBO: Rice Brawn Oil; JOB20: Jatropha Oil Biodiesel (20%) + Diesel (80%); ISO10: Fuel Additive (Di Iso Propylether 10%) + Diesel (90%); ZrO_2: Zirconium dioxide; $La_2Zr_2O_7$: Lanthanum Zirconate; Y_2O_3: Yttrium Oxide; Fly Ash: (silica SiO_2:45%, alumina Al_2O_3:30 %, iron Fe_2O_3:10%, magnesium MgO:0.5%); ZrO_3: Partially stabilized Zirconia; PSZ: Partially stabilized Zirconium PSZ; Mo: Molybdenum; CH: Cylinder Head; CL: Cylinder Liner; PC: Piston Crown; V: Intake and Exhaust Valves

2.8.1. Performance characteristics

Engine performance parameters such as BTE, BSFC, and brake Specific Energy consumption (BSEC) of the biofuels are reviewed in Figure 2.10. The results were tabulated under two conditions which were; (i) uncoated biofuel to coated biofuel (UB to CB), and (ii) uncoated diesel to coated biofuel (UD to CB). Each of the important parameters will be discussed in the next sections.

(a)

(b)
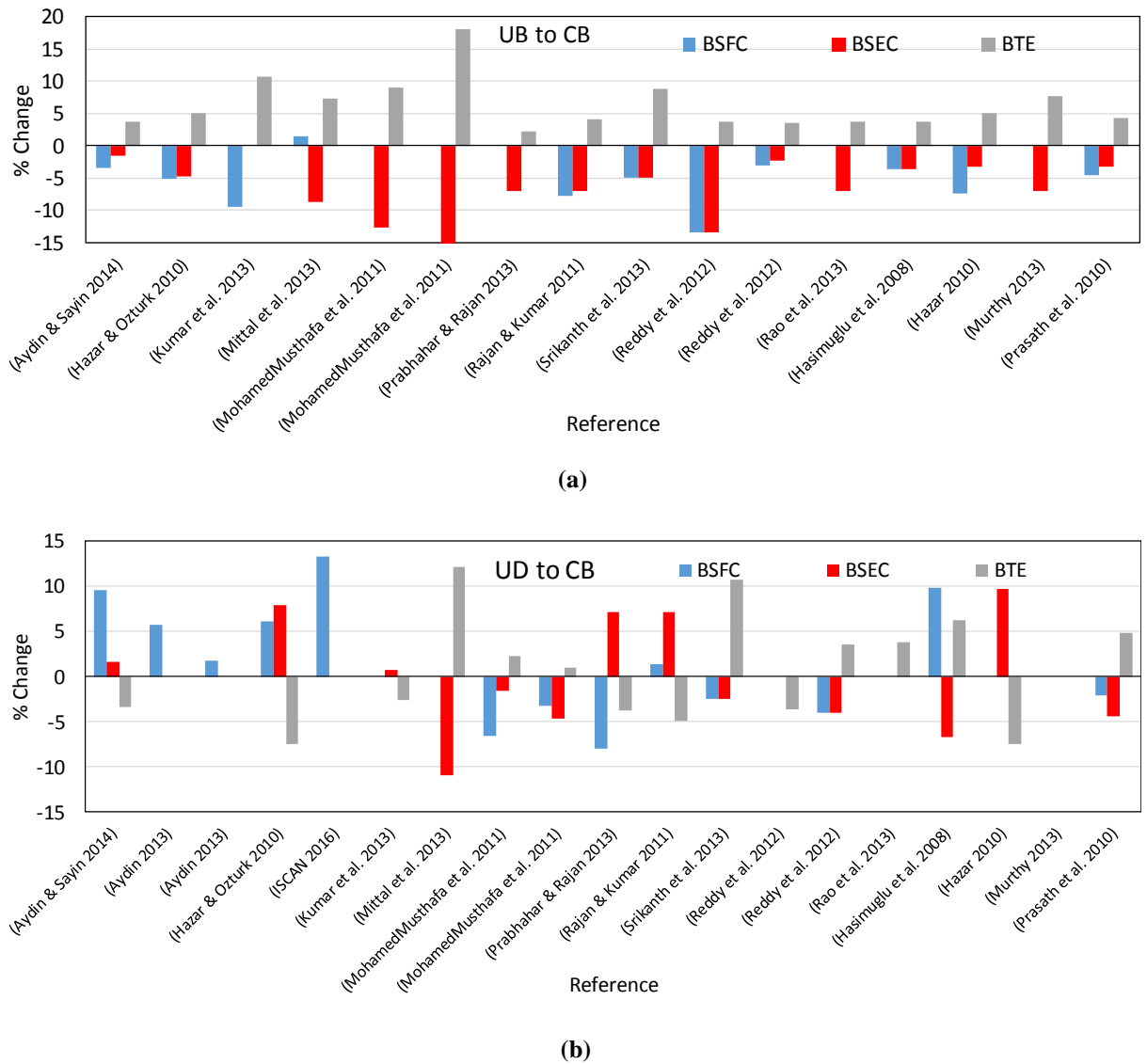
Figure 2.9: Comparison of engine performance before and after coating - (a) for UB to CB scenario (b) for UD to CB scenario, adapted from (Masera and Hossain, 2019).

2.8.1.1.   *Brake specific fuel consumption*

It is known that the BSFC of the biofuels are generally high relative to fossil diesel operation, due to lower heating value (Canakci and Gerpen, 2003; Dorado *et al.*, 2003; Lin and Li, 2009; Öner and Altun, 2009; Behçet, 2011; Hulwan and Joshi, 2011; Zhu *et al.*, 2011; Hossain and Davies, 2012). However, according to Figure 2.10, the TBC technique clearly improved the BSFC of the biofuels due to the heat retained by the coating. The maximum reduction for UB to CB conditions was observed as 13.4% (Reddy *et al.*, 2012). This can be explained by the shortened ignition delay and improved combustion of biodiesel as a result of higher combustion temperatures. Overall, BSFC of biodiesel operation can be improved up to 13.4% by the TBC modification.

35

2.8.1.2. Brake specific energy consumption

BSEC of the biofuels were also considered to have better comparison between fuels with different lower heating values. Unlike BSFC, the BSEC takes LHV of fuels into account too (Krishna *et al.*, 2016). As a result of retained heat diesel and biofuel had up to 7.4% and 15.4% improvements on BSEC (MohamedMusthafa *et al.*, 2011; Kumar *et al.*, 2013). Literature agreed that BSEC can also be reduced by injector opening pressure, fuel preheating and injection timing adjustment (Reddy *et al.*, 2012; Srikanth *et al.*, 2013; Krishna *et al.*, 2016). The injection timing should be arranged according to cetane number of any fuel (Masera and Hossain, 2019). Srikanth et al. (2013) reported 5.6% and 4.4% lower BSEC for cottonseed biodiesel (lower cetane number compared to diesel was reported for this biodiesel) after advancing the injection by 6° and 3° crank angles. The improvement was attributed to earlier fuel injection which leads to better air/fuel fraction (Srikanth *et al.*, 2013).

2.8.1.3. Brake thermal efficiency

It is known that biofuel operation generally increases the BTE of an engine due to the oxygen content of the fuel (Kumar *et al.*, 2013). Despite this, further improvements were reported with the TBC modification. According to the Figure 2.10, the maximum increases in BTE were 17% for UB to CB case. Moreover, some studies reported 4.9%, 6.3% and 10.7% increased BTE for UD to CB scenario (Hasimuglu *et al.*, 2008; Prasath, Porai and Shabir, 2010; Srikanth *et al.*, 2013). Properly arranged injection timing along with TBC modification could even result in higher improvement in BTE (Masera and Hossain, 2019). Masera and Hossain, (2019) stated that increase in BTE is likely to be achieved with the increasing injector opening pressure. This can be attributed to the improved combustion as a result of upgraded spray characteristics (Srikanth *et al.*, 2013). Preheating of biofuels has also a positive effect on BTE of both coated and uncoated engines (Reddy *et al.*, 2012; Srikanth *et al.*, 2013; Krishna *et al.*, 2016). The increased temperature of the fuel reduces the viscosity of fuel, with which droplet sizes gets smaller during the spray injection (Masera and Hossain, 2019).

The best BTE may be obtained at various injection timings according to fuel properties of biofuel and specifications of engine used. To illustrate, Murthy (2013) reported that 30°bTDC as the optimum injection timing for coated engine under rice brawn oil application. Whereas, Reddy *et al.*, (2012) stated the optimum injection timing as 28.5°bTDC for coated engine under Mohr oil application. This was due to the different ignition delays and combustion durations of the fuels (Masera and Hossain, 2019).

2.8.2. Exhaust gas emissions characteristics

Figure 2.11 illustrate the effects of TBC modification on exhaust gas emissions of biofuels. Like engine performance analyses, exhaust gas emissions were also reviewed under two conditions: (i) uncoated biofuel to coated biofuel (UB to CB), and (i) uncoated diesel to coated biofuel (UD to CB).

(a)

(b)
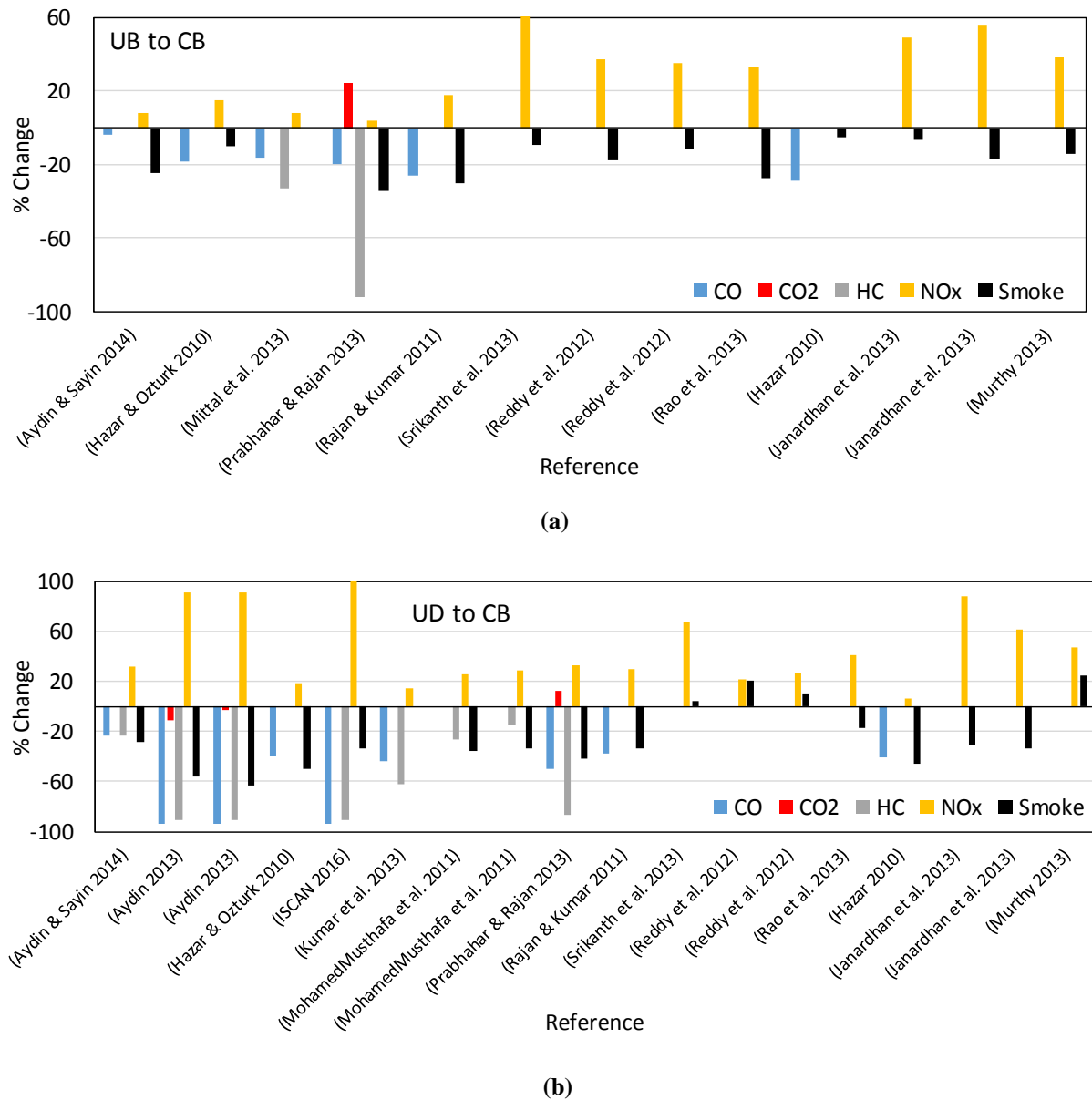
Figure 2.10: Deviations in exhaust emissions and smoke - (a) for UB to CB scenario (b) for UD to CB scenario (Masera and Hossain, 2019).

2.8.2.1. CO Emission

Many studies noted reduced CO emission with biofuel operation on unmodified engines as a result of the oxygen content (Canakci and Gerpen, 2003; Dorado *et al.*, 2003; Hulwan and Joshi, 2011; An *et*

al., 2012; Hossain and Davies, 2012). Figure 2.11 showed even further decrease in CO after TBC modification with all three considered cases. Use of ZrO_2, ZrO_3, TiO_2 and Mo coating materials helped to achieve better CO gas reduction than other types (Masera and Hossain, 2019). Iscan (2016) and Aydin (2013) stated maximum 81.3% and 93.8% reductions in the CO emissions diesel and biofuel after TBC modification, respectively.

2.8.2.2. CO_2 Emission

Significant influences of the engine speed and TBC modification on CO_2 emission was addressed (Aydin, 2013). Aydin (2013) expressed that CO_2 emission of diesel was decreased by about 19.4% at low and medium engine speed, whereas 29.2% increase was noted at the high engine speed. For coated biofuel operation, CO_2 emissions of cottonseed biodiesel-diesel blend (35/65 volume fraction) and sunflower oil biodiesel-diesel blend (35/65 volume fraction) were reduced by 11.1% and 2.8% respectively at low- and medium-range engine speeds; however, at high speed, they were increased by 20% and 23% respectively (Aydin, 2013). It can be concluded that in coated engines, CO_2 emission was decreased at low to medium speed operation; however, at high speed and high load operation, CO_2 emission could increase (Masera and Hossain, 2019a).

2.8.2.3.   HC Emission

As mentioned earlier, HC emissions are caused by incomplete combustion of fuels (Behçet *et al.*, 2015). The reviewed studies in this thesis reported significantly reduced HC emissions with TBC modification Figure 2.11b. Higher lean flammability and reduced distance for quenching due to the thermal barrier caused this (Chan and Khor, 2000; Mittal *et al.*, 2013). Up to 92.5% reduction in HC gas emission was reported when biofuel was used in a coated engine instead of an uncoated engine (Prabhahar and Rajan, 2013).

2.8.2.4. NO_x Emission

Unlike other emissions, for UB to CB case, all studies measured increased NOx emissions between 4% and 62.9% for TBC modification Figure 2.11b. The increased combustion temperature was linked to this increase which resulted in more interaction between nitrogen and oxygen (MohamedMusthafa *et al.*, 2011). The more coated components, the more increase in NOx emission (Masera and Hossain, 2019). The lowest increase in NOx emission was 4% and the only coated component was the piston crown in the specified study (Prabhahar and Rajan, 2013). Injection timing also has an important effect on NOx emission. To illustrate this, Kumar *et al.* (2013) and Alkidas and Cole (1983) reported decreased NOx emission when the injection timing was advanced. Moreover, Buyukkaya et al (2006)

noted 2.44% reduction in NO_x emission with the combined TBC and injection timing modifications. 350 µm $MgZrO_3$ was used in the primary and 150 µm NiCrAl was applies in bond coating layer in the mentioned study. Similarly, Sathiyagnanam et al. (2010) observed 46.5% decrease in NO_x emission for diesel after TBC modification (with Al_2O_3 material). However, they used the fuel additive of di-isopropyl ether in diesel, which may also have contributed to NO_x reduction.

According to Srikanth *et al.* (2013), advancing the injection timing to 3°b TDC result in 7% reduction in NOx emission for cottonseed biodiesel in TBC engine. This was attributed to enhanced air/fuel ratio as a result of lower combustion temperature in the particular study (Srikanth *et al.*, 2013). Similar reductions in NOx emissions under coated engine operation were also provided by other studies reviewed such as; 50 ppm (4.2%) for tobacco seed oil biodiesel operation with advancing the injection timing by 3°b TDC (Rao *et al.*, 2013), 40 ppm (3.9%) for mohr oil operation with advancing the injection timing by 1.5°b TDC (Reddy *et al.*, 2012). Same studies also reported 80 ppm and 150 ppm NOx reductions accounted for the fuel preheating and increased injector pressure modifications. Even though injection pressure, injection timing and preheating can reduce the NOx emission in coated engine, it was higher than the uncoated engine operation for most of the cases (Masera and Hossain, 2019).

2.8.2.5.   *Smoke and particulate matter*

This review noticed further reduced particulate matter and smoke emissions with TBC modification for biofuels Figure 2.11. The maximum reduction of smoke emission was noted by 63% for UD to CB case (Aydin, 2013). Furthermore, around 40% reduced PM emission was measured with TBC modification (Büyükkaya *et al.*, 2006). Moreover, turbocharged engines showed relatively higher PM and smoke reductions due to the increased air (or oxygen) content available for combustion in each cycle. Literature states that that smoke emission shall be further decreased by rearrangement of the injection time, fuel injection pressure (Reddy *et al.*, 2012; Janardhan *et al.*, 2013; Murthy, 2013; Rao *et al.*, 2013; Srikanth *et al.*, 2013). This can be linked to better combustion characteristics of fuel due to improved spray injection. The number of fuel droplets increased as the droplet diameter got smaller and as a result of higher injection pressures (Masera and Hossain, 2019). Another modification is the preheating of fuel, which helps to decrease viscosity of fuel in turn provide improved combustion. In addition, density of the fuel decreases by the preheating application which is directly proportional to the smoke emission (Reddy *et al.*, 2012; Masera and Hossain, 2019). Srikanth *et al.* (2013) reported 70% decrease in smoke intensity for cottonseed biodiesel with TBC modification combined with all three mentioned modifications.

2.9. NOx emission mitigation technologies

Various solutions to lower NOx emissions are reviewed in this section. Modern NOx reduction techniques were categorised under three sections: fuel treatment, engine adjustment and aftertreatment. Firstly, fuel treatment refers to fuel chemistry modification such as emulsifying, blending and doping fuel additives. In this technique, the main aim is to reduce the combustion temperature of fuel, hence lower NOx emissions can be achieved. As a second method, the engine can be modified for the needs of selected biofuel properties in a way that lower NOx emissions produced. In the third approach, aftertreatment systems are placed on the exhaust pipe. Various aftertreatment techniques exist in the literature like Diesel Particulate Filter (DPF), Selective Catalytic Reduction (SCR), and Diesel Oxidation Catalysts (DOC). Figure 2.12 summarises the mentioned three methods in NOx emission combating and their specific examples.
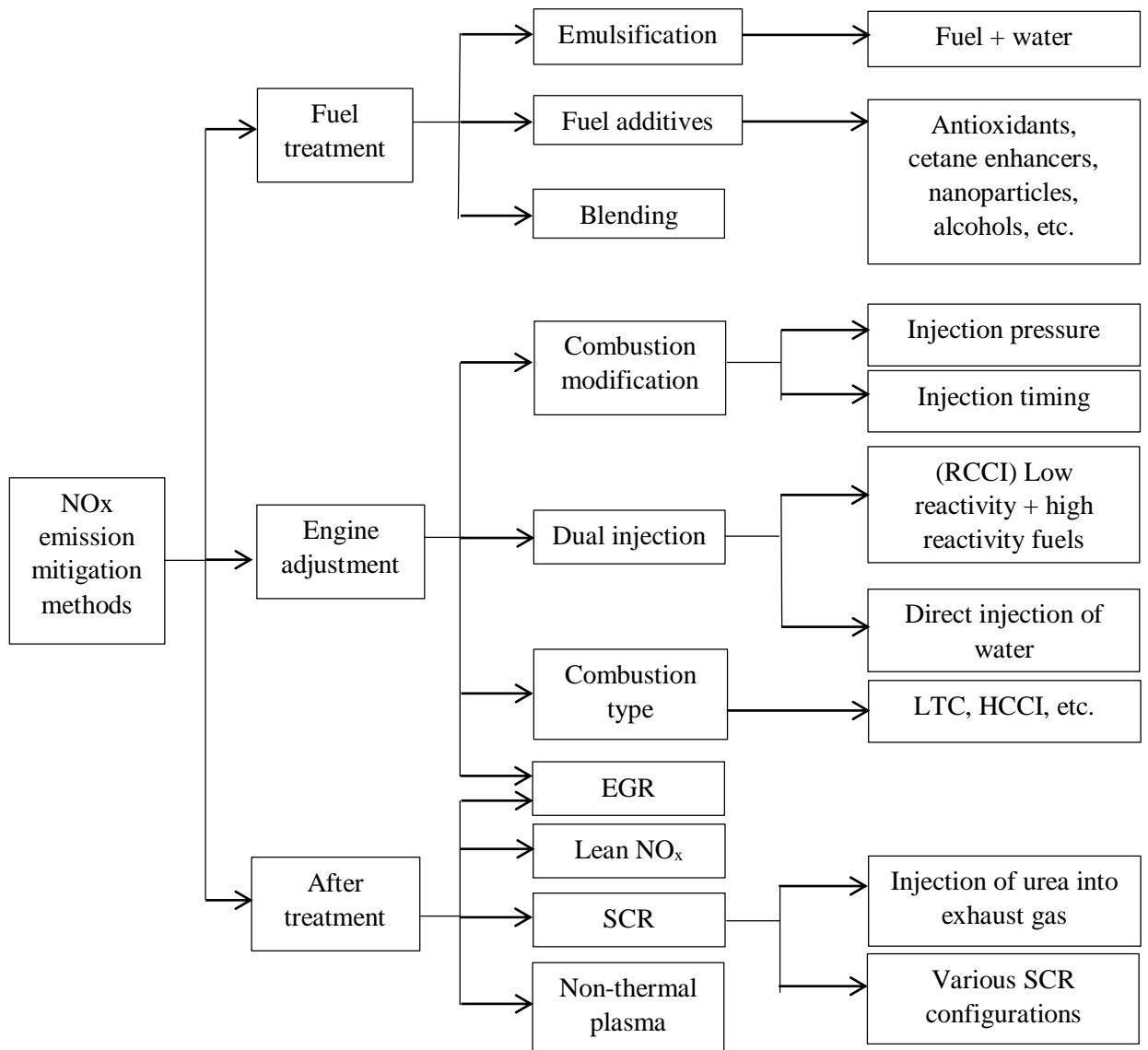
Figure 2.11: NOx mitigation techniques are categorised under three groups which were (i) Fuel treatment, includes any changes on the fuel composition, (ii) Engine modifications and (iii) Exhaust aftertreatment technologies.

2.9.1. Fuel treatment to reduce NOx emission

This section covers physical or chemical changes made to the fuel to reduce NOx emission. The three popular fuel treatment techniques are emulsification, diesel blending and usage of fuel additives (Figure 2.12). This section also explains the emulsification method and investigates some real case studies related to all three techniques.

2.9.1.1. *Emulsification of biodiesels for lower NOx emission*

Emulsification refers to mixing multiple fluids which are immiscible under normal conditions, like biodiesel and water. By using this technique, non-polar and polar fluids can be mixed thermodynamically stable (Debnath *et al.*, 2015). The general aim in the emulsification of biofuels with water is to improve combustion and reduce harmful tile pipe gases like NOx. Having tinier fuel droplets increases the total surface area. In other words, increased contact between the oxygen and fuel yields more rapid and upgraded combustion in the engine (Annamalai *et al.*, 2016). Water, having a lower boiling temperature, vaporises in the oil which in turn disintegrates the biodiesel cell and results in smaller fuel droplets (Subramanian, 2011). Furthermore, additional pressure which occurs due to the spontaneous water explosion contributes to the total force acting on the piston crown and positively affects the engine torque (Abu-Zaid, 2004). Figure 2.13 represents the microexplosion process schematically.

Aston University

Illustration removed for copyright restrictions

Figure 2.12: Schematic of micro explosion process (Basha and Anand, 2011).

Although emulsification results in favourable performance of the engine, it is not a straightforward process to mix water with biodiesel. By nature, some liquids contain uneven charge distribution in their molecules – these are called polar liquids. For example, in the water molecule, negative charge is biased towards the oxygen atom. This uneven distribution of charge results in an unbalance of repulsive and attractive forces (Debnath *et al.*, 2015). In contrast to polar liquids, distributions of charges on each molecule are even in nonpolar liquids such as vegetable oils and biodiesel. As a result, additives have to be used to blend nonpolar and polar liquids. These agents are called surfactants or surface acting agents. The presence of both polar and nonpolar group of molecules makes the surfactants capable of integrating two immiscible liquids. In addition, as surfactants make water suspend in the fuel, water molecules do not undergo direct contact with the metallic surfaces of the engine (Ghojel *et al.*, 2006). However, although, all surfactants have an affinity to both polar and nonpolar agents, their affinity levels to each agent differ. Surfactants can be divided into two types in terms of their affinity namely, hydrophilic and lipophilic surfactants (Krutof and Hawboldt, 2016). The former have more affinity towards polar liquids like water; the latter more affinity towards

lipophilic surfactants have more affinity to oil type liquids i.e. biodiesel (methyl esters). Hydrophilic-lipophilic balance (HLB) number was introduced in the literature as Equation 2.3 (Debnath *et al.*, 2015).

$$HLB = \frac{20\ M_h}{(M_h + M_l)} \tag{2.3}$$

Where M_l and M_h stands for molecular weight of lipophilic and hydrophilic molecule portions. HLB value of a surfactant can be maximum 20 which represents surfactant is made up of hydrophilic constituents only. Whereas, minimum HLB value of 0 reveals a surfactant which comprises of totally lipophilic molecules. For biodiesel emulsification (water-in-oil) HLB range between 4 and 6 suggested by Debnath et al. (2015).

Table 2.7 examines some emulsification studies from the literature and their maximum NOx reductions. Qi et al (2010) studied the ethanol-soybean biodiesel-water micro emulsion in a one cylinder DI engine. 1 ml of water was emulsified with 80 ml biodiesel, 20 ml ethanol and 4 grams of Span 80 surfactant. They reported that emulsified fuel had 12.5% lower NOx emission than neat biodiesel. However, this significant reduction was not solely from emulsification, but the contribution of ethanol should not be ignored. In another study, Basha and Anand (2011) emulsified 83% jatropha biodiesel with 15% of the water in the presence of 2% of Span 80 and Tween 80 surfactants. The experiments were carried out in a single-cylinder DI diesel engine. They reported up to 23% reduction on NOx emission with emulsified biodiesel compared to neat biodiesel. This study showed that increasing the water fraction in emulsification can result in more reduction in NOx emission. This was confirmed by Annamalai et al (2016). In their study, the neat waste cooking oil was emulsified with diesel and different percentages of water i.e. 10%, 20% and 30%. They reported 35%, 50% and 53% reductions of NOx emissions compared to diesel-WCO blend. Note that these reductions proved that NOx did not decrease linearly; hence an optimum water fraction must be determined.

Table 2.7: Biodiesel emulsification case studies from the literature and provided NOx reductions.

Reference	Biodiesel	Diesel	Additive	Water	Surfactant	Engine type	Maximum reduction in NOx	Compared to
(Qi *et al.*, 2010)	Soybean biodiesel (80 ml)	None	Ethanol (20 ml)	(1 ml)	Span 80 (4 g)	1CY, DI	12.5%	Neat biodiesel
(Basha and Anand, 2011)	Jatropha biodiesel (83%)	None	None	(15%)	Span 80 and Tween 80 (2%)	1CY, DI	23%	Neat biodiesel
(Basha and Anand, 2011)	Jatropha biodiesel (83%)	None	Alumina nanoparticle (100 ppm)	(15%)	Span 80 and Tween 80 (2%)	1CY, DI	27.7%	Neat biodiesel
(Annamalai *et al.*, 2016)	WCO (not given)	Diesel (not given)	None	(10%) (20%) (30%)	Type and amount not given	DI	45% 57.7% 60.6%	Diesel Diesel Diesel
(Silambarasan *et al.*, 2015)	Annona biodiesel (20%)	Diesel (80%)	None	(5%) (7.5%)	Span 80 and Tween 80 (2%)	Not given	2.6% 5.2%	Diesel Diesel
(Rao and Anand, 2014)	Jatropha biodiesel (88%)	None	None	(10%)	Span 80 and Tween 80 (2%)	1CY, DI	30.3%	Neat biodiesel
(Rao and Anand, 2014)	Pongamia biodiesel (88%)	None	None	(10%)	Span 80 and Tween 80 (2%)	1CY, DI	35.4%	Neat biodiesel

1CY: 1 Cylinder, DI: Direct Injection, WCO: Waste cooking oil

2.9.1.2.   *Fuel additives for lower NOx emission*

The number of studies investigating the use of antioxidants for NOx reduction has increased especially in the past few decades Table 2.8. Rizwanul Fattah et al (2014) studied the 2(3)-tert-butyl-4-methoxyphenol (BHA) and 2,6-ditert-butyl-4-methylphenol (BHT) synthetic antioxidants as biodiesel additive to reduce NOx emission. The NOx emission of biodiesel (20%)-diesel (80%) blend lowered by 7.78% and 3.84% with the 2000 ppm BHA and BHT additives. However, some negative aspects of the antioxidant doped fuels were also reported. For example, 8%-9% increase in CO, 17% and 27% increases in HC, and 16% and 19% increase in smoke emissions were reported for BHA and BHT doped biofuels, respectively. Similarly, Adam et al (2018) studied the antioxidants for NOx reduction which were namely, N,N′-diphenyl-1,4-phenylenediamine (DPPD), N-phenyl-1,4-phenylenediamine (NPPD), 2(3)-tert-Butyl-4-methoxyphenol (BHA), and 2-tert-butylbenzene-1,4-diol (TBHQ). The four antioxidants were added into diesel-palm oil biodiesel blends (50/50% by volume) at different

fractions (Table 2.8). They report a reduction in NOx emission by 9% compared to the base biofuel without additives. However, similar to the previous case study, they also reported approximately, 25% increase in CO, a 42% increase in HC and a 32% increase in smoke opacity. The reason for CO increase can be attributed to antioxidants inherent property of hindering the CO to CO_2 conversion (Palash *et al.*, 2014). The increase in HC is due to the reduced hydroxyl radicals (OH) which helps to form H_2O by breaking down the HC molecules (Varatharajan and Cheralathan, 2013). Finally, the reduced oxygen content and increased aromatic compounds with the addition of antioxidants can explain the increase in smoke opacity (Rizwanul Fattah *et al.*, 2014).

Table 2.8: Influence of biodiesel fuel additives on NOx emissions and reported side effects on other exhaust gases.

Reference	Biodiesel	Diesel	Additive	Engine type	Reduction in NOx	Increase in
(Rizwanul Fattah *et al.*, 2014)	Coconut biodiesel (20%)	(80%)	2(3)-tert-butyl-4-methoxyphenol (BHA) (2000 ppm)	4CY, IDI	7.78%	8% CO 17% HC 16% smoke
(Rizwanul Fattah *et al.*, 2014)	Coconut biodiesel (20%)	(80%)	2,6-ditert-butyl-4-methylphenol (BHT) (2000 ppm)	4CY, IDI	3.84%	9% CO 27% HC 19% smoke
(Adam *et al.*, 2018)	Palm oil biodiesel (50%)	(50%)	N,N′-diphenyl-1,4-phenylenediamine (DPPD) (2000 ppm)	4CY, IDI	9%	25% CO 33% HC 20% smoke
(Adam *et al.*, 2018)	Palm oil biodiesel (50%)	(50%)	N-phenyl-1,4-phenylenediamine (NPPD) (2000 ppm)	4CY, IDI	9%	8% CO 42% HC 24% smoke
(Adam *et al.*, 2018)	Palm oil biodiesel (50%)	(50%)	2(3)-tert-Butyl-4-methoxyphenol (BHA) (2000 ppm)	4CY, IDI	9%	25% CO 50% HC 33% smoke
(Adam *et al.*, 2018)	Palm oil biodiesel (50%)	(50%)	2-tert-butylbenzene-1,4-diol (TBHQ) (2000 ppm)	4CY, IDI	7.5%	33% CO 42% HC 38% smoke

4CY:4 cylinder, IDI: Indirect injection

2.9.2. Engine modifications to reduce NOx emission

This section involves some popular engine modifications on CI engines for the purpose of NOx reduction. The changes on the fuel injection parameters such as (i) injection pressure and timing, (ii) advanced combustion techniques like LTC, HCCI, (iii) dual fuel injection strategies like RCCI, and (iv) water injection methods were investigated. The maximum NOx reductions (typically at full load condition) for each technique was reviewed from the literature along with any draw backs on other exhaust gases such as an increase in CO, HC or smoke opacity.

2.9.2.1.   Injection timing and injection pressure arrangement for lower NOx emission

Biodiesel can be used in diesel engines without any modification but its performance, combustion characteristics and exhaust gas emissions can be upgraded by injection timing and pressure adjustment. As biodiesel has different fuel properties to diesel, the fuel injection system may be modified in accordance with the needs of selected biodiesel. To illustrate, injection timing can be reset with respect to cetane number, and injection pressure can be changed with respect to viscosity and density of the biodiesel. The effects of injection timing and injection pressure were also studied earlier in Section 2.8.

Agarwal et al. (2015) studied the influence of different injection pressures as 300, 500, 750 and 1000 bar and injection timings between -24° and 4°CA on common rail direct injection CI engine fuelled with karanja biodiesel-diesel (50/50 by volume) blend. They reported decreased NOx emissions with respect to increased pressure. It was also addressed that NOx emissions were reduced with the retarded injection timing at 300 and 500 bar injection pressures. On the other hand, slightly increasing NOx emissions were reported with the retarded injection timing at 750 and 1000 bar injection pressures (Agarwal *et al.*, 2015). The lowest NOx emissions were achieved at 300 and 500 bar injection pressures at -9° and -3°CA injection timings. However, HC and CO had increased by approximately 69% and 27% at the mentioned injection operation points.

Similarly, Gnanasekaran et al. (2016) studied the effect of injection timing on NOx emission of fish oil biodiesel. They reported that NOx emission was reduced by approximately 2.1% by advancing the injection timing from 24°bTDC to 27°bTDC. However, CO was increased around 20% whilst smoke and HC was not changed. Deep *et al.* (2017) also investigated the influence of injection pressure and injection timing on a single-cylinder diesel engine fuelled with castor biodiesel-diesel (20/80 by volume). They reported around 16% and 32% reductions in NOx emission by retarding the injection timing from 25° to 23°bTDC and 23° to 21°bTDC, respectively. Similarly, reducing injection pressure from 300 to 250 bar and from 250 to 200 bar resulted in 13% and 16% reductions in NOx emission at

300 bar. However, CO, HC and smoke opacity were negatively affected by reducing injection pressure and retarding injection timing.

2.9.2.2.   *HCCI combustion for NOx reduction*

Various advanced combustion studies targeted low NOx emission by low-temperature combustion (LCT) (Lawler *et al.*, 2017). Homogeneous Charge Compression Ignition (HCCI) can be the most popular example of advanced combustion techniques which reduces NOx and provides high engine performance (Imtenan *et al.*, 2014; Yousefi, Gharehghani and Birouk, 2015). The main principle is to avoid high combustion temperature due to flame propagation like in the cases of SI and CI engines (Imtenan *et al.*, 2014). In HCCI combustion, fuel and air are mixed homogenously through the combustion chamber and local burning of fuel droplets is achieved simultaneously to avoid flame propagation (Figure 2.14). However, Komninos (2009) addressed about 9% increased HC emission with HCCI combustion. The difficulty of low combustion control and high mechanical stress on the combustion chamber were also noted as further disadvantages of HCCI technique (Benajes *et al.*, 2017). To solve these problems, Bessonette et al. (2007) conducted a test on a caterpillar 3401E single-cylinder oil test engine under HCCI conditions. They reported that some drawbacks of HCCI technique can be solved by arranging engine operating conditions i.e. using higher CN fuels at low engine loads and low CN fuels at higher loads. Variable valve timing (Mahrous *et al.*, 2009), optimisation of valve lift (Cinar *et al.*, 2015), residual gas trapping (Xie *et al.*, 2014) were the other studies to improve HCCI combustion operation. Although those studies reduce the side effects of HCCI applications, the operating range of HCCI is still not wide enough (Benajes *et al.*, 2017).
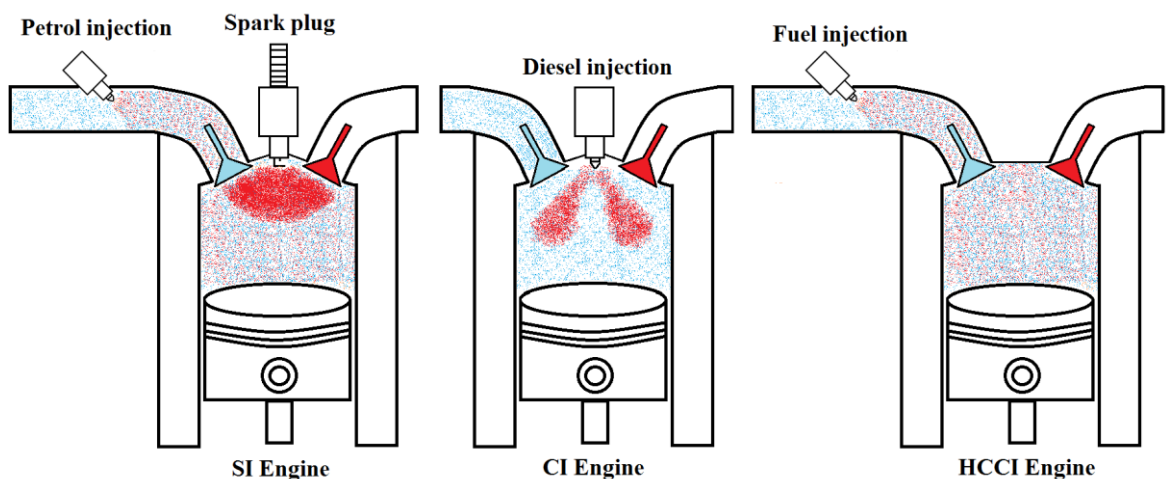
Figure 2.13: Comparison schematic of combustion initiation on spark ignition, compression ignition and Homogeneous Charge Compression Ignition engines.

2.9.2.3. *RCCI combustion for NOx reduction*

The dual fuel injection process which is also known as Reactivity Controlled Compression Ignition (RCCI) is another popular advance combustion technique (Salahi *et al.*, 2017). In this type of combustion high reactivity (thus high cetane number) fuels like biodiesel is injected into combustion chamber, whereas low reactivity fuels with high octane number like natural gas, alcohols, gasoline etc. are injected typically from intake manifold at early combustion stroke (Imtenan *et al.*, 2014; Gharehghani *et al.*, 2015; Zhou *et al.*, 2015) (Figure 2.15). The combustion starts with the fuel having high reactivity at the top of the combustion chamber after that it expands towards the bottom of the combustion chamber. By this method, the overall combustion duration increases due to the high reactivity differences of two various fuels, thus the cylinder temperature reduces which in turn reduces the NOx formation (Poorghasemi *et al.*, 2017).
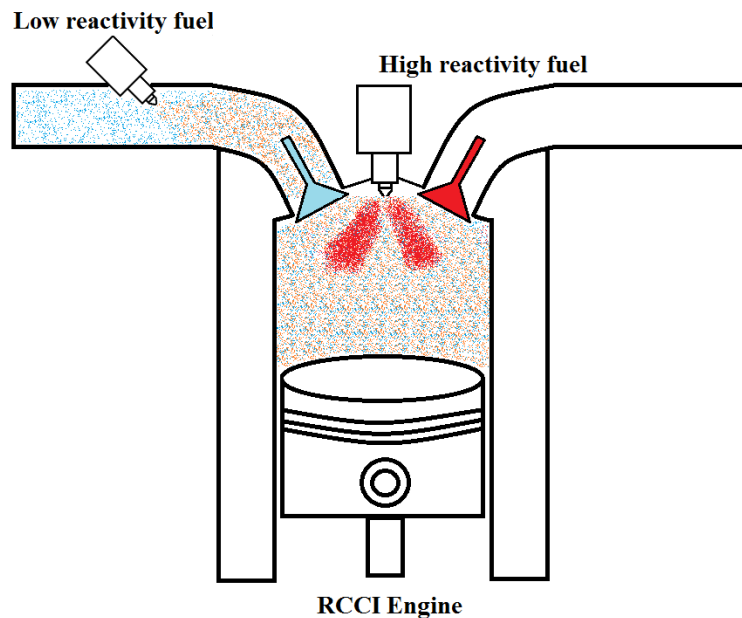
Figure 2.14: The schematic of RCCI engine operation. Low reactivity fuel is injected from the inlet manifold and high reactivity fuel is injected from the injector.

Salahi *et al.* (2017) studied RCCI combustion in an IDI diesel engine with natural gas and diesel. They stated that the fraction of highly reactive fuel should be kept relatively low due to the pre-chamber. This shows that engines with direct injection are more applicable to the RCCI application. Moreover, the compression ratio of the diesel engine should be reduced, as a low reactivity fuel will be used. In this regard, Benajes et al. (2017) reduced the compression ratio of a 4-cylinder Volvo/d5k240 CI engine from 17.5:1 to 15.3:1 by enlarging the piston bowls. Mahla et al. (2018) studied the duel fuel injection Compressed Natural Gas (CNG) and 20% jatropha biodiesel blended with diesel in a single

cylinder DI CI engine. They reported a 13% increase in NOx emission with CNG-biodiesel dual injection relative to simple diesel injection. However, with the addition of EGR system at 15% valve opening, the NOx emission was dropped by 25% relative to neat diesel operation at the full load. Similarly, Gharehghani et al. (2015) tested the biodiesel-natural gas fuels on a single-cylinder variable compression ratio engine. Firstly, they tested WCO biodiesel as a single fuel which had around 15% higher NOx emission than diesel. Then, biodiesel and natural gas fuels were experimented in RCCI mode at 17:1 compression ratio. They reported by 85% and 87% reduced NOx emissions with RCCI mode relative to neat diesel and neat biodiesel operations. However, for the RCCI combustion, the same study reported approximately 50% higher CO emission and 8 times increased HC emissions compared to neat biodiesel operation. The natural gas might be the reason behind the increased CO and HC emissions. This problem can be minimised by using biofuels as a low reactivity fuel too like bioethanol or syngas. However, the reviewed studies prove that even though the RCCI method can reduce the NOx emission, other emissions can be increased. Moreover, a complex fuel supply system along with a smart operational algorithm should be developed for the RCCI method.

2.9.2.4. Water injection for NOx reduction

There is a significant amounts of studies on the effect of water injection into combustion chamber both on spark ignition and compression ignition engines (Tauzia *et al.*, 2010; Subramanian, 2011; Adnan *et al.*, 2012; Tesfa *et al.*, 2012; Chintala and Subramanian, 2014; Kettner *et al.*, 2016; Mingrui *et al.*, 2017). The main advantage of this technique over the catalytic converter and EGR is the capability of NOx reduction at any engine load without increasing the PM emissions (Tauzia *et al.*, 2010). Like in the case of emulsification, the injected water reduces the combustion temperature by absorbing the heat during the combustion (Tesfa *et al.*, 2012). Consequently, NOx emission reduces with diminished peak flame temperature. The water can be injected from different places. To illustrate, Stanglmaier et al. (2008) developed a multi-functional injection system which can inject both fuel and water through the same injector. For the diesel (70%) + water (30%) operation, they reported a reduction in NOx emission by approximately 15% relative to neat diesel application. However, around 50% and 65% higher CO and HC were observed. The second and most common water injection place is the intake manifold. This may be because of the easier modification of the water injector on the intake manifold rather than on the combustion chamber. Subramanian (2011) injected 40% (by mass) of the consumed diesel through the intake manifold into a one-cylinder diesel engine. The study reported 41% NOx reduction, whereas CO, HC and smoke emissions were increased by 6.7%, 33% and 26% respectively. Similarly, Tesfa et al. (2012) were successful in reducing NOx emission of neat rapeseed biodiesel by 50% by injecting water through the intake manifold at the flow rate of 3 kg/h. This study also reported a 40% increase in CO emission. Adnan et al. (2012) also used water injection through the intake manifold. They reported 100% improvement in NOx emission when the water was injected at 2 bar

pressure. However, SO_2 emission was 17% higher than without water application. Similar to previously reviewed studies, Chintala and Subramanian (2014) also observed 37% reduction in NOx emission by the 270 g/kWh water injection. However, the drawbacks in CO, HC and smoke emissions were also reported as they increased by 100%, 54% and 55%, respectively. Table 2.9 summarises the case studies according to their operation conditions, maximum NOx reductions and main drawbacks on other emissions. To sum up, direct water injection found to be a good way of reducing NOx emission. However, it was noticed that the other exhaust gases like CO, HC, SO_2 and smoke emissions were negatively affected by this technique. This can be due to the reduced combustion temperature. Another disadvantage of the system is the direct contact between the water and the metallic surfaces such as manifold and combustion chamber which can be rusted and damaged.

Table 2.9: Summary of the direct water injection studies with their details, the maximum NOx reduction at full load and negative aspects of other exhaust gases.

Reference	Fuel	Water injection	Engine type	Reduction in NOx	Increase in
(Subramanian, 2011)	Diesel	40% of diesel by mass	1CY, water injected through intake manifold	41%	6.7% CO 33% HC 26% smoke
(Tesfa et al., 2012)	Rapeseed biodiesel (100%)	3 kg/h	4CY, DI, turbocharged, water injected through intake manifold	50%	40 % CO
(Adnan et al., 2012)	Diesel and Hydrogen (5 l/m)	2 bar	DI, naturally aspired, duel fuel, water injected through intake manifold	100%	17% SO_2
(Chintala and Subramanian, 2014)	Pilot fuel: Diesel (80%) + Biodiesel (20%) Main fuel: Hydrogen (100%)	270 g/kWh	1CY, naturally aspired, water injected through intake manifold	37%	100% CO 54% HC 55% smoke
(Stanglmaier et al., 2008)	Diesel (70% by volume)	(30%)	Volvo D-12, DI, water injected directly into the combustion chamber	15%	50% CO 65% HC

2.9.2.5.   *Selective Catalytic Reduction (SCR)*

Selective Catalytic Reduction (SCR) is considered as the most efficient after-treatment technology in terms of NOx mitigation (Guan et al., 2014; Zhang et al., 2018). It was first commercialised for heavy duty CI engines in 2005 (Cho et al., 2017). In this technique, water-urea solution is injected into exhaust gases. When the solution reacts with the flowing hot gases, the solution decomposes to

ammonia and reacts with the NOx gases to N_2 at the catalyst (Zhang *et al.*, 2018). The system used a honeycomb monolith catalyst made of V_2O_5-WO_3/TiO_2. After 2010, the material of the catalyst mainly shifted to Fe-promoted zeolite due to its better durability, reliability and improved activation with NO_2 (Cho *et al.*, 2017). The following equation 2.4 shows the decomposition of urea [$CO(NH_2)_2$] into ammonia [NH_3], equation 2.5 shows how ammonia [NH_3] converts nitrogen oxide [NO] and oxygen [O_2] into nitrogen [N_2] and water [H_2O], and equation 2.6 shows the same conversion for both nitrogen oxide [NO] and nitrogen dioxide [NO_2] (Haridass and Jayaraman, 2018).

$$(NH_2)_2CO + H_2O \rightarrow 2NH_3 + CO_2 \qquad (2.4)$$
$$4NH_3 + 4NO + O_2 \rightarrow 4N_2 + 6H_2O \qquad (2.5)$$
$$4NH_3 + 2NO + 2NO_2 \rightarrow 4N_2 + 6H_2O \qquad (2.6)$$

Figure 2.16 shows a schematic diagram and Figure 2.17 shows a picture of a typical SCR system. Cheruiyot et al (2017) stated that the SCR system operates more efficiently at higher engine loads. This is because of the higher NOx formation at high engine loads due to increased combustion temperatures.

Figure 2.15: Schematic diagram of SCR (Haridass and Jayaraman, 2018).

Figure 2.16: SCR system (Haridass and Jayaraman, 2018).

Scientists have been testing the efficiency of the SCR method under various conditions. For example, Tadano et al (2014) reported 68% reduced NOx emission for biodiesel with the application of SCR. Haridass and Jayaraman (2018) tested the mahua biodiesel in a multi-cylinder diesel engine with and without an SCR system. They reported that the SCR system reduced the NOx emission by approximately 8.7%. Sachuthananthan et al (2018) studied the effects of Butylated hydroxytoluene antioxidant and SCR system on a single cylinder diesel engine fuelled with neem biodiesel. They reported that neem biodiesel had around 11% higher NOx emission than the diesel without antioxidant

and SCR applications. When 100 mg of antioxidant added into 1 kg of neem biodiesel, the NOx emission dropped by 12.5% and 22.2% compared to diesel and neat biodiesel. The NOx emission was further reduced by 82% via the application of SCR (Sachuthananthan *et al.*, 2018). In another study, Zhang et al (2018) investigated the durability of a 6-cylinder turbocharged diesel engine fuelled with B20 (produced from WCO) with common rail fuel injection system and aftertreatment components of DOC and SCR. Their results indicated a 25% increase in NOx emission after 500 hours operation of the engine.

The main disadvantage of the SCR system is the N_2O generation. N_2O is a harmful greenhouse gas which is not a typical product of the fuel combustion (Cho *et al.*, 2017). Its global warming potential was reported as 298 times greater than CO_2 (Cho *et al.*, 2017). Moreover, it is a very stable gas in the atmosphere with approximately 114 years of lifetime (Lambert *et al.*, 2014). Grossale et al (2008) defined the N_2O formation from NO_2 emission in equation 2.7, 2.8 and 2.9. They reported that when nitrogen dioxide (NO_2) and ammonia (NH_3) reacts, they form ammonium nitrate (NH_4NO_3) equation 2.7 which then decomposes to nitrous oxide (N_2O) and water (H_2O) equation 2.8. The sum of the reactions 2.7 and 2.8 gives equation 2.9 which describes the N_2O formation from NO_2.

$$2NH_3 + 2NO_2 \rightarrow NH_4NO_3 + N_2 + H_2O \qquad (2.7)$$
$$NH_4NO_3 \rightarrow N_2O + 2H_2O \qquad (2.8)$$
$$2NH_3 + 2NO_2 \rightarrow N_2O + N_2 + 3H_2O \qquad (2.9)$$
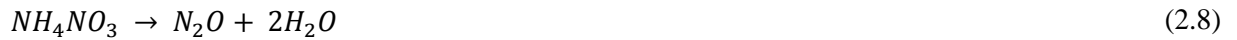
Cho et al (2017) also agreed with the equation 2.9. Moreover, Djerad et al (2006) addressed other possible N_2O formation reactions for NO emission when reacts with O_2 equations 2.10 and 2.11.

$$4NH_3 + 4NO + 3O_2 \rightarrow 4N_2O + 6H_2O \qquad (2.10)$$
$$2NH_3 + 2O_2 \rightarrow N_2O + 3H_2O \qquad (2.11)$$

To sum up, although SCR systems can reduce the NOx emission very effectively (up to 82%), it produces another harmful greenhouse gas, N_2O, which is not normally produced through fuel combustion (Cho *et al.*, 2017). This fact can be considered as the main drawback of the SCR application.

2.10.   Review summary and gaps in the literature

In the chapter, literature was reviewed in detail in terms of biodiesel feedstock, transesterification details, biodiesel quality, engine tests, engine modifications and NOx reduction technologies. After understanding the already published studies and careful analysis of the literature, the following knowledge gaps were found:

- Fuel properties of biodiesels produced from waste cooking oils (including inedible vegetable oils) and animal fats were very different (i.e. Tables 2.2 and 2.3). For example, waste cooking oil and inedible vegetable oil biodiesels were superior to animal fat biodiesels mainly in terms of viscosity and acid value. On the other hand, animal fat biodiesels were better than waste cooking oil and inedible vegetable oil biodiesels in terms of higher heating value, cetane number and iodine value (Table 2.10). From the literature review it was discovered that fuel properties could be optimised by blending these opposite groups of biodiesels. Hence, it was decided to investigate the biodiesel-biodiesel blends for improved fuel properties and better combustion in the internal combustion engines.

Table 2.10: Pros and cons of the selected biodiesels relative to diesel and BS EN 14214 standard.

Biodiesel	Viscosity	HHV	Iodine value	transesterification difficulty	Cetane number
Waste cooking oil	Good	Normal	Bad	Good	Normal
Sheep fat	Bad	Good	Good	Bad	Good
Cottonseed oil	Good	Normal	Normal	Good	Normal
Chicken fat	Bad	Good	Good	Bad	Good

- Literature review showed that biodiesels derived from vegetable oils were blended with each other before for various purposes like cheap production, enhance fuel properties and ease transesterification (Usta *et al.*, 2005; Sanjid *et al.*, 2016; Sharma and Ganesh, 2019). However, biodiesels derived from waste cooking oil and vegetable oils were likely to have similar fuel properties as they mainly compose of unsaturated FAMEs (Table 2.2). On the other hand, animal fats, which are composed of saturated FAMEs, are also important feedstock used for biodiesel production in the world and their blends with unsaturated biodiesels could provide promising fuel properties and engine results. To the best of author's knowledge, hardly any study could be found in the literature blending waste cooking oil biodiesel or inedible

vegetable oil biodiesels with animal fat biodiesel to test diesel engine performance, combustion and emissions.

- The effect of degree of unsaturation was investigated in the literature up to some extent (Schönborn, 2009; Benjumea *et al.*, 2011; Balakrishnan *et al.*, 2016). The previous studies tested different source biodiesels produced from soy, canola, rapeseed, palm, linseed and tallow to understand the effect of degree of unsaturation. However, effect of other fuel properties such as viscosity, density, heating value, volatility, carbon, hydrogen and oxygen contents etc. are also influences the results. It is believed that this parameter can be analysed in more detail when the effects of fuel properties other than degree of unsaturation are minimised. In this regard, two biodiesels having different degree of unsaturation values can be blended with each other at different volume fractions. Then, a range of biomixtures having various degree of unsaturation can be compared to each other. Highly saturated biodiesel and relatively unsaturated biodiesel blends at volume fractions such as 60/40, 50/50 and 30/70 would contribute to understanding of the effect of degree of unsaturation on diesel engine performance, combustion characteristics and exhaust emissions.

- Literature showed that biodiesels have comparable and even higher NOx emissions compared to diesel. Researchers have investigated various techniques to reduce the NOx emission i.e. fuel treatment, engine modifications and after-treatment. Among these options, fuel additives such as alcohols and antioxidants are found effective way of NOx reduction but their side effects were also observed on other emissions like CO, HC and smoke opacity (Figure 2.12). Hardly any study could be found in the literature investigating 2-Butoxyethanol as a fuel additive. As 2-Butoxyethanol is an ether compound with an alcohol branch, it has promising properties for biodiesel blending. It could be doped into biodiesel and/or biodiesel-biodiesel mixtures to test fuel properties, engine performance, combustion characteristics and exhaust emissions.

- According to literature, after-treatment system such as SCR is also promising way of NOx mitigation, as urea injection could led up to 82% NOx reduction efficiency (Sachuthananthan *et al.*, 2018). However, the use of catalytic may cause problems like high back pressure, erosion, clogging, expensive cost and limited life time (Javed *et al.*, 2007). After-treatment equipment without any catalytic could be designed in order to reduce the NOx emission and to avoid catalytic related problems. The after-treatment system could compensate (to some extend) the absence of the catalytic by upgrading the turbulence and residence time of injected fluid and exhaust gases.

Chapter 3

3. METHODOLOGY

3.1. Introduction

This chapter introduced techniques and methods followed during the feedstock analyse and biodiesel production. Fuel properties were introduced in accordance with BS EN 14214 standard. Moreover, equipment to conduct this research, and data analysis were described in this section.

3.2. Feedstock

The four main feedstock used in this study were waste cooking oil (WCO), waste sheep fat/tallow, inedible cottonseed oil and waste chicken fat (Figure 3.1). WCO was collected from the *Matayb* restaurant located in Birmingham UK. Both waste animal fats, which were sheep fat and chicken skin, were obtained from the *Euroasia* butcher located in Loughborough UK. Inedible cottonseed oil was purchased from commercial suppliers. Initially, feedstock collected and pre-treatment processes applied according to the need of feedstock. For example, WCO was filtered through a 5 µm sock filter to remove any remaining cooking particles. Waste sheep fat and waste chicken skin were both rendered i.e. crashed into small parts and owned at approximately 150 °C for 35-45 minutes. The released tallow/oil was used in the next stage to measure out Free Fatty Acid (FFA) content by titration.

Figure 3.1: The four feedstock used in this research, (from left to right) rendered chicken fat, waste cooking oil, cottonseed oil and rendered sheep fat.

3.2.1. Titration of feedstock

The oils having FFA value less than 2% are allowed to proceed with the transesterification process (Ramadhas *et al.,* 2005). If it is higher than 2%, the esterification process was recommended to reduce FFA value before transesterification (Ramadhas *et al.,* 2005). Titration was carried out at Aston University mechanical engineering laboratory by prepared titration solution and oil sample as follows;

- Preparation of titration solution: 1 gram of catalyst (KOH) dissolved into 1 litre of distilled water.

- Preparation of oil sample: 10 ml of isopropyl alcohol, 1 ml of oil sample and few drops of pH indicator (phenolphthalein) added and mixed in a testing vial.

- Titration: Titration solution was added into testing vail until the colour turns into pink. Then, the amount of titration solution spent was recorded.

The catalyst required for the transesterification, acid value and FFA value of the each feedstock were calculated through the titration results. To determine catalyst amount to be used in transesterification, the titration result was divided by the purity of the KOH used and added on the base value 7 g/litre (Masera and Hossain, 2017). Acid value and FFA value were calculated by using equations 2.1 and 2.2.

3.3. Biodiesel production procedure

Figure 3.2 demonstrates the flow diagram of feedstock conversion into biodiesel. Biodiesels were produced at the Aston University mechanical engineering and chemical engineering laboratories.
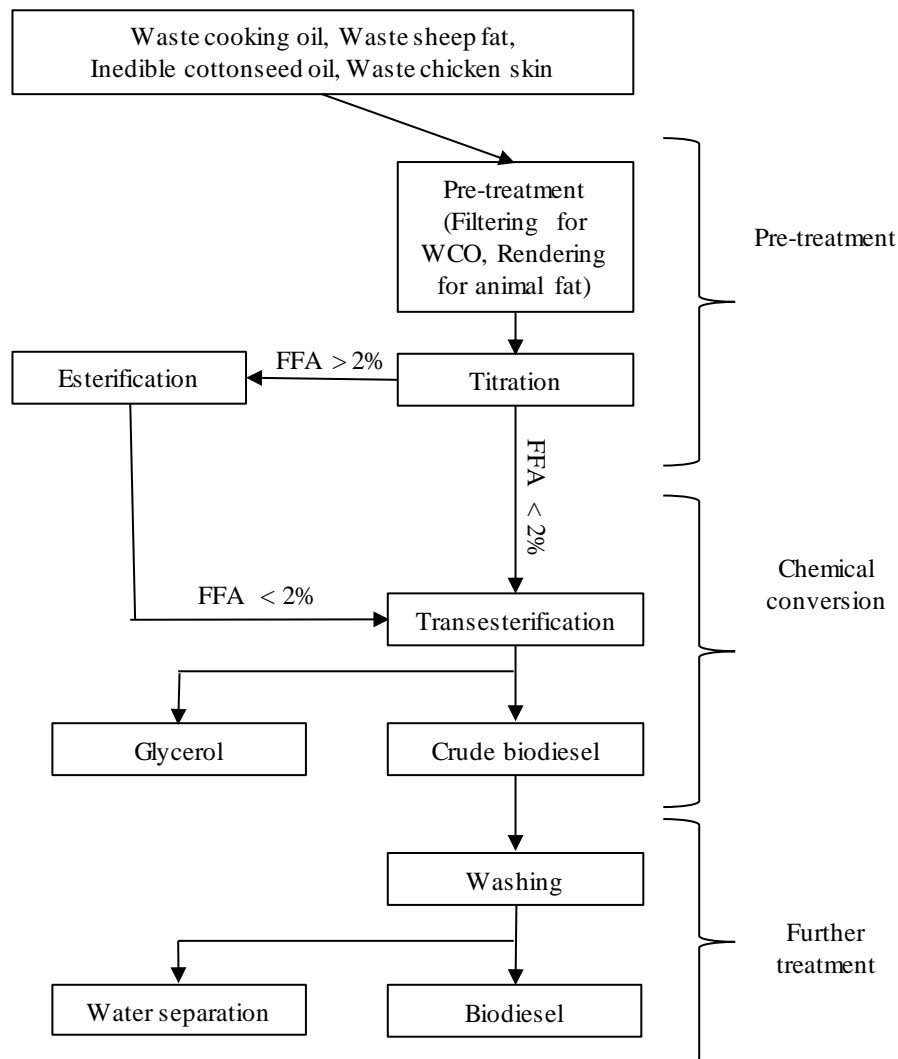
Figure 3.2: Flow diagram of feedstock conversion into biodiesel.

Transesterification process was carried out in the presence of KOH catalyst and methanol. Initially, feedstock was heated up to 65 °C. KOH catalyst was dissolved in methanol (5:1 oil to alcohol ratio). Then, the KOH - methanol solution was added into the heated feedstock. Note that transesterification above 60 °C could be a critic as the methanol evaporates around 64 °C (Methyl-Alcohol, 2018). Therefore, the condenser was used to condensing any evaporating methanol vapour back into the

transesterification flask. The transesterification process was kept heated at 65 °C and mechanically stirred by magnetic stirrers both simultaneously for 3 hours Figure 3.3.

Figure 3.3: Transesterification setup which includes heating from the bottom, continuous mechanical string with a help of magnets and condenser at the top (Aston University chemistry laboratories).

After three hours of heating and stirring, the solutions were transferred to separator funnels and left for 24 hours. Glycerol was settled down and crude biodiesel was formed at the top layer as shown in Figure 3.4 a. Next, glycerol was removed and crude methyl ester collected for enhancing the quality. Biodiesels were washed by spraying distilled water on top Figure 3.4 b. Water cleaned any unreacted methanol and other impurities, and settled down. This process was repeated several times (each allowed 24 hours for separation) until a clear colour was observed in biodiesel Figure 3.4 d. Finally, biodiesel and water separated. The biodiesel can also be heated after this process to evaporate any remaining water.
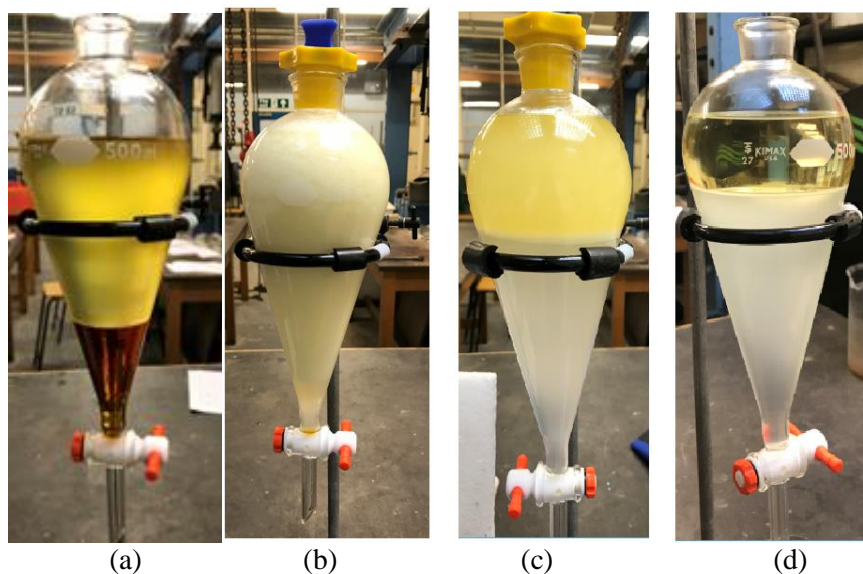
Figure 3.4: The products of transesterification process (a) two layers biodiesel on the top glycerine at the bottom, (b) water spraying on top of crude biodiesel (c) water reacting with unreacted methanol, (d) biodiesel on top and washed water at the bottom.

3.4. Biodiesel quality and British biodiesel standard

This section explains fuel characterisation methods used to define biodiesel physiochemical properties. The test methods declared in British and European biodiesel standard were taken as reference for the fuel characterisation (Table 3.1). Biodiesels were characterised at Aston University mechanical engineering, chemical engineering and EBRI laboratories except for elemental analysis which was conducted at the University of Birmingham.

Biodiesels produced from various feedstock are likely to have different fuel properties. This can be due to the different chemical compositions of the feedstock and methods used during the transesterification process. In this regard, different standards are in use in Europe and America. Table 3.1 introduces the biodiesel standards for Europe and UK (BS EN 14214) and America (ASTM D 6751) along with the European petroleum diesel standard (EN 590). It should be noted that EN 590 diesel standard also involves 7% biodiesel in its content (European Standard EN 590:2013, 2009). The European standard for biodiesel last updated in 2008 and named as EN 14214:2008 (Masera and Hossain, 2017). The British biodiesel standard is the same as the European standard and named as BS EN 14214 (British Standard Institution, 2010). According to Table 3.1, European biodiesel standard is more restricted than American standard. For example, some important fuel properties such as density, total contamination, unsaturated methyl esters, iodine value etc., were not considered in American standard, whereas European standard has strict ranges on the mentioned parameters. Moreover, ASTM D 6751 standard allow the usage of biodiesels having a viscosity in the range of $1.9 - 6.0$ mm^2/s,

whilst this range is only 3.5 – 5.0 mm^2/s in BS EN 14214. The purpose of the biodiesel standard is to provide safe and efficient biodiesel utilisation in terms of storage, transport and engine operation.

Table 3.1:European and American standards for biodiesel and petroleum diesel (British Standard Institution, 2010; Deka and Basumatary, 2011).

Fuel Characteristic	Test Method	Unit	Europe	America	Europe
Specification			BS EN 14214:2008	ASTM D 6751-07b	EN 590:2009
Applies to			Biodiesel	Biodiesel	Diesel
Density 15°C	EN ISO 3675 EN ISO 12185	g/cm³	0.86-0.90	n/a	0.82-0.845
Viscosity 40°C	EN ISO 3104 ISO 3105	mm²/s	3.5-5.0	1.9-6.0	2.0-4.5
Distillation	EN ISO 3405	% @ °C	n/a	90%,360°C	85%,350°C - 95%,360°C
Flash point	EN ISO 3679	°C	101 min	93 min	55 min
Sulphur content	EN ISO 20846 EN ISO 20847 EN ISO 20884	mg/kg	10 max	15 max	50 max
Carbon residue (10%distillation residue)	EN ISO 10370	%(mol/mol)	0.3 max	n/a	0.3 max
Sulphated ash	ISO 3987	%(mol/mol)	0.02 max	0.02 max	0.01 max
Water	EN ISO 12937	mg/kg	500 max	500 max	200 max
Total contamination	EN 12662	mg/kg	24 max	n/a	24 max
Copper strip corrosion	EN ISO 2160	3h/50°C	1 max	3 max	1 max
Oxidation stability	EN 14112	hours;110°C	6 hours min	3 hours min	(25 g/m3)
Cetane number	EN ISO 5165		51 min	47 min	51 min
Acid value	EN 14104	mg KOH/g	0.5 max	0.5 max	n/a
Methanol	EN 14110	%(mol/mol)	0.20 max	0.2 max or Fp <130°C	n/a
Ester content	EN 14103	%(mol/mol)	96.5 min	n/a	7% FAME
Unsaturated methyl esters (≥ 4 double bonds)		%(mol/mol)	1 max	n/a	n/a
Monoglyceride	EN 14105	%(mol/mol)	0.8 max	n/a	n/a
Diglyceride	EN 14105	%(mol/mol)	0.2 max	n/a	n/a
Triglyceride	EN 14105	%(mol/mol)	0.2 max	n/a	n/a
Free glycerol	EN 14105 EN 14106	%(mol/mol)	0.02 max	0.02 max	n/a
Total glycerol	EN 14105	%(mol/mol)	0.25 max	0.24 max	n/a
Iodine value	EN 14111		120 max	n/a	n/a
Linolenic acid content	EN 14103	%(mol/mol)	12 max	n/a	n/a
Phosphorus	EN 14107	mg/kg	4 max	n/a	n/a
Alkaline metals (Na,K)	EN 14108 EN 14109	mg/kg	5 max	5 max	n/a

3.4.1. **Kinematic viscosity**

The kinematic viscosity of fuel is one of the most important parameters as it directly relates the flow of fuel through a fuel supply line and inside the engine. By definition, the viscosity is the resistance of a fluid to flow. By this means, high viscosity fuels are not preferred to use in engines as their slow movement in the fuel supply line may cause problems. In addition, it is more difficult to atomise viscous fuels through injectors (Agarwal *et al.*, 2015). According to standards of EN ISO 3104 for Europe (Knothe, 2006) and ASTM D445 for USA (Nabi *et al.*, 2015), measurement of kinematic viscosity undergoes at 40°C, it was also recommended to measure this property of biofuels at the room temperature as well. The reason for this measurement is to check the behaviour of the biofuel mobility from a tank to an engine and at the cold start-up condition. According to the viscosity of a biofuel, some modifications on the fuel supply line may be required such as an auxiliary fuel pump or preheating.

The viscosities were measured in accordance with EN ISO 3104 method. The Cannon-Fenske viscometer M100 size viscometer which can be used for an estimated viscosity range of 3 to 15 was used during the test with the uncertainty of 0.16%. The viscometer was embedded into a water bath and fixed by support as shown in Figure 3.5. The electronically controlled heater was heating and circulating the water to have a uniform heat distribution. The temperature was both measured on the heater and additional thermometer placed away from the viscometer to make sure that the system was at the steady state before the measurement. Firstly, biodiesel placed into the viscometer. Then, the fuel level on the scaled leg of the viscometer was raised above the start line by using the suction pump (Figure 3.6). Next, the suction pump and the pipe were removed to let atmospheric pressure apply on both legs of U-tube viscometer. The time measured for the fuel from the start line to the end line. To find the viscosity, measured time was multiplied by the constant provided for the used viscometer (Cannon, 2012). The experiment was conducted several times to check the consistency of the readings.
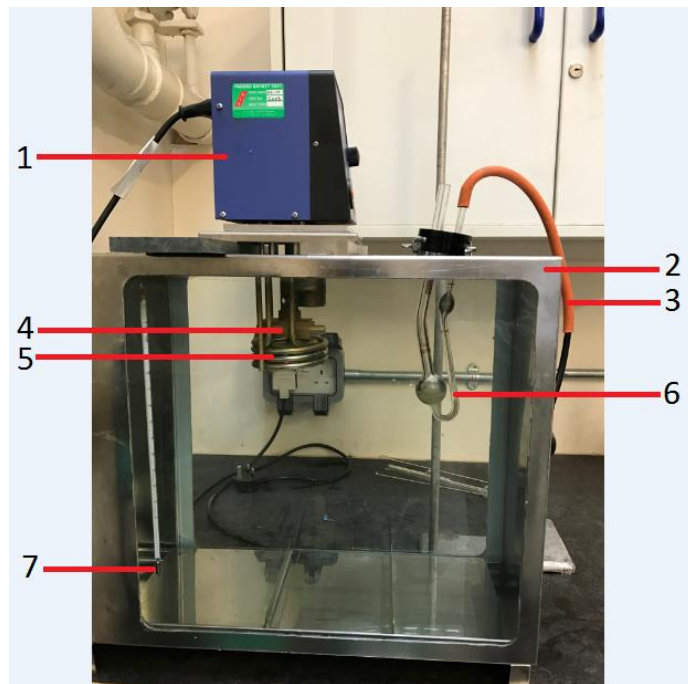
Figure 3.5: Viscosity measurement equipment, composed of 1 power unit, 2 water bath, 3 hand pump, 4 water circulation pump, 5 electrical heater, 6 viscometer, 7 thermometer (Aston University mechanical engineering laboratory).
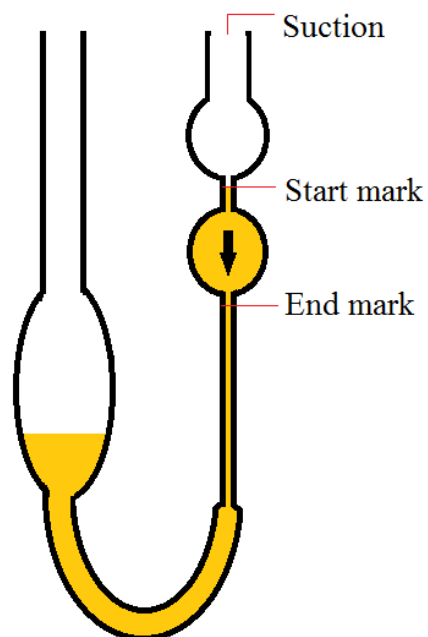
Figure 3.6: U-Tube viscometer application.

3.4.2. Density

Amount of fuel sent into the combustion chamber generally controlled by volume or time bases (Piaszyk, 2012). When biofuel is used in an unmodified diesel engine, the volume of biofuel transferred is assumed to be the same with the case of diesel. Thus, it directly affects the mass of fuel. In this perspective, a higher density may be desired for better engine efficiency. However, density also directly affects the atomisation of fuels. According to literature, higher densities lead to the higher formation of particulates which results in poor atomisation (Emiroğlu *et al.,* 2018).

Densities of biodiesels were measured by hydrometer method in accordance with EN ISO 3675. Initially, A graduated cylinder filled with a test fuel and hydrometer placed into it. Then the corresponding value reads on the hydrometer scale (Figure 3.7). It should be noted that fuel meniscus could lead to an inaccurate density reading (Piaszyk, 2012). A schematic of the true reading was shown in Figure 3.7 b.

(a)   (b)
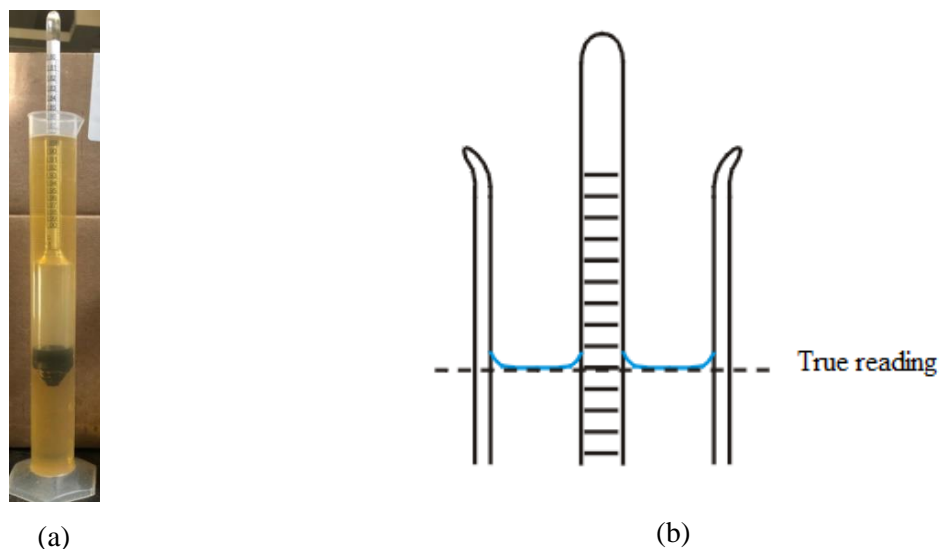
Figure 3.7: (a) Density measurement apparatus - hydrometer and (b) accurate measurement technique.

3.4.3. Flash point

The flash point of a fuel is an important parameter mainly in terms of safety. Fuels having low flash points can cause explosions during the storage, handling or transport (Kirubakaran and Selvan, 2018). Knowing the flash point of such fuels allows the user to take necessary precautions to avoid any fire hazard. The flash point of biodiesel should be measured in accordance with the standard given by EN ISO 3679 for Europe. The minimum allowed flash point is declared as $101\,^{0}C$ for biodiesels in Europe (Table 3.1).

Flash points were measured in accordance with EN ISO 3679 method. Biodiesel samples were tested through Setaflash Series 3 Closed Cup flash point tester with the accuracy of ±0.5 Figure 3.8.

Approximately 2 ml of biodiesel was placed into the closed cup thermally control room of the equipment. As it was recommended by the suppliers, biodiesel was tested in Auto mode. That is, setting a temperature value lower than the estimated value, upon the ready comment (steady temperature) the burning flame on top of the closed cup was met with the fuel by operating the equipment's trigger. In the case of any flash detection at this stage, the procedure had to be repeated with lower temperature. If there was no flash detected, the temperature was increased and tested again with a few °C increments. This experiment was also repeated several times for each fuel to check the consistency of the reading.

Figure 3.8: Flash points of biodiesels were measured through Setaflash Series 3 Closed Cup flash point tester (Aston University mechanical engineering laboratory).

3.4.4. Cloud and pour points

The cloud point can be explained as the temperature at which wax crystals start to settle up. This temperature is highly important especially in cold countries where there is a risk of fuel to freeze inside the components of the engine like injectors, fuel supply system or fuel tank. Nabi *et al.* (2015) used ASTM 5773 to measure the cloud point of their fuels. Knothe (2006) states that the method of ASTM D2500 can be used to figure out the cloud point of test fuel. However, by European standard, there is no specified cold filter plugging point temperature (Knothe, 2006). Nevertheless, EN 116 method can be used for determining the cold filter plugging point temperature (CFPP). Cold filter plugging point temperature represents the minimum temperature at which the liquid fuel can flow. It is also called as the Pour point. It can be measured through ISO 3016 test method. Similar to cloud point, there is no specific value of pour point on EN 14214 European standard for vehicle usage of biodiesel (Hasimuglu *et al.*, 2008; Kumar *et al.*, 2013). However, as the climate conditions vary from country to country, individual countries in Europe may define their own pour point temperatures according to the time of the year (Hasimuglu *et al.*, 2008; Kumar *et al.*, 2013). British standard BS EN 14214 classifies

CFPP of biodiesels differently for the temperate climates Table 3.2 and for the arctic climates Table 3.3 (British Standard Institution, 2010). Note that, climate related CFPP requirements do not apply for FAMEs to be blended with fossil diesel under EN 590 standard (British Standard Institution, 2010).

Table 3.2: Temperate climate related Cold Filter Plugging Point requirements.

Property	Unit	Grade A	Grade B	Grade C	Grade D	Grade E	Grade F	Test method
CFPP	⁰C, min	+5	0	-5	-10	-15	-20	EN 116

Table 3.3: Arctic climate related Cold Filter Plugging Point requirements.

Property	Unit	Class 0	Class 1	Class 2	Class 3	Class 4	Test method
CFPP	^{0}C, max	-20	-26	-32	-38	-44	EN 116

These parameters were not measured in the scope of this research as they do not exist in the BS EN 14214 standard. Equipment limitation was another reason. However, no indication of wax formation was observed on biomixtures at the room temperature.

3.4.5. Water content

Feedstock may contain a significant amount of water in their contents, especially the waste cooking oils. However, the presence of water in the internal combustion engines could create very important problems. To illustrate, water contamination may lead to corrosion of engine components. Furthermore, water can react with the glycerides which in turn produce glycerine and soap which is absolutely undesired scenario (Felizardo *et al.*, 2007). In addition, it also reduces energy content of biofuel. To avoid any problems caused by water contamination in biodiesel, BS EN 14214 standard limits the water content as maximum 500 mg per kg of biodiesel. The water content of any biodiesel can be measured through EN ISO 12937 method, Karl Fisher titration. This property was not measured in this research due to equipment limitation. However, water content of biodiesel was minimised by allowing each separation process minimum 24 hours during the production stage.

3.4.6. Higher heating value

Higher Heating Value (HHV) which is also known as calorific value or energy content represents the amount of energy released per unit mass of fuel. This value also includes the energy release from the condensation of water vapour (product of combustion) (Michael *et al.,* 2011). Although neither European nor American standards have limitation over HHV for biodiesels, it is a very important

property in terms of engine efficiency (Piaszyk, 2012). DIN 51900-3 is one of the recommended methods for measuring HHV (Rutz and Janssen, 2006).

Higher heating values of fuels were measured through the Parr 6100 boom calorimeter shown in Figure 3.9 with the accuracy of 0.1%. Its working principle was specific heat equation, Equation 3.3. Initially, the mass of fuel sample was measured and placed into a close system surrounded by the water. Then, equipment started the combustion by burning fuse wire. Measuring the temperature rise on the water before and after the fuel burned, knowing the mass of the fuel burned and specific heat capacity of the system components the software can calculate energy content by using Equation 3.3.

$$Q = mc \, \Delta T \qquad (3.3)$$

Figure 3.9: Parr 6100 calorimeter used for Higher Heating Value measurement (Aston University mechanical engineering laboratory).

3.4.7. Acid value

The acid value indicates the amount of free acids in the sample. The presence of free acids negatively effects the biodiesel aging (Predojević, 2008). The acid values of the samples were measured by the same titration method explained in Section 3.2.1. Initially the 0.1 N KOH titration solution was prepared and filled in the burette. At the same time, 1 ml biodiesel was dissolved in 10 ml isopropyl alcohol and some phenolphthalein indicator was added. The amount of titration solution spent to

convert the colour to pink was recorded as a result. This value was then used to calculate acid value through Equation 3.4 (Jagadale and Jugulkar, 2012; Heroor and Bharadwaj, 2013).

$$\text{Acid Value} = \frac{(\text{titration result})(\text{Normality})(28.2)}{(\text{weight of sample})} \tag{3.4}$$

3.4.8. Elemental analysis (CHN analysis)

As the name refers elemental analysers are useful devices to analyse the compounds of carbon, hydrogen, nitrogen and sulphur in organic substances. There is no specified test method for the carbon, hydrogen and oxygen content of the biodiesels in BS EN 14214 standard (Table 3.1). The main working principle of elemental analysers is separating the oxygen molecules attached to carbon, hydrogen, nitrogen and sulphur by the help of copper. During this process test sample generally carried by additional gases which are known as carrier gas such as helium (Thompson, 2008). Figure 3.10 presents the CHN analyser used in this study located at University of Birmingham. It should be noted that it was very challenging to conduct EA analysis for the biomixtures. This was because of the possibility of a biodiesel agent to be more dominant in a vail where the sample was taken. Therefore, four measurements conducted for each sample and averages of the results were used.

Figure 3.10: Elemental analyser equipment used to measure carbon, hydrogen and nitrogen contents of biodiesels and biomixtures (University of Birmingham).

3.4.9. Thin layer chromatography

Thin layer chromatography (TLC) of each feedstock was conducted at Aston University, European Bioenergy Research Institution (EBRI) laboratories. This analyse was conducted to determine fractions of triglycerides (TAG), diglycerides (DAG), monoglycerides (MAG) and free fatty acids in the sample.

The solvent was prepared by mixing 70 ml of hexane, 30 ml of dimethyl ether and 1 ml of acetic acid, and placed into a chromatography tank. A TLC silica plate was activated by heating. The 0.5 ml oil samples were diluted with 1.5 ml hexane and 50 µl of samples were applied on the plate. Plate was transferred into tank and time allowed for solvent to separate TAG, FFA, DAG and MAG. Then, the plate was introduced into an iodine tank which made the separation visible.

To quantify the fractions, corresponding areas of TAG, FFA, DAG and MAG were scraped separately for each sample and transferred into tubes. Internal standard of C17:0 was added into tubes by 25 µl. The samples were transesterified by adding 2 ml of 2.5% sulfuric acid-methanol solution at 80°C for 1.5 hours. Then, samples were analysed through gas chromatography and mass spectrum analysis at EBRI.

3.4.10. Gas chromatography and mass spectrum analysis

Gas Chromatography and Mass Spectrum (GC-ms) analyses was given as the standard measurement method of the following parameters; methanol content, ester content, unsaturated methyl esters which have ≥ 4 double bonds, monoglyceride content, diglyceride content, triglyceride content, free glycerol, total glycerol and linolenic acid contents (British Standard Institution, 2010). The test methods for the mentioned properties were given in BS EN 14214 standard like EN 14110, EN 14103, EN 14105 and EN 14106 (Table 3.1). Additionally, some other fuel properties such as iodine value, cetane number, lower heating value, degree of unsaturation were calculated by using mass fractions of each FAME forming biodiesel.

Two different Gas Chromatography and Mass Spectrum (GC-ms) analyses was conducted in this research. Firstly, biodiesels tested the find FAME compositions at Aston University chemical engineering laboratories Figure 3.11. Secondly, biodiesel (and feedstock oil) samples were separated into TAG/FAME, FFA, DAG and MAG on a Thin Layer Chromatography (TLC) plate and quantified through GC-ms at EBRI Figure 3.12.

Figure 3.11: Gas Chromatography and mass spectrum equipment used to determine FAME compositions (Aston University, chemical engineering laboratory).

Figure 3.12: Gas Chromatography and mass spectrum equipment used to quantify FAME, TAG, DAG and MAG (Aston University, European Bioenergy Research Institute).

The gc-ms analysis was carried out with the help of helium carrier gas which was supplied to the inlet of the system and flows through detector under controlled pressure. The test sample injects from the injection port and carried to the column by the carrier gas after volatilised. Separation occurred inside the long column. After elution, carrier gas carried the sample into a detector where the electronic signal generated as a response to a physicochemical property of substances. The data system measures the electronic signal and produces results as a chromatogram (Masada, 1976). In the scope of the GC-ms analysis, every test was duplicated for each sample to check the consistency of the results. The equipment was measuring different peaks at different times which were indicating the type of FAME. The probabilities of the FAME determination were around 80% throughout the experiment.

3.4.10.1. Sample preparation for gas chromatography and mass spectrum analysis

All biodiesels were separately tested in the Trace 1300 type Thermo Scientific Gas Chromatography and the ISQLT Mass spectrum (Aston University chemical engineering laboratories). The 0.05 g of biodiesels were dissolved in 50 ml of methanol. Samples were prepared in 50 ml volumetric flasks (Figure 3.13) and placed into ultrasonificator for 15 minutes. Then, 0.1µl of the prepared samples were transferred into test tubes and loaded to GC-ms equipment. The Perkin Elmer column was used in the analysis which was 30 m long, 0.22 mm diameter and 0.25 µm film thickness. A split mode was used with 1:10 ratio and injector temperature was set to 280 ℃. The initial temperature of the oven was 100 ℃ and it was increased up to 275 ℃ with the increments of 10 ℃ per minute. Electron impact ionisation (at 200 ℃) with the operation range of 50-600 m/z was used at the mass spectrometer (250 ℃).

| (a) | (b) | (c) |
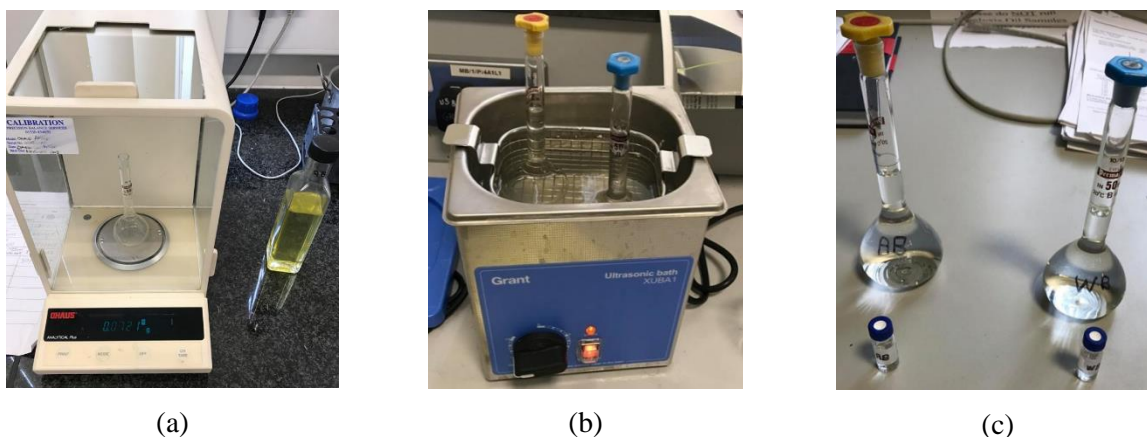
Figure 3.13: Sample preparation for GC-ms analysis (a) weight 0.05g of sample and fill 50 ml of solvent, (b) place in ultrasonificator and (c) pipette out 0.1 µL of sample into test vial.

Additionally, biodiesel and feedstock oil samples which were separated into TAG/FAME, FFA, DAG and MAG on a Thin Layer Chromatography (TLC) plate were also tested in the Agilent Technologies 6890N GC system (Aston University EBRI laboratories). A DB-23 capillary column was used which has length of 30 m, internal diameter of 0.25 mm and film thickness of 0.25 µm. The GC injector was operated in split mode 50:1 with an inlet temperature of 250°C. The column temperature was kept at 50°C for 1 min then increased at 25°C /min to 175°C, followed by a second ramp with a heating of 4°C/min up to 235°C held for 15 min. Assignments of main FAME were made by using a NIST08 MS library.

3.4.11. Iodine value and degree of unsaturation

Iodine Value (IV) is a measure of the Degree of Unsaturation (DU) in oils and fats (Mata *et al.*, 2014). The physical interpretation of the iodine number can be described as the amount of iodine in grams consumed by 100 gram of fat, thus it is an unitless parameter (Balakrishnan *et al.*, 2016). Like all other saturation level measurements, the principle is the same for estimation of iodine value. Iodine added into unsaturated oil breaks the double bonds between carbon atoms and becomes a part of the molecular structure by attaching themselves. Consequently, higher consumption of iodine indicates a higher degree of unsaturation level (Ham *et al.*, 1998; Soares, Lima and Rocha, 2017). British standard for biodiesel BS EN 14214 stated an updated alternative technique to determine the iodine number of biodiesel (British Standard Institution, 2010). According to this technique, firstly FAME composition of biodiesel is defined through gas chromatography and mass spectrum (GC ms) experiments. Next, iodine value can be calculated by multiplying the mass fractions of each FAMEs with the defined constants (Table 3.4) (British Standard Institution, 2010). Equation 3.5 was used to calculate overall iodine value of biodiesels.

Table 3.4: Factors used in the calculation of iodine value (British Standard Institution, 2010).

Methyl ester of the following acids	Factor
Myristic C14:0	0
Palmitic C16:0	0
Palmitoleic C16:1	0.95
Stearic C18:0	0
Oleic C18:1	0.86
Linoleic C18:2	1.732
Linolenic C18:3	2.616
Eicosanoic C20:0	0
Eicosenoic C20:1	0.785
Docosanoic C22:0	0
Docosenoic C22:1	0.723

$$\text{Iodine value}_{\text{biodiesel}} = \sum (\text{Iodine value}_{\text{FAME}})(\text{mass persentage of FAME}) \qquad (3.5)$$

Although degree of unsaturation does not take place in the standard, this method was generally preferred by the researchers (Ramos *et al.*, 2009; Redel-Macías *et al.*, 2013; Balakrishnan *et al.*, 2016; Dhamodaran *et al.*, 2017; Han Li *et al.*, 2018). The principle is very similar to the iodine value calculation. However, in the calculation of DU, number of double bonds was considered rather than type of FAME. There was no certain empirical definition defined in the literature and it was defined

slightly different by each researcher. Table 3.5 summarises the various definitions of DU found in literature and in this study.

Table 3.5: Different definitions of degree of unsaturation (DU) in the literature and this study.

Reference	Equation	
(Ramos *et al.*, 2009)	$DU = (mono) + 2\,(poly)$	(3.6)
(Redel-Macías *et al.*, 2013)	$DU = \dfrac{(mono) + 2\,(di) + 3\,(tri)}{100}$	(3.7)
(Balakrishnan *et al.*, 2016)	$DU = \dfrac{(2\,C + 2 + N - X - H)}{2}$	(3.8)
(Dhamodaran *et al.*, 2017)	$DU = (mono) + (poly)$	(3.9)
(Han Li *et al.*, 2018)	$DU = (mono) + 2\,(poly)$	(3.10)
This study	$DU = (mono) + 2\,(di) + 3\,(tri)$	(3.11)

mono: Weight percentage of FAMEs having 1 double bond; poly: Weight percentage of FAMEs having 2 or more than 2 double bonds; di: Weight percentage of FAMEs having 2 double bonds; tri: Weight percentage of FAMEs having 3 double bonds; C: Number of carbon atoms; N: Number of nitrogen atoms; X: Number of halogen atoms; H: Number of hydrogen atoms

Although there were different equations found in the literature, most of the equations were build up with the same logic i.e. weight percentages of unsaturated FAMEs. Among the equations defined in the literature, only the Equation 3.7 was differentiating FAMEs with 2 and 3 double bonds. Considering the significant difference in iodine values of 2 and 3 double bond FAMEs, Equation 3.7 found to be the best option in the analysis of this study. However, a small modification decided to be made i.e. not dividing by 100. This was made to have larger DU differences between the test fuels, which in turn provide easier analysis to have a better understanding of the effect of DU. Ultimately; Equation 3.11 was modified from previous equations and used in this study.

3.4.12. Cetane number

Cetane number (CN) is a dimensionless parameter represents ignition delay period of a biodiesel after being injected into the combustion chamber (Knothe *et al.*, 2003). In other words, CN value represents the readiness of fuel to self-ignition after its injection into combustion chamber (Sivaramakrishnan and Ravikumar, 2012). According to Rao *et al.* (2010), there is a direct relation between CN and other fuel properties such as heating value and density. Higher cetane number fuels provide shorter ignition delay. There are also significant amount of studies correlating higher CN with reduced exhaust gas emissions, specifically NOx and unburned hydrocarbons (HC) (Knothe *et al.*, 2003; Tong *et al.*, 2011).

Cetane number of biodiesels was estimated with the same principle as iodine value. This technique was also frequently used in the literature (Kurtz and Polonowski, 2017; Masera and Hossain, 2019). It should be noted that, unlike iodine value, British standard does not provide any factors to calculate cetane number. Various factors were used by different researchers in the literature Table 3.6. The values were summarised in Table 3.6 and noticed that they were very close to each other. Cetane number factors provided by Ramírez-Verduzco *et al.,* (2012) were selected to be used in this study. Equation 3.12 represents the calculation method of the cetane number for biodiesels (Kurtz and Polonowski, 2017; Masera and Hossain, 2019).

Table 3.6: Cetane numbers of FAMEs declared by various studies.

		Reported cetane numbers				
		(Bamgboye *et al.,* 2008)	(Knothe *et al.,* 2003)	(Tong *et al.,* 2011)	(Ramírez-Verduzco *et al.,* 2012)	(Murphy *et al.,* 2004)
Myristic	C14:0			66.2	65.4	
Palmitic	C16:0	74.4	74.5	74.3	73.9	81
Palmitoleic	C16:1	51	51	51	53.3	
Stearic	C18:0	76.3	86.9	75.6	82.3	89
Oleic	C18:1	57.2	55-59.3	56.5	61.7	62
Linoleic	C18:2	36.8	42.2-38.2	38.2	41.1	42
Linolenic	C18:3	21.6	20.6-22.7	22.7	20.5	
Arachidic	C20:0			100	90.8	
gadoleic	C20:1			64.8	70.2	
Erucic	C22:1			76	78.7	

$$\text{Cetane number}_{\text{biodiesel}} = \sum (\text{Cetane number}_{\text{FAME}})\,(\text{mass persentage of FAME}) \tag{3.12}$$

3.5. Test engine

This section describes the engine testing facilities used to conduct this research. A three-cylinder Lister Petter LPWS 3 CI engine having an indirect injection system was used. Figure 3.14 illustrates the test engine coupled to a dynamometer. Table 3.7 shows the engine specifications. The engine had a natural aspiration system and there was not any EGR facility installed. A heat exchanger (Bowman UK, header tank type) other than radiator was used for engine cooling (Figure 3.14). The water reservoir located under the building was used as a cooling agent for the heat exchanger. Exhaust gases were diverted outside the building by a pipe system with the help of a suction fan (Figure 3.15). In

addition, an extra opening with a valve was placed on the exhaust pipe inside the engine cell for the purpose of emission measurement.

Table 3.7: Test engine specifications.

Manufacturer	Lister Petter (UK)
Model	LPWS Bio3 water cooled
Cylinder number	3
Bore/Stroke	86/80 mm
Rated speed	1500 rpm
Continuous power at rated speed	9.9 kW
Overload power at rated speed	10.9 kW
Fuel injection type	Indirect injection. Self-vent fuel system with individual fuel injection pumps
Fuel pump injection timing	20° BTDC
Aspiration	Naturally aspired
Exhaust gas recirculation	0%
Cylinder capacity	1.395 litre
Compression ratio	1:23.5
Firing order	1-2-3
Minimum full load speed	1500 rpm
Maximum permissible exhaust back pressure	75 mbar
Continuous power fuel consumption at 1500 rpm	3.19 L/hr (fossil diesel)
Glow plug	Combustion-chamber glow plugs
Exhaust gas flow	41.4 L/sec at full loads at 1500 rpm
Jacket water flow at full load	33 L/min (at 1500 rpm)
Maximum engine jacket water temperature	99 - 102 °C
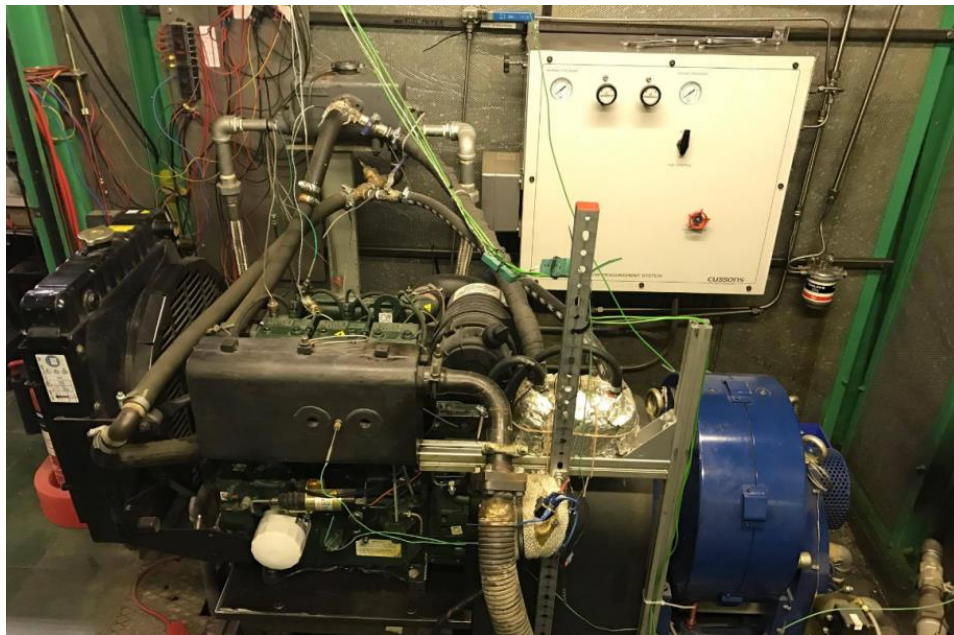
Figure 3.14: Engine – dynamometer coupling and water cooling system (Aston University mechanical engineering laboratory).

Figure 3.15: Main switches for cooling water pump and exhaust gas fan (Aston University mechanical engineering laboratory).

The test engine was equipped with a dual fuel supply system which can be operated manually by a T-junction valve Figure 3.16. By this means, it was possible to switch from one fuel to another without stopping the engine. This allows avoiding cold start effect of any test fuel, unless it was the main scope. In this research, the engine was started on diesel and switched to test fuels after engine warmup. Similarly, the fuel switched back to diesel to avoid any contamination in the engine at the end of experiments. The original (unmodified) fuel injection system provided by the engine manufacturer was used in this research. The detailed information and part numbers were provided in the Lister Petter LPW, LPWT and LPWS Masters part manual (Lister-Petter, 2001).

Figure 3.16: T-junction placed on the dual fuel supply system.

Figure 3.17 illustrates the schematic of experimental setup used for this research. Engine and dynamometer were coupled to each other and located in a properly isolated test cell (room). The engine load and speed were controlled from the control panel located just outside test cell. Similarly, combustion analyser was placed at the same place and a computer was connected to log and observe measured data Figure 3.18. The fuel supply system was located on the outer wall of the test cell. Exhaust gas analyser was also located outside.
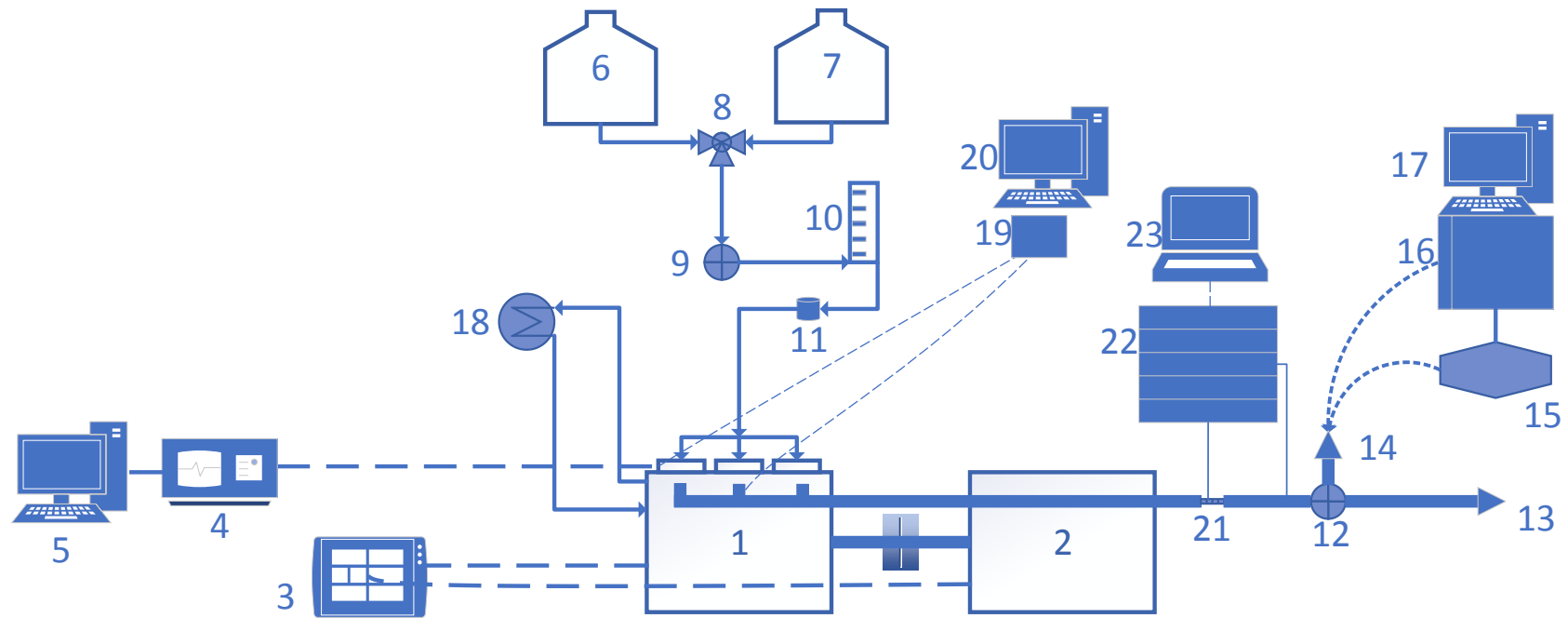
Figure 3.17: The schematic of the engine test rig. 1 engine; 2 dynamometer; 3 dynamometer controller; 4 Kister combustion analyser; 5 computer to collect and visualise combustion data; 6 fossil diesel tank; 7 biodiesel tank; 8 three-way valve; 9 valve; 10 graduated cylinder to measure fuel consumption; 11 fuel filter; 12 valve on the exhaust line; 13 exhaust gas exit; 14 branch on the exhaust line to measure smoke opacity; 15 smoke opacity unit; 16 data acquisition for BOSCH exhaust gas analyser; 17 computer to collect and visualise exhaust gas emissions; 18 engine cooling; 19 deq card to measure and log temperature; 20 computer with LabView to monitor temperature readings; 21HORIBA tailpipe attachment; 22 HORIBA gas analyser; 23 data acquisition for HORIBA gas analyser.

Figure 3.18: Control panel of the engine - dynamometer coupling and combustion.

3.6. Data acquisition systems and instruments

An eddy current type *Froude Hofmann AG80HS* dynamometer which had ±1 rpm speed and ±0.4 Nm torque accuracies were used for this experiment. The constant speed variable engine load was performed to analyse test fuels. The rated engine speed of 1500 rpm was used in this research. Data collected at six different engine loads which were corresponding approximately to 20%, 40%, 60%, 70%, 80% and 100% of the full load. Fuel consumption of the engine was measured manually. A graduated cylinder was placed on the fuel supply line to observe amount of fuel used (Figure 3.19). By this means, time to consume 100 ml of fuel was measured via stopwatch.

Figure 3.19: Graduated cylinder installed on fuel supply system to measure fuel consumption.

Two different gas analyser systems were used for the different chapters of this research. As the degree of unsaturation study requires advance emission measurement, the HORIBA OBS-ONE measurement system was borrowed from the company for the mentioned analyse only (Chapter 4).

Figure 3.20 shows the HORIBA OBS-ONE-GS02 which is a portable emissions measurement system (PEMS) designed for engine/vehicle certification under real road conditions. The Gas-PEMS measures concentrations of CO, CO_2, NO, NO_2 and NO_x emissions, air-to-fuel ratio, exhaust flow rate, GPS

data, environmental conditions (e.g. atmospheric temperature, humidity and pressure) and calculates mass emissions. HORIBA OBS-ONE features the highly adaptable, intelligent operating platform called "HORIBA ONE PLATFORM" which integrates other ONE series product data and optimises test cell operation. During the experiment, some parameters such as GPS data was ignored, as it was not related to stationary engine test.

Figure 3.20: Horiba OBS-ONE-GS02 gas analyser.

The cold gas pump sucks the exhaust gas through the analysers, which are all designed as semi-vacuum types. The power consumption of the cold pump was 450W with a heated line of 191°C. In this study, the gas analyser OBS-ONE-GS02 was used for NO and NO_x measurements. The Non Dispersive Infrared (NDIR) analyser was heated to 95 °C and measured the CO, CO_2 and water. Using this measurement the water quenching effect in NO_x analyser and the water interference of the CO and CO_2 analysers were compensated by means algorithm (Nakamura *et al.,* 2002). The water concentration was not displayed in the control software. The Chemiluminescent Detectors (CLD) analyser used to measure NO or NO_x. This measurement was hot and wet at 95 °C. The used analysers were also robust against vibration.

Figure 3.21 shows the tailpipe attachment including a pitot placed on the exhaust system to measure the exhaust gas temperature and gas sampling. Masses of the gas emissions were calculated by the system using the measured flow rate and concentration data.

Figure 3.21: Tailpipe attachment, sampling part with water trap.

Apart from the degree of unsaturation analysis (Chapter 4), the rest of the research was conducted with the commercially available Bosch BEA 850 five-gas emission analyser for measuring exhaust emissions Figure 3.22. By this device, it was possible to measure the exhaust gases of HC, CO, CO_2, O_2, NO and excess air ratio (lambda). Besides these emissions, the smoke intensity was analysed through the Bosch RTM 430 smoke opacity measurement instrument. The emission data observed simultaneously and collected when all readings were steady.

Figure 3.22: The Bosch BEA 850 gas analyser.

Combustion characteristics of test fuels were investigated on the first cylinder of the engine. The first cylinder which was located close to radiator side was modified to collect in-cylinder pressure and crank angle data. Kistler 6125C11 pressure sensor with the Kister 5064B11 charge amplifier was installed for the measurement of in-cylinder pressure. The Kister 4065A500A0 pressure sensor along with the Kister 4618A0 amplifier was used to observe and log the fuel injection pressure. Crank angle was detected by using the optical encoder, Kister 2614A. The Kister product, 2893AK8 model KiBox was installed to the system to log the gathered data by the encoder and the amplifier. Then a computer having KiBoxCockpit software (to analyse the combustion parameters) was used to connect KiBox through an ethernet connection. Details of the used equipment are given in Table 3.8.

Table 3.8: Details of the data acquisition components.

Measured parameter	Equipment	Details	Accuracy
Torque	Eddy Current Dynamometer	Froude Hofmann AG80HS	± 0.4Nm
Engine speed	Eddy Current Dynamometer	Froude Hofmann AG80HS	± 1 rpm
Time to consume 100 ml of fuel	Scaled cylinder and stopwatch	Manually tested	± 0.1 s
Exhaust gas temperature	Horiba OBS-ONE-GS02	Tailpipe attachment with pitot	± 0.1 °C full scale (0°C - 800°C)
CO	Horiba OBS-ONE-GS02	Heated NDIR	± 0.01 vol. %
CO_2	Horiba OBS-ONE-GS02	Heated NDIR	± 0.1 vol. %
NO	Horiba OBS-ONE-GS02	Heated dual CLD	± 1 ppm
NO_x	Horiba OBS-ONE-GS02	Heated dual CLD	± 1 ppm
Smoke opacity	Bosch	RTM 430	± 0.01 m^{-1}
CO	Bosch	BEA 850	± 0.001 vol. %
CO_2	Bosch	BEA 850	± 0.01 vol. %
NO	Bosch	BEA 850	± 1 ppm
O_2	Bosch	BEA 850	± 0.01 vol. %
HC	Bosch	BEA 850	± 1 ppm
In-Cylinder pressure	Kistler	6125C11 pressure sensor, 5064B11 charge amplifier	± 0.1 bar
Fuel injection pressure	Kistler	4065A500A0 pressure sensor, 4618A0 amplifier	± 0.1 bar
Crank angle	Kistler	an optical encoder, 2614A	± 0.1 °
To log the combustion data	Kistler	2893AK8 model KiBox	
Combustion software	Kistler	KiBoxCockpit	

NDIR: Non dispersive infrared detection, CLD: Chemiluminescence detection

3.7. Data analysis

In this section, empirical equations necessary to work collected data were examined. By this means, compression ignition engines were investigated theoretically in terms of heat transfer and thermodynamics principles. Understanding the engine theory was highly important for converting any experimental data into physical interpretation accurately.

3.7.1. Combustion chamber geometry

Internal combustion engine converts chemical energy stored in fuel into mechanical energy in the form of rotating crank shaft. By the design of the cylinder piston geometry (combustion chamber) released energy transferred to the crankshaft via connecting rod Figure 3.23. Thus, the design geometry of the engine directly affects the operating parameters.
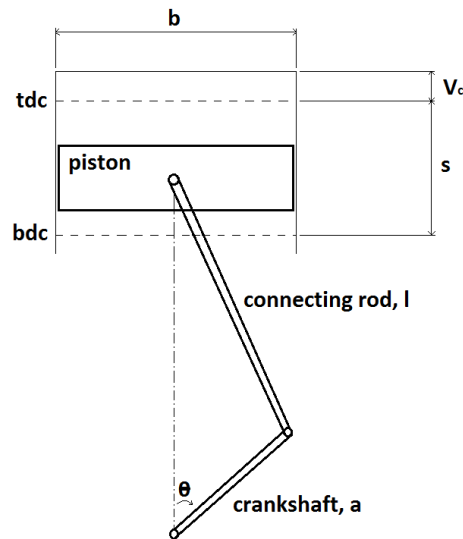
Figure 3.23: Schematic of a typical piston cylinder assembly.

Geometric parameters of a piston and cylinder assembly are presented in Figure 3.23. Where bore dimension is designated by b. Connecting rod is an intermediate component of the system which transfers power to the crankshaft. In addition, connecting rod together with crankshaft, convert the linear motion of piston into the circular motion; their lengths are denoted by l and a sequentially. Note that crank radius a is equal to half of the stroke distance s.

Top Dead Centre (TDC) is the upper limit that piston reaches in each stroke. Typically this point corresponds to crank angle at $\Theta=0^{\circ}$ (Ferguson and Kirkpatrick, 2015). The volume of the cylinder when the piston is at TDC is called as clearance volume V_c. Similarly, Bottom Dead Centre (BDC) is the lowest level of piston crown which corresponds to $\Theta=180^{\circ}$ crank angle and maximum volume V_1 was obtained at this position. Compression ratio r, of an engine, is defined as a ratio of total volume to clearance volume Equation 3.13 (Ferguson and Kirkpatrick, 2015).

$$r = \frac{\text{clearance volume}}{\text{maximum volume}} = \frac{V_c}{V_1} \tag{3.13}$$

By the geometry, the maximum volume is equal to the summation of clearance volume V_c, and displacement volume V_d. The displacement volume is also presented in Equation 3.14.

$$V_d = \frac{\pi}{4} b^2 s \tag{3.14}$$

Beside of total displacement volume, instantaneous volume $V(\Theta)$, of the combustion chamber with respect to the reciprocating motion of the piston is calculated by Equation 3.15 (Ferguson and Kirkpatrick, 2015).

$$V(\Theta) = V_c + \frac{\pi}{4} b^2 \left(l + a - \left(\sqrt{l^2 - a^2 \sin^2 \Theta} + a \cos\Theta\right)\right) \tag{3.15}$$

3.7.2. Engine performance

The torque of the engine T and engine speed N are measured through the dynamometer. Thus, brake power $\dot{P}_b$ can be calculated via Equation 3.16. Brake power is rate of work done.

$$\dot{P}_b = 2 \pi TN \tag{3.16}$$

Indicated mean effective pressure (imep) can be defined as net work per unit displacement volume of gas during the combustion. Imep is equal to break mean effective pressure (bmep) plus friction pressure. Thus, bmep can be defined as the useful work which makes it the real interest in this research (Ferguson and Kirkpatrick, 2015). Equation 3.17 was used in the calculation of bmep.

$$\text{bmep} = \frac{4\,\pi\,T}{V_d} \tag{3.17}$$

Brake specific fuel consumption (BSFC) shows the rate of fuel consumed divided by the brake power obtained Equation 3.18. Although BSFC is a crucial parameter to compare different engines, in the case of fuel comparison brake specific energy consumption (BSEC) is as crucial as the BSFC. Because, lower heating value (LHV) of fuel is also taken in to account in BSEC calculation Equation 3.19.

$$\text{BSFC} = \frac{\dot{m}_f}{\dot{P}_b} \tag{3.18}$$

$$\text{BSEC} = \frac{\dot{m}_f\,\text{LHV}}{\dot{P}_b} \tag{3.19}$$

The brake thermal efficiency BTE is another important engine performance parameter. It can be explained by the ratio of the brake power $\dot{P}_b$ to the mass flow rate of the fuel $\dot{m}_f$ and lower heating value of fuel Equation 3.20.

$$\text{BTE} = \frac{\dot{P}_b}{\dot{m}_f\,\text{LHV}} \tag{3.20}$$

Volumetric efficiency represents the mass ratio of actual air to theoretical air Equation 3.21. Where theoretical air refers to the amount of air which could occupy the cylinder under ideal atmospheric conditions and can be calculated by Equation 3.22 (Ferguson and Kirkpatrick, 2015). The actual air intake can be measured during the experiment. However, this parameter was not considered in this research as the aspiration system was the same throughout the research.

$$\eta_v = \frac{(\dot{m}_{air})_{actual}}{(\dot{m}_{air})_{theoretical}} \tag{3.21}$$

$$(\dot{m}_{air})_{theoretical} = \frac{2 \, N \, i \, V_d \, \rho_{std}}{j} \tag{3.22}$$

Where i is the number of cylinders, ρ_{std} is standard air density and j is a number of strokes. Standard air density ρ_{std} can be calculated by the ratio of standard atmospheric pressure P_{std}, over standard atmospheric temperature T_{std}, multiply by the gas constant of air R_{air} Equation 3.23.

$$\rho_{std} = \frac{P_{std}}{R_{air} \, T_{std}} \tag{3.23}$$

Air-fuel ratio of an engine is also important. A related parameter is called excess air coefficient (lambda) λ and can be defined as the ratio of actual air-fuel ratio to theoretical air-fuel ratio Equation 3.24.

$$\lambda = \frac{(A/F)_{actual}}{(A/F)_{theoretical}} \tag{3.24}$$

3.7.3. Combustion characteristics

Cylinder pressure p is one of the fundamental combustion parameter as it affects most of the combustion parameters like heat release rate. Pressure was measured with respect to changing crank angle and recorded during the experiments. Combustion analyses were conducted for the all samples with the data collected from the first cylinder of the engine. In this regard, heat release, heat release rate, in-cylinder pressure, combustion start and finish times, total combustion duration, fuel injection pressure and knock intensity were analysed. Note that for in-cylinder pressure and heat release, a selected typical cycle (among 51 measured cycles) was presented with respect to crank angle. Whereas, for the rest of combustion parameters, (which are illustrated with respect to engine load) the arithmetic average of 51 indication cycles was used i.e. knock intensity, start and end of the combustion, combustion duration, maximum heat release and fuel injection pressure. Combustion parameters were determined by considering the geometry of the engine, the first law of

thermodynamics and pressure versus volume cycle. Heat losses to walls neglected and adiabatic expansion and compression were assumed.

3.7.3.1. Heat release rate

To analyse the heat release from the combustion process Q, can be calculated by applying the first low of the thermodynamics (Schönborn, 2009). The effect of pre-chamber was neglected at this calculations due to lack of pressure data. The combustion chamber was selected as a control volume and the assumptions made were; cylinder gases have ideal gas behaviour, no mass transfer and adiabatic conditions.

These assumptions were also used in the literature (Schönborn, 2009; Emiroğlu et al., 2018). Under these circumstances, the net heat release can be equal to the gross heat release as a result of combustion Q_{gross}, and the heat transfer to combustion chamber walls Q_{walls} (Schönborn, 2009). However, as the temperature of the controlled volume is typically much higher than the surroundings i.e. combustion chamber, transferred heat to combustion chamber walls may be s negative value by the convention. The governing equation of heat release with respect to crank angle can be written as Equation 3.25.

$$\frac{dQ_{net}}{d\theta} = \frac{dQ_{gross}}{d\theta} + \frac{dQ_{walls}}{d\theta} \qquad (3.25)$$

Applying the first law of thermodynamics over the combustion chamber Equation 3.26, net heat release is must be equal to the addition of work delivered to the piston and internal energy of the gases.

$$\frac{dQ_{net}}{d\theta} = p\frac{dV}{d\theta} + \frac{dU_{gases}}{d\theta} \qquad (3.26)$$

Equation 3.27 recalls the ideal gas behaviour assumption. Thus, change of the internal energy rate of the gases can be calculated from Equation 3.28.

$$pV = mRT \qquad (3.27)$$

$$\frac{dU_{gases}}{d\theta} = m\, c_v \frac{dT}{d\theta} \tag{3.28}$$

Equation 3.29 obtained after rewriting Equation 3.26 with substituting Equation 3.28;

$$\frac{dQ_{net}}{d\theta} = p\frac{dV}{d\theta} + m\, c_v \frac{dT}{d\theta} \tag{3.29}$$

By taking the derivatives of both sides of Equation 3.29 and assuming R is constant, it was possible to rewrite Equation 3.30 as follows (Equation 3.29) (Heywood, 1988).

$$\frac{dp}{p} + \frac{dV}{V} = \frac{dT}{T} \tag{3.30}$$

Then both sides of the Equation 3.30 were multiplied by $\left(\frac{P\,V}{R}\right)$ and (Tm), which are equal to each other by the ideal gas law (Equation 3.31) (Heywood, 1988).

$$(V\, dp + p\, dV)\frac{1}{R} = m\, dT \tag{3.31}$$

Substation of Equation 3.31 into Equation 3.29 for replacing the $(m\, dT)$;

$$\frac{dQ_{net}}{d\theta} = p\frac{dV}{d\theta}\left(1 + \frac{c_v}{R}\right) + \frac{c_v}{R}V\frac{dp}{d\theta} \tag{3.32}$$

Recalling the basic thermodynamic equations;

$$\gamma = \frac{c_p}{c_v} \tag{3.33}$$

$$R = c_p - c_v \tag{3.34}$$

Rearranging Equation 3.32 by considering Equations 3.33 and 3.34, the final equation can be driven for calculation of heat release rate Equation 3.35.

$$\frac{dQ_{net}}{d\theta} = p\frac{dV}{d\theta}\left(\frac{\gamma}{\gamma - 1}\right) + V\frac{dp}{d\theta}\left(\frac{1}{\gamma - 1}\right) \tag{3.35}$$

The specific heats ratio γ may be assumed constant for both strokes of compression and power as the gas contents do not change significantly. Schönborn (2009) recommended using $\gamma \approx 1.35$ for compression stroke and range in between $\gamma \approx 1.35$ and $\gamma \approx 1.35$ for the power stroke.

3.7.3.2. Cumulative Heat release

As the name refers cumulative heat release was the total chemical energy release from the fuel Equation 3.36. Generally, this parameter is calculated between specific crank angles as there is no continuous release at every crank angle. For example, heat release measurement was started from the crank angle at which fuel injection occurs to the opening of the exhaust valve.

$$dQ_{gross} = \int_{\theta_{start\ point}}^{\theta_{end\ point}} \frac{dQ_{gross}}{d\theta}\ d\theta \tag{3.36}$$

3.7.3.3. Combustion start and finish

Pressure data was used to analyse the start of injection (SOI), start of combustion (SOC), ignition delay (ID), end of combustion (EOC) and combustion duration (CD). The crank angle when the fuel injection pressure was built up was assumed as a SOI point. Moreover, 5% and 90% of heat release were assumed as the start and end of combustion. Ignition delay corresponds to crank angle difference between the SOC and SOI. Similarly, combustion duration was the crank angle difference between the EOC and SOC (Kistler Group, 2017; Emiroğlu *et al.,* 2018; Masera and Hossain, 2019).

3.8. Summary

This chapter studied the feedstock analysis in detail. In addition, the biodiesel production strategy for the research was given. British and European standard for biodiesel was introduced and fuel characterisation methods were explained. Moreover, experimental setup to conduct this research, data acquisition equipment, tools and methods were explained. Furthermore, analytical equations to convert observed raw data into useful results were demonstrated.

Chapter 4

4. EFFECTS OF BIODIESELS UNSATURATION ON FUEL PROPERTIES AND ENGINE PERFORMANCE

This chapter investigates waste cooking oil biodiesel and waste sheep fat biodiesel blends at different volume fractions. A set of biomixtures, having different degrees of unsaturation (DU) as a result of blending, was tested to provide a better understanding of biodiesel DU on engine test results. Moreover, new biomixture blends with an optimised degree of unsaturation were analysed thoroughly in terms of physicochemical fuel properties and engine test results. Therefore, the suitability of the biomixtures with the BS EN 14214 standard was checked and volume fractions which complied with the standard identified.

4.1. Introduction

The most popular and used waste biodiesel feedstock are waste cooking oils and animal fats (Hajjari *et al.*, 2017). However, biodiesels derived from WCO hardly comply with the BS EN 14214 standard especially in terms of iodine value (Demirbas, 2009; Refaat, 2009). This is due to the high degree of unsaturation of WCO. On the other hand, animal fats are highly saturated (relatively low degree of unsaturation) and biodiesels derived from this feedstock generally are too viscous, hence also failing to comply with BS EN 14214 standard. As the degree of unsaturation is a crucial fuel property for biodiesel, it was chosen for further investigation.

4.2. Literature review for biodiesel degree of unsaturation

The FAMEs which have no double bond, like C14:0, C16:0 and C18:0, are named as saturated FAMEs. On the other side, FAMEs having at least one double bond are categorised as unsaturated FAMEs (Lanjekar and Deshmukh, 2016). The degree of unsaturation (DU) and iodine value (IV) of any FAME depends on the number of double bonds in its content. Therefore, FAMEs having only one double bond are called monounsaturated whereas FAMES having two or more double bonds are called as polyunsaturated. DU and IV are very important for biodiesels as it directly affects the combustion characteristics (Rao *et al.,* 2010). Hence, some researchers have investigated the influence of

molecular structure, the degree of unsaturation and carbon chain length of FAMEs on diesel engine performance, combustion characteristics and exhaust emissions. However, results have not yet provided any consensus as effect of DU on NOx, smoke emission, start of combustion (SOC) and heat release rate (HRR) were conflicting Table 4.1. Moreover, a significant gap in the literature was noticed regarding the effect of DU on CO_2 emission (Table 4.1).

Table 4.1: How parameters were affected by the decreasing degree of unsaturation, DU (increasing saturation level).

Case study	NO_x	CO	CO_2	Smoke opacity	Start of combustion	HRR	Engine Performance
(Lapuerta and Armas, 2009)	↓	n/a	n/a	↑	retarded	↓	No change
(Benjumea *et al.*, 2011)	↓	n/a	n/a	↓	advanced	↓	No change
(Altun, 2014)	↑	n/a	n/a	↓	n/a	n/a	No change
(Rao *et al.*, 2010)	↓	n/a	n/a	n/a	n/a	n/a	n/a
(Schönborn *et al.*, 2009)	↓	n/a	n/a	n/a	advanced	n/a	n/a
(Fareez *et al.*, 2016)	↓	n/a	n/a	n/a	n/a	n/a	n/a
(Dhamodaran *et al.*, 2017)	↓	↑	n/a	↑	retarded	↓	No change
(Li *et al.*, 2018)	↓	↑	n/a	↓	advanced	No change	n/a
(Redel-Macías *et al.*, 2013)	↑	↑	n/a	n/a	n/a	n/a	n/a

Lapuerta and Armas (2009) produced biodiesels from three different feedstock: waste cooking olive oil, waste cooking sunflower oil and neat sunflower oil. These were blended with diesel. Biofuels having different iodine values were tested in a direct injection (DI) type 2.2 litre four-cylinder turbocharged diesel engine. As a result of the study, no significant effect of IV on the engine performance was reported. In terms of emissions, a 10% increase in NO_x emissions was reported with higher IV fuels. However, high IV fuels released particulates with reduced diameters. In addition, saturated fuels resulted in more delay on the ignition start time and lower heat release rates. However, considerable variations among the viscosities and lower heating values could also have influenced the combustion and emission parameters, and the possible effects of these parameters on the results should also be taken into account.

Benjumea et al (2011) conducted an experimental study on a 4-cylinder turbocharged direct injection diesel engine to observe the effect of degree of unsaturation of palm oil and linseed oil biodiesels. Similar to Lapuerta et al (2009), no significant effect of degree of unsaturation was addressed on engine performance. According to the study, combustion start time of higher DU biodiesel (linseed oil biodiesel having iodine value of 185.4) was 2°CA later than the lower DU biodiesel (palm oil biodiesel having iodine value of 52). Moreover, peak heat release rate (HRR) of the higher DU fuel (linseed oil biodiesel) was 40% higher than the lower DU fuel (palm oil biodiesel). In terms of the exhaust emissions, higher DU biodiesel released higher NO_x and slightly higher smoke opacity

compared to low DU biodiesel. This was mainly explained by the reduced cetane number and by the increasing degree of unsaturation which in turn delays the start of combustion.

Altun (2014) produced three different biodiesels from palm oil, cottonseed oil and anchovy fish oil, having different iodine values of 59, 115 and 185 respectively. The experiments were carried out on a direct injection naturally aspired 3-cylinder diesel engine. As in other studies, no change in engine performance as a result of changing DU was indicated. The NOx emissions of palm, cottonseed and fish biodiesels were reported as 960, 900 and 970 ppm..

Rao et al (2010) investigated the influence of iodine value and cetane number of biodiesels produced from various feedstock on a single cylinder naturally aspired DI diesel engine. The biodiesels used for the mentioned study were obtained from coconut oil (IV: 10), palm kernel (IV: 52), mahua (IV: 74), pongamia pinnata (IV: 81), jatropha curcas (IV: 93), rice bran (IV: 100) and sesame seed (IV: 110) (Rao et al 2010). The study revealed a linear relationship between the iodine value and the NO_x emissions at the full load Figure 4.1.
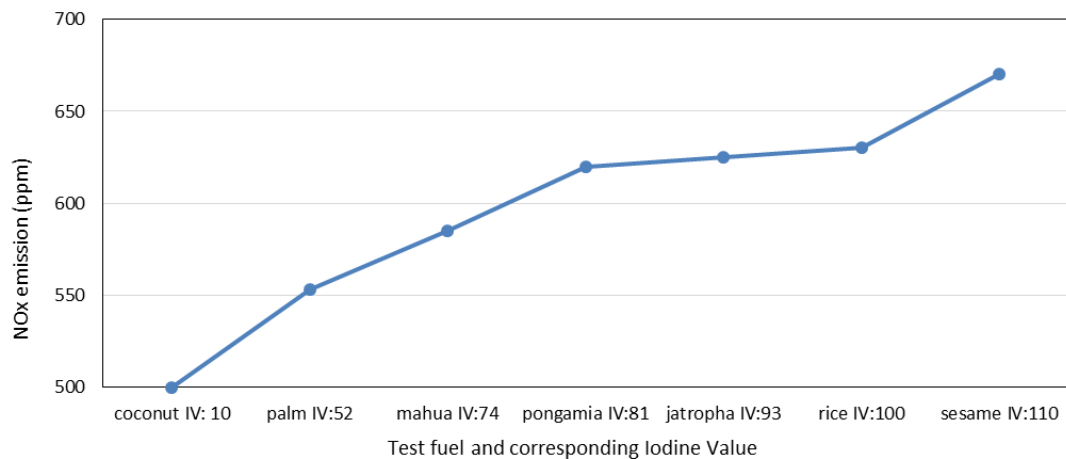
Figure 4.1: Relationship between the NO_x emission and iodine value, values are taken from (Rao *et al.,* 2010).

Schönborn *et al.*, (2009) studied the effect of biodiesel molecular structure on the combustion and exhaust gas emissions. 2-ethylhexy nitrate was used to adjust ignition properties. Hence, the effect of ignition delay did not change the combustion temperature which was a crucial parameter affecting the NO_x formation. According to the study, decreased DU and increased chain length of fatty acids resulted in decreased ignition delay. As a result of the study, it was observed that longer premixed combustion phase results in higher NO_x formation. This means, lower DU biodiesels having higher cetane number and less premixed combustion fraction develops less NOx emission.

Fareez et al (2016) examined the saturation degrees of the biodiesel to understand their effect on NO_x emission and Fourier Transform Infrared Spectroscopic characteristics. Biodiesels having various iodine values obtained from canola oil (IV: 110-120), palm oil (IV: 44-58), and coconut oil (IV: 8-10) (Fareez *et al.*, 2016). The mentioned biodiesels were blended with diesel at three different percentages 10%, 15% and 20% and tested in a naturally aspired DI diesel engine. The results stated that the blend having lowest IV (20% coconut oil biodiesel blended with diesel) emitted 1% and 5% less NO_x than the medium IV blend (20% palm oil biodiesel) and the highest IV blend (20% canola oil biodiesel) respectively.

Dhamodaran *et al.*, (2017) compared the biodiesels produced from three different feedstock sources which were rice bran, neem and cottonseed oil having DUs of 79.3 (weight %), 77.7% (weight %) and 71% (weight %) respectively. 20% blends of the biodiesels with the diesel were tested on a single cylinder diesel engine for the analysis. Like other reviewed studies, they also provided comparable engine performance between the biofuels having various DU. Ignition delay of the highest DU biodiesel blend was approximately 2°CA and 3°CA less than the lowest DU biodiesel blend and diesel respectively. Similarly, peak HRR of the highest DU fuel was around 11% and 15% higher than the lowest DU biodiesel blend and diesel at the premixed combustion phase respectively. Most of the exhaust gas emissions such as HC, CO and smoke opacity were increasing with the decreasing DU. On the other hand, the highest DU biodiesel blend (rice bran) emitted approximately 33% higher NO_x than the lowest DU biodiesel blend (cottonseed oil). However, there was inconsistency between the FAME compositions which used to estimate DU of the biodiesels with the literature. Although, Dhamodaran *et al.*, (2017) estimated the DUs of biodiesel-diesel blends by using only the C18:1, C18:2 and C18:3 FAMEs, (Sachuthananthan *et al.*, 2018) reported 17% of C16:0 in the content of neem biodiesel. Therefore, the mentioned DUs can be changed after the consideration of neglected FAMEs like C16:0 for neem biodiesel.

Li *et al.,* (2018) tested six different biodiesels which were obtained from palm, olive, rapeseed, soybean and grapeseed feedstock and having degrees of unsaturation as 64.2, 92.8, 121.9, 143.8 and 157.9 respectively. A turbocharged 4-cylinder DI engine with common rail fuel injection system was used in the study. Li *et al.,* (2018) sated that combustion starts earlier with the decreasing DU and this was mainly attributed to the reduced kinematic viscosity that provides better turbulence and spray characteristics. It was also reported that NO_x and smoke opacity emissions increased with increasing DU whereas; CO emission was decreasing with the increasing DU.

Redel-Macías *et al.*, (2013) investigated the influence of the degree of unsaturation over CO, NO_x emissions and noise characteristics of a 3-cylinder DI diesel engine. In the study; coconut, palm, olive-pomace, sunflower, and linseed oils were used as feedstock to produce biodiesels having DU of 12, 61, 98, 151 and 217, respectively. Results of the study indicated that the CO emission and noise of the

engine were reduced with increasing DU. However, according to their NOx results, there was an uneven relationship between NO_x and DU noticed.

The literature investigated the effects of the degree of unsaturation, especially on NO_x and PM emissions. However, studies mainly compare the biodiesels from various feedstock sources which have different degrees of unsaturation (iodine values) or their blends with diesel. In this chapter, on the other hand, the main aim is to investigate the effect of degree of unsaturation by keeping the feedstock the same i.e. biodiesel-biodiesel blends (100% biomixtures). This technique minimises any effects of fuel properties other than DU on engine operation. For example, biomixtures obtained from the same sources would have very similar carbon chain lengths, carbon, hydrogen, oxygen contents, densities, viscosities, flash points, heating values and acid values. By this means, the degree of unsaturation was the main parameter creates some changes on engine performance, combustion characteristics and exhaust gas emissions. In this study, moreover, another significant novelty was achieved by understanding the effect of biodiesel's DU on CO_2 emission.

4.3. Horiba emission analyser for accurate emission readings

Although BOSCH BEA 850 was the main gas analyser used in this PhD research (as described in Chapter 3), for this specific chapter a more advanced emission measurement system, i.e. HORIBA OBS-ONE-GS02 was used to detect emissions more accurately (Figure 4.2). This was due to the expected small changes in biomixtures emissions as a result of the minimised effect of fuel properties other than DU. In addition, NO_2 and NO_x were also measured with the HORIBA OBS-ONE-GS02. Smoke opacity was monitored by BOSCH analyser by placing the probe into the exhaust system.
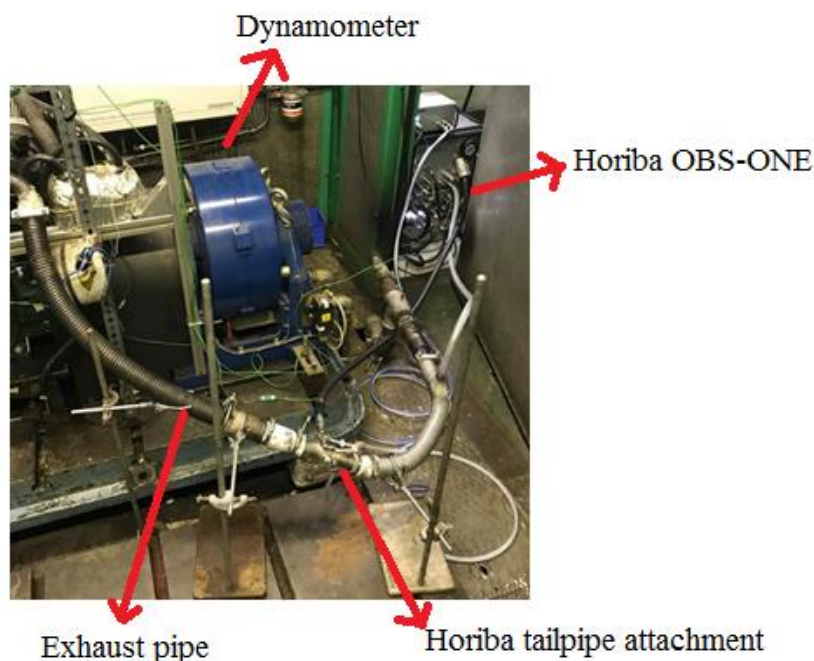
Figure 4.2: Engine test rig equipped with HORIBA exhaust gas analyser.

4.4. Biomixture blends for the degree of unsaturation study

Two biodiesel sources were selected according to their degrees of unsaturation (iodine values). The low DU biodiesel was produced from sheep fat (DU: 47), whereas high DU biodiesel was derived from waste cooking oil (DU: 167). Approximately 1.576 kg of sheep tallow was rendered from 1.8 kg of sheep fat; hence the rendering yield was calculated as 88%. The each feedstock was converted into biodiesel separately by the transesterification technique described in Chapter 3. The titration results of the fat and oil, amounts of KOH and methanol used for transesterification are given in Table 4.2.

Table 4.2: Titration results and chemicals used to convert feedstock into biodiesel.

Feedstock	Volume of titration solution consumed (ml)	KOH used for Transesterification (g/litre)	Methanol used for 1 litre of feedstock (ml)
WCO	1	8.2	200
Sheep tallow	0.6	7.7	200

Fuel properties of 7 biofuels were tested, namely 2 neat biodiesels, 100% WCO biodiesel (W100), 100% waste sheep tallow biodiesel (A100), and 5 biomixtures at different volume ratios. The biomixtures were composed of waste cooking oil biodiesel to sheep biodiesel volume ratios of 80/20,

60/40, 50/50, 30/70 and 10/90; and named as W80A20, W60A40, W50A50, W30A70 and W10A90 respectively Figure 4.3. The reference ULSD diesel was purchased from Esso UK and it was satisfying the BS EN 590 specifications (Esso, 2019).

Figure 4.3: Biomixtures obtained by blending waste cooking oil biodiesel (W100) and sheep fat biodiesel (A100); from left to right W100, W80A20, W60A40, W50A50, W30A70, W10A90 and A100.

Fuel characterisations of all test fuels were carried out and their suitability to British and European biodiesel standard BS EN14214 were checked. Next, selected biomixtures i.e. W60A40, W50A50 and W30A70 along with both neat biodiesels and diesel were tested in the engine to measure engine performance, combustion characteristics and exhaust gas emissions.

4.5. Fuel characterisation results for the waste cooking oil biodiesel – sheep fat biodiesel blends

FAME compositions of each biodiesel were analysed and presented in Table 4.3. In addition, total percentages of saturated FAMEs (C14:0, C16:0 and C18:0), monounsaturated FAMEs (C16:1 and C18:1), and polyunsaturated FAME (C18:2) were summarised in Table 4.3. According to the GS-ms results, W100 was mainly formed of C18:2 as 76.8% which was the most unsaturated FAME in this chapter. In contrast, A100 was only containing 1.1% of C18:2. Whilst, the main FAMEs found in the structure of A100 were C18:1, C18:0 and C16:0 with the percentages of 43.5%, 29.3% and 21.6%, respectively. The blends of biodiesels (W100 and A100) had extremely different FAME percentages which also result in a significant difference on degrees of unsaturation. Figure 4.4 presents the distribution of the neat biodiesels as well as the biomixtures according to total percentages of saturated, monounsaturated and polyunsaturated FAMEs. The major changes were observed on saturated and polyunsaturated FAMEs. On the other hand, a relatively minor change was spotted on

monounsaturated FAMEs. To illustrate, the overall percentage of saturated FAMEs was 15.1% for the W100 and it was increased to 22.9% by the addition of 20% (by volume) A100 into W100. It was followed by increases to 30.5%, 34.9%, 42.5%, and 50.8% as the addition of A100 by 40%, 50%, 70% and 90% respectively. Finally, the highest percentage of saturated FAME was spotted in the content of A100 as 54.4%. However, as described earlier in Chapter 3, the degree of unsaturation was defined by the unsaturated FAMEs such as monounsaturated and polyunsaturated. Similar to saturated FAMEs, linear variations were observed in the changes of both monounsaturated and polyunsaturated FAMEs after blending of the two neat biodiesels Table 4.3 and Figure 4.4.

Table 4.3: Mass percentages of each FAME compound found in the test fuels, adapted from the author's published paper (Masera and Hossain, 2017).

FAME	W100	W80A20	W60A40	W50A50	W30A70	W10A90	A100
C14:0	0.1	0.5	0.9	1.2	1.7	2.3	2.8
C16:0	11.0	13.1	14.8	15.8	18.2	20.6	21.6
C16:1	0.0	0.0	0.4	1.0	1.4	1.9	0.9
C18:0	4.0	9.3	14.7	17.9	22.6	27.9	29.3
C18:1	2.6	3.8	5.0	5.9	6.8	7.9	43.5
C18:2	76.8	68.9	60.5	55.0	47.1	38.2	1.1
C18:3	5.4	4.5	3.6	3.1	2.2	1.2	0.8
Saturated	15.1	22.9	30.5	34.9	42.5	50.8	54.4
Monounsaturated	2.6	3.8	5.4	7.0	8.2	9.8	44.4
Polyunsaturated	82.2	73.4	64.1	58.1	49.3	39.4	1.1
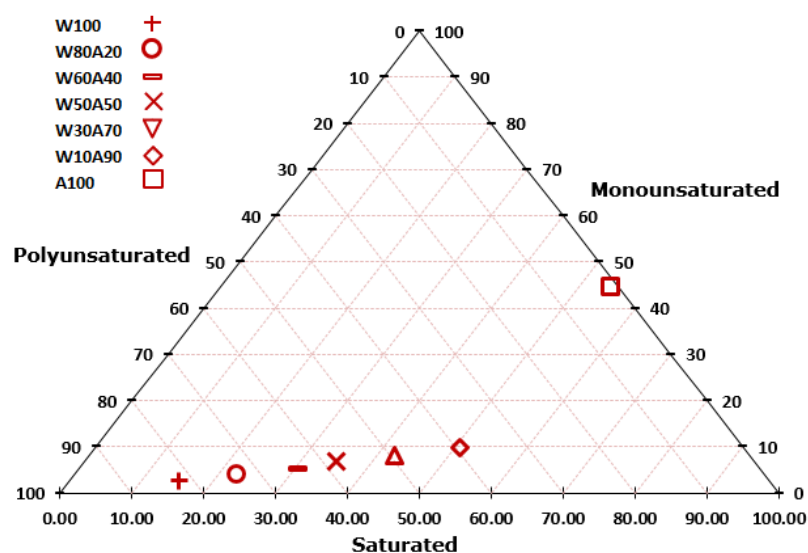
Figure 4.4: Distribution of test samples according to polyunsaturated, saturated and monounsaturated methyl esters, adapted from the author's published paper (Masera and Hossain, 2017).

Figure 4.5 demonstrates the TLC chromatography results of the waste cooking oil, sheep fat and their biodiesel versions. According to Figure 4.5, TAGs were the most dominant compound in the oils. Figure 4.6 also showed that TAGs were main source of the feedstock that was converted into

biodiesel. Note that FFA, DAG and MAG compounds could not be quantified as their concentrations were below the detection point.

(a)   (b)
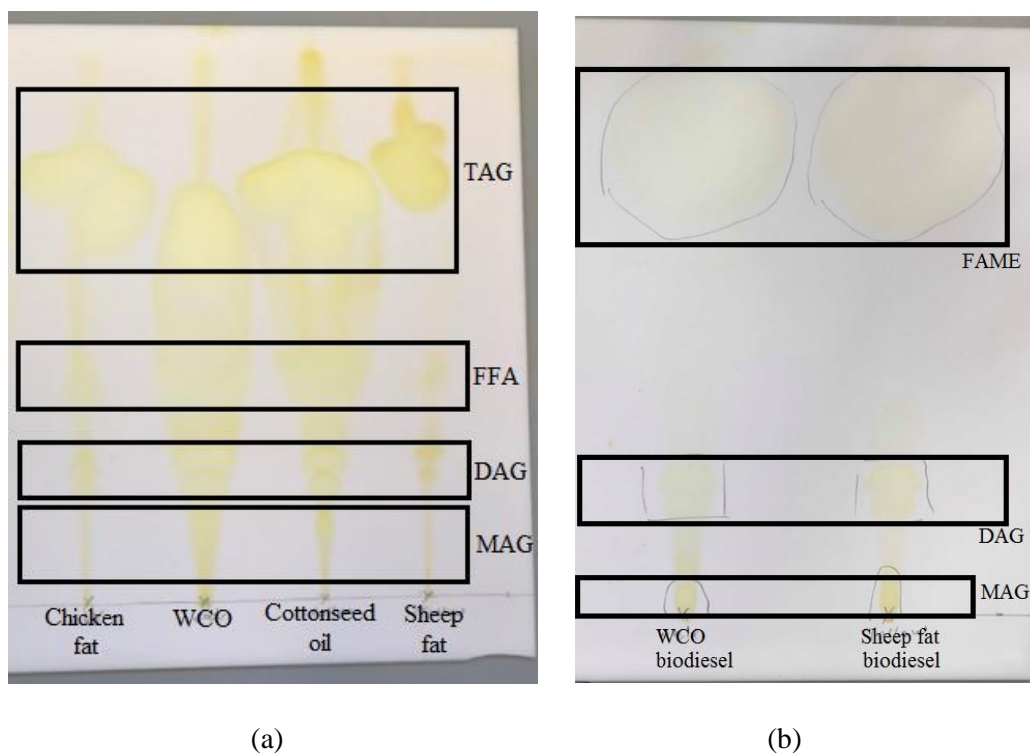
Figure 4.5: Thin layer chromatography (TLC) results (a) feedstock and (b) biodiesel samples.
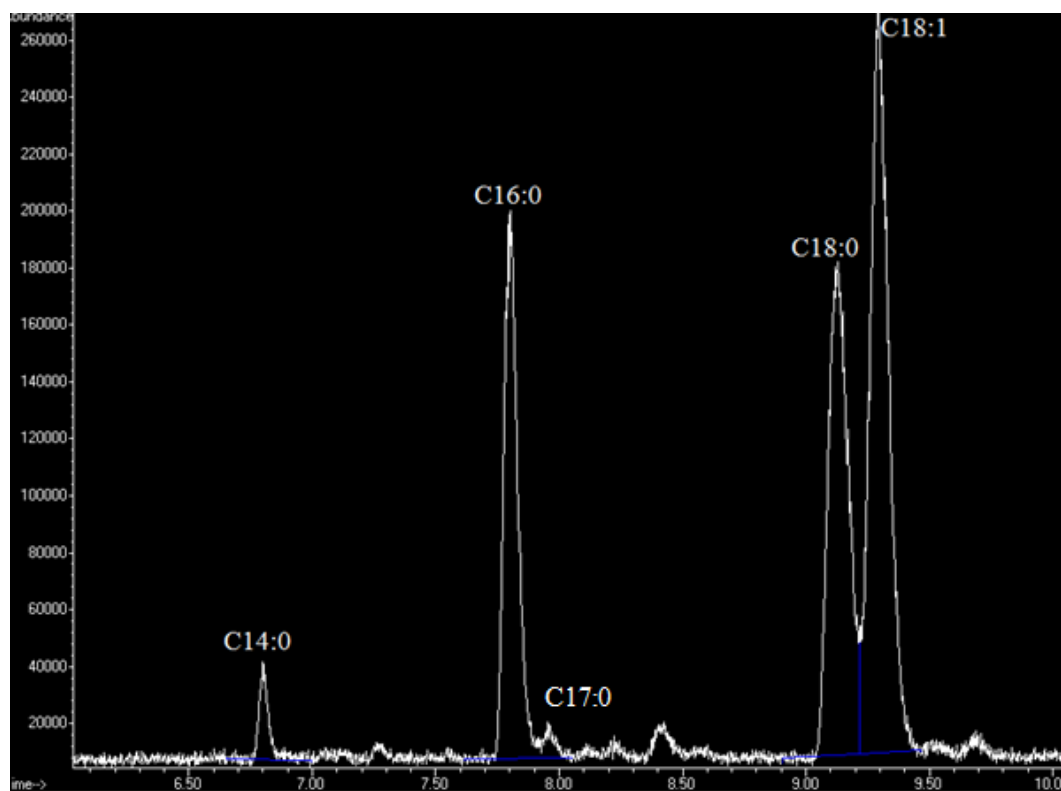
(a)
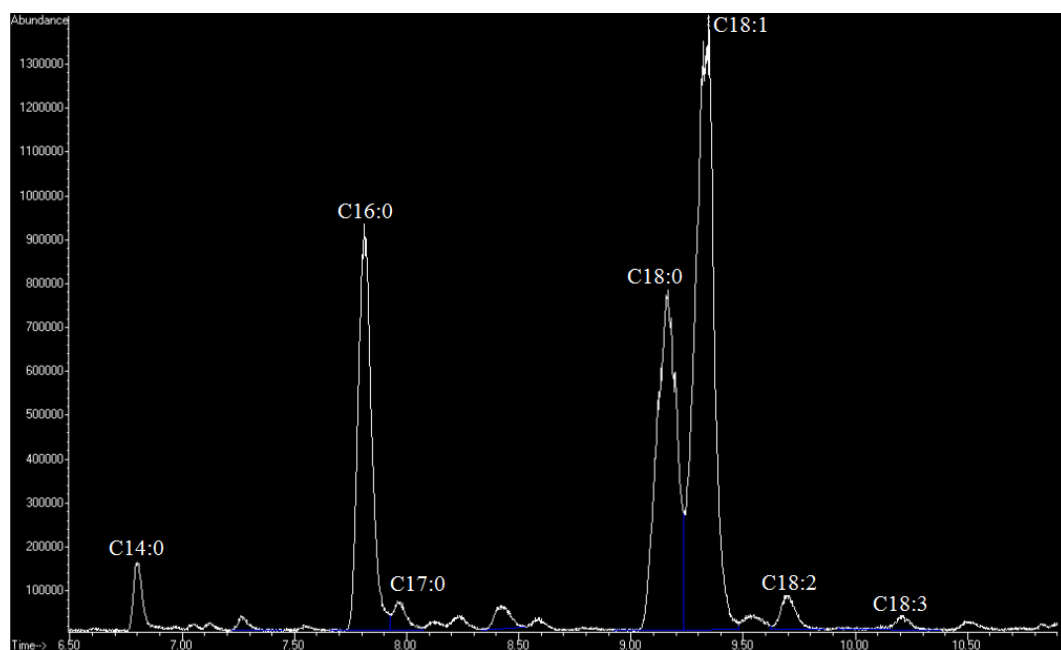
(b)

Figure 4.6: GC-ms results of the (a) Sheep fat TAG and (b) sheep biodoesel FAME. Sheep biodiesel A100 mainly composed of C16:0, C18:0 and C18:1 (C17:0 was added as an internal standard).

Table 4.4 shows the fuel properties of the neat biodiesels, the biomixtures, diesel, British biodiesel standard BS EN 14214 and European diesel standard EN 590 (European Standard EN 590:2013, 2009;

British Standard Institution, 2010). Note that the EN 590 diesel standard allows the presence of 7% biodiesel by volume to be blended with diesel (not shown in Table 4.4). According to measured fuel properties, neither W100 nor A100 satisfied the BS EN 14214 biodiesel standard. For example, W30A70, W10A90 and A100 did not comply with the BS EN 14214 standard in terms of their viscosities higher than 5.0 mm^2/s. Moreover, W100 and W80A20 did not comply with the standard due to cetane numbers being lower than 52 and iodine values being greater than 120. In the light of fuel characterisation analysis, W60A40 and W50A50 were the only two biomixtures meeting the BS EN 14214 standard (Masera and Hossain, 2017).

Table 4.4: Fuel properties of the test fuels along with BS EN 14214 British/European biodiesel standard and EN 590 diesel standard (European Standard EN 590:2013, 2009; British Standard Institution, 2010).

Fuel Properties	Units	Biofuels							Diesel	BS EN 14214 Biodiesel Standard	EN 590 Diesel Standard
		W100	W80A20	W60A40	W50A50	W30A70	W10A90	A100			
Viscosity at 40°C	(mm^2/s)	4.80	4.85	4.90	4.93	5.15	5.33	5.48	2.78	3.5 - 5.0	2.0 - 4.5
Density	(g/cm^3)	0.882	0.880	0.874	0.872	0.870	0.868	0.865	0.828	0.86 - 0.90	0.820 - 0.845
Flash Point	(°C)	169	170	168	168	172	172	170	61.5	min 101	min 55
Cetane number[a]	()	47	50	53	55	58	62	70	53.5	min 51	min 51
Cetane number[b]	()	44	47	51	52	55	58	66	53.5	min 51	min 51
Carbon, theoretical	(%)	77.27	77.16	77.04	76.96	76.84	76.71	76.48	n/a	n/a	n/a
Carbon, measured	(%)	76.56	n/a	77.48	77.1	75.01	n/a	76.89	86.6[c]	n/a	n/a
Hydrogen, theoretical	(%)	11.74	11.84	11.93	11.99	12.08	12.18	12.43	n/a	n/a	n/a
Hydrogen, measured	(%)	11.86	n/a	12.12	12.66	12.58	n/a	12.81	13.4[c]	n/a	n/a
Oxygen, theoretical	(%)	10.99	11.01	11.03	11.05	11.08	11.11	11.09	n/a	n/a	n/a
Oxygen, measured	(%)	11.58	n/a	10.41	10.24	12.41	n/a	10.30	0.07[c]	n/a	n/a
HHV	(MJ/kg)	38.4	39.8	39.5	39.4	39.2	39.0	40.5	45.16	n/a	n/a
LHV	(MJ/kg)	37	37	37	37	37	37	37	42	n/a	n/a
Iodine number	(g/100g)	145	130	116	107	92	77	40	n/a	max 120	n/a
Linolenic acid methyl ester	(%mol/mol)	5.4	4.5	3.6	3.1	2.2	1.3	0.8	n/a	max 12	n/a
Monoglyceride (MAG)	(%mol/mol)	ND	ND	ND	ND	ND	ND	ND	ND	max 0.8	n/a
Diglyceride (DAG)	(%mol/mol)	ND	ND	ND	ND	ND	ND	ND	ND	max 0.2	n/a
Triglyceride (TAG)	(%mol/mol)	ND	ND	ND	ND	ND	ND	ND	ND	max 0.2	n/a
Methanol	(%mol/mol)	0	0	0	0	0	0	0	n/a	max 0.2	n/a
Acid value	(mg KOH/g)	0.200	0.229	0.259	0.289	0.289	0.290	0.291	0.091	max 0.5	n/a
Degree of Unsaturation	(Weight %)	167	150	133	123	107	89	47	n/a	n/a	n/a

a= (Ramírez-Verduzco *et al.,* 2012); b= (Tong *et al.*, 2011); c= (Schönborn *et al.*, 2009); ND= Not detected

Relations between DU-cetane number and DU-viscosity were noticed. For example, viscosity and cetane number of the biofuels were observed to be increasing with the decreasing DU Figure 4.7. This can be due to the chemical structures of the saturated FAMEs such as carbon chain lengths Table 2.1. DU of the biofuels was decreasing by adding more A100 into W100. Thus, the percentage of saturated FAMEs was also increasing (Table 4.3 and Figure 4.4). These results are in good agreement with the literature (Schönborn *et al.*, 2009).
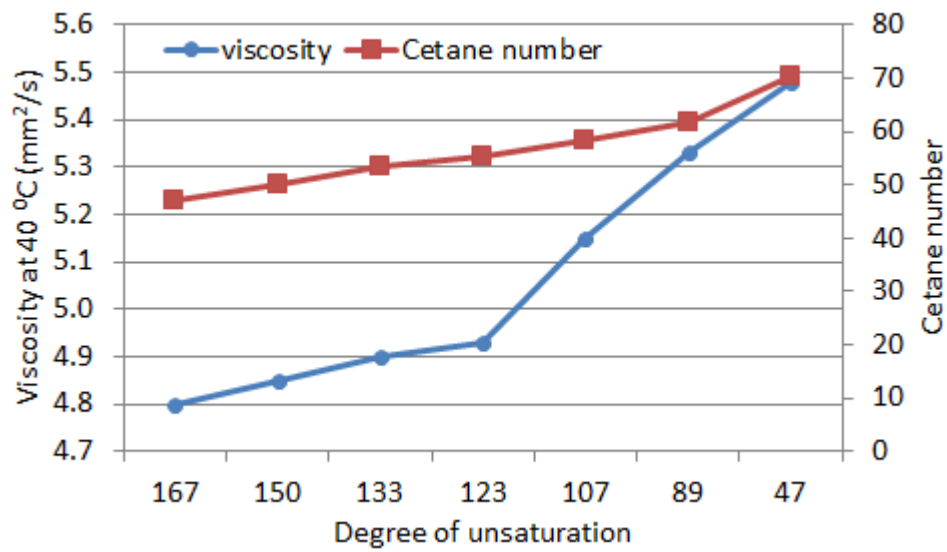
Figure 4.7: Effect of degree of unsaturation on viscosity and cetane number of biodiesel.

Although some biofuels (i.e. W100, W30A70 and A100) did not comply the BS EN 14214 standard, they were also tested in the engine to understand the effect of degree of unsaturation on engine performance, combustion characteristics and exhaust gas emissions. Among the characterised biofuels, W100, W60A40, W50A50, W30A70 and A100 were tested in the engine along with the ULSD diesel as a reference fuel.

4.6. Combustion characteristics and degree of unsaturation

Combustion parameters were collected from the first cylinder of the engine. Various combustion parameters such as combustion start and end times, overall combustion duration, peak knock, in-cylinder pressure, heat release, heat release rate were collected and analysed through KiBoxCockpit software. Averages of 51 consecutive cycles were used to analyse combustion characteristics of the test fuels.

Figure 4.8 presents combustion (a) start (b) finish times, and (c) total combustion duration in terms of crank angle position. From Figure 4.8 (a) it can be understand that combustion of the test fuels started almost at the same crank angle at each engine load. However, combustion end time increases with respect to increasing engine load Figure 4.8 (b), as the amount of fuel consumed increased to overcome increased resistance. This increase in combustion end time affects the overall combustion duration which was also increased with respect to increasing engine load Figure 4.8 (c). Figure 4.9 studies the ignition delay and combustion durations of the test fuels including the diesel.

Results also showed that there was a relatively long ignition delay period for all fuels. In other words, combustion took place after about 4 °CA Top Dead Centre (TDC), which was not the desired scenario and shows that the injection system of the engine shall be rearranged. Under the mentioned circumstances, biodiesels having higher cetane number than diesel (Table 4.4) performed slightly shortened ignition delay periods. Presumably, ignition delays of the biofuels would be better than that of diesel with an advanced fuel injection arrangement of the engine. It was also presumed that biofuels would provide even shorter ignition delays than diesel in a direct injection engine.
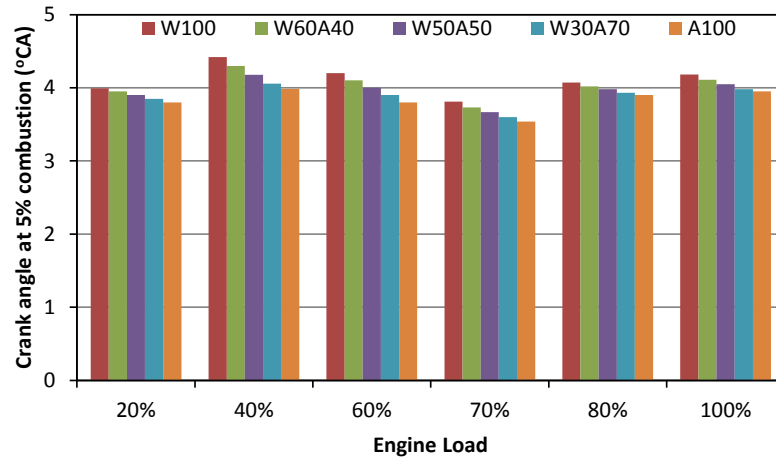
(a)
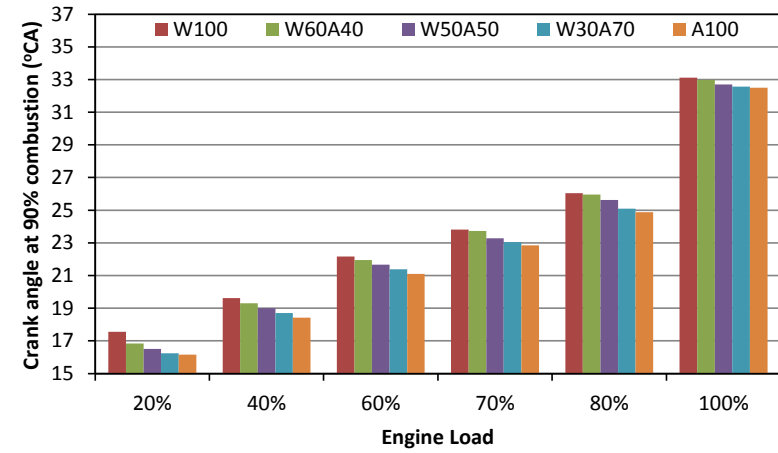
(b)
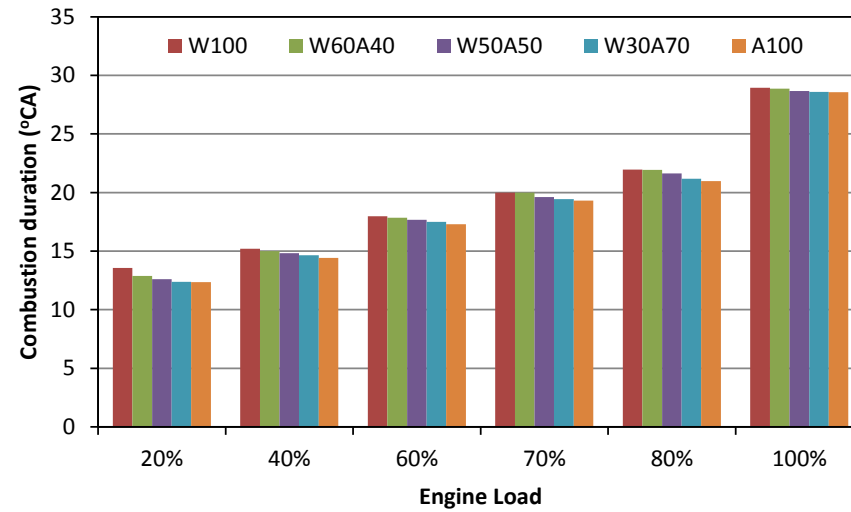
(c)

Figure 4.8: Crank angle positions at different stages of the combustion; (a) at the beginning, (b) at the end, and (d) total combustion duration.
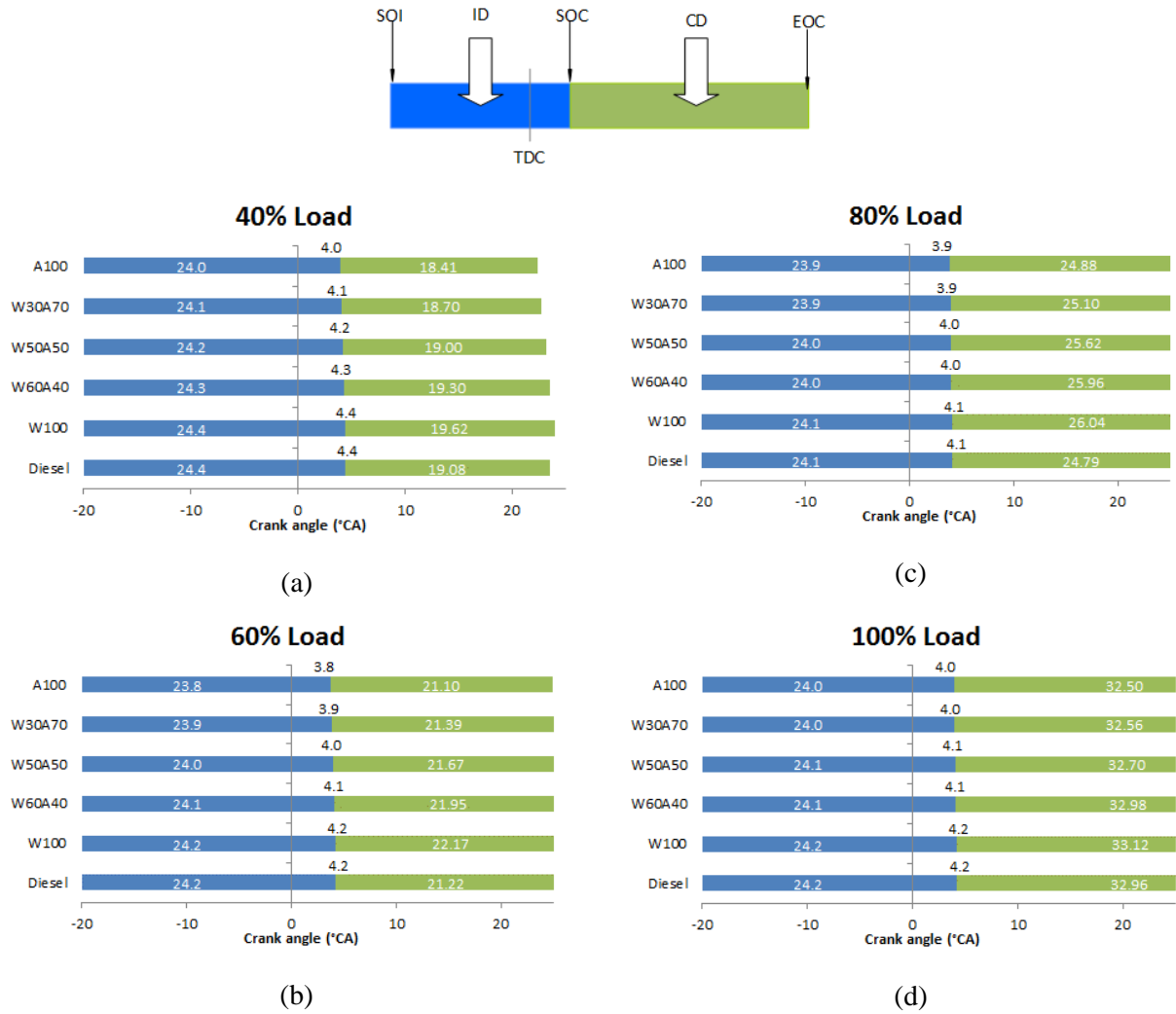
Figure 4.9: Ignition delay and combustion durations with respect to crank angles at 40%, 60%, 80% and 100% engine loads.

The influence of the degree of unsaturation on ignition delay and total combustion duration were investigated in detail at 40% and 80% engine loads at 1500 rpm (Figure 4.10 and Figure 4.11). Results indicated that the ignition delay reduces with the reducing DU. The highest ignition delay was observed as 24.03 °CA for W100, which was 7% higher than that of A100 at 40% engine load (Figure 4.10). Similarly, total combustion duration also reduced for the low DU biodiesels (Figure 4.11). At 40% engine load, the highest combustion duration was observed as 15.20 °CA for the W100 and it decreased with the 0.2 °CA decrements for W60A40, W50A50, W30A70 and A100 which had DU's of 133, 123, 107 and 47, respectively. The decreasing trend was the same at the 80% load operation but with decrements of approximately 0.5 °CA between the biomixtures. The decreasing ignition delay and combustion duration trends with respect to decreasing DU were in good agreement with the literature (Schönborn *et al.*, 2009;

Benjumea *et al.*, 2011; Li *et al.*, 2018). This was attributed to increased cetane number of the biodiesels in the literature. However, relatively complex molecular structures of saturated FAMEs like having double bonds should also be considered. It was assumed that high DU FAMEs take longer time to burn due to the extra time/energy spent for breaking the double bunds.

(a)   (b)
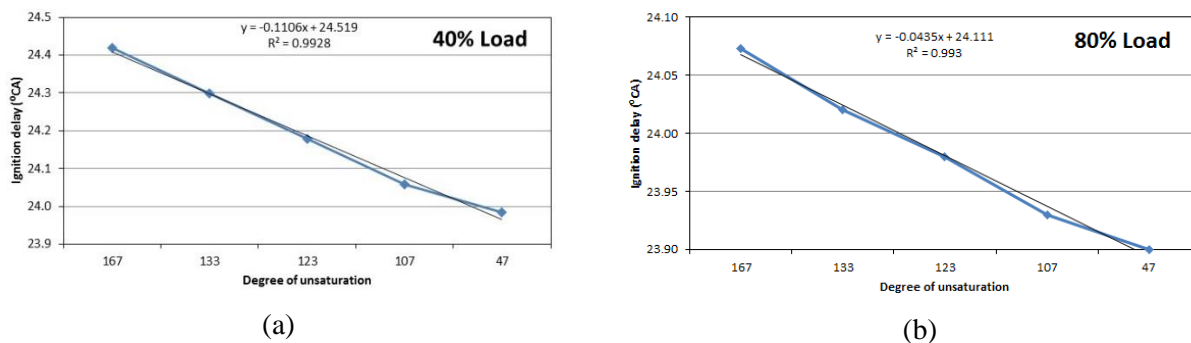
Figure 4.10: Effect of degree of unsaturation on ignition delay at 40% and 80% engine loads.

(a)   (b)
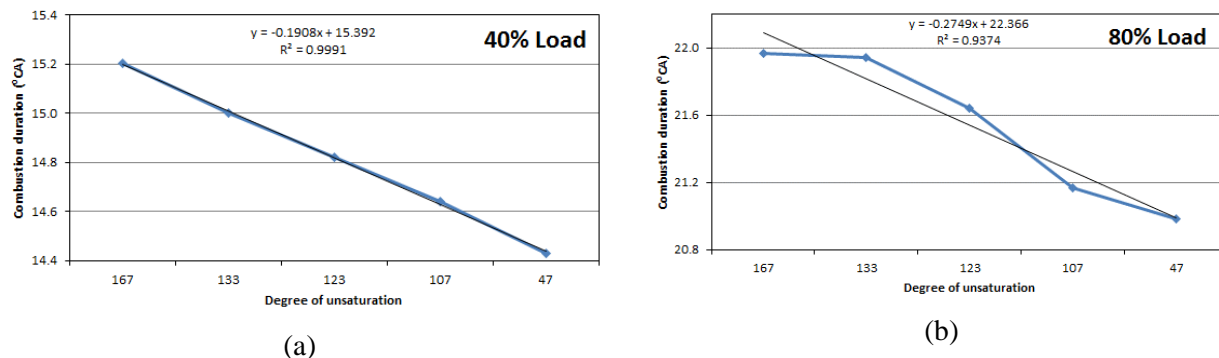
Figure 4.11: Effect of degree of unsaturation on combustion duration.

Engine knocking is a vital parameter for the smooth operation of an engine. Zhen *et al.*, (2012) reviewed various methods to measure this parameter which were analysis based on in-cylinder pressure, the vibration of the engine block, the temperature of the exhaust gases, heat release and intermediate radicals and species. In this study, engine knocking was investigated through the in-cylinder pressure. According to the peak knock results provided in Figure 4.12, it can be reported that the engine was running smoothly on every test fuel. Peak knockings were in the order of 0.1 and 0.2 bars which were negligible for the engine operating around 70 bar in-cylinder pressure. It was also noticed that biofuels burned smoother at the higher engine loads (above 70%). This small knocking at low engine loads can be attributed to higher

viscosities and densities of the biofuels which cause relatively poor atomisation properties at lower temperatures compared to diesel. It was also believed that the test engine was not responding well at low engine loads as it has indirect injection system and a relatively high compression ratio of 1:23.5. Moreover, late fuel injection could cause some peak knock fluctuations especially at the low engine loads; where the effect of high viscosity biofuels (i.e. W30A70 and A100) observed more dominant under low combustion temperatures.
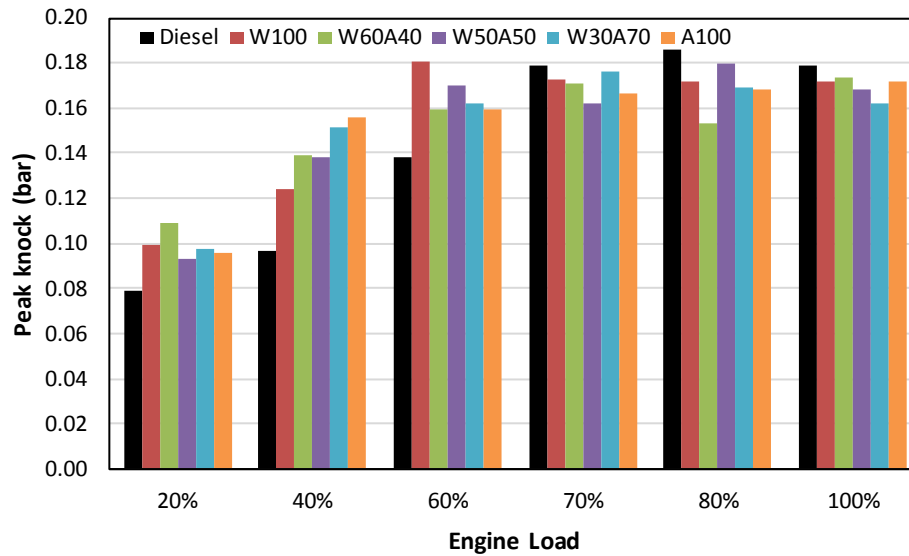
Figure 4.12: Peak knock at different engine loads.

Exhaust gas temperature (EGT) was increasing almost linearly with the increased engine load (Figure 4.13). This was because of the longer combustion durations at the higher engine loads (Emiroğlu *et al.,* 2018). Longer combustion duration may cause a significant amount of fuel to be burned at the late power stroke where the volume is getting larger, hence released energy creates less impact on the pressure applied on piston head (Awad *et al.,* 2014). Note that it is also known that high EGT negatively effects the NO_x emissions (Dhamodaran *et al.*, 2017). This is because of the combining tendency of oxygen and nitrogen molecules to at higher temperatures. The results also indicate a reducing exhaust gas temperature with respect to decreasing DU of the biofuels. To illustrate, exhaust gas temperatures of 215°C, 211°C, 209°C, 206°C and 206°C were reported for W100, W60A40, W50A50, W30A70 and A100 at 70% engine load, respectively.
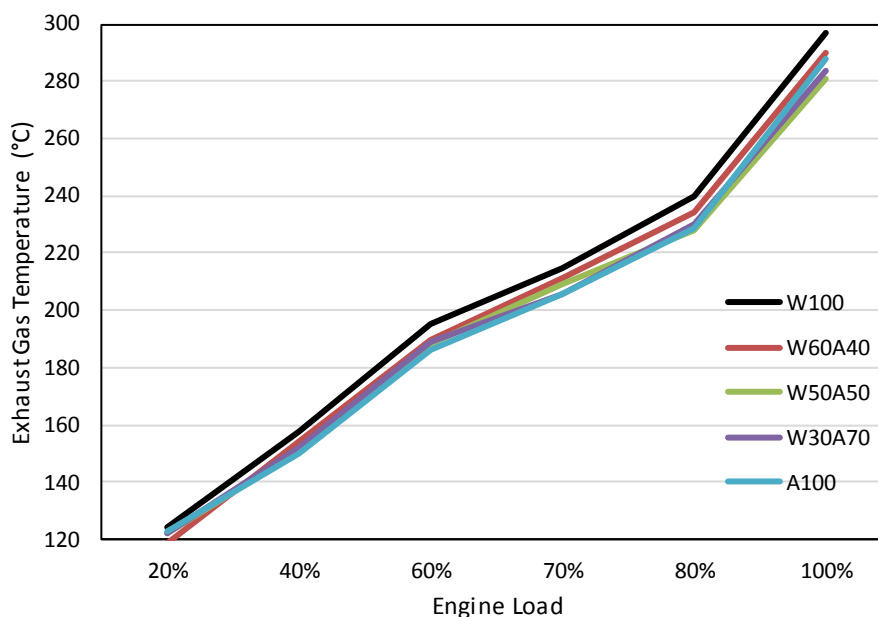
Figure 4.13: Exhaust gas temperatures of biofuels at different engine loads.

According to the in-cylinder results, all biofuels provided higher in-cylinder pressure, by a few bars, than the diesel as a result of improved combustion due to their inherent oxygen contents (Figure 4.14). Among the biofuels, W50A50 provided the maximum pressure at almost every engine load. For example, the peak in-cylinder pressure of W50A50 was 67.9 bar at 10.5 °CA, 68.9 bar at 10.3 °CA and 67.5 bar at 12.0 °CA which were 4.3%, 5.2% and 2.8% higher than both neat biodiesels at 70%, 80% and 100% engine loads, respectively. This was deemed to its optimised fuel properties which provide relatively medium viscosity (4.93 mm^2/s) and relatively medium DU of 123 (34.9% saturated, 7.0% monounsaturated and 58.1% polyunsaturated). At the 20% engine load, W60A40 was the other well-performing biomixture after the W50A50 in terms of maximum in-cylinder pressure. The reason was again the optimised fuel properties. Optimised fuel characteristics of biomixtures such as DU and viscosity, lead to optimum molecular structure (carbon chain length, number of double bonds) and atomisation characteristics of the fuel molecules to create best in-cylinder pressure. However, at 60% engine load, highly saturated biofuels like W30A70 and A100 provided in-cylinder pressure as 66 bar which was at the level of W50A50. This can be explained by the reduced viscosities of the highly saturated biofuels at the high temperatures of the higher engine load. At the 80% engine load, W50A50 provided approximately 2 bar higher peak in-cylinder pressure at around 10 °CA aTDC compared to other fuels. To sum up, in-cylinder pressure analysis demonstrated that biodiesel-biodiesel blends (biomixtures) could provide slightly higher peak in-cylinder pressures compared to their neat biodiesel versions due to optimised fuel properties. For example,

maximum peak in-cylinder pressure was observed by W50A50 and W30A70 which was 2 bar (2.9%) higher than the neat biodiesels and diesel at 100% load.
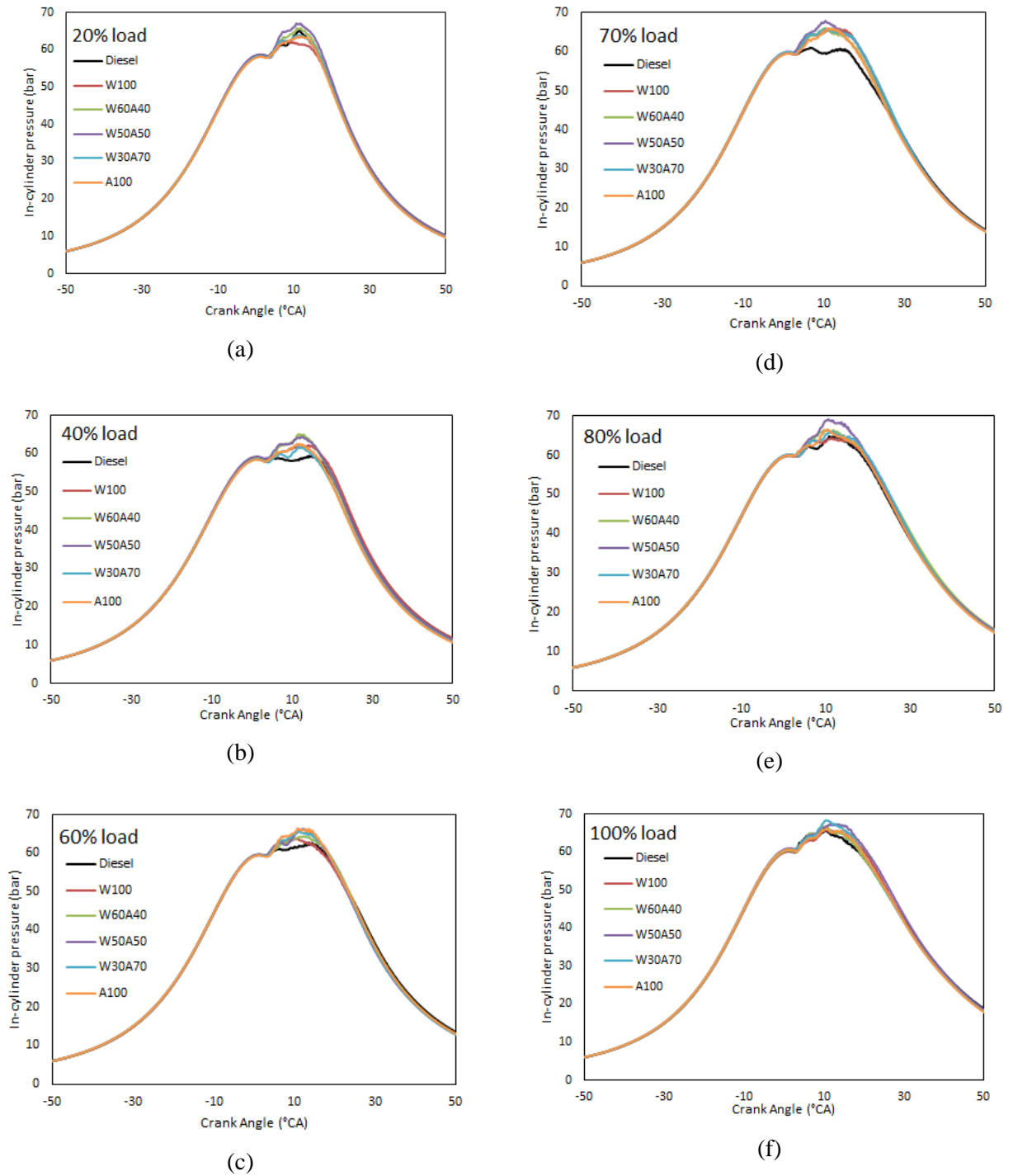
Figure 4.14: In-cylinder pressures versus crank angle for all test fuels at different engine loads.

Figure 4.15 demonstrates the heat release (HR) of the test fuels with respect to crank angle at different engine loads. Negative heat release values just before the combustion can be attributed to evaporation of the fuel (Bowden *et al.,* 1969). At 20% engine load, it was observed that W60A40 and W50A50 biomixtures provided around 10 joules and 20 joules higher HR than the diesel at each crank angle (during the combustion period). At the initial phase of combustion, the lowest DU biodiesel A100 had the highest HR approximately 4% higher than other fuels at almost all engine loads. For example, A100 had 15 joules higher HR than average of other fuels at 7°CA at 60% engine load. On the other hand, A100 had 5.5% lower HR than the other fuels towards the end of combustion i.e. released 20 joules less than the average of other fuels at 35°CA at 60% engine load. The results were almost the same for the 80% engine load too. In contrast, highly unsaturated biodiesel W100 which contains only 15.1% saturated FAMEs exhibited better heat release performance towards the end of the combustion rather than at the initial phase. This was due to the number of double bonding in FAMEs and cetane number. As it consumes more energy and time to break down the second bonds, energy release on highly saturated biofuels like A100 and W30A70 was more significant at the beginning of the combustion period. On the other hand, HR of the highly DU W100 was more effective towards the end of the combustion period. Ultimately, it can be concluded that lower DU biodiesels had quicker and higher HR at the early phase of the combustion, whereas higher DU biofuels had higher HR at the late combustion phase.
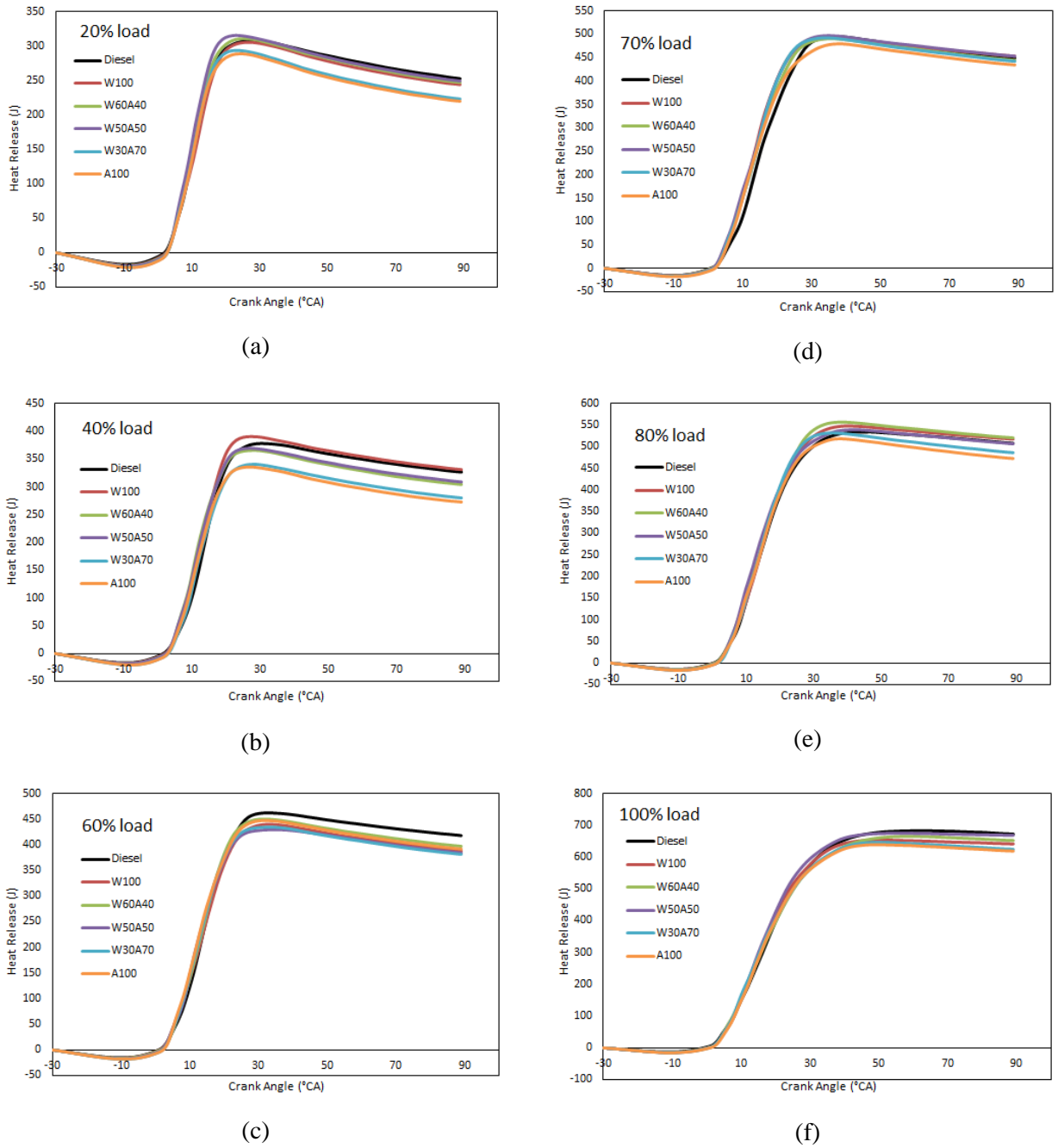
Figure 4.15: Heat release of the test fuels at various engine loads.

Figure 4.16 shows the heat release rates (HRR) of the test fuels at different engine loads at 1500 rpm. Biodiesels had higher HRR than the diesel at almost all engine loads due to their oxygen content. The rapid burning at the premixed combustion phase was due to higher cetane numbers of the biofuels compared to diesel Table 4.4. The HRR trends of the biofuels were similar at all loads. The low DU

biodiesels such as A100 and W30A70 found to be burning rapidly at all engine loads because of the easier breakdown of the saturated FAME molecules and high cetane numbers. However, their maximum HRR (25 J/°CA at 20% engine load) at low engine loads were not as much as at the high engine loads (30 J/°CA at 100% engine load) due to their relatively higher viscosities and densities. The effect of DU on maximum HRR was investigated at 80% load for the biomixtures. According to Figure 4.17, the maximum HRR values were 27.8 J°CA, 28.4 J°CA and 29.6 J°CA for W60A40, W50A50 and W30A70, respectively. The similar increasing maximum HRR trend for the decreasing DU was also observed on 70% engine load. However, according to results shown in Figure 4.17, W50A50 biomixture gave the highest maximum heat release rate as 32 J/°CA at the full engine load. The heat release rate results also show that optimised fuel properties like DU, density, viscosity, cetane number and carbon chain length could provide optimum combustion characteristics at all engine loads.
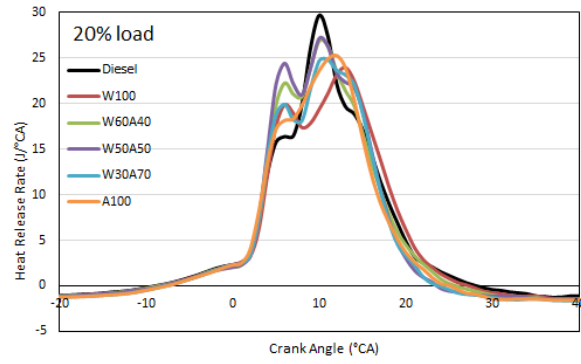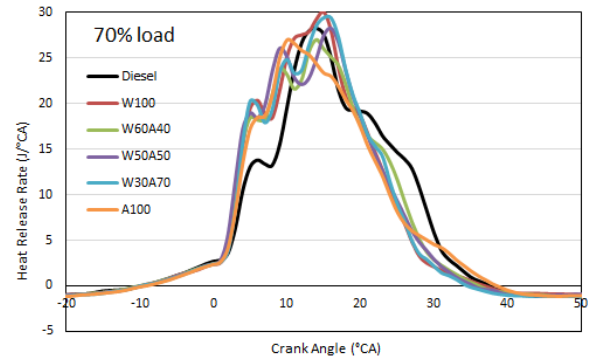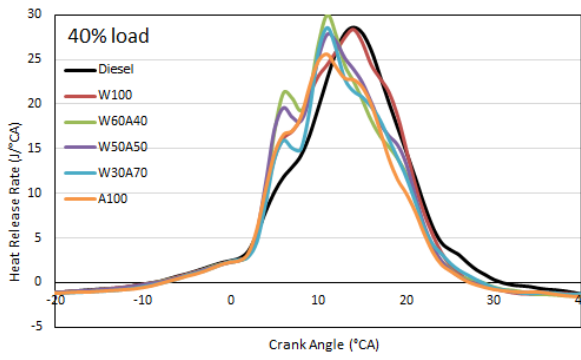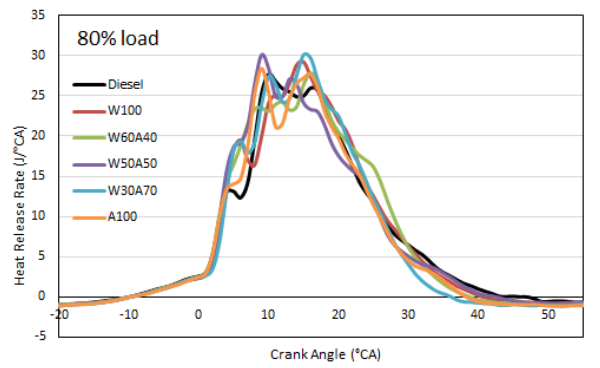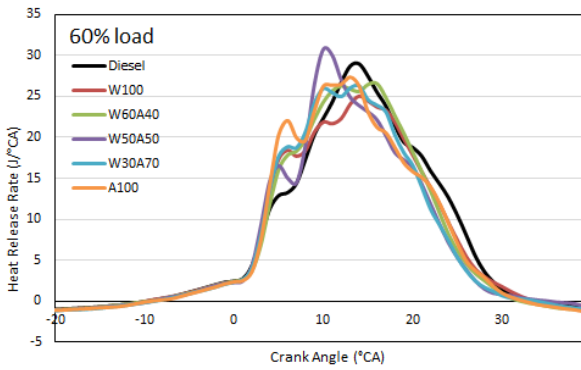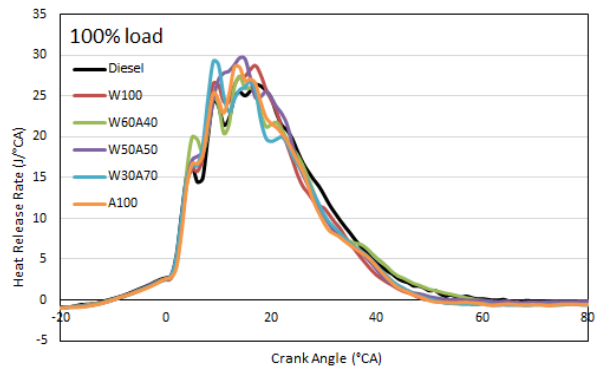
Figure 4.16: Heat release rate of test fuels vs crank angles at different engine loads.
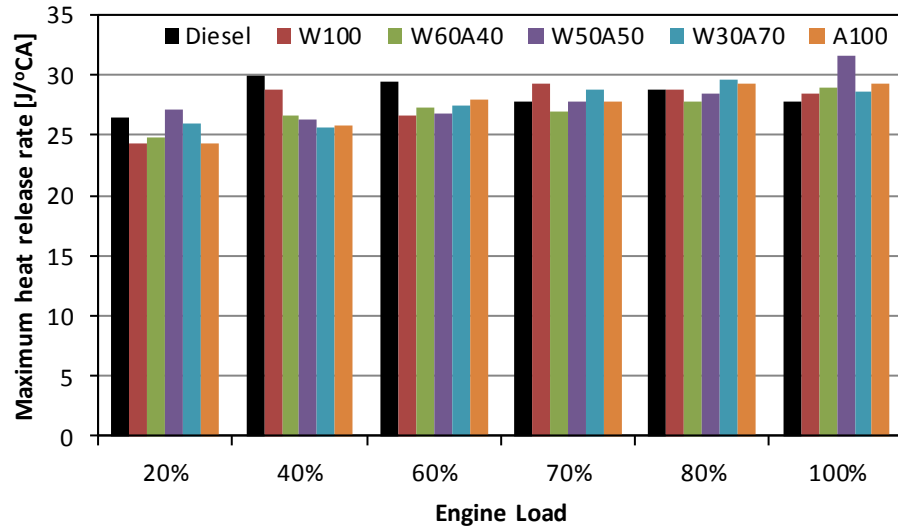
Figure 4.17: Maximum heat release rate of the test fuels at different engine loads.

4.7. Engine performance and degree of unsaturation

Brake specific fuel consumption (BSFC), Brake Specific Energy Consumption (BSEC) and Brake Thermal Efficiency (BTE) of the indirect injection CI engine operating at 1500 rpm were measured and analysed in the scope of engine performance evaluation. Figure 4.18 demonstrates the BSFC of the test fuels at different engine loads. All biodiesels had higher BSFC than diesel at every engine load. This was in good agreement with the literature and can be linked to lower LHV of biodiesels (Özener *et al.*, 2014). The differences between each BSFCs were similar as 1% at the lowest engine load. A100 had the highest BSFC as 0.433 kg/kWh, followed by W30A70 with 0.426 kg/kWh, W50A50 with 0.412 kg/kWh, W60A40 with 0.400 kg/kWh, W100 with 0.390 kg/kWh and diesel with 0.369 kg/kWh at 40% engine load. The biofuels having low DU values like A100 and W30A70 had the same BSFC value of 0.36 kg/kWh which was approximately 2.8% higher than the other biodiesels at 60% engine load. The differences between the BSFC values of the biofuels were decreasing and approaching to zero as the engine load increased. Hence, there was no BSFC difference among the biodiesels at the full load. It was very clear that DU had not a significant effect on the BSFC at medium and high engine loads as the BSFC values were very close to each other. The slight difference at the low engine loads can be attributed to relatively highly viscosities of low DU biodiesels. Due to the poor combustion characteristics of relatively low DU biodiesels like A100 and W30A70 at low engine loads, more amount of fuel consumed to provide the same power output compared to relatively less saturated fuels. W100 and W50A50 were the best

116

performing biofuels by having 3.4%, 5.1% and 8.5% less BSFC than W60A40, W30A70 and A100, respectively; but 6.8% higher BSFC than the diesel at the lowest engine load. As the combustion temperature increases proportionally to engine loading, viscosities of the A100 and W30A70 biofuels reduced and similar BSFC levels with the other biofuels achieved after 70% engine load. However, average BSFC of the biodiesels was 14.5% higher than diesel at medium and high engine loads. This can be attributed to the low LHV of the biofuels which caused more amount of fuel to be burned in order to provide the same power output with the diesel operation. Unlike the lowest engine load condition, A100 having the lowest DU biodiesel provided the lowest BSFC which was 3.2% less than that of W100.
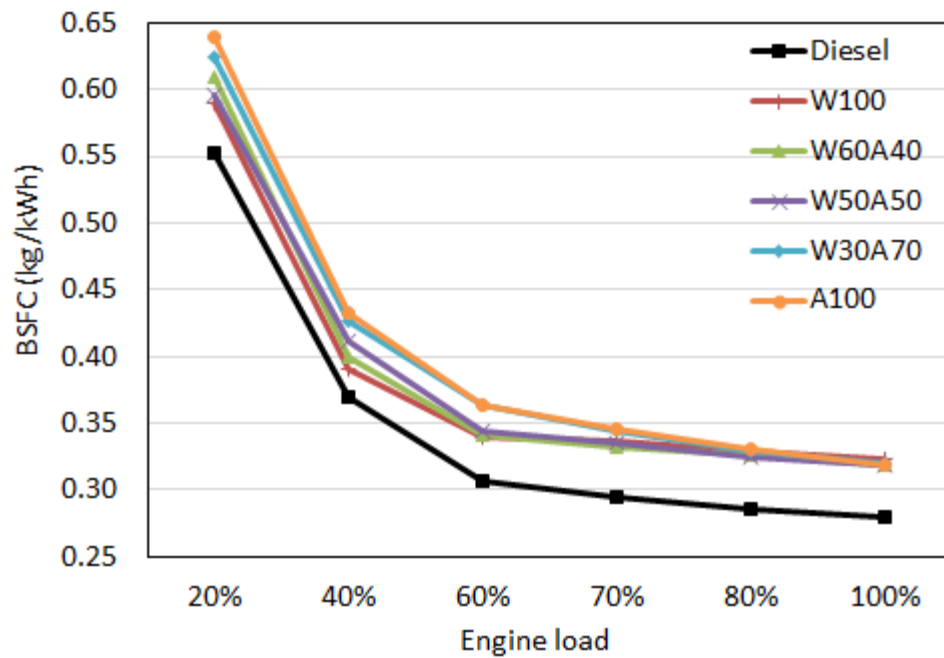
Figure 4.18: Brake specific fuel consumptions of the test fuels at different engine loads.

Although BSFC's of the biodiesels were analysed, BSEC analysis was also crucial as the compared fuels had different LHV properties (Krishna *et al.*, 2016). Unlike BSFC analysis, BSEC did not only consider the amount of fuel consumed but LHV were taken into account. According to BSEC analysis provided in Figure 4.19, the energy consumptions of the biodiesels were comparable with the diesel. Moreover, relatively high DU biodiesels W100, W60A40 and W50A50 had around 1.9% lower BSEC than the diesel at 60% engine load. Comparing the BSEC's of the biodiesels at the low and medium engine loads, A100

had the highest BSEC as 16.0 MJ/kWh, followed by W30A70 with 15.6 MJ/kWh, W50A50 with 15.1 MJ/kWh, W60A40 with 14.8 MJ/kWh and W100 with 14.5 MJ/kWh at 40% engine load.
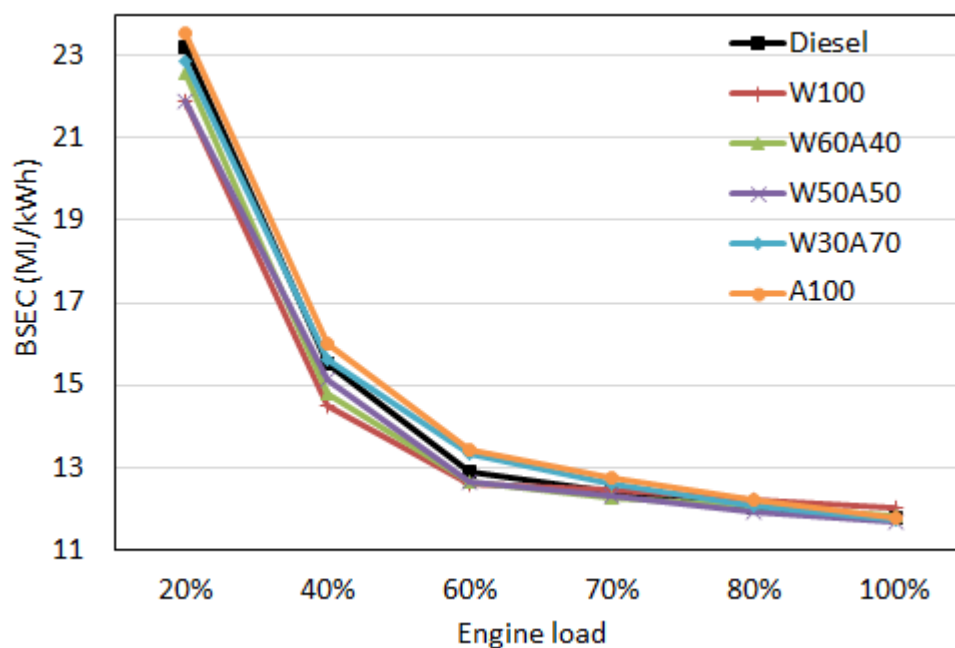
Figure 4.19: Brake specific energy consumptions of the test fuels at different engine loads.

Figure 4.20 illustrates the BTE of the engine operating at 1500 rpm at different loads. The highest DU biodiesel W100 had the highest BTE which was 8% and 10% greater than the diesel and the lowest DU biodiesel A100 at medium engine loads, respectively. Moderate DU biomixtures such as W60A40 and W50A50 exhibited approximately 2% higher BTE than the diesel between 20% and 60% loads. The presence of oxygen in molecular structures of the biodiesels believed to be the main reason for improved BTE. However, A100 and W30A70 addressed 3.3% and 3.0% lower BTE than the diesel at 60% load. This was due to their limited combustion characteristics due to high viscosities at low combustion temperatures. On the other hand, at the highest engine load, W100 with high DU provided 2% lower BTE than all other fuels. This could be due to the energy loss to breakdown excessive double bonds for unsaturated FAMEs.
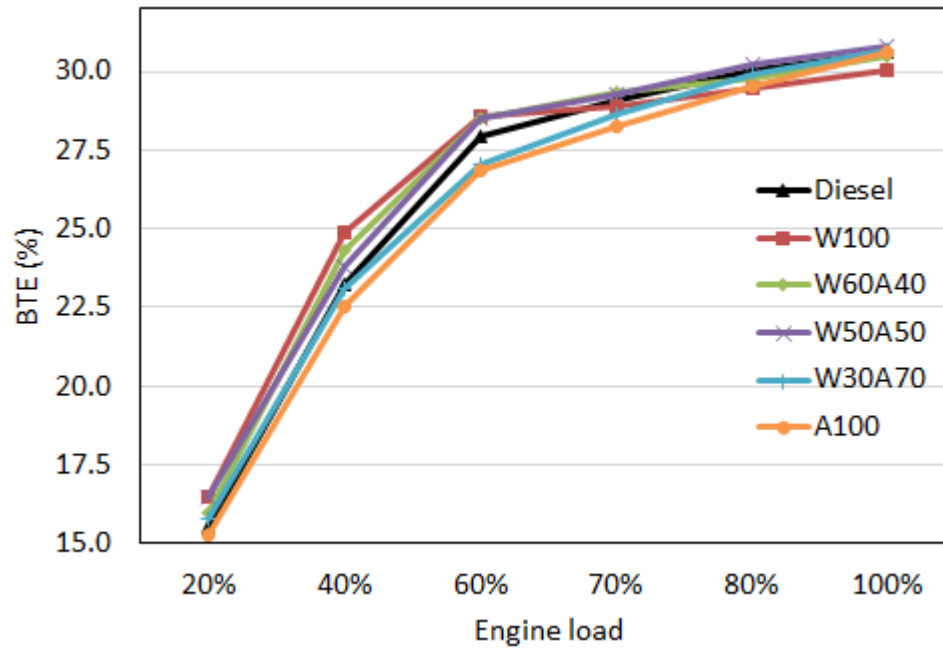
Figure 4.20: Brake thermal efficiency at different engine loads.

To sum up, all biodiesels performed almost the BSEC and comparable BTE among themselves and diesel, especially at the full load. Therefore, no significant effect of DU was observed on the engine performance parameters. This finding also matches with the literature (Lapuerta and Armas, 2009; Benjumea *et al.*, 2011; Altun, 2014; Dhamodaran *et al.*, 2017).

4.8. Exhaust emissions and degree of unsaturation

In the scope of exhaust gas analysis, CO, CO_2, NO, NO_2, NO_x and smoke opacity emissions were analysed for all biodiesels and compared to diesel emissions. Simultaneous readings were collected in %volume for CO and CO_2; and ppm for NO and NO_x emissions. In addition, data was also collected in grams for a defined time interval after the steady-state condition. Effects of DU on the mentioned emissions were investigated in detail. To contribute to the literature, not only the different biodiesels (i.e. W100 and A100) but also the biomixtures (i.e. W60A40, W50A50 and W30A70), which were blends of the two neat biodiesels, were analysed to have a deep understanding on DU. In this way, all changes on the exhaust gas emissions were solely caused by the direct effect of the DU property.

Carbon content, oxygen content and burning efficiency are the three main factors which effect the CO_2 and CO emissions (Kumar and Subramanian, 2017). Hence, CO_2 emission of any fuel shows its combustion efficiency. During the combustion process, carbon atoms oxidise with the presence of oxygen and form CO and CO_2 gases sequentially. Under these circumstances, lack of oxygen prevents the second phase of the oxidation and carbon atoms release as CO before turning into CO_2 (Wakode and Kanase-Patil, 2017). CO_2 Results of all fuels indicated linear increases on CO_2 emissions with the increasing engine loads Figure 4.21 and Table 4.5. This was due to the increasing amount of fuel with the engine load. It was also observed that all biofuels, except W100, released around 6% (15 g/100s at full load) reduced CO_2 than the diesel on average. W50A50 biomixture provided 3.6% and 6.7% reduced CO_2 emission compared to diesel and W100 respectively at the full load. W100 had the highest CO_2 emission at 240.4 g/100s and it was the only biodiesel having the CO_2 emission greater than the diesel by 3.1%. All other biodiesels like W60A40, W50A50, W30A70 and A100 released 1.8%, 3.3%, 2.6% and 2.9% lower CO_2 emissions than diesel at the full load condition respectively. The effect of degree of unsaturation on CO_2 emission was investigated by comparing the CO_2 emissions of the biomixtures at 80% and 100% engine loads Figure 4.22. According to results, no significant change in CO_2 emissions was observed at biomixtures having DU range between 167 and 123. The largest CO_2 emission changes were only 1 g/100s (0.005%) and 3 g/100s (0.013%) at 80% and 100% engine loads.
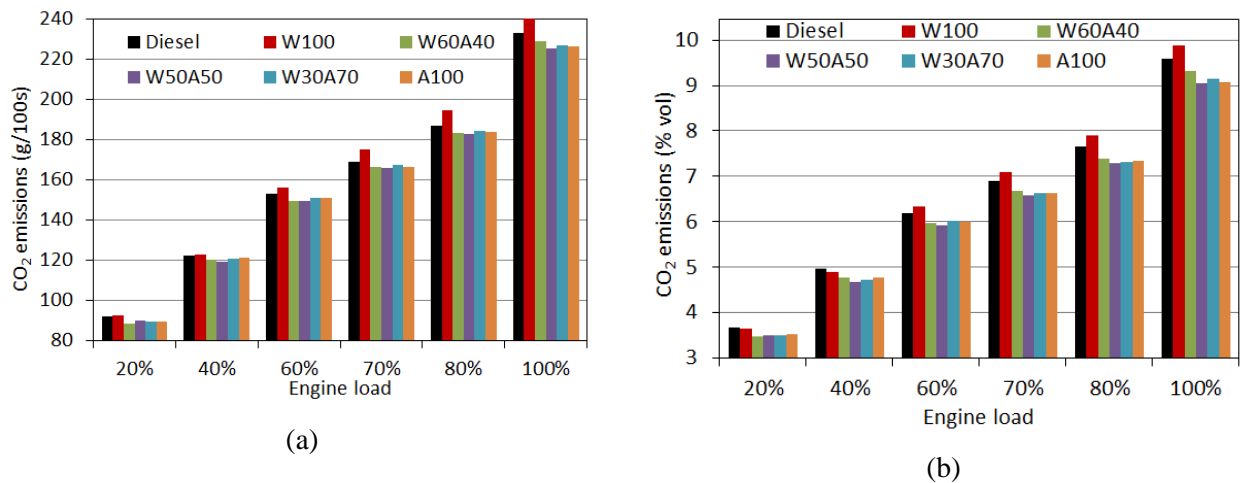
Figure 4.21: CO_2 emissions of test fuels in (a) g/100s and (b) % volume.

Table 4.5: Mass (gram) of CO_2 emitted in 100 seconds.

Fuel	Engine load					
	20%	40%	60%	70%	80%	100%
Diesel	92.3	122.3	152.9	169.0	186.8	232.9
W100	92.6	122.8	156.0	175.3	194.5	240.4
W60A40	88.4	120.4	149.6	166.3	183.1	228.8
W50A50	89.8	119.0	149.6	165.6	182.8	225.3
W30A70	89.5	120.6	150.8	167.1	184.0	226.8
A100	89.7	121.2	150.9	166.3	183.9	226.0

(a)   (b)
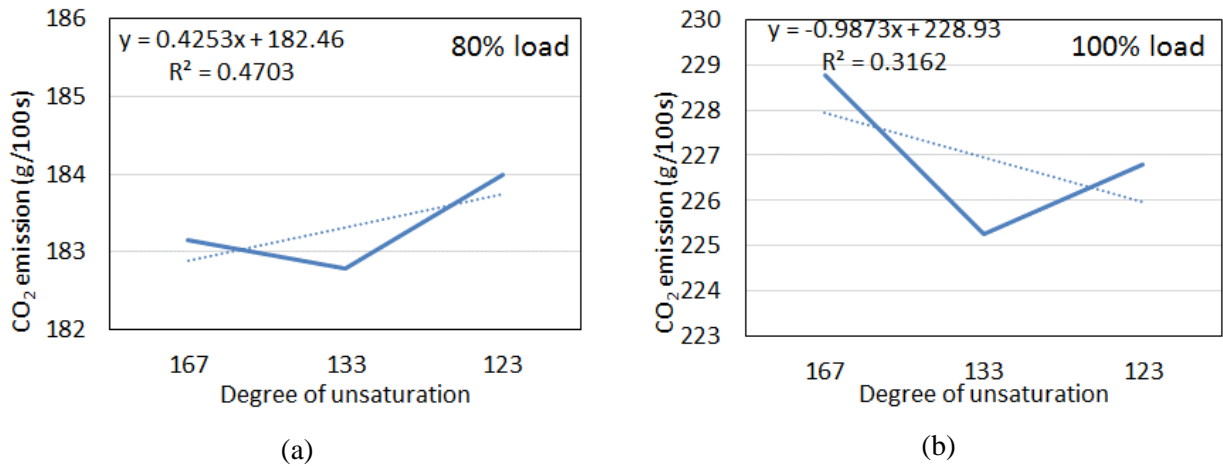
Figure 4.22: Effect of degree of unsaturation on biodiesel's CO_2 emission at (a) 80% and (b) 100% engine load.

Figure 4.23 presents CO emissions of the test fuels in grams per 100 seconds. Like CO_2, CO emissions were also increasing with the engine load. This can be explained by the increased fuel content and combustion duration at high engine loads. Although the majority of biodiesels emitted lower CO than the diesel at all engine loads, W100 had approximately 0.30 g/100s higher CO than the other biodiesels. It can be concluded that W100 had relatively poor combustion efficiency when compared to other biodiesels. Moreover, W100 had the highest carbon content among the biodiesels. The highest DU biodiesel W100 had the highest CO emission as 0.461 g/100s and it was followed by the other biodiesels; W60A40 of 0.132 g/100s, W50A50 with 0.127 g/100s, W30A70 with 0.123 g/100s and A100 with 0.109 g/100s at 80% engine load. All of these CO emissions were lower than that of diesel by 5.9%, 73.0%, 74.2%, 74.8% and 77.7% respectively. The slight differences in biodiesels CO emissions were also due to variation in their carbon contents Table 4.4. For example, it was noticed that the carbon content of the biomixtures decreased with the increasing percentage of A100 in the blend, which in turn resulted in lower carbon

atoms to form CO emission. Hence, A100 with the lowest carbon content and DU provided the least CO emissions, which was 67% (approximately 0.35 g/100s) less than the diesel at low and medium engine loads Figure 4.23 and Table 4.6. W50A50 found to be least CO emitting fuel as 0.211 g/100s at full engine load which was 70% and 63% lower than the diesel and W100 at the full load.
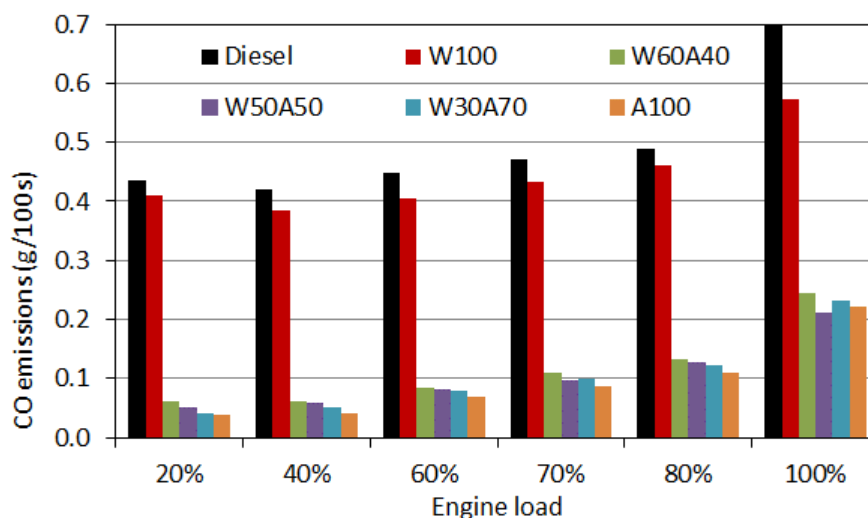
Figure 4.23: CO emissions of the test fuels in g/100s.

Table 4.6: Mass (grams) of CO emitted in 100 seconds.

| Fuel | Engine load | | | | | |
	20%	40%	60%	70%	80%	100%
Diesel	0.437	0.420	0.447	0.471	0.490	0.696
W100	0.410	0.385	0.406	0.432	0.461	0.574
W60A40	0.062	0.060	0.084	0.110	0.132	0.244
W50A50	0.052	0.059	0.082	0.096	0.127	0.211
W30A70	0.042	0.051	0.080	0.099	0.123	0.232
A100	0.039	0.042	0.070	0.088	0.109	0.222

The effect of degree of unsaturation on CO emission was investigated by comparing the CO emissions of the biomixtures at 80% engine loads Figure 4.24. According to the results, CO was slightly increased with increasing DU. The highest CO emission increases were of 3.8% and 5.3% at 80% and 100% engine loads. This can be attributed to increasing the carbon content of the biomixtures with the increasing DU. It can be concluded that the carbon content of any fuel has more impact than its DU on CO emission.
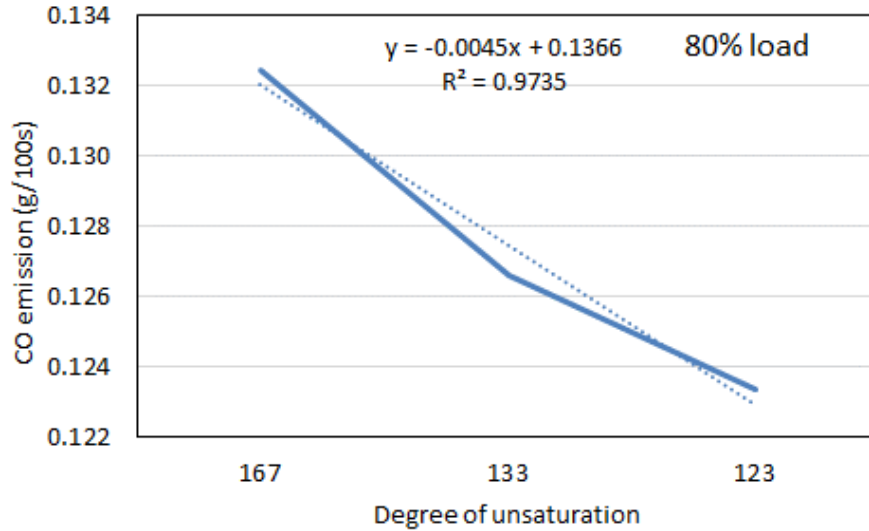
Figure 4.24: Effect of degree of unsaturation on biodiesel's CO emission at 80% engine load.

Figure 4.25 and Table 4.7 illustrates the NO, NO_2 and NO_x measurements of the test fuels at different engine loads. NO_x was the combination of the nitrogen oxide (NO) and nitrogen dioxide (NO_2) emissions. Unlike CO_2 and CO emissions, all biodiesels emitted higher NO and NO_x emissions, especially at low and moderate engine loads. This can be explained by their inherent oxygen content which results in improved combustion. It was also noticed that NO and NO_x emissions of all test fuels exhibited a decreasing trend at the full load condition. This can be attributed to reduced oxygen to nitrogen contents ratio at the 100% load. More specifically, W100, W60A40 and A100 released lower NO emission than diesel by 0.5%, 1.2%, and 2.9% at the full load respectively. On the other hand, W50A50 and W30A70 released higher NO emission than diesel by 2.4% and 1.7% at the full load respectively. However, NO_2 emissions of all biofuels were higher than diesel by 25%, 25%, 6%, 29% and 29% at the full load respectively. Ultimately, the NO_x emissions of the W100, W50A50 and W30A70 were higher than the diesel by 0.7%, 2.5% and 2.9% at the full load respectively. However, the NO_x emissions of the A100 and W60A40 were comparable to that of diesel as they released 1.4% lower and the same NO_x emissions compared to diesel, respectively. Note that, W60A40 was one of the biomixtures complies with the BS EN14214 standard.
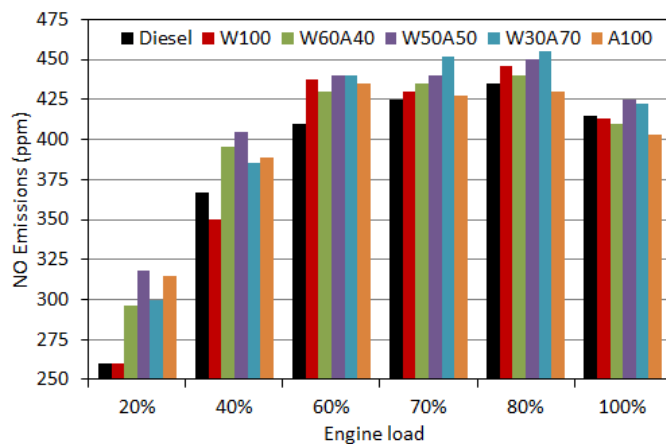
(a)
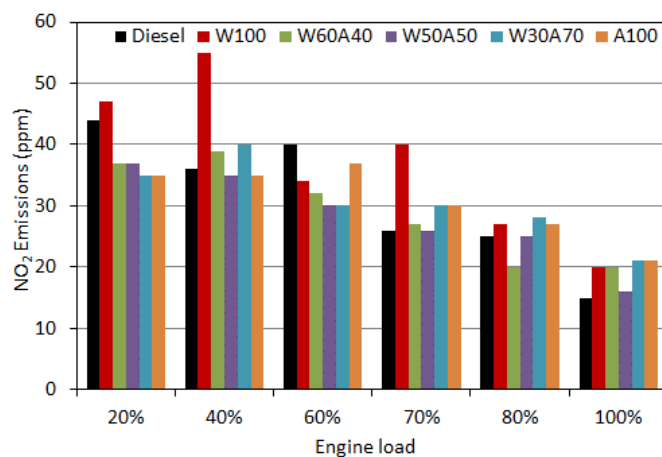
(b)
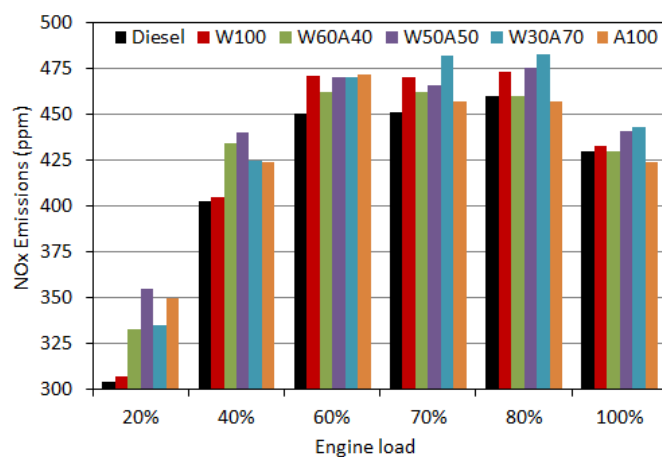
(c)

Figure 4.25: NO, NO₂, and NOₓ emissions of the test fuels at different engine loads.

Table 4.7: NO, NO$_2$, and NO$_x$ emissions of test fuels at different engine loads (ppm).

	NO					
	Engine load					
Fuel	**20%**	**40%**	**60%**	**70%**	**80%**	**100%**
Diesel	260	367	410	425	435	415
W100	260	350	437	430	446	413
W60A40	296	395	430	435	440	410
W50A50	318	405	440	440	450	425
W30A70	300	385	440	452	455	422
A100	315	389	435	427	430	403
	NO$_2$					
Diesel	44	36	40	26	25	15
W100	47	55	34	40	27	20
W60A40	37	39	32	27	20	20
W50A50	37	35	30	26	25	16
W30A70	35	40	30	30	28	21
A100	35	35	37	30	27	21
	NO$_x$					
Diesel	304	403	450	451	460	430
W100	307	405	471	470	473	433
W60A40	333	434	462	462	460	430
W50A50	355	440	470	466	475	441
W30A70	335	425	470	482	483	443
A100	350	424	472	457	457	424

Figure 4.26 compares the two neat biodiesels and illustrates that W100 had higher NO and NO$_x$ emissions than A100 by 3.6% and 3.4% at 80% engine load. Similarly, the same differences were 2.4% and 2.1% at the full load condition. This analysis between two different neat biodiesels matches with the literature, as NO$_x$ emission was decreasing with respect to decreasing DU of biodiesel (Dhamodaran *et al.*, 2017). However, when the same analysis conducted with the biomixtures, the trend was exactly the opposite. According to Figure 4.27, NO$_x$ emission was increasing with respect to decreasing DU of the biomixture. For example, 15 ppm increase on NO$_x$ emission was reported when the DU of biomixture reduced from 167 to 133. Similarly, another 8 ppm increase on NO$_x$ was observed with the reduction of DU from 133 to 123. Lanjekar and Deshmukh (2016) depicted bulk modulus of biodiesel, which is directly proportional to density but in inverse relationship to the NO$_x$ emission. Increase in the biodiesel's bulk modulus was also addressed with the higher DU FAMEs (Giakoumis, 2013; Lanjekar and Deshmukh, 2016). In this regard, the results of this study match with the mentioned theory as NOx increased with decreasing densities and DU. In addition, the higher NO$_x$ emission with the lower DU biomixtures can be attributed to improved combustion characteristics of the low DU biomixtures like shorter ignition delay, shorter combustion duration, and higher heat release at the early period of the combustion. It is known from the literature that

improved combustion characteristics cause higher NO_x emission as a result of the increase in combustion temperature (Shameer and Ramesh, 2017). Consequently, NO_x was in an inverse relationship with the DU due to improved combustion properties.
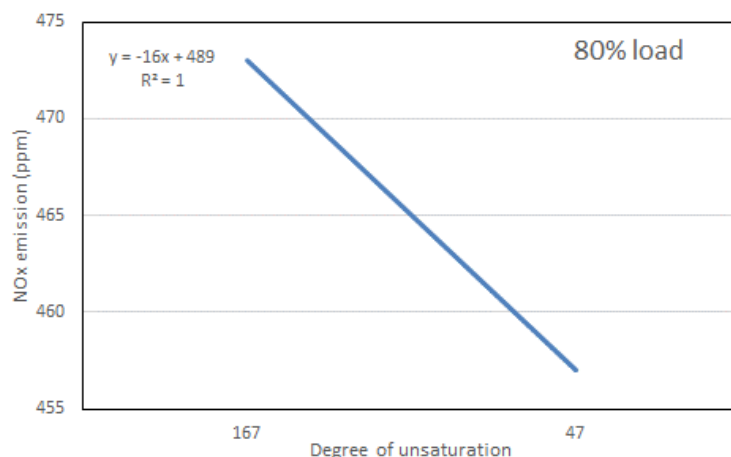
Figure 4.26: The effect of degree of unsaturation when observed on different biodiesels.
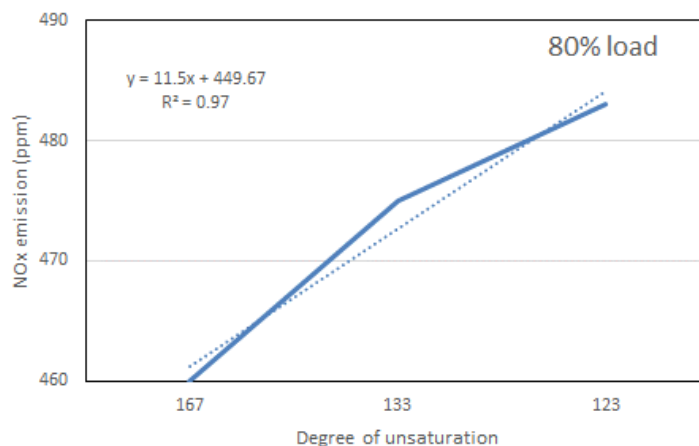
Figure 4.27: The effect of degree of unsaturation when observed on biomixtures (biodiesel-biodiesel blends).

Figure 4.28 demonstrates smoke opacity measurements of the test fuels at different engine loads. The smoke opacity was the same for biodiesels and lower than diesel at all engine loads. This can be attributed to the aromatic hydrocarbon content of the diesel. The aromatic compounds decompose during the combustion and form visible side-products which are known as smoke (as well as soot) in the absence of

the oxygen (Dhamodaran *et al.*, 2017). According to the results, average smoke opacity of biofuels was approximately 56%, 92% and 96% lower than the diesel at low (40%), medium (70%) and high (100%) engine loads respectively. The lower smoke emissions of biofuels were due to the improved combustion efficiency as a result of the inherent oxygen content of biofuels. The increasing smoke opacity trend with respect to increasing engine load can be explained by the reduced oxygen content in the combustion chamber. It was also previously reported that combustion behaviour like air turbulence and spray characteristics; and fuel properties such as cetane number, density and viscosity affects the smoke opacity (Ragit *et al.*, 2010; Dhamodaran *et al.*, 2017). The filter of the gas analyser was observed after the test of diesel fuel Figure 4.29a. Then the filter was replaced with the new one and contamination was observed again after testing the biofuels Figure 4.29b.
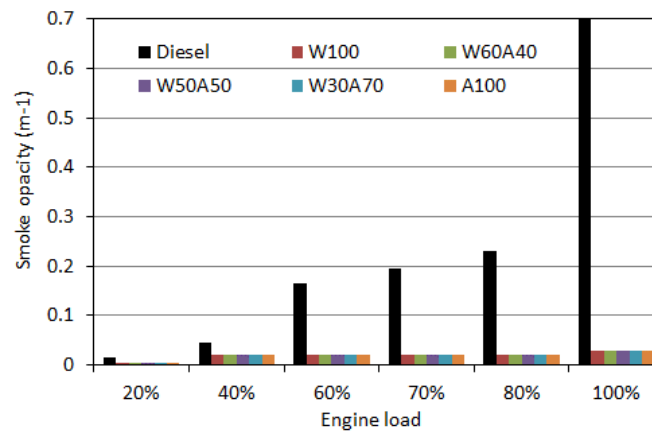
Figure 4.28: Smoke opacity of the test fuels at various engine loads.
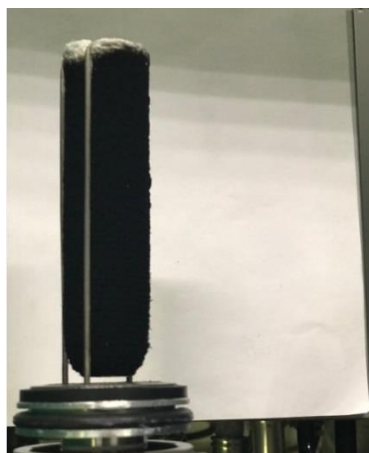
| (a) | (b) |

Figure 4.29: Condition of the Horiba gas analyser filter, after testing (a) the diesel, and (b) biomixtures.

4.9. Repeatability of the results

The results provided in this chapter were validated through repeatability analysis. The experiments were repeated for W50A50 with a 1 year aged biomixture and new sets of produced biodiesels. Moreover, apart from the HORIBA gas analyser, the exhaust emissions were also measured by another exhaust gas analyser BOSCH BEA 850 (described in Chapter 3). Standard errors for the CO_2, CO, HC, O_2, NO, smoke emission and time to consume 100 ml fuel were given in Table 4.8. The first measurement for smoke opacity of diesel was recorded extremely higher than another tests which can be related to inconsistency of diesel quality purchased from commercial supplier, ESSO UK.

The repeatability analysis also proved that there was not any significant effect of 1-year storage of biomixtures on engine results. The biomixtures were stored at the room temperature in glass containers; lids were closed and kept in the dark.

Table 4.8: Repeatability of test results for W50A50 biomixture. The measurements conducted on 15/02/2019 was 1 year aged biomixture, whereas measurements on 20/02/2019 were for new biomixture.

1.9 kW (20%)	Test dates					standard	standard
W50A50	26/10/2017	19/12/2018	15/02/2019	20/02/2019	average	deviation	error
CO_2 (% vol)	3.5	3.43	3.5	3.55	3.50	0.05	0.02
CO (% vol)	0.01	0.012	0.005	0.002	0.007	0.005	0.002
HC (% vol)	-	1	1	1	1	0	0.00
O_2 (% vol)	-	16.15	16.16	16.00	16.10	0.09	0.04
NO (ppm)	318	265	304	309	299	23	11.70
Smoke (m^{-1})	0.01	0.01	0.01	0.01	0.010	0.00	0.00
Time for 100 ml fuel (s)	273	276	267	266	271	5	2.40
Gas analyser	HORIBA	BOSCH	BOSCH	BOSCH			

3.8 kW (40%)	Test dates					standard	standard
W50A50	26/10/2017	19/12/2018	15/02/2019	20/02/2019	average	deviation	error
CO_2 (% vol)	4.67	4.24	4.76	4.77	4.61	0.25	0.13
CO (% vol)	0.01	0.006	0.003	0.003	0.01	0.003	0.002
HC (% vol)	-	3	2	2	2	1	0.29
O_2 (% vol)	-	14.98	14.43	14.37	14.59	0.34	0.17
NO (ppm)	405	361	394	394	389	19	9.53
Smoke (m^{-1})	0.02	0.01	0.01	0.01	0.01	0.01	0.00
Time for 100 ml fuel (s)	206	206	199	198	202	4	2.17
Gas analyser	HORIBA	BOSCH	BOSCH	BOSCH			

5.7 kW (60%)		Test dates					standard	standard
W50A50	**26/10/2017**	**19/12/2018**	**15/02/2019**	**20/02/2019**	**average**	**deviation**	**error**
CO_2 (% vol)	5.92	6.12	6.34	6.23	6.15	0.18	0.09
CO (% vol)	0.01	0.003	0.006	0.005	0.01	0.003	0.001
HC (% vol)	-	2	1	2	2	1	0.29
O_2 (% vol)	-	12.59	12.35	12.35	12.43	0.14	0.07
NO (ppm)	440	460	480	481	465	19	9.71
Smoke (m^{-1})	0.03	0.02	0.025	0.02	0.02	0.00	0.00
Time for 100 ml fuel (s)	160	163	155	162	160	4	1.78
Gas analyser	**HORIBA**	**BOSCH**	**BOSCH**	**BOSCH**			

6.65 kW (70%)		Test dates					standard	standard
W50A50	**26/10/2017**	**19/12/2018**	**15/02/2019**	**20/02/2019**	**average**	**deviation**	**error**
CO_2 (% vol)	6.58	6.95	7.05	6.97	6.89	0.21	0.10
CO (% vol)	0.01	0.003	0.008	0.003	0.01	0.004	0.002
HC (% vol)	-	1	2	1	1	1	0.29
O_2 (% vol)	-	11.64	11.44	11.48	11.52	0.11	0.05
NO (ppm)	440	459	480	489	467	22	10.98
Smoke (m^{-1})	0.03	0.02	0.02	0.02	0.02	0.00	0.00
Time for 100 ml fuel (s)	141	146	141	146	144	3	1.44
Gas analyser	**HORIBA**	**BOSCH**	**BOSCH**	**BOSCH**			

7.6 kW (80%)		Test dates					standard	standard
W50A50	**26/10/2017**	**19/12/2018**	**15/02/2019**	**20/02/2019**	**average**	**deviation**	**error**
CO_2 (% vol)	7.29	7.82	7.87	7.82	7.70	0.27	0.14
CO (% vol)	0.01	0.005	0.009	0.008	0.01	0.002	0.001
HC (% vol)	-	2	1	1	1	1	0.29
O_2 (% vol)	-	10.66	10.38	10.32	10.45	0.18	0.09
NO (ppm)	450	447	501	490	472	28	13.77
Smoke (m^{-1})	0.03	0.02	0.02	0.02	0.02	0.00	0.00
Time for 100 ml fuel (s)	128	130	128	130	129	1	0.58
Gas analyser	**HORIBA**	**BOSCH**	**BOSCH**	**BOSCH**			

9.75 kW (100%)		Test dates					standard	standard
W50A50	**26/10/2017**	**19/12/2018**	**15/02/2019**	**20/02/2019**	**average**	**deviation**	**error**
CO_2 (% vol)	9.05	10.15	10.09	10.07	9.84	0.53	0.26
CO (% vol)	0.01	0.009	0.012	0.011	0.01	0.001	0.001
HC (% vol)	-	0	0	0	0	0	0.00
O_2 (% vol)	-	7.85	7.53	7.46	7.61	0.21	0.10
NO (ppm)	425	420	478	477	450	32	15.91
Smoke (m^{-1})	0.21	0.04	0.02	0.02	0.07	0.09	0.05
Time for 100 ml fuel (s)	101	103	103	102	102	1	0.48
Gas analyser	**HORIBA**	**BOSCH**	**BOSCH**	**BOSCH**			

4.10.   Conclusion

Two neat biodiesels of W100 and A100 were blended at different ratios to produce biomixtures at different levels of DU. According to engine tests of the tested fuels, the following conclusions were made;

1. Viscosity, iodine value and cetane number were the three main fuel properties which were directly affected by the degree of unsaturation.

2. Ignition delay of the biomixtures was slightly shortened by 0.05 °CA each time DU reduced from 133 to 123 and 123 to 47. Similarly, total combustion duration was shortened by 0.5 °CA each time the DU of the biomixtures reduced.

3. Exhaust gas temperature was the highest for the highest DU biodiesel W100 as 215°C, followed by W60A40, W50A50, W30A70 and A100 as 211°C, 209°C, 206°C and 206°C at 70% engine load respectively.

4. The highest peak in-cylinder pressure was provided by the W50A50 biomixture having moderate DU of 123 at almost all engine loads i.e. 67.9 bar at 10.5 °CA, 68.9 bar at 10.3 °CA and 67.5 bar at 12.0 °CA which were 4.3%, 5.2% and 2.8% higher than the neat biodiesels at 70%, 80% and 100% engine loads respectively.

5. The maximum HRR values were 27.8 J/°CA, 28.4 J/°CA and 29.6 J/°CA for W60A40, W50A50 and W30A70 at the 80% engine load respectively. The study also shows that biodiesels having low DU values burned slightly quicker by around 15 joules (4%) at the early phase of the combustion. On the other hand, high DU biodiesels were burning approximately 30 Joules (5.5%) higher than the low DU biodiesels at the late combustion phases at 80% engine load.

6. No significant effect of DU was observed on engine performance at full engine load. However, the highest DU biodiesel W100 provided maximum BTEs at the low and medium engine loads by approximately 8% and 10% higher than the diesel and the lowest DU biofuel A100 respectively.

7. A100 had the highest BSFC as 0.433 kg/kWh and followed by W30A70 as 0.426 kg/kWh, W50A50 as 0.412 kg/kWh, W60A40 as 0.400 kg/kWh, W100 as 0.390 kg/kWh and diesel as 0.369 kg/kWh at 40% engine load. However, there was no difference among all fuels BSFC values at the high engine loads. This shows no significant effect of DU on the BSFC of biodiesels.

8. Biodiesels having DU greater than 123 like W100, W60A40 and W50A50 had around 1.9% lower BSEC than the diesel at 60% engine load. However, all biodiesels and diesel had the same BSEC as 11.7 MJ/kWh at the full engine load.

9. W100 had the highest CO_2 emission as 240.4 g/100s and it was also 3.1% higher than the diesel. All other biodiesels like W60A40, W50A50, W30A70 and A100 released 1.8%, 3.3%, 2.6% and 2.9% lower CO_2 emissions than diesel at the full load condition respectively.

10. The highest DU biodiesel W100 had the highest CO emission which was 5.9% less than the diesel. CO emissions were reduced as reduced DU. For example, W60A40, W50A50, W30A70 and A100 released 73.0%, 74.2%, 74.8% and 77.7% lower CO emissions than the diesel at 80% engine load respectively.

11. NO_x emissions of the W100, W50A50 and W30A70 were higher than the diesel by 0.7%, 2.5% and 2.9% but A100 and W60A40 released comparable NO_x emissions with the diesel at the full engine load. When the results of the biomixtures compared at the 80% engine load, NO_x emission increased with respect to decreasing DU value due to improved combustion.

To sum up, this chapter recommends the blending of two different biodiesels to optimise the fuel properties especially viscosity, cetane number, degree of unsaturation and iodine value. Improved combustion characteristics and exhaust gas emissions were also observed with the biomixtures as a result of optimised fuel properties. In this regard, the next chapter will be concentrated on chicken biodiesel which has advantages; high availability, high energy content, high cetane number and low degree of unsaturation. At the same time, chicken biodiesel has the main disadvantage of high viscosity. The disadvantages of the mentioned biodiesel will be minimised in light of the blending technique proved in this chapter.

Chapter 5

5. CHARACTERISATION AND ENGINE PERFORMANCE OF CHICKEN FAT BIODIESEL AND COTTONSEED OIL BIODIESEL BLENDS

This chapter present studies on improvement of the waste chicken fat biodiesel fuel properties by blending with cottonseed biodiesel. The targets were: (i) to achieve the fuel properties to meet the BS EN 14214 standard, (ii) to have improved combustion characteristics and reduced exhaust emissions with optimised biomixture fuel. In the beginning part of this chapter, negative aspects of the produced chicken biodiesel were spotted in terms of fuel properties. Cottonseed biodiesel was selected for blending with the chicken fat biodiesel. Characterisation of the chicken fat biodiesel – cotton seed oil biodiesel mixtures were carried out. Optimised biomixture fuels were tested in the engine to evaluate the combustion and emission advantages.

5.1. Introduction

During the last decade, animal fats have become more popular feedstock for biodiesel production due to relatively cheaper price and availability of the feedstock (Adewale *et al.,* 2015). Furthermore, they are considered as wastes and their disposal is subjected to some procedures in the UK (Environment Agency, 2015). The number of reported chickens as waste (landfilled either as whole or parts of poultry) was 86 million in 2015 in the UK, this makes it a promising candidate as biodiesel feedstock (McDougal, 2015). Chicken skin, offal, blood, trims, feathers etc. can be used as feedstock for fats extraction and biodiesel production (Alptekin and Canakci, 2011). Typically, the mentioned feedstock is rendered and chicken oil obtained for transesterification process (Adewale *et al.,* 2015). According to the type of selected waste chicken feedstock, a pre-treatment may be required due to high acid content (Alptekin and Canakci, 2010). Researchers are working to develop new techniques particularly for converting waste chicken feedstock into biodiesel. For example, Marulanda *et al.,* (2010) experimented supercritical transesterification of chicken fat at temperature of between 300-400 °C and 41.1 MPa pressure. The

authors reported that this technique gave higher biodiesel yield than the conventional technique (Marulanda *et al.,* 2010).

5.2. Literature review for improving fuel properties

The viscosity of biodiesels directly affects the combustion characteristics (Masera and Hossain, 2019). High viscosities cause poor atomisation and/or vaporisation of fuel droplets, which may also lead to higher pollution (Barrios *et al.*, 2014). As per BS EN 14214 standard, the maximum allowable viscosity was set as 5 mm^2/s (British Standard Institution, 2010). Nevertheless, animal fat biodiesels hardly meet the standard and have difficulties in direct usage in engines (Adewale *et al.*, 2015; Ashraf *et al.*, 2017; Kirubakaran and Selvan, 2018). Significant amount of studies reported viscosity higher than 5 mm^2/s for chicken biodiesel (Bhatti *et al.*, 2008; Mata *et al.*, 2010, 2011, 2014; Alptekin and Canakci, 2011; Jagadale and Jugulkar, 2012; Ashraf *et al.*, 2017). Various techniques were used to overcome this challenge, such as pre-heating of biodiesel, use of additives and diesel blending. Nonetheless, each technique had its own drawbacks. Blending with diesel may be the most popular among the mentioned solutions. However, this method cannot be reliable as the literature forecasts fossil fuel depletion in the future (Day and Day, 2017; Wang *et al.*, 2017). The other solution was the pre-heating of biodiesel with various engine modifications. To illustrate, Nanthagopal *et al.* (2017) used the heat from the exhaust system to pre-heat the blend of ethanol-diesel by approximately 50 °C. Similarly, Hossain and Davies (2012) raised the temperatures of karanja and jatropha oils by 75 °C which in turn decreased the viscosities from 80 cSt to 11 cSt and from 58 cSt to 9 cSt via hot jacket water, respectively. Even though the mentioned modifications were successful, they need significant modifications on the engine cooling or exhaust systems which means extra cost and weight (Masera and Hossain, 2019). Finally, fuel additives such as alcohols are doped into biodiesels to reduce high viscosities (Tosun *et al.*, 2014; Yasin *et al.*, 2014; Imdadul *et al.*, 2016; Yilmaz and Atmanli, 2017). To illustrate, Yasin *et al.* (2014) doped methanol 5% (by volume) into palm oil biodiesel-diesel blend (20%/75%). The study addressed 1.38 mm^2/s improvement on the blend's viscosity. However, alcohol additive causes a reduction on the engine performance and increase on exhaust emissions. The study reported that engine power was reduced by 8.3% and increased the NO emission by 7% at medium brake mean effective pressure (Yasin *et al.*, 2014).

Another biodiesel which has promising fuel properties to compensate weak fuel properties of chicken biodiesel can be blended. This technique may help to meet BS EN 14214 standard and utilise chicken fat biodiesel in a more efficient manner (Masera and Hossain, 2019).

Cottonseed biodiesel with a relatively low viscosity value can be a good candidate to be blended with the chicken biodiesel. Alhassan *et al.* (2014) measured 4.38 mm^2/s viscosity for the cottonseed biodiesel at 40°C. Similarly, Venkatesan *et al.,* (2017), Alptekin and Canakci (2009), and Ramírez-Verduzco *et al.,* (2012) all reported relatively low viscosities for cottonseed biodiesels as 3.75, 4.06 and 4.12 mm^2/s, respectively. These values were considered relatively low for biodiesel, thus viscosity of chicken biodiesel-cottonseed biodiesel blend can be reduced to comply with the BS EN 14214 standard. Moreover, literature also reported reduced NO$_x$ emission for cottonseed biodiesel compared to diesel. Aydin and Bayindir (2010) investigated need biodiesel obtained from cottonseed in a one cylinder DI diesel engine. The study reported approximately 18% reduction in NOx emission for the cottonseed biodiesel compared to diesel operation. Similarly, 5% reduction in NOx emission was reported for a cottonseed biodiesel pre-heated to 90 °C (Karabektas *et al.,* 2008). Furthermore, Yucesu and Ilkilic (2006) investigated neat cottonseed biodiesel in a one cylinder CI engine and recorded 16% lower NO$_x$ emission relative to diesel.

The purpose of this chapter is to improve the viscosity of chicken biodiesel and comply with the BS EN14214 standard by cottonseed biodiesel blending. By this means, fuel properties such as viscosity could be optimised and blends could be directly used in CI engines without any engine modification, diesel blending or fuel additive. Furthermore, combustion characteristics and exhaust gas emissions of novel blends could be superior to neat biodiesels and diesel.

5.3. Cottonseed biodiesel and chicken fat biodiesel blending

Initially, the waste chicken skin was collected from EURO ASIA CASH & CARRY, Loughborough UK and cottonseed oil (origin Greece) was purchased from Mystic Moments, UK. Next, they were converted into biodiesel at the Aston University mechanical engineering and chemical engineering laboratories as described in Chapter 3. Figure 5.1 shows the chicken skin rendering fat and cottonseed oil feedstock used in this research.
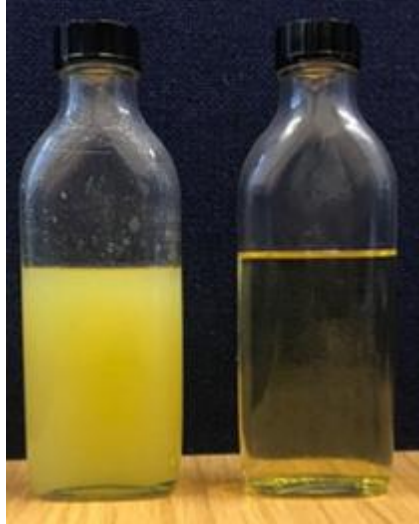
Figure 5.1: Chicken skin rendering fat (on the left) and cottonseed oil (on the right).

Biomixtures were prepared by blending cottonseed biodiesel (CO100) and chicken fat biodiesel (CH100) at 80/20, 60/40, 50/50, 30/70 and 10/90 volume ratios and named as CO80CH20, CO60CH40, CO50CH50, CO30CH70 and CO10CH90 as shown in Table 5.1. The commercially available Esso ULSD diesel (in the UK) was used as a reference fuel which contain 5% biodiesel in accordence with EN 590 standard. The biomixtures kept undisturbed for 2 weeks at room temperature and there was no phase separation or miscibility problem observed Figure 5.2.

Table 5.1. Biodiesel percentages of the biomixtures, adapted from the author's published paper (Masera and Hossain, 2019).

Fuel Name	Volume percentage of		Fuel Characterisation	Engine Testing
	Cottonseed biodiesel	Chicken biodiesel		
CO100	100%	0%	Yes	Yes
CO80CH20	80%	20%	Yes	NO
CO60CH40	60%	40%	Yes	Yes
CO50CH50	50%	50%	Yes	Yes
CO30CH70	30%	70%	Yes	Yes
CO10CH90	10%	90%	Yes	NO
CH100	0%	100%	Yes	Yes
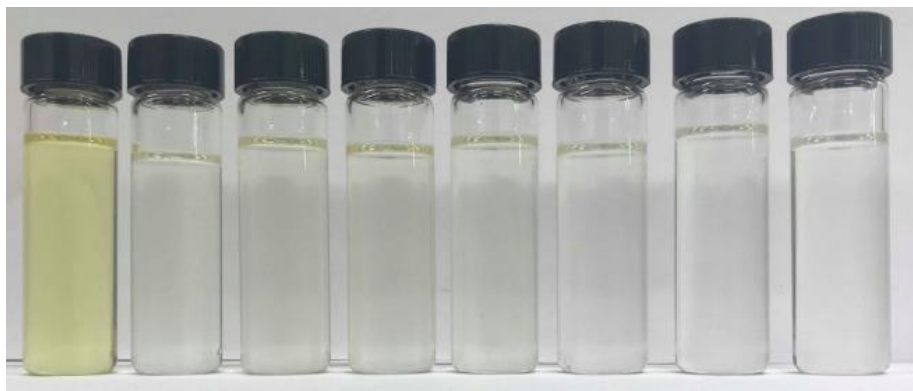
Figure 5.2. The appearance of the test fuels which are from left to right; Diesel, CO100, CO80CH20, CO60CH40, CO50CH50, CO30CH70, CO10CH90 and CH100, adapted from the author's published paper (Masera and Hossain, 2019).

5.4. Fuel characterisation results for cottonseed biodiesel-chicken biodiesel blends

Around 2.2 kg of oil was rendered from 5kg waste chicken skin; hence rendering yield was 43.5%. On the other hand, biodiesel yields of both transesterifications of the chicken and cottonseed oil were approximately 92%.

Table 5.2 illustrates the mass percentages of saturated FAMEs for CO100 and CH100 as 26.7% and 28.8%, respectively. Similarly, overall unsaturated FAMEs were also close to each other as 73.3% and 71.2%. However, a significant difference was observed on the type of unsaturated FAME i.e. monounsaturated and polyunsaturated. This was an important detail as the type of unsaturated FAME play a crucial role in fuel properties (Masera and Hossain, 2017). According to the results, CO100 was mainly composed of C18:2 as 51.7%, whereas CH100 mainly had C16:1 and C18:1 as 48.8% in total.

Table 5.2. Fatty Acid Methyl Ester compositions of the biofuels, adapted from the author's published paper (Masera and Hossain, 2019).

FAME	Mass percentage (%)						
	CO100	CO80CH20	CO60CH40	CO50CH50	CO30CH70	CO10CH90	CH100
C14:0	0.7	0.6	0.6	0.6	0.6	0.6	0.6
C16:0	23.2	21.8	21.7	21.5	21.6	21.5	21.7
C16:1	0.5	1.4	2.1	3.1	4	5.1	5.4
C18:0	2.8	3.8	5.2	5	5.7	6.2	6.6
C18:1	20.9	25.8	30.9	32.6	36.8	40.9	43
C18:2	51.7	46.5	39.4	37.3	31.3	25.4	22.4
C18:3	0.2	0.2	0	0	0	0.3	0.4
C20:0	0.1	0	0	0	0	0	0
Total saturated	26.7	26.2	27.6	27.1	27.9	28.3	28.8
Monounsaturated	21.6	27.3	33	35.7	40.8	46.3	48.8
Polyunsaturated	51.7	46.5	39.4	37.3	31.3	25.4	22.4

Figure 5.3 demonstrates the TLC chromatography results of the cottonseed oil, chicken fat and their biodiesel versions. According to Figure 5.3, TAGs were the most dominant compound in the oils. Figure 5.4 also showed that TAGs were main source of the feedstock that was converted into biodiesel. Note that FFA, DAG and MAG compounds could not be quantified as their concentrations were below the detection point.

(a)   (b)
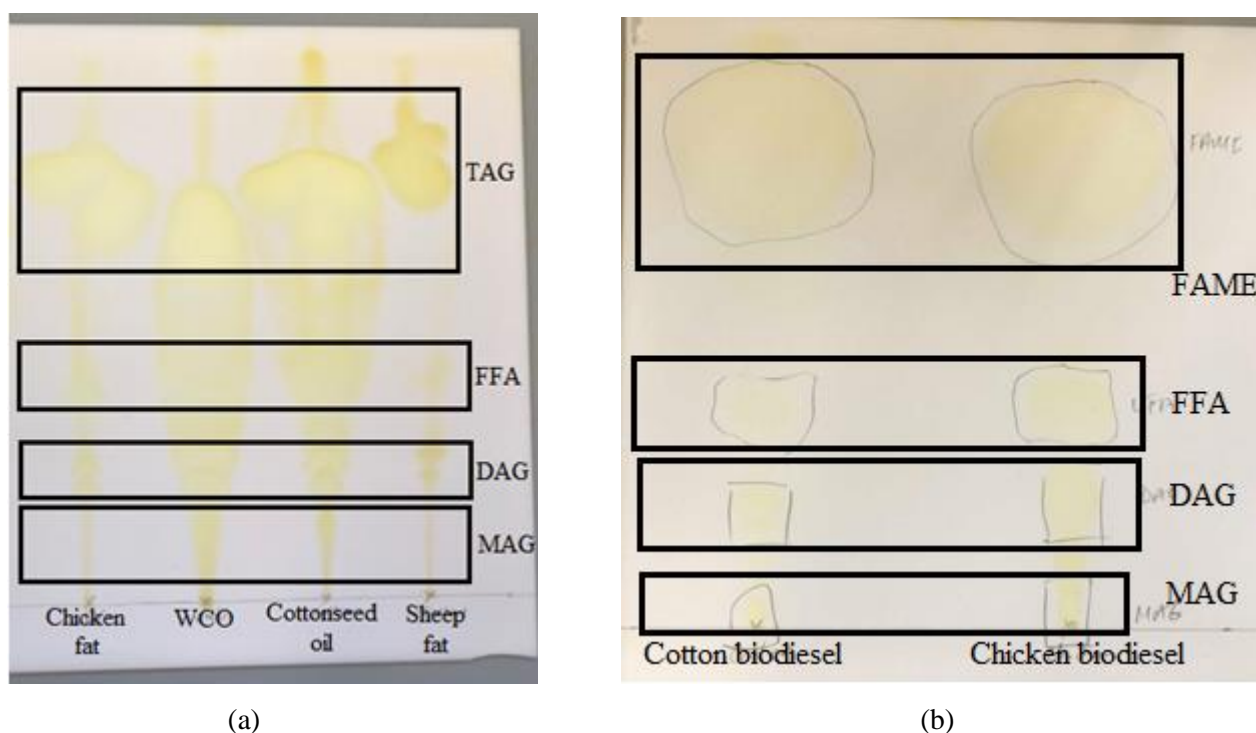
Figure 5.3: Thin layer chromatography (TLC) results of (a) feedstock and (b) biodiesel samples.
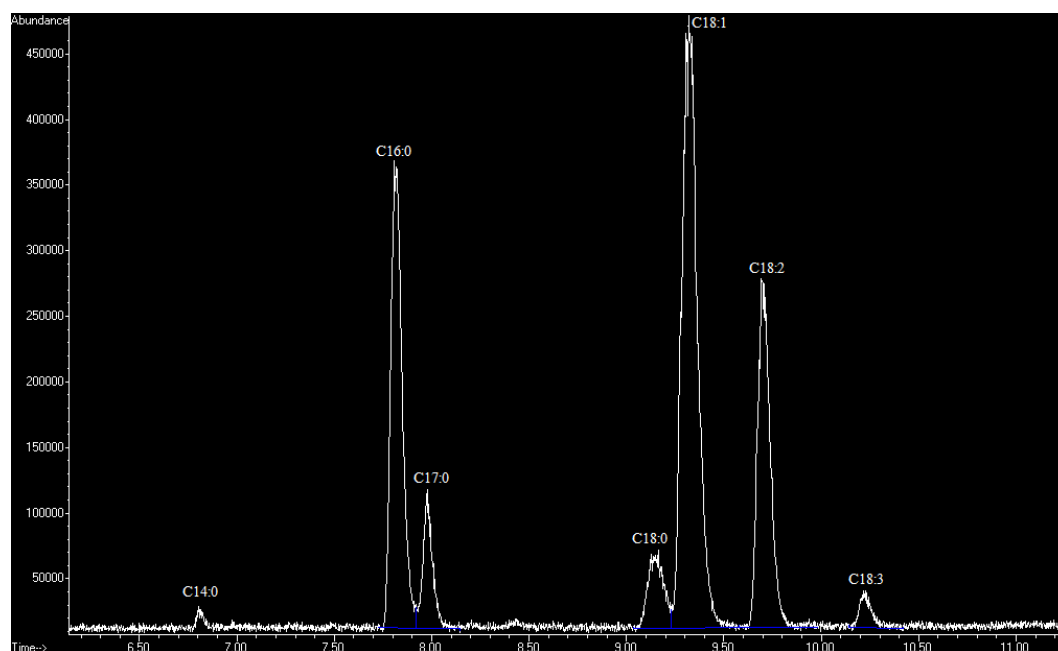
(a)
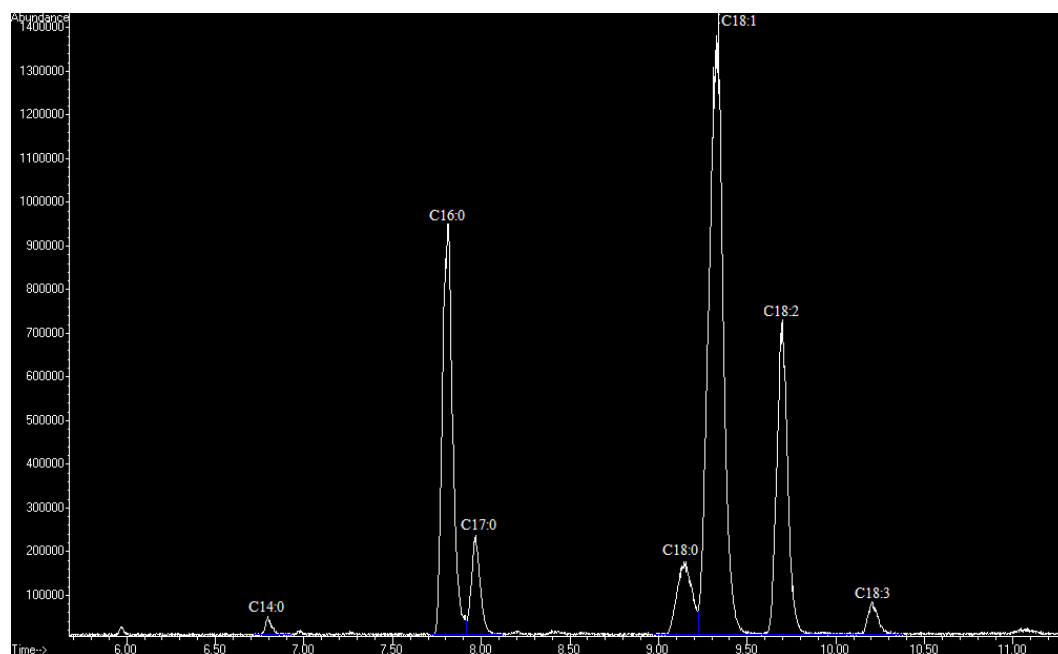
(b)

Figure 5.4: GC-ms results of the (a) chicken fat TAG and (b) chicken biodoesel FAME. Chicken biodiesel CH100 mainly composed of C16:0, C18:1 and C18:2. (C17:0 was added as an internal standard).

Fuel properties of the test biodiesels and diesel are shown in Table 5.3. Moreover, BS EN 14214 biodiesel standard (British Standard Institution, 2010) and EN 590 diesel standard (European Standard EN 590:2013, 2009) are also included as reference. The biggest differences of the neat biodiesels were on cetane number, viscosity, degree of unsaturation and iodine value. Therefore, they were the major parameters affected from cottonseed-chicken biodiesel blending. Influence of blend ratio on cetane number and viscosity was given in Figure 5.5. Both cetane number and viscosity were increased as the chicken biodiesel fraction of blends increased. This can be attributed to the relatively low amount of polyunsaturated FAME content of the CH100 as 22.4% (Masera and Hossain, 2019).

Table 5.3. Fuel properties of the test fuels with the corresponding EN14214 biodiesel (British Standard Institution, 2010) and EN 590 diesel (European Standard EN 590:2013, 2009) standard, adapted from the author's published paper (Masera and Hossain, 2019).

Fuel Properties	Units	Biofuels							Diesel	BS EN 14214 Biodiesel Standard	EN 590 Diesel Standard
		CO100	CO80CH20	CO60CH40	CO50CH50	CO30CH70	CO10CH90	CH100			
Viscosity at 40°C	(mm^2/s)	4.33	4.48	4.66	4.92	5.10	5.16	5.36	2.78	3.5 - 5.0	2.0 - 4.5
Density	(g/cm^3)	0.884	0.882	0.882	0.881	0.880	0.880	0.878	0.828	0.86 - 0.90	0.820 - 0.845
Flash Point	(°C)	176	176	173	171	168	165	165	61.5	min 101	min 55
Cetane number[a]	()	54	55	57	57	59	60	60	53.5	min 51	min 51
Cetane number[b]	()	52	52	54	54	56	56	57	53.5	min 51	min 51
Carbon, theoretical	(%)	76.69	76.77	76.85	76.84	76.79	76.49	76.44	n/a	n/a	n/a
Carbon, measured	(%)	77.58	n/a	74.69	74.20	76.12	n/a	75.67	86.6[c]	n/a	n/a
Hydrogen, theoretical	(%)	11.93	11.98	12.05	12.06	12.09	12.09	12.10	n/a	n/a	n/a
Hydrogen, measured	(%)	12.33	n/a	12.49	12.41	11.33	n/a	11.96	13.4[c]	n/a	n/a
Oxygen, theoretical	(%)	11.08	11.08	11.10	11.11	11.11	11.08	11.08	n/a	n/a	n/a
Oxygen, measured	(%)	10.09	n/a	12.82	13.40	12.55	n/a	12.38	0.07[c]	n/a	n/a
HHV	(MJ/kg)	39.4	39.4	39.6	39.4	39.1	39.6	39.3	45.2	n/a	n/a
LHV	(MJ/kg)	37	37	37	37	37	37	37	42	n/a	n/a
Iodine number	(g/100g)	108	104	97	95	90	84	81	n/a	max 120	n/a
Linolenic acid methyl ester	(%mol/mol)	0.2	0.2	0	0	0	0.3	0.4	n/a	max 12	n/a
Monoglyceride (MAG)	(%mol/mol)	ND	ND	ND	ND	ND	ND	ND	ND	max 0.8	n/a
Diglyceride (DAG)	(%mol/mol)	ND	ND	ND	ND	ND	ND	ND	ND	max 0.2	n/a
Triglyceride (TAG)	(%mol/mol)	ND	ND	ND	ND	ND	ND	ND	ND	max 0.2	n/a
Methanol	(%mol/mol)	0	0	0	0	0	0	0	n/a	max 0.2	n/a
Acid value	(mg KOH/g)	0.228	0.200	0.200	0.171	0.172	0.172	0.172	0.091	max 0.5	n/a
Degree of Unsaturation	(Weight %)	125	120	112	110	103	97	94	n/a	n/a	n/a

a= (Ramírez-Verduzco *et al.,* 2012); b= (Tong *et al.,* 2011); c= (Schönborn *et al.,* 2009); ND= Not detected
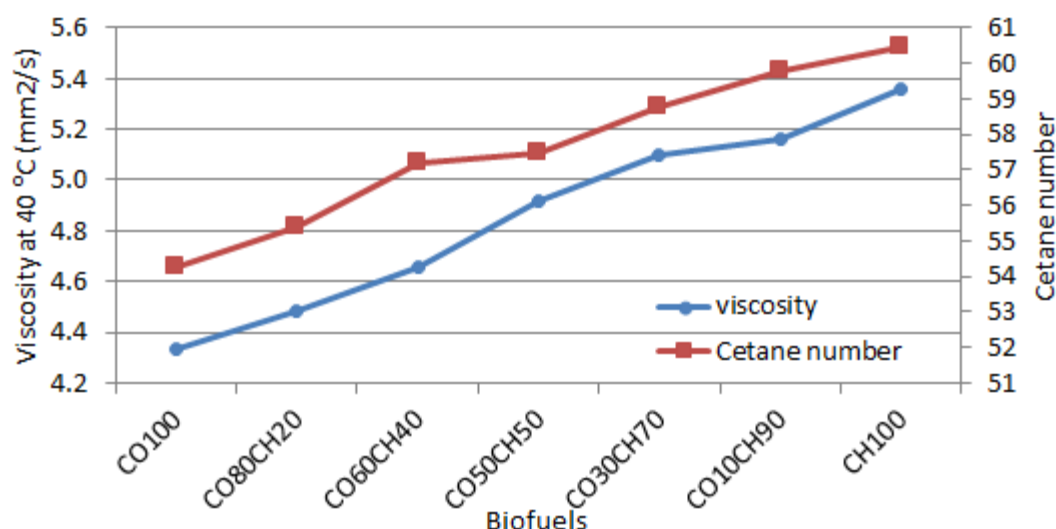
Figure 5.5. Variation of viscosity and cetane number with respect to cottonseed-chicken biodiesel ratio, adapted from the author's published paper (Masera and Hossain, 2019).

Literature pointed viscosity as one of the most important fuel property due to its direct effect on fuel combustion (Alptekin and Canakci, 2009). Viscosity of chicken biodiesel was not complied with the BS EN 14214 standard as it was measured as 5.36 mm^2/s at 40°C. This can be linked to relatively low iodine value of the chicken biodiesel which was 81 g/100g. The literature also stated higher viscosities for low iodine value FAMEs (Schönborn *et al.*, 2009). However, viscosity was improved when cottonseed biodiesel was added into chicken biodiesel and blends with minimum 50% cottonseed biodiesel met the BS EN 14214 standard in terms of viscosity Figure 5.5. Density is another fuel property directly effects engine performance and combustion (Emiroğlu *et al.*, 2018). All biodiesels found suitable with the BS EN 14214 standard in terms of density. The highest density was measured for CO100 as 0.884 g/cm^3. Densities of blends were increased by the cottonseed biodiesel blending. Flash point is an important parameter for safe storage and transport of the fuels (Masera and Hossain, 2019). The flash points of all biodiesels complied with the standard and measured between 176°C and 165°C. Cetane number is a good measure of the ignition quality of any fuel (Kurtz and Polonowski, 2017). All biodiesels met the BS EN 14214 standard in terms of cetane number as they were above the minimum limit of 51. However, the highest CN measured for chicken biodesel as 60 was reduced with the cottonseed biodiesel blending. This was the biggest drawback of cottonseed biodiesel blending of chicken biodiesel. Nevertheless, this scarify from cetane number can be acceptable as the CN of optimised biomixtures such as CO60CH40 and CO50CH50 were 57 and higher than diesel having CN of 53.5. The carbon, hydrogen and oxygen contents of the test biodiesels similar to each other and good agreement with the literature (Giakoumis, 2013). The HHV and LHV of biodiesels were very similar to each other as 39.4 MJ/kg and 37 MJ/kg; these values were slightly lower than diesel Table 5.3. As mentioned earlier, DU and IV are both measuring the same fuel property which is saturation

level (Schober and Mittelbach, 2007). All biodiesels complied with the BS EN14214 iodine value standard declared as maximum 120 g iodine/100g. IV of blends increased with the increased cottonseed biodiesel fraction. Acid value of a biodiesel shows its resistance to ageing (Predojević, 2008). Acid values were all measured within the range declared by the BS EN 14214. This was a good indication of biodiesels safe usage in CI engines in terms of corrosion and pump plugging and (Predojević, 2008; Emiroğlu *et al.,* 2018). Ultimately, the high viscosity of CH100 was successfully reduced and 5.00 mm^2/s viscosity requirement of BS EN 14214 standard was met by cottonseed biodiesel blending. For example, CO60CH40 and CO50CH50 were high quality biomixtures which also complied with the standard.

Fuel characterisation of the biomixtures i.e. CO50CH50 were in good agreement with the similar studies in the literature. For example, Benjumea *et al.,* (2011) studied palm/linseed biodiesel blends at 50/50 volume fraction. The blend had similar HHV as 39.8 MJ/kg, density as 0.885 g/cm^3 and iodine value as 112.7 g/100g with the CO50CH50. However, the blend had 10% lower CN as 51.3 than CO50CH50 biomixture. In another study, Sanjid *et al.* (2016) studied the kapok biodiesel-Moringa biodiesel-diesel blend with volume ratio of 10/10/80 respectively. The biofuel had around 30% lower viscosity value than CO50CH50, this can be attributed to the high percentage of diesel as 80%. However, CN of the biofuel was around 16% lower than CO50CH50. To sum up, the biomixtures produced and analysed in this chapter had comparable fuel characteristics with similar types of biofuel blends in the literature. Furthermore, the biomixtures produced in this research like CO60CH40 and CO50CH50 had superior cetane numbers over the literature due to relatively high CN of chicken biodiesel as 60.

5.5. Engine performance of cottonseed biodiesel-chicken biodiesel blends

Figure 5.6 shows the BTE of the test fuels at various engine loads. Biomixtures with relatively higher fractions of cottonseed biodiesel had better BTE at low and medium engine loads. BTE of CO100, CO60CH40 and CO50CH50 was approximately 10% higher than other biodiesels and diesel at 40% load. This was linked to the presence of oxygen content of biodiesels which improves the combustion. However, all biodiesels had slightly lower BTE by about 1.6% than diesel at the full engine load. The result was in good agreement with the literature. Diesel had higher BTE than biodiesels at the full load due to its higher LHV than biodiesel (Emiroğlu *et al.,* 2018).
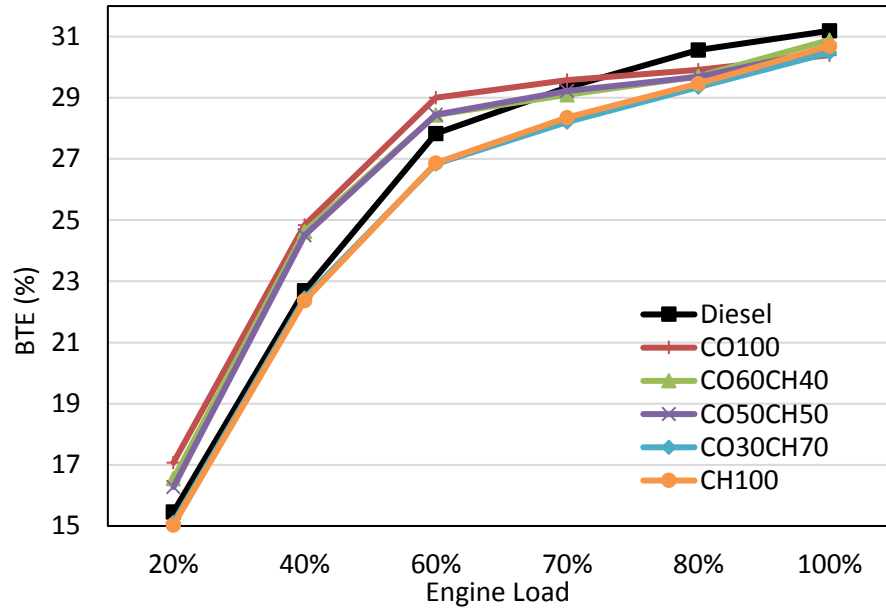
Figure 5.6. BTE of the test fuels at different engine loads, adapted from the author's published paper (Masera and Hossain, 2019).

Figure 5.7 demonstrates (a) BSFC and (b) BSEC of the test fuels at different engine loads. BSFC of all biodiesels were measured 15.4% higher than diesel at the full load. BSFC of lower IV biodiesels were higher at the low and medium loads. For example, CH100 and CO30CH70 biodiesels with relatively high IV provided 5.6% and 14.4% higher BSFC than diesel and other biodiesels at 60% load, respectively. However, BSFC of the all biodiesels were comparable at the full load due to similar LHV. To minimise the influence of LHV, BSEC of biodiesels could be analysed (Reddy *et al.*, 2012; Krishna *et al.*, 2016). This allows comparing the test fuels in terms of the energy consumed to produce the same power output (Masera and Hossain, 2019). Figure 5.7 (b) states that CO100, CO60CH40, CO50CH50 provided 11.8% reduced BSEC than CO30CH70, CH100 and diesel at 40% load. Furthermore, all biodiesels and diesel gave comparable BSEC at the full engine load. To sum up, diesel did not provide any superiority over biodiesels at the full engine load.
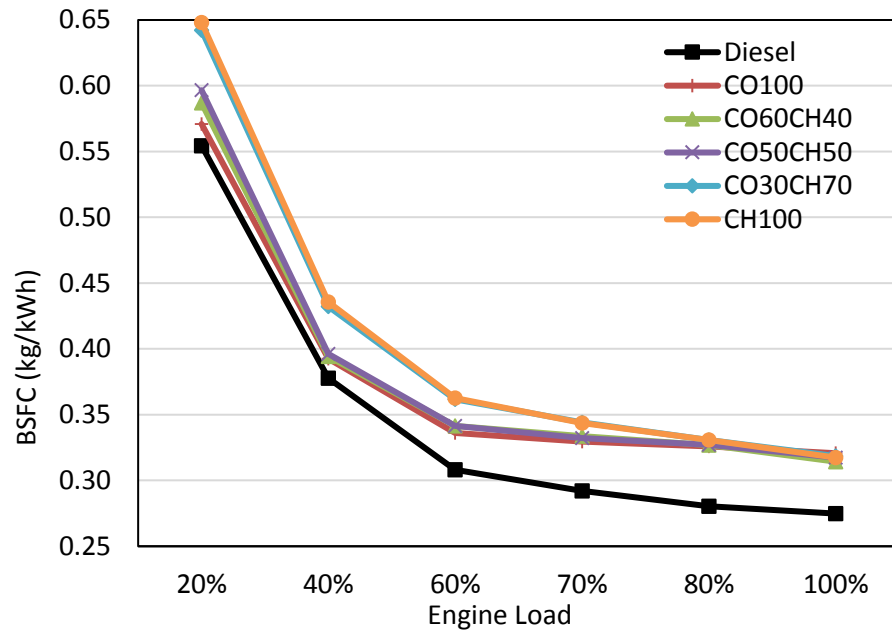
(a)
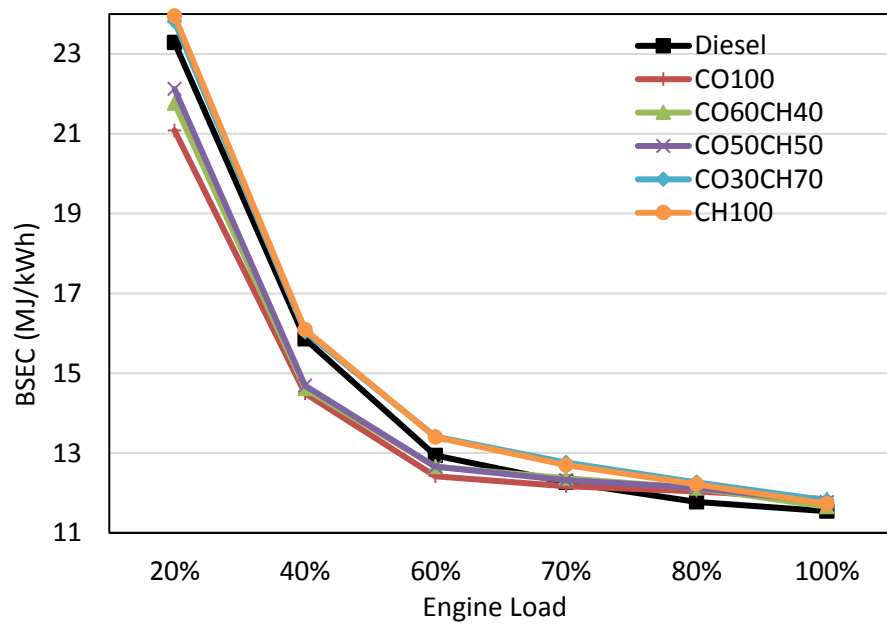
(b)

Figure 5.7. BSFC and BSEC of the test fuels at different engine loads, adapted from the author's published paper (Masera and Hossain, 2019).

5.6. Injection and combustion characteristics of cottonseed biodiesel-chicken biodiesel blends

Figure 5.8 illustrates start of combustion (SOC), end of combustion (EOC) and total combustion duration (CD) of a test fuel. All test fuels had very similar SOC regardless of engine load, whereas EOC were linearly increasing for the all test fuels as a result of increased fuel to overcome increasing resistance. Consequently, CD was also increased for the test fuels at higher engine loads.

(a)

(b)

(c)
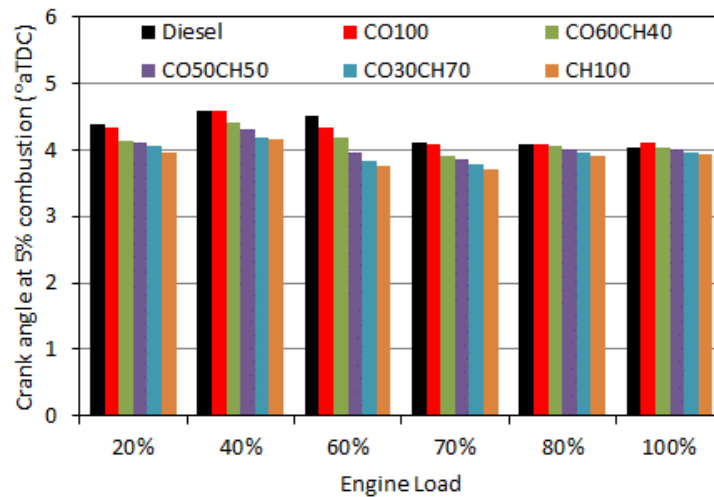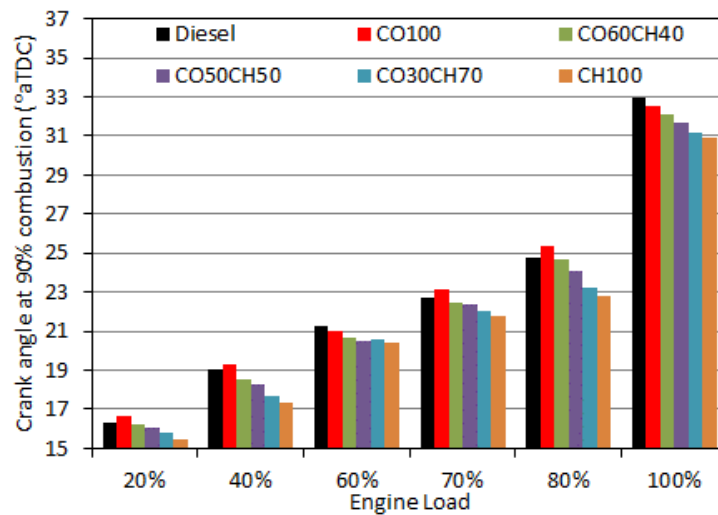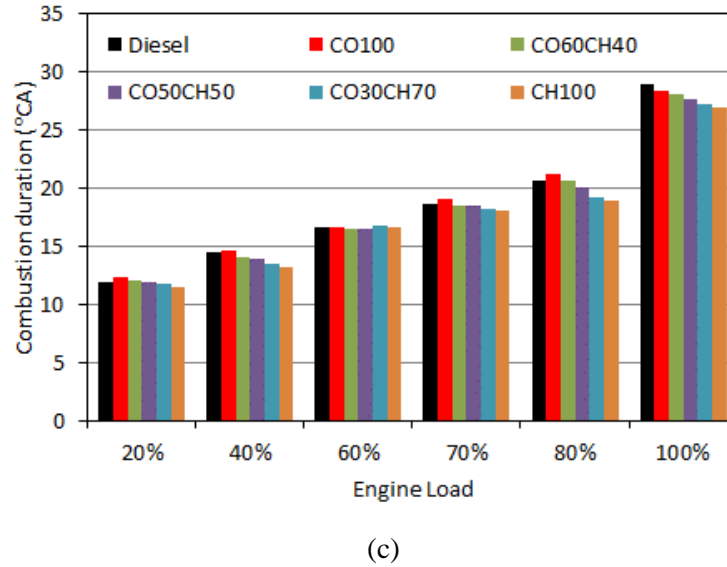
Figure 5.8. Combustion (a) start, (b) end times and (c) combustion duration in terms of crank angles, adapted from the author's published paper (Masera and Hossain, 2019).

Deep investigation over ignition delay (ID) and combustion durations were analysed and given Figure 5.9. CO100 had the shortest ID as a result of its high CN and low DU. Around 0.2°CA and 0.1°CA longer IDs were observed with each 2 CN decrements at medium and high loads. This means, both ID and CD were increased with the increased cottonseed biodiesel fraction in a blend. This was due to the relatively high density, IV and lower CN of the cottonseed biodiesel. The biomixtures of CO60CH40 and CO50CH50 gave average ID and CD values as 4.0°CA and 28°CA at the full load.
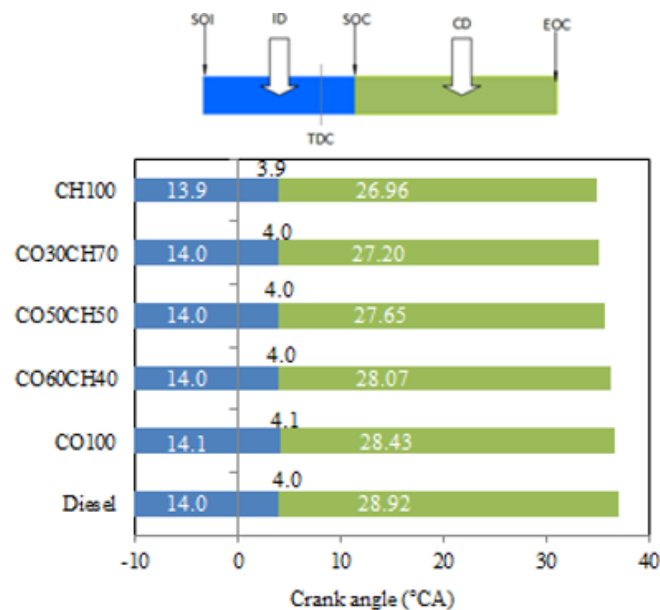
Figure 5.9. Ignition delay and combustion duration of the test fuels at the full engine load, adapted from the author's published paper (Masera and Hossain, 2019).

Exhaust gas temperature (EGT) is an important parameter to understand effective heat energy of a fuel (Dhamodaran *et al.*, 2017). High EGT indicates lower energy conversion into useful work (Emiroğlu *et al.*, 2018). In addition, BSFC and NO_x emission are typically increase under higher EGT (Dhamodaran *et al.*, 2017). EGTs of the test fuels were measured and given in Figure 5.10. Similar to CD, EGT was also increased with the increasing load. Overall, the biodiesels had lower EGT than diesel. The CO50CH50 biomixture had the lowest EGT at each engine load i.e. 7.8%, 6.9% and 2.4% lower than diesel, CO100 and CH100 at full engine load, respectively. Diesel had the highest EGT and it was followed by the CO100 and CO60CH40 at each engine load. Longer combustion durations may cause some of the fuel to be burned in the expansion stroke where the combustion chamber volume gets larger (Masera and Hossain, 2019). This phenomena results in converting the fuel energy into exhaust temperature rather than useful energy, which explained the reason of higher EGT of diesel, CO100 and CO60CH40 (Awad *et al.*, 2014). For example, diesel had 0.5°CA longer CD than CO50CH50 at 60% engine load which result in 10°C higher EGT.

Figure 5.10. Exhaust gas temperature of the test fuels at different engine loads, adapted from the author's published paper (Masera and Hossain, 2019).

The in-cylinder pressures of the biodiesels and diesel were given in Figure 5.11. Smooth in-cylinder pressure patterns were obtained for all biodiesels like diesel which indicated no abnormality for the biodiesels operation (Hossain *et al.*, 2016). The maximum in-cylinder pressure was observed for CO50CH50 as 71.8 bar at 10.7°CA. This value was around 4.2% and 4.5% higher than diesel and average of other biodiesels at the full load. The optimised fuel properties (by blending) of CO50CH50

was the reason why the pressure of CO50CH50 was the highest (Masera and Hossain, 2019). To illustrate, although CO100 had the minimum viscosity as 4.33 mm^2/s; it had lower CN as 54 and higher DU as 125 compared to CH100 having CN as 60 and DU value as 94. This proved that high viscosity detriment of CH100 and low CN drawback of the CO100 were both minimised with the CO50CH50 blend. Figure 5.12 demonstrates HR of the test fuels with respect to crank angles. Like in-cylinder pressure, CO50CH50 had the maximum HR at the early (pre-mixed) phase of combustion i.e. between 5°CA and 25°CA aTDC. For example, Figure 5.12(b) shows that CO50CH50 had 249 J of heat at 12°CA, but diesel had only 238 J of HR which was 4.4% lower than CO50CH50. Beyond the 35° CA, CO60CH40 had the maximum HR around 3.8% higher than the neat biodiesels and diesel at 69°CA. Iodine value, degree of unsaturation, cetane number and viscosity were the main fuel parameters affecting the HR. It was noticed that biodiesels with lower IV burned relatively faster due to presence of less number of double bonds in their chemical structures (Masera and Hossain, 2017). Nevertheless, their relatively high viscosities led to poor atomisation which reduces the burning quality of the fuel (Kirubakaran and Selvan, 2018). Therefore, CO50CH50 and CO60CH40 had the highest HR due to optimised fuel properties such as IV and viscosity.
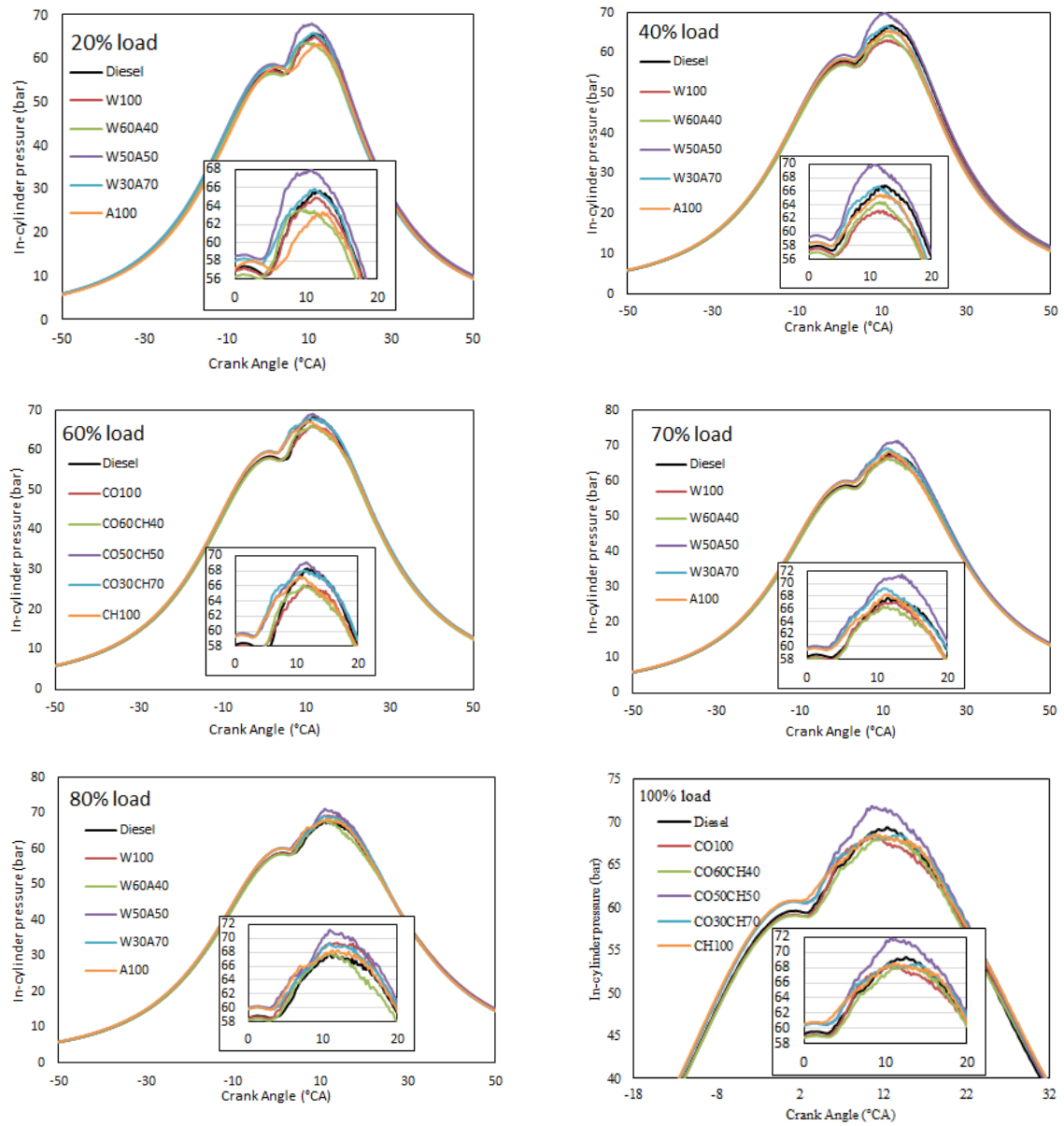
Figure 5.11. In-cylinder pressure versus crank angle of the test fuels at different engine loads.
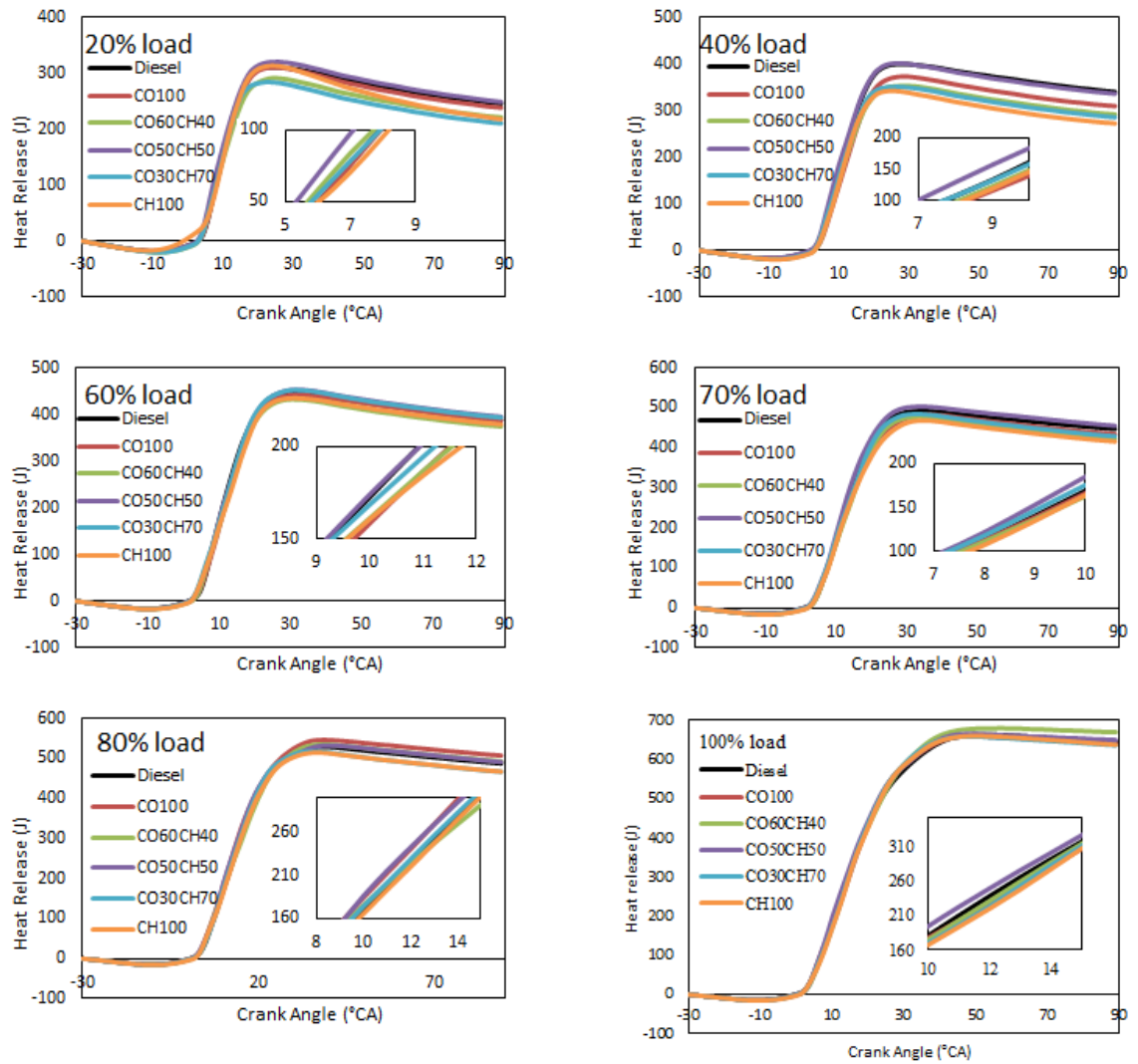
Figure 5.12. Heat release of test fuels at versus crank angles whole combustion period, and early combustion phase (enlarged view).

5.7. Exhaust emissions of cottonseed biodiesel-chicken biodiesel blends

CO_2, CO and NO emissions were measured via BOSCH BEA 850 gas analyser and instantaneous readings were captured for the neat biodiesels, the biomixtures and diesel. According to Figure 5.13, all CO_2 emissions were increasing in accordance with increasing engine load. This can be linked to increased carbon atoms in combustion reaction as a result of increased fuel consumption at high engine loads. On contrary, O_2 emissions were decreasing with the increasing engine load, as the air aspiration kept constant at the speed of 1500 rpm (Figure 5.14). Oxygen content and burning efficiency were the other important factors stated in literature in CO_2 emission (Kumar and Subramanian, 2017). However, carbon, hydrogen and oxygen contents of the biodiesels were very similar to each other as given in Table 5.3. Consequently, variations on CO_2 were linked to burning

efficiency of the fuels. Comparing the two neat biodiesels, CO100 released 5.4% higher CO_2 compared to CH100. Moreover, CO100 released 2.8% higher CO_2 than diesel, whereas CH100 released 2.8% lower CO_2 then diesel. However, even though CH100 had viscosity challenge according to BS EN 14214 standard and cannot be directly used in an engine, lower CO_2 emission advantage of the chicken biodiesel effected the CO_2 emission of the CO50CH50 biomixture positively. The CO50CH50 released the minimum CO_2 at almost each load. It was 5.8% and 2.9% lower than CO100 and diesel at the full load respectively. To sum up, CO_2 emission at high engine loads was successfully decreased by cottonseed biodiesel and chicken biodiesel blending.
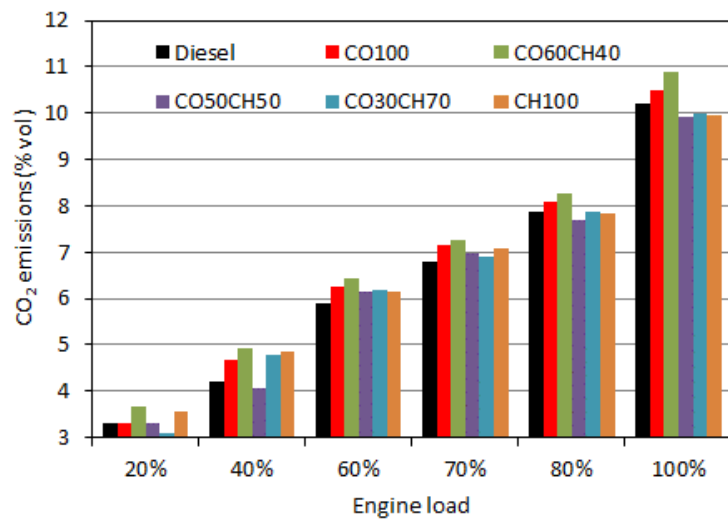

Figure 5.13. CO_2 emissions of the test fuels at different engine loads, adapted from the author's published paper (Masera and Hossain, 2019).
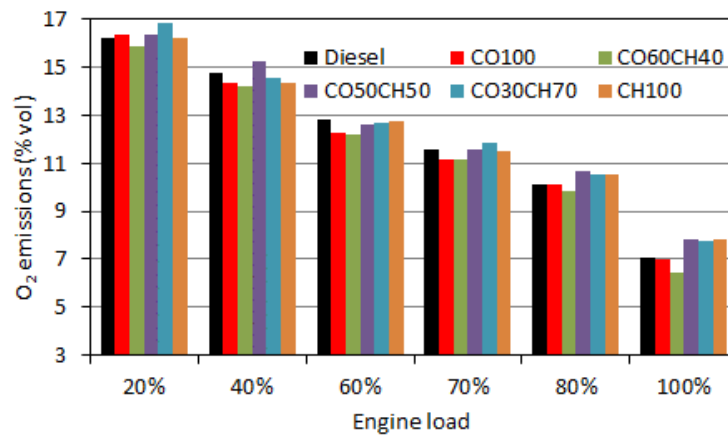
Figure 5.14: O_2 emissions of the test fuels at different engine loads.

Figure 5.15 presents CO emissions of the biodiesels and diesel under various load conditions. CO50CH50 released the same CO with diesel and it was 15% lower than both neat biodiesels at the full load. In contrast, CO60CH40 and CO30CH70 released approximately 17% higher CO than the neat biodiesels. Consequently, in average CO50CH50 biomixture proved that blending of cottonseed biodiesel with chicken biodiesel was successfully reduced the CO emission.
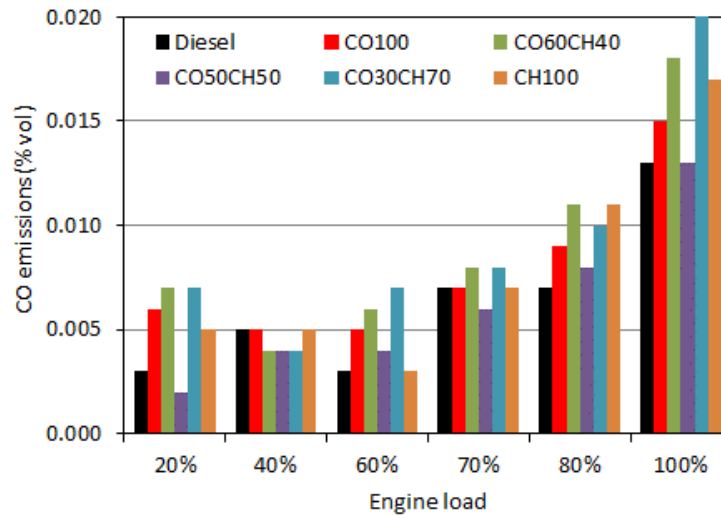
Figure 5.15. CO emissions of the test fuels at different engine loads, adapted from the author's published paper (Masera and Hossain, 2019).

NO emissions of the test fuels presented in Figure 5.16. Although the NO_x emission was not measured directly, the manufacturer of the equipment stated that NO_x can be estimated as approximately 1.2 times greater than the measured NO emission (Masera and Hossain, 2019). NO emissions of all fuels were increasing with the increasing engine load up to 70%, then remained similar at the 80% load and slightly decreased at the full load. This reduction at the full load was attributed to relatively low oxygen content to form NO. Comparing the neat biodiesels, CO100 released around 3%, 4% and 2% reduced NO than diesel at high engine loads like 70%, 80% and 100%, respectively. On the other side, CH100 released comparable NO with diesel. The reduced NO emissions of CO100 were in good agreement with the literature (Yucesu and Ilkilic, 2006; Karabektas *et al.,* 2008; Aydin and Bayindir, 2010). Similar to CO100, CO60CH40 also released 6.5% mitigated NO compared to diesel at full load. The reduction on NO emission was attributed to the lower in-cylinder pressure, which indicates lower combustion temperature because of lower LHV of CO60CH40 (Masera and Hossain, 2019). However, it must be noted that different factors influences the NO formation which might result in conflicting measurements. The ambient conditions, fuel spray characteristics, gas residence time of the fuels, EGR application, physical condition of the experimental equipment, oxygen content, and fluctuations can all affect the NO and NO_x formations, thus it is difficult to determine the most

dominant parameter causing the difference (Omari *et al.*, 2017; Ramalingam and Rajendran, 2017; Emiroğlu *et al.*, 2018; Ulusoy *et al.*, 2018).
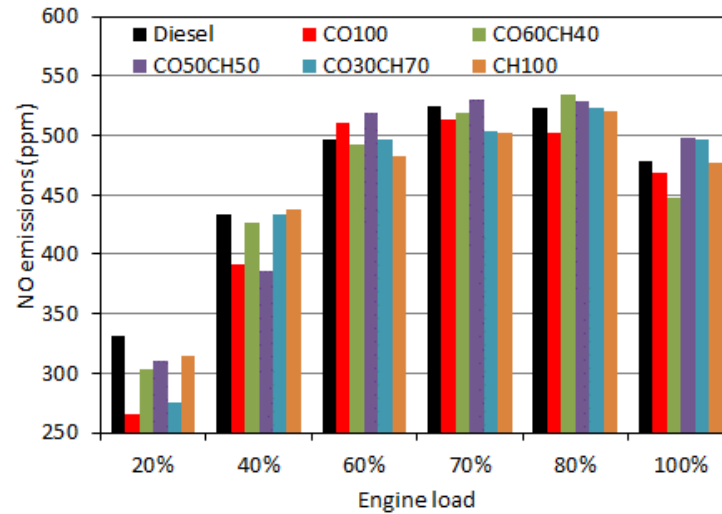
Figure 5.16. NO emissions of the test fuels at different loads, adapted from the author's published paper (Masera and Hossain, 2019).

Smoke opacities of the biodiesels along with diesel were also measured Figure 5.17. Smoke opacities of the biodiesels were comparable among themselves and lower than that of diesel at each engine load. For example, biodiesels had around 90% reduced smoke opacity than diesel at the full engine load.
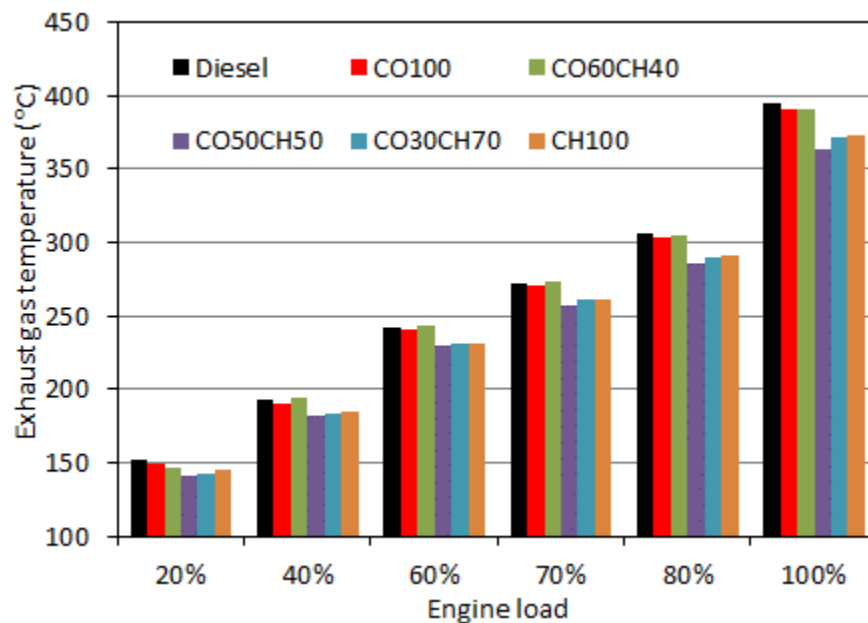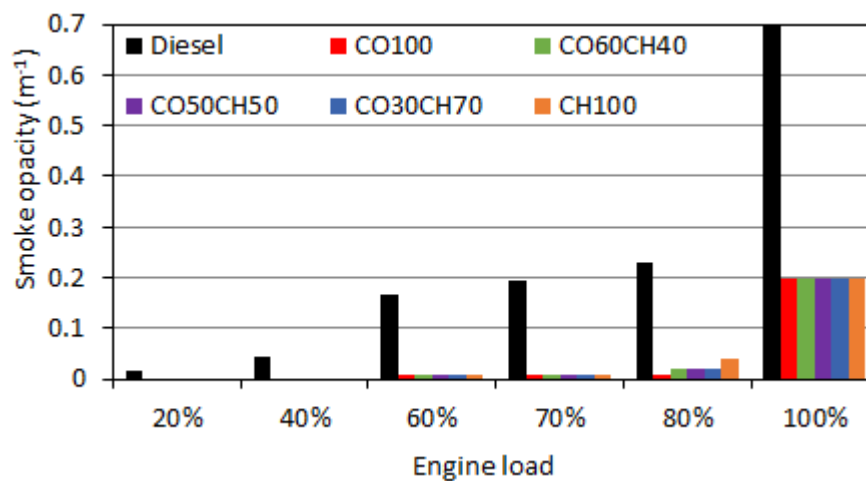

Figure 5.17: Smoke opacity of the test fuels at different engine loads, adapted from the author's published paper (Masera and Hossain, 2019).

5.8. Repeatability of test results

The results provided in this chapter were validated through repeatability analysis. The experiments were repeated for CO50CH50 biomixture with 1 year aged biomixture and new sets of produced biodiesels. Standard errors were found comparable with the Chapter 4 (Table 5.4). Like in the Chapter 4, the first measurement for smoke opacity of diesel was recorded higher than other tests at full load which can be related to inconsistency of diesel quality purchased from ESSO UK.

The repeatability analysis also proved that there was not any significant effect of a 1 year aged biomixtures on engine results. The biomixtures were stored at the room temperature in glass containers; lids were closed and placed in dark.

Table 5.4: Repeatability of test results for CO50CH50 biomixture. The measurements conducted on 15/02/2019 was 1 year aged biomixture, whereas measurementson 20/02/2019 were for new biomixture.

1.9 kW (20%)	Test dates				standard	standard
CO50CH50	19/03/2018	15/02/2019	20/02/2019	average	deviation	error
CO_2 (% vol)	3.31	3.44	3.58	3.44	0.14	0.08
CO (% vol)	0.002	0.004	0.003	0.003	0.001	0.001
HC (% vol)	1	1	1	1	0	0.00
O_2 (% vol)	16.37	16.13	16.09	16.20	0.15	0.09
NO (ppm)	310	278	313	300	19	11.20
Smoke (m^{-1})	0.01	0.01	0.01	0.01	0.00	0.00
Time for 100 ml fuel (s)	280	270	265	272	8	4.41
Gas analyser	**BOSCH**	**BOSCH**	**BOSCH**			

3.8 kW (40%)	Test dates				standard	standard
CO50CH50	19/03/2018	15/02/2019	20/02/2019	average	deviation	error
CO_2 (% vol)	4.06	4.8	4.86	4.57	0.45	0.26
CO (% vol)	0.004	0.004	0.003	0.004	0.001	0.000
HC (% vol)	1	0	0	0	1	0.33
O_2 (% vol)	15.25	14.23	14.25	14.58	0.58	0.34
NO (ppm)	386	392	391	390	3	1.86
Smoke (m^{-1})	0.02	0.02	0.02	0.02	0.00	0.00
Time for 100 ml fuel (s)	220	217	210	216	5	2.96
Gas analyser	**BOSCH**	**BOSCH**	**BOSCH**			

5.7 kW (60%)	Test dates				standard	standard
CO50CH50	19/03/2018	15/02/2019	20/02/2019	average	deviation	error
CO_2 (% vol)	6.15	6.12	6.29	6.19	0.09	0.05
CO (% vol)	0.004	0.008	0.005	0.006	0.002	0.001
HC (% vol)	2	3	0	2	2	0.88
O_2 (% vol)	12.59	12.44	12.39	12.47	0.10	0.06
NO (ppm)	519	485	483	496	20	11.68
Smoke (m^{-1})	0.03	0.03	0.03	0.03	0.00	0.00
Time for 100 ml fuel (s)	163	163	160	162	2	1.00
Gas analyser	**BOSCH**	**BOSCH**	**BOSCH**			

6.65 kW (70%)	Test dates				standard	standard
CO50CH50	19/03/2018	15/02/2019	20/02/2019	average	deviation	error
CO_2 (% vol)	6.99	6.98	7.1	7.02	0.07	0.04
CO (% vol)	0.006	0.007	0.005	0.006	0.001	0.001
HC (% vol)	1	2	1	1	1	0.33
O_2 (% vol)	11.55	11.38	11.33	11.42	0.12	0.07
NO (ppm)	530	497	498	508	19	10.84
Smoke (m^{-1})	0.03	0.03	0.03	0.03	0.00	0.00
Time for 100 ml fuel (s)	143	145	142	143	2	0.88
Gas analyser	BOSCH	BOSCH	BOSCH			

7.6 kW (80%)	Test dates				standard	standard
CO50CH50	19/03/2018	15/02/2019	20/02/2019	average	deviation	error
CO_2 (% vol)	7.68	7.89	7.96	7.84	0.15	0.08
CO (% vol)	0.008	0.009	0.006	0.008	0.002	0.001
HC (% vol)	2	0	0	1	1	0.67
O_2 (% vol)	10.64	10.26	10.24	10.38	0.23	0.13
NO (ppm)	529	477	502	503	26	15.01
Smoke (m^{-1})	0.03	0.02	0.02	0.02	0.01	0.00
Time for 100 ml fuel (s)	128	129	128	128	1	0.33
Gas analyser	BOSCH	BOSCH	BOSCH			

9.75 kW (100%)	Test dates				standard	standard
CO50CH50	19/03/2018	15/02/2019	20/02/2019	average	deviation	error
CO_2 (% vol)	9.92	10.07	10.18	10.06	0.13	0.08
CO (% vol)	0.013	0.014	0.013	0.013	0.001	0.000
HC (% vol)	0	1	0	0	1	0.33
O_2 (% vol)	7.85	7.47	7.45	7.59	0.23	0.13
NO (ppm)	498	468	469	478	17	9.84
Smoke (m^{-1})	0.2	0.02	0.02	0.08	0.10	0.06
Time to 100 ml fuel (s)	102	102	102	102	0	0.00
Gas analyser	BOSCH	BOSCH	BOSCH			

5.9. Conclusion

In this chapter, waste chicken fat biodiesel was chosen as base biodiesel because of high feedstock availability and promising fuel properties such as cetane number, iodine value and heating value. However, viscosity of chicken biodiesel was high, thus did not comply with the BS EN 14214 standard. In this regard, it was blended with cottonseed biodiesel for the purpose of fuel property improvement. It was found that blends with minimum 50% volume fraction of cottonseed biodiesel met the British and European standard. The major conclusions of the CO60CH40 and CO50CH50 biomixtures were;

1. BSEC of the all biodiesels found similar to that of diesel at the full engine load. Similarly, BTE of the biodiesels were comparable to diesel, BTE was only 1.6% lower than diesel at full load.

2. The lowest exhaust gas temperature was measured for CO50CH50; at full engine load, they were 7.8%, 6.9% and 2.4% lower than diesel, CO100 and CH100 respectively.

3. The in-cylinder peak pressure was maximum for CO50CH50 biomixture fuel, 4.2% higher than diesel. Moreover, heat release of the biomixture was observed 4.4% higher than diesel [between 5°CA and 25°CA aTDC (early combustion phase)].

4. The lowest CO_2 was observed with CO50CH50. It was 5.8% and 2.9% lower than CO100 and diesel fuels, respectively. Similarly, CO was of CO50CH50 was around 15% lower than the both neat biodiesels and comparable to diesel at the full load. However, CO50CH50 gave 6% higher NO emission compared to diesel. On the other hand, biomixture CO60CH40 gave 6.5% lower NO emission than diesel at full load.

To sum up, this part of the research proved that fuel properties of the chicken biodiesel were improved and met the BS EN 14214 standard when blended with cottonseed biodiesel. However, non-investigated properties such as metals content, oxidation stability, water content etc. should also be measured, they were out of scope of the current study and recommended as a future work to be able to declare that the biomixtures fully complies with the BS EN 14214 standard. Biomixtures CO50CH50 and CO60CH40 were provided comparable engine performance, improved combustion characteristics and reduced exhaust emissions.

Chapter 6

6. EXPERIMENTAL INVESTIGATION OF THE 2-BUTOXYETHANOL AS A BIODIESEL ADDITIVE

This chapter studies the 2-Butoxyethanol, which is an ether component having an alcohol branch, as a biodiesel additive. The additive was tested with the biomixtures introduced in the previous chapters i.e. W50A50 and CO50CH50 by 15% (by volume) and analysed in detail. Moreover, it was also tested with some popular biodiesels in the UK such as waste cooking biodiesel (W100) and rapeseed biodiesel (R100). Previous chapters proved that the biomixtures had improved engine test results compared to neat biodiesels due to their optimised fuel properties. Further upgrades on fuel properties and engine test results were investigated by the novel biodiesel additive in the present chapter.

6.1. Introduction

Renewable alternative fuels could potentially be used in diesel engines to reduce the harmful gas emissions (Atabani *et al.*, 2012; Hossain and Davies, 2012b, 2013; Masera and Hossain, 2017). Biodiesels are considered as one of the most promising alternative to fossil diesel due to promising physico-chemical properties and life-cycle emission mitigation potential. Literature reported that biodiesel fuel significantly reduced the PM, HC, CO and CO_2 emissions; however, most researchers reported that the use of neat biodiesels fuels in the unmodified CI engines gave higher NOx emissions than those obtained for diesel (Hoekman and Robbins, 2012; Mofijur *et al.*, 2013; Palash *et al.*, 2013). Other technical issues associated with neat biodiesel use are: (i) starting the engine in cold weather, (ii) sticking and clogging of fuel injector holes, fuel filters, and inlet/exhaust vales, and (iii) compatibility of fuel supply pipe materials with the biodiesel (Bhale *et al.*, 2009; Verma *et al.*, 2016; Datta and Mandal, 2017).

6.2. Literature review for alcohol fuel additives

Blending biodiesel with fossil fuels or alcohol additives improved engine performance and reduced emissions (Varatharajan and Cheralathan, 2012; Mofijur *et al.*, 2013). Blending neat biodiesel with additives gave lower NO_x and PM emissions than neat biodiesel operation (Zhu *et al.*, 2010; Yilmaz,

2012b; Yasin *et al.*, 2014; Datta and Mandal, 2017). Datta and Mandal (2017) reported that blending palm biodiesel with 15% methanol (or ethanol) decreased the peak in-cylinder pressure with respect to the neat biodiesel. The NO_x emissions were reduced by 19% and 30% due to methanol and ethanol addition respectively (Datta and Mandal, 2017). The smoke opacity was decreased dramatically when the biodiesel-alcohol blend was used (Datta and Mandal, 2017). In another study, the effects of PM and PAHs emissions were investigated when 1-3% acetone and 1% isopropyl were added in the waste cooking oil biodiesel (Tsai *et al.*, 2014). The authors reported that the use of both additives helped to reduce the PAH and PM emission by 24.1% and 53.2%, respectively. Vedaraman *et al.*, (2011) reported that NO_x emissions were decreased when ethanol, methanol, diethyl ether and distilled water was added separately into fossil diesel-palm oil biodiesel blend. Addition of methanol and water reduced the NO_x emission by up to 2.7% and 7%, respectively (Vedaraman *et al.*, 2011). However, HC emission was increased with the distilled water addition (Vedaraman *et al.*, 2011).
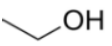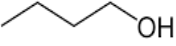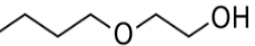
On the other hand, increase in the NOx emissions were also observed by the researchers when additives were added to neat biodiesel or diesel-biodiesel blends. Yilmaz (2012a) compared the effects of ethanol and methanol on diesel-biodiesel blends in a two cylinder direct injection type Kubota diesel generator set. Four different blends 40%Biodiesel-40%Diesel-20%Alcohol and 45%Biodiesel-45%Diesel-10%Alcohol and neat diesel were tested. The author reported that the BSFC of ethanol and methanol blends were increased by 28.6% and 58.3%, respectively. The methanol blends did not help to decrease the NO_x emissions. Whereas, ethanol blends reduced the NO_x emission by approximately 20% at medium loads (Yilmaz, 2012a). Another study conducted by Tosun *et al.* (2014) investigated the influences of ethanol, methanol and butanol addition separately on the peanut oil biodiesel in a multi-cylinder direct injection type diesel engine. They reported that 20% blends of methanol, ethanol and butanol with peanut oil biodiesel enhanced the engine torque output by 1.2%, 3.4% and 6.1% respectively as compared to neat biodiesel operation. The CO emissions of methanol, ethanol and butanol blends were decreased by 4.8%, 1.8% and 9.1%, respectively. They observed that the NO_x emissions were increased by 13.8%, 4.1% and 17.4% for 20% blends of methanol, ethanol and butanol respectively (Tosun *et al.*, 2014). Yasin *et al.* (2014) investigated the effects of 5% methanol addition on B20 blend with diesel. Methanol was mixed with the biodiesel-diesel blend using an ultrasonic agitator operated at 40 kHz frequency. They found that the brake power for B20 M5 fuel was decreased by approximately 7% and 10% than B20 and neat diesel fuels respectively. The BSFC of the engine was increased by about 4-6% (Yasin *et al.*, 2014). A reduction of approximately 17-18% in CO and CO_2 emissions, and an increase of 13% in NO_x emission was reported when the engine was fuelled with B20 M5 fuel (Yasin *et al.*, 2014). Yilmaz (2012b) studied the effects of air intake temperature when the engine was fuelled with 85%biodiesel-15%alcohol blends. The author reported that the CO and HC emissions were reduced by increasing the air intake temperatures and with the increasing percentage of alcohol additives (Yilmaz, 2012b).

The above studies demonstrated that blending biodiesel with alcohols improved engine performance characteristics. However, in the case of emission characteristics, no specific conclusions could be reached on whether adding alcohol helped to decrease the harmful gas emissions or not. So far, the effects of ethanol, methanol and butanol on biodiesel fuelled engine operation were found in the literature. In this chapter, a new additive '2-Butoxyethanol' will be used to assess the performance and emission characteristics of the engine operated with biodiesel-2-butoxyethanol blends. 2-Butoxyethanol is an ether compound with ethanol branch containing additional oxygen molecule. It is not a naturally occurring compound but obtained via different techniques in the laboratory environment like ethoxilation and etherification of butanol (Sievers and Wenzel, 1981; Rogers *et al.*, 2015). Additional oxygen content would further help to combust the biodiesel fuels more efficiently. Furthermore, the flash point of the 2-Butoxyethanol is close to diesel and higher than other alcohols used previously by the researchers (Fisher Scientific, 2018). In addition, 2-Butoxyethanol have better surfactant properties which may help to reduce the corrosion rate of a biodiesel fuel on engine components (Rogers *et al.*, 2015). Due to these promising fuel properties, investigation of the 2-Butoxyethanol as a biodiesel additive will be carried out in this chapter. It is important to note that no such study was found in the literature.

6.3. Biomixtures with 2-Butoxyethanol additive

2-Butoxyethanol (99% purity) purchased from Thermo Fisher Scientific was used as a biodiesel additive in this study. Fuel properties of the 2-Butoxyethanol and popular alcohol additives were tabulated in Table 6.1.

Table 6.1: Properties of common alcohols and 2-Butoxyethanol.

	Methanol (Methyl-Alcohol, 2018)	**Ethanol** (Ethanol, 2018)	**Butanol** (Butyl-Alcohol, 2018)	**2-Butoxyethanol** (2-Butoxyethanol, 2018; Fisher Scientific, 2018)
Structure	$\diagup$OH	$\diagdown\diagup$OH	$\diagdown\diagup\diagdown$OH	$\diagdown\diagup\diagdown_O\diagdown\diagup$OH
Linear formula	CH_3OH	CH_3CH_2OH	$CH_3(CH_2)_3OH$	$CH_3(CH_2)_3OCH_2CH_2OH$
Molecular weight (g/mol)	32.042	46.069	74.123	118.176
Heat of vaporisation (kJ/mol at 25C)	37.34	42.32	52.35	56.59
Miscibility with organic solvents	Yes	Yes	Yes	Yes
Kinematic viscosity (mm^2/s)	0.69 at 25°C	1.36 at 20°C	3.14 at 25°C	3.15 at 25°C
Density (g/ml)	0.79	0.79	0.81	0.90
Flash point (°C)	12	17	29	62
Boiling point (°C)	64.7	79	117.6	171
Melting point (°C)	-98	-117	-90	-75

Amount of the 2-Butoxyethanol to be doped into biodiesels was selected by a set of fuel characterisation experiments. In this regard, the additive was added into W50A50 biomixture at the volume fractions of 10%, 15% and 20%. Next, the mostly affected properties which were viscosity and HHV were measured. Figure 6.1 indicates the changes on viscosity and HHV with the 0%, 10%, 15% and 20% 2-Butoxyethanol. Both viscosity and HHV reduced with the increasing percentage of the additive. Although viscosity reduction was considered as improvement, HHV reduction was the disadvantage of the additive. Therefore, 15% volume of the additive was decided to be used in this research as HHV was around 38.5 MJ/kg. This means, doping 15% of the 2-Butoxyethanol additive caused 14% reduction in viscosity and 2.5% reduction in HHV.
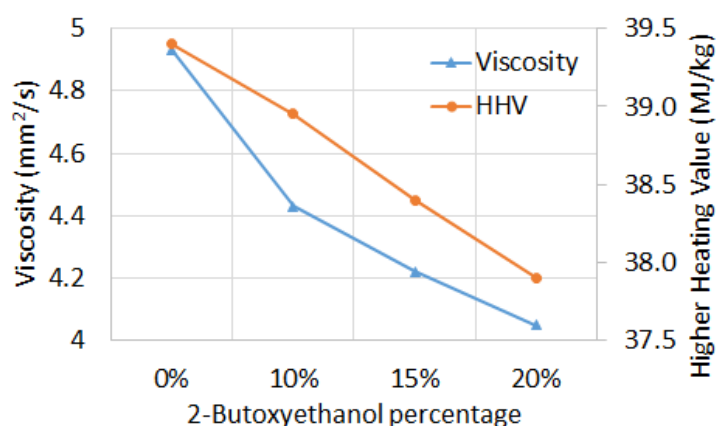
Figure 6.1: Effect of the 2-Butoxyethanol percentage on viscosity and higher heating value.

The mentioned additive was added into W50A50 and CO50CH50 biomixtures by 15% (by volume) and new biofuels were named as W42.5A42.5B15 and CO42.5CH42.5B15. Furthermore, the most common biodiesels in the UK were also tested with the additive which were waste cooking oil and rapeseed oil biodiesels (Alberici and Toop, 2014). Therefore, seven different fuels were tested in this study which were: ultra-low sulphur diesel (ULSD) as a reference fuel; neat waste cooking oil biodiesel (W100); blend of 85% waste cooking oil biodiesel and 15% of 2-Butoxyethanol (W85); neat rapeseed oil biodiesel (R100); blend of 85% rapeseed oil biodiesel and 15% of 2-Butoxyethanol (R85), blend of 42.5% waste cooking biodiesel-42.4% sheep biodiesel and 15% of 2-Butoxyethanol (W42.5A42.5B15); blend of 42.5% cottonseed biodiesel-42.4% chicken biodiesel and 15% of 2-Butoxyethanol (CO42.5CH42.5B15) Figure 6.2. The miscibility of biodiesels with 2-Butoxyethanol was successful. Thus, there was no need of any surfactant or mechanical stirring. The reference ULSD diesel was purchased from Esso UK and it was satisfying the BS EN 590 specifications (see Appendix) (Esso, 2019).

Figure 6.2: Fuel samples from left to right: Diesel, W100, W85, R100, R85, W42.5A42.5B15, and CO42.3CH42.5B15.

6.4. Fuel characterisation results for cottonseed biodiesel-chicken biodiesel blends

The FAME compositions of the biodiesels with and without 2-Butoxyethanol additive are shown in Table 6.2. The major FAMEs found in this study were C16:0, C18:0, C18:1 and C18:2. Peaks for the mentioned FAMEs were clearly observed on the mass spectra and presented in Figure 6.3. According to GCms results for W100, W85, R100 and R85, the first peaks were obtained at retention time around 18 minute which were representing the presence of the C16:0 (Figure 6.3 a, b, c and d). On the other hand, the following peaks between 21 and 22 minutes were accounted for C18 group FAMEs such as C18:0, C18:1 and C18:2. It was clearly observed that 2-Butoxyethanol additive reduced the mass fraction of the C18:2 FAME in the neat biodiesels around 3% in W100 and 7% in R100. It was

assumed that 2-Butoxyethanol (i.e. oxygen atoms) break the second double bonds in the content of C18:2. This phenomena directly influences the fuel properties especially cetane number and iodine value. Because, according to BS EN 14214 standard for biodiesel, iodine value of biodiesel is directly proportional to FAME breakdown of any biodiesel (British Standard Institution, 2010). Similarly, other fuel properties such as cetane number, lower heating value (LHV), density and cloud point can be predicted through FAME composition (Ramírez-Verduzco *et al.,* 2012).

Table 6.2: Mass fractions of the measured Fatty Acid Methyl Esters in the biodiesels.

FAME			Biodiesels					
Formula	Fatty acid	Designation	W100	W85	R100	R85	W42.5A42.5B15	CO42.5CH42.5B15
$C_{15}H_{30}O_2$	Myristic	C14:0	0.0	0.0	0.0	0.0	1.2	0.6
$C_{17}H_{34}O_2$	Palmitic	C16:0	10.4	10.1	4.1	4.3	15.9	22
$C_{17}H_{32}O_2$	Palmitoleic	C16:1	0.0	0.1	0.1	0.0	1.0	3
$C_{19}H_{38}O_2$	Stearic	C18:0	3.3	3.4	1.5	1.6	17.9	5
$C_{19}H_{36}O_2$	Oleic	C18:1	32.8	36.0	65.8	72.3	5.9	33
$C_{19}H_{34}O_2$	Linoleic	C18:2	52.9	50.0	26.0	19.2	58.1	37
$C_{19}H_{32}O_2$	Linolenic	C18:3	0.0	0.1	0.0	0.0	0.0	0.0
$C_{21}H_{42}O_2$	Arachidic	C20:0	0.2	0.0	0.5	0.5	0.0	0.0
$C_{21}H_{40}O_2$	gadoleic	C20:1	0.2	0.4	1.3	1.4	0.0	0.0
$C_{23}H_{46}O_2$	Behenic	C22:0	0.2	0.0	0.2	0.2	0.0	0.0
$C_{23}H_{44}O_2$	Erucic	C22:1	0.0	0.0	0.5	0.5	0.0	0.0
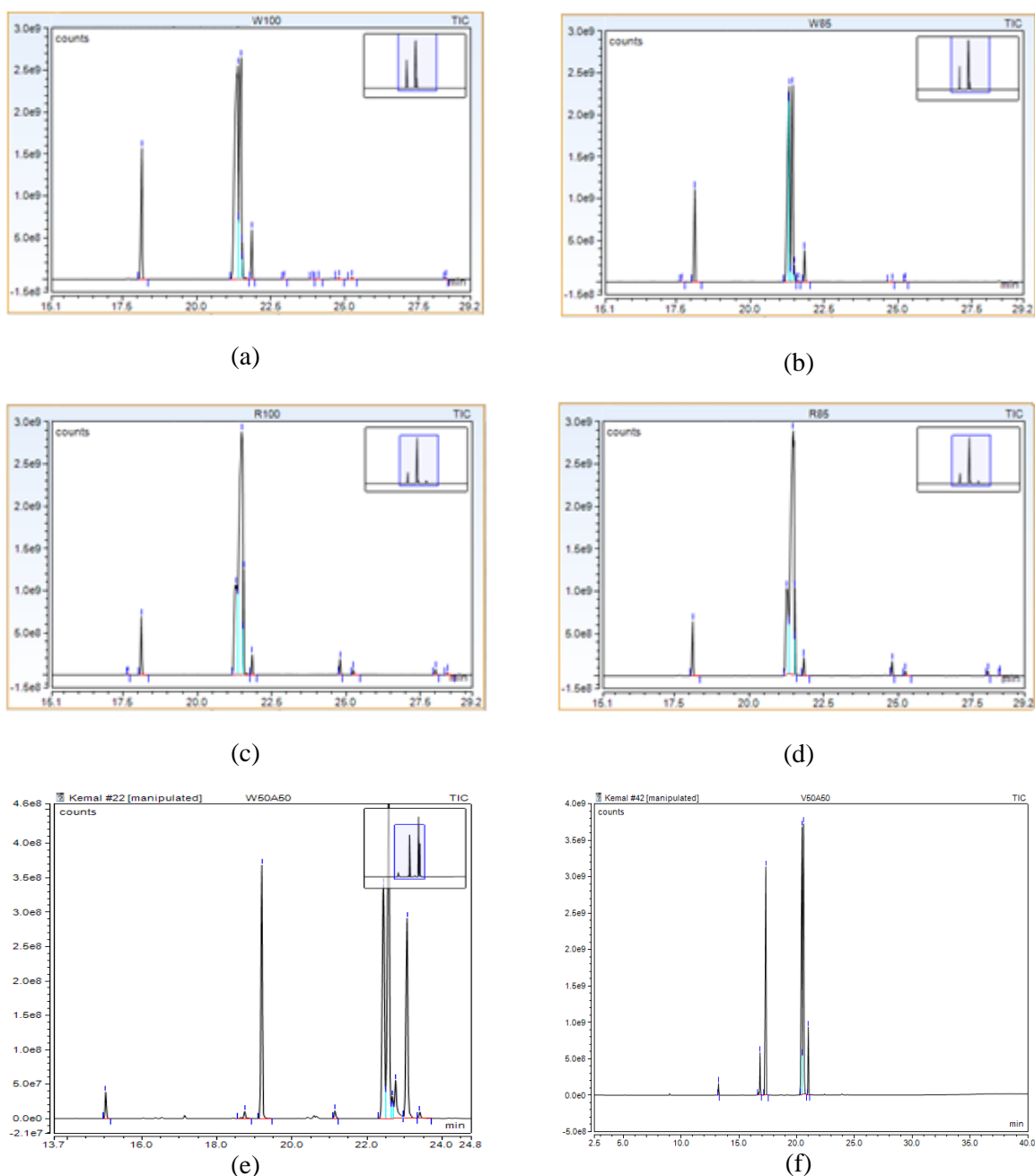
Figure 6.3: Gas chromatography and mass spectrum analyse of (a) W100, (b) W85, (c) R100, (d) R85, (e) W42.4A42.5B15 and (f) CO42.5CH42.4B15.

Table 6.3 shows the fuel properties of the test fuels and the British biodiesel norms BS EN 14 214. Visocsities (at 40 °C) of the W100 and R100 biodiesels were reduced by 12.5% and 9.8% with the addition of 15% 2-Butoxyethanol additive, respectively. Densities of the biodiesels did not change with the additive as 2-Butoxyethanol has similar density value with biodiesels as 900 kg/m^3 (Table 6.1). Flash points were also reduced by the 2-Butoxyethanol additive. They were measured relatively low for biodiesels, between 80 °C and 90 °C. This requires more precautions in the storage and transportation safety of the 2-Butoxyethanol doped biodiesels. Similarly, HHV of the biodiesels were reduced by 1-2.5%. Iodine value and degree of unsaturation were also slightly reduced with the

additive addition. On the other hand, cetane number was slightly increased. Carbon, hydrogen and oxygen contents were not significantly affected by the 2-Butoxyethanol additive. Overall, fuel characterisation results proved that 2-Butoxyethanol (by 15% volume) can be used as biodiesel additive, especially for the purpose of viscosity reduction.

Table 6.3: Fuel properties of the test fuels and BS EN 14214 standard.

Fuel Property	Unit	Diesel	W100	W85	R100	R85	W42.5A42.5B15	CO42.5CH42.5B15	BS EN 14214
Kinematic Viscosity at 40°C	(mm^2/s)	2.78	5.05	4.42	4.6	4.15	4.22	3.95	3.5-5.0
Kinematic Viscosity at 20°C	(mm^2/s)	4.39	7.61	6.66	6.69	6.21	6.31	5.91	n/a
Density	(kg/m^3)	828	882	882	880	880	872	881	860-900
HHV	(MJ/kg)	45.16	38.4	38	39.2	38.5	38.4	38.3	n/a
LHV	(MJ/kg)	42	36	35	37	36	36	36	n/a
Flash point	(^{o}C)	61.5	169	87	173	81	86	90	101 min
Iodine value	(g iodine/100 g)	n/a	120	118	103	97	109	97	120 max
Linolenic acid methyl ester	(% mol/mol)	n/a	0	0	0	0	0	0	12 max
Cetane number[a]	()	54	53	53	58	59	55	57	51 min
Cetane number[b]	()	54	49	50	53	55	53	55	51 min
Degree of u nsaturation	(% m/m)	n/a	239	237	220	213	121	108	n/a
Carbon content	(% m/m)	86.6[c]	77.14	77.13	77.12	77.08	76.96	76.84	n/a
Hydrogen content	(% m/m)	13.4[c]	11.91	11.93	12.04	12.08	11.99	12.06	n/a
Oxygen content	(% m/m)	0.07[c]	10.95	10.95	10.84	10.84	11.05	11.11	n/a

a= (Ramírez-Verduzco *et al.,* 2012); b= (Tong *et al.*, 2011); c= (Schönborn *et al.*, 2009)

6.5. Engine performance of 2-Butoxyethanol doped biodiesels

The alcohol blends of biodiesels provided higher BSFC than neat biodiesels and diesel, Figure 6.4 a. On average, BSFC of the W85 was 4.3% and 14.1% higher than the W100 and diesel respectively. Similarly, BSFC of the R85 was observed as 5.2% and 18.8% greater than R100 and diesel respectively. The scenario was the same with the biomixtures as BFSC of W42.5A42.5B15 was around 5% higher compared to W50A50. On the other hand, CO50CH50 and CO42.5CH42.5B15 had comparable BSFC values. This increase on BSFC can be attributed to the reduced LHV of the biodiesels with the alcohol addition (Table 6.3). However, BSFC of the alcohol blends were improved by the increasing engine load. Therefore, BSFC of the alcohol blends were very close to that of the neat biodiesels, only 1% higher, at the highest engine load. This was mainly due to the higher enthalpy of vaporisation of alcohol blends, which leads to better performance under higher engine loads (temperatures) (Yilmaz, 2012). Comparing the 15% alcohol blends, all W85, R85, W42.5A42.5B15 and CO42.5CH42.5B15 presented the same trend but BSFC of W85 and CO42.5CH42.5B15 was slightly (0-3%) lower than that of R85 and W42.5A42.5B15 (Figure 6.4 a). Brake Specific Energy Consumptions (BSEC) of the fuels were also analysed and given in Figure 6.4 b. The trends off all biofuels were the same with BSFC. However, most of the biofuels (except R85 and W42.5A42.5B15) had approximately 7% lower BSEC than diesel at the low and medium engine loads.

(a)

(b)
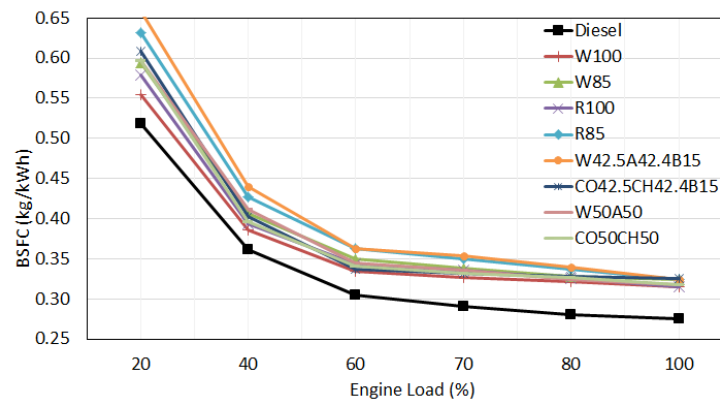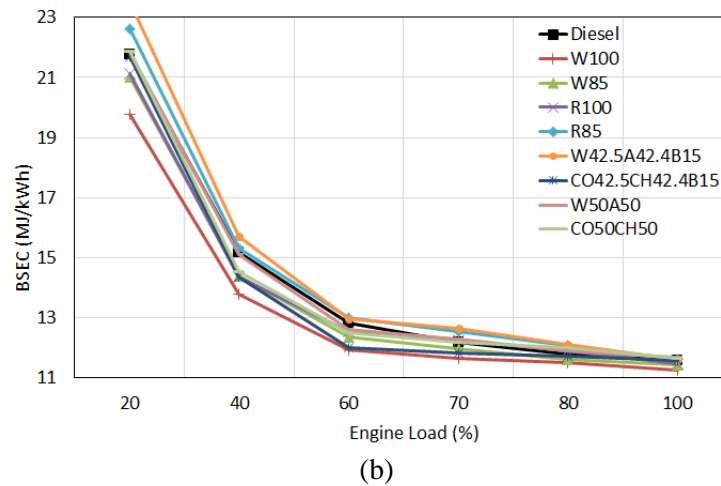
Figure 6.4: (a) BSFC and (b) BSEC of the test fuels at different engine loads.

Figure 6.5 presents the relationship between Brake Thermal Efficiency (BTE) and engine load for the test fuels. BTE of the engine was observed 1.5% lower for W85 and R85 compared to their base biodiesels at the full load. The reduction in BTE with the additive can be explained by the reduction on LHV with the 2-butoxyethanol addition Table 6.3. In contrast, 0.6% and 3.7% increase with W42.5A42.5B15 and CO42.5CH42.5B15 were observed compared to W50A50 and CO50CH50 at the full load. Moreover, W100 and CO42.5CH42.5B15 had 5% higher BTE than the diesel (in average) were clearly the best fuels among the tested fuels. They were followed by the W50A50 and CO50CH50 as around 3% higher BTE was reported than that of the diesel. The improved BTE's can be explained by the higher oxygen content of the biodiesels which in turn enhances the combustion (Vellguth, 1983; Tashtoush, Al-Widyan and Al-Jarrah, 2004). To sum up, in average BTE of the biodiesels were slightly reduced by 2.6% with the 2-Butoxyethanol additive due to reduced LHV.
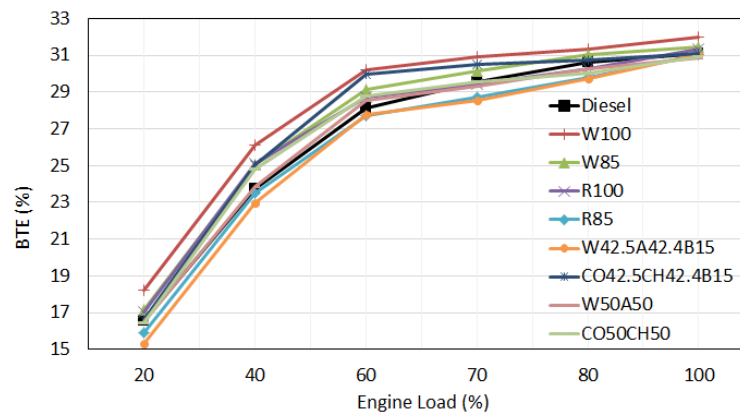
Figure 6.5: BTE of test fuels at different engine loads.

6.6. Combustion characteristics of 2-Butoxyethanol doped biodiesels

There was not any stability problem spotted during the engine operations. Figure 6.6 represents in-cylinder pressure behaviour of the test fuels at low, mid-range, and high loads. At the lowest load (20%), in-cylinder pressures of the neat biodiesels W100 and R100 were quite similar to that of the diesel. Whereas, the same parameter for alcohol blends (W85 and R85) was measured approximately 6% higher at the peak point, Figure 6.6a. This increase at the low loads was presumably caused by increased volatility of the alcohol blends. However, at the same time, W42.5A42.5B15 and CO42.5CH42.5B15 gave 6% lower peak pressure than W50A50 and CO50CH50. The results indicated that difference of peak pressures of all test fuels reduced with respect to increased load and comparable pressures were measured at the medium load. For example, at 60% engine load, R100 provided a similar peak in-cylinder pressure with the alcohol blends by 7.7% higher than the diesel, Figure 6.6b. Then, increase on the peak in-cylinder pressure was observed at 80% engine load for W100, Figure 6.6c. Finally, at the full load condition, biodiesels were provided 6-11% higher peak in-cylinder pressure than the diesel, Figure 6.6d. Besides, around 5°CA shift in peak in-cylinder pressure was detected between the diesel and all biofuels especially at the 100% load, Figure 6.6d. The alcohol blends of the biomixtures W42.5A42.5B15 and CO42.5CH42.5B15 gave further increase in peak pressure which was around 5% higher than W50A50 and CO50CH50. This is due to reduced viscosity and increased volatilities of the biodiesels with the 2-Butoxyethanol additive. Moreover, cetane number, density and iodine value were not negatively affected by the additive. In addition, increased in-cylinder pressures with the biodiesels and their alcohol blends proved that combustion was improved due to the presence of oxygen in their content.
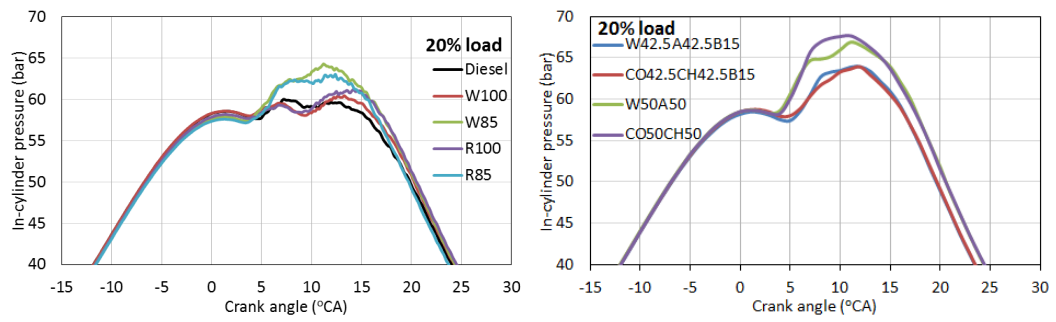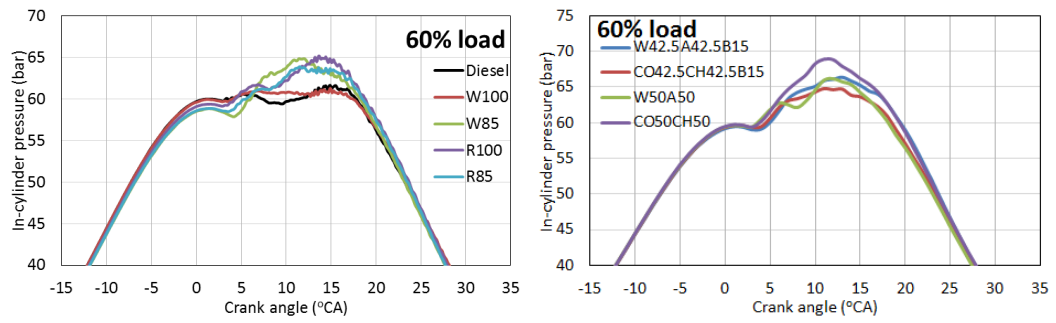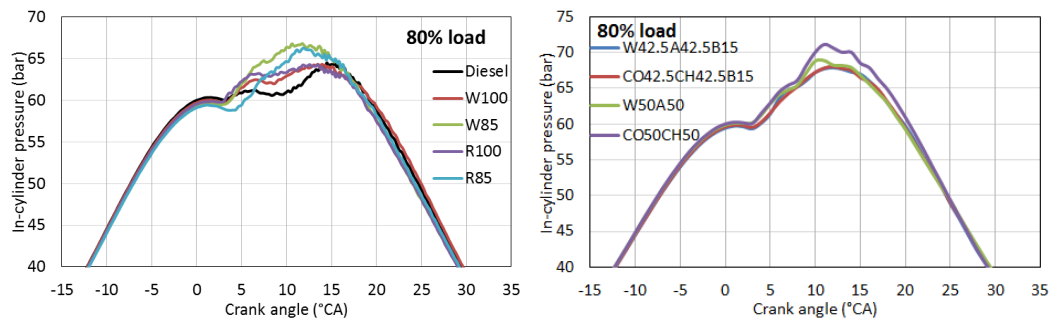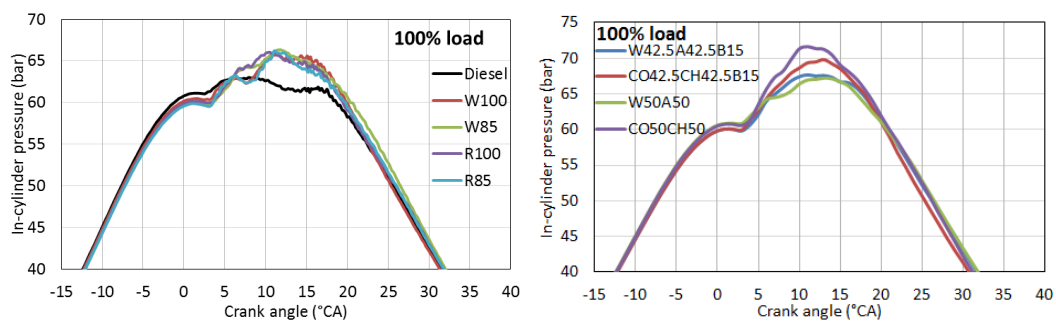
Figure 6.6: Relationship between the in-cylinder pressure and the crank angles at (a) 20%, (b) 60%, (c) 80% and (d) 100% engine loads.

The start and end of combustion processes were analysed and presented for each sample in Figure 6.7. Combustion start angle was measured when 5% of the combustion took place and similarly combustion finish angle was recorded at 90% of the total combustion via the help of KiBox cockpit software, Figure 6.7a and 6.7b. Differences between the finish and start angles were reported to identify the total combustion duration, Figure 6.7c. According to the results, combustion of all biodiesels started similar to diesel at low loads. However, higher ignition delays were addressed for the alcohol blends by 18% and 6% at mid-range and high engine loads respectively, Figure 6.7a. These results agree with the similar studies (with different alcohol blends) in the literature (Zhu *et al.*, 2010; Anand *et al.,* 2011). Enhanced ignition delay can be explained by the alcohol presence in the blend (Datta and Mandal, 2017), On the other hand, It was clearly observed that combustion of W85, R85, W42.5A42.5B15 and CO42.5CH42.5B15 ended few ^{0}CA earlier than the diesel and slightly earlier than their neat versions at almost every load Figure 6.7b. This early completion of the combustions automatically reflected into the combustion duration. According to Figure 6.7c, combustion durations of the W85, W42.5A42.5B15 and CO42.5CH42.5B15 were 0-6 ^{0}CA and 0-3 ^{0}CA less than the diesel and their neat versions (without additive) respectively (except 80% load for W85). Similarly, combustion duration of the R85 was reported 1-2 ^{0}CA less than both diesel and R100 at low and mid-range loads. Maximum reductions on the combustion durations were observed at the full load by approximately 3^0, 4^0, 4^0, 3^0, 2^0, 3^0, 3^0 and 1^0 for the W100, W85, R100, R85, W50A50, W42.5A42.5B15, CO50CH50 and CO42.5CH42.5B15, respectively Figure 6.7c. This analysis proved that the 2-Butoxyethanol blends of biodiesels burn quicker than the diesel and neat biodiesels. This can belinked to reduced viscosity and iodine value. Moreover, increased cetane number and volatility also contributed in rapid burning of the 2-Butoxyethanol blends.
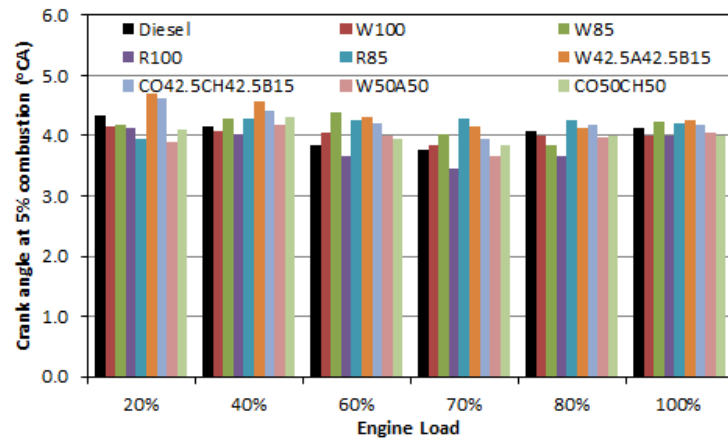
(a)
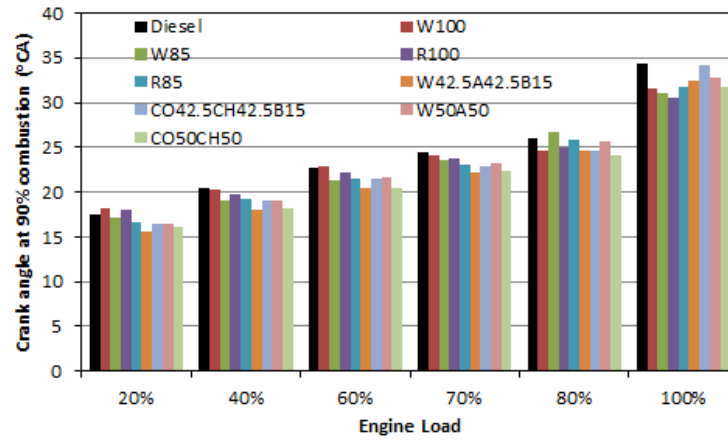
(b)
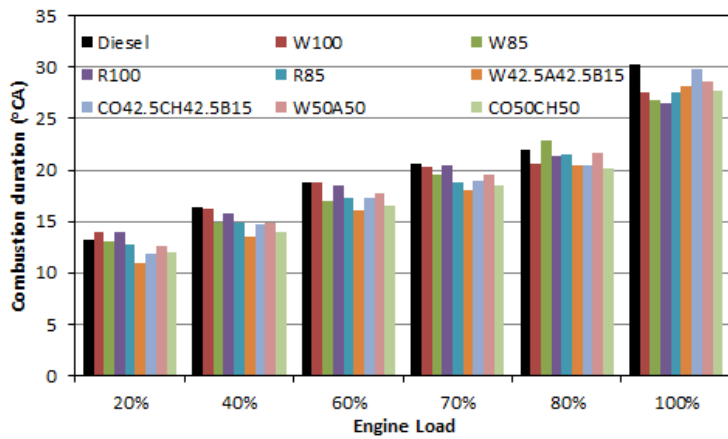
(c)

Figure 6.7: Analyse of combustion (a) start, (b) finish and (c) combustion duration.

Energy releases of the test fuels at corresponding angles were measured at the different engine load conditions and were illustrated in Figure 6.8. W85 and R85 were providing higher heat release especially during the early phases i.e. between approximately 3° and 15° CA at all engine loads. For example, heat releases of both W85 and R85 at 10° CA were 17% (23 Joules) higher than the diesel and neat biodiesels at the low (20%) and medium (60%) engine loads. The higher heat releases of alcohol blends of biodiesels (W85 and R85) can be attributed to their increased volatility and viscosity with presence of alcohol which results in faster combustion. However, in accordance with the lower peak pressures, W42.5A42.5B15 and CO42.5CH42.5B15 had around 11% lowered energy release than W50A50 and CO50CH50 at the low engine load. At the full engine load, on the other hand, heat releases of alcohol blends and neat biodiesels were comparable as the high combustion temperatures makes the atomisation of neat biodiesels easier. All biofuels were releasing around 16% (24 joules) higher heat than the diesel at 10° CA at the highest engine load. Although, however, alcohol blends burned quicker, their maximum heat release was 2.6-11% less than neat biodiesels at the end of combustion at almost each engine load. This was because of the shorter combustion durations of the alcohol blends. Maximum heat release rates of the fuels were measured for 51 cycles and the arithmetic mean was calculated for all loads Figure 6.9. Like in heat release case, in maximum heat release rate have an uneven distribution for fuels at low loads. However, after the 60% engine load, the deviations between the biofuels were not that significant. The first reason of this was believed to be the relatively higher combustion temperature which eliminates the effect of high viscosities. Secondly, the higher enthalpy of vaporisation of alcohol results in better maximum heat release rates at the higher combustion temperatures (Armas *et al.,* 2012).
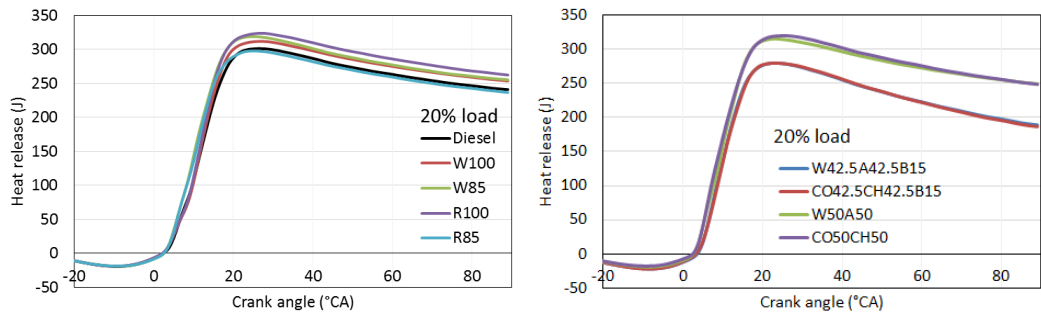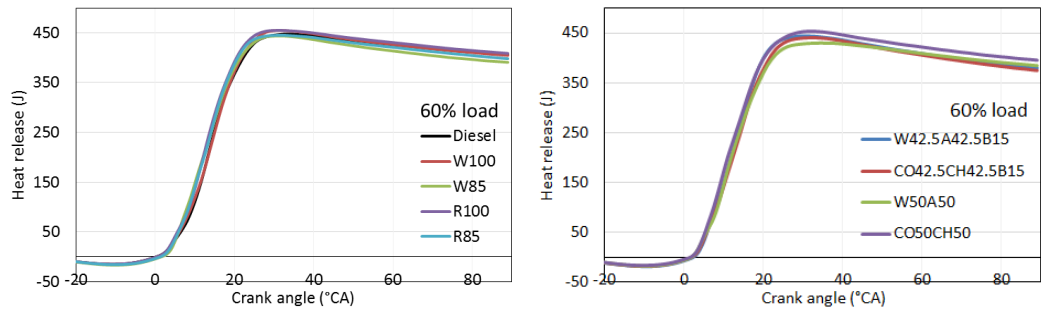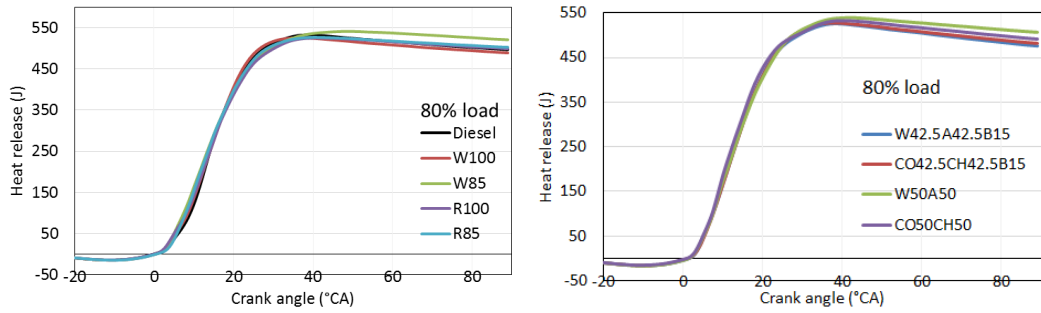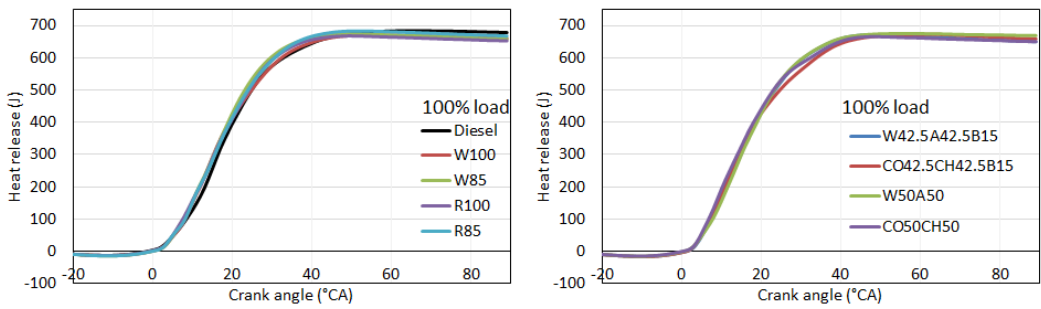
Figure 6.8: Heat release of test fuels at corresponding crank angles a) at 20%, b) at 60%, c) at 80% and d) at 100% engine loads.
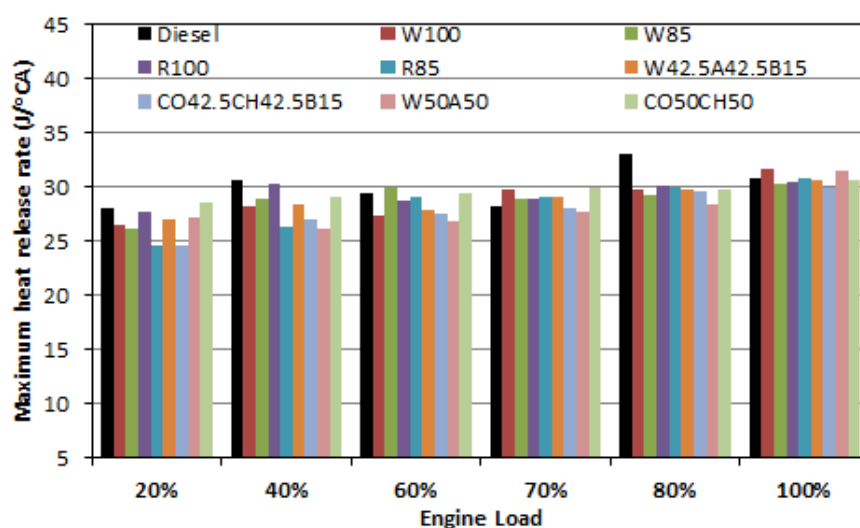
Figure 6.9: Maximum heat release rates of the fuels at different engine loads.

Consequently, 2-Butoxyethanol additive slightly reduced the combustion characteristics at the low engine loads due to reduced cetane number and LHV. However, combustion characteristics of alcohol blends found comparable with the base biodiesels at high engine loads. This was in good agreement with the literature and can be linked to higher enthalpy of vaporisation of alcohol additives, which gave better combustion under high temperatures (Nour *et al.*, 2017).

6.7. Exhaust emissions of 2-Butoxyethanol doped biodiesels

Exhaust gas emissions of the engine were tested at six engine loads for each fuel. Emissions were monitored instantaneously and captured at the steady state condition. Figure 6.10 indicates variation of CO_2 emissions with respect to increasing loads. It is clear that there was a linear relationship between the CO_2 emitted and the engine load. This can be explained by increased amount of fuel to overcome increasing load. Although all the test fuels exhibited comparable CO_2 emissions, the alcohol blends were emitting slightly higher (approximately 1-3%) CO_2 than their neat biodiesels. The highest CO_2 emission was noticed for the W42.5A42.5B15 which was 10.8% higher than W50A50 at the full load. This slight increased may be due to rapid burning of the 2-Butoxyethanol blends which turns more carbon atoms in to carbon dioxide. Unlike CO_2 emission, O_2 emissions were linearly decreasing with the increasing engine load for the all test fuels Figure 6.11. This was due to the increased reaction between the relatively higher amount of fuel molecules and the same amount of air (oxygen)

molecules at the higher loads. As the amount of air is constant at the CI engines, more O_2 was taking place in the combustion as an oxidiser at the higher engine loads.
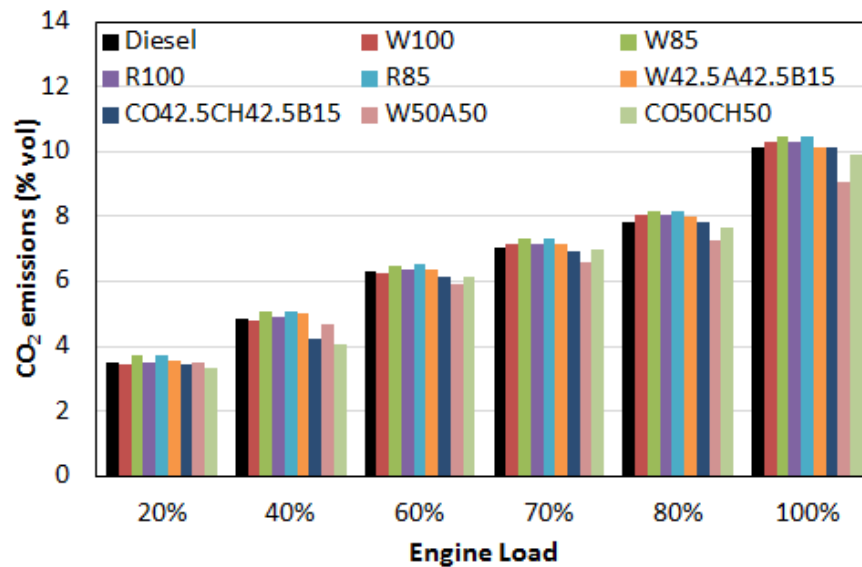
Figure 6.10: CO_2 emissions of the test fuels at different engine loads.
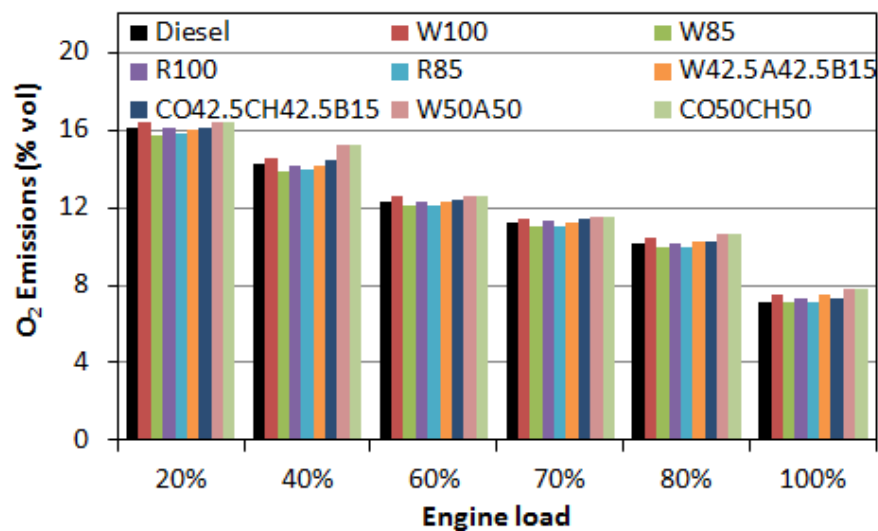
Figure 6.11: O_2 emissions of the test fuels at different engine loads.

Theoretically, biodiesels are likely to reduce the HC emission as the additional oxygen content provides more complete combustion (Li *et al.*, 2015). Hence, alcohol blends of biodiesels were expected to emit reduced HC emission as overall oxygen content increases

with presence of alcohol. Experimental results proved the theory as most of the biodiesels emitted almost 100% reduced HC emissions than diesel. Moreover, the alcohol blends had around 50% lower HC emissions than their neat biodiesel versions in average (Figure 6.12). The dramatic decrease on the HC emission can be a result of the extra oxygen molecules in the 2-butoxyethanol (both ether and alcohol) content.
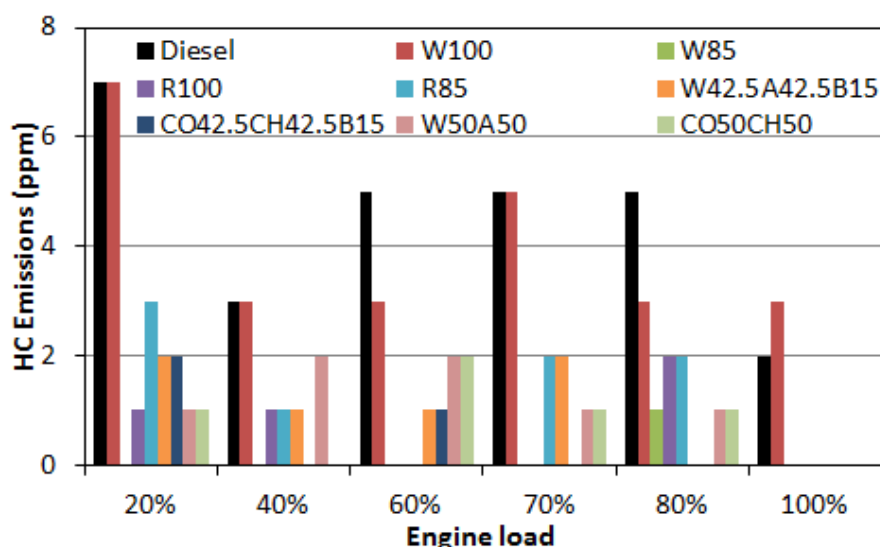
Figure 6.12: HC emissions of the test fuels at different engine loads.

Figure 6.13 provides CO emissions of the test fuels at different loads. It can be clearly deemed that 2-butoxyethanol addition into WCO biodiesel decreased the CO emission by approximately 25% on average. Similarly, CO of W42.5A42.5B15 and CO42.5CH42.5B15 were reduced by 10% and 30% compared to W50A50 and CO50CH50 at the full load respectively. In contrast, the additive increased the CO emission by around 12% when it was added into the rapeseed biodiesel. This result shows that the type of feedstock is very important for the 2-butoxyethanol blending in terms of the CO emission. The effect of oxygen content of any feedstock on the CO and CO_2 emissions were addressed in the literature (Vedaraman *et al.*, 2011). W85 emitted 10% less CO (on average) compared to diesel. Furthermore, the maximum reduction in CO emission of W85 was observed by 36.4% less than W100 at 70% engine load and by 30% less than the diesel at 60% load. At full load, W42.5A42.5B15 and CO42.5CH42.5B15 gave approximately 44% lower CO than diesel. The reduction in CO emission was presumably due to the reduced viscosities of the alcohol blends

which in turn leads to better vaporisation and of the fuel (Imdadul *et al.*, 2017). It is presumed that 2-butoxyethanol increased the atomisation characteristic and volatility of the alcohol blends during injection which in turn improved the combustion.
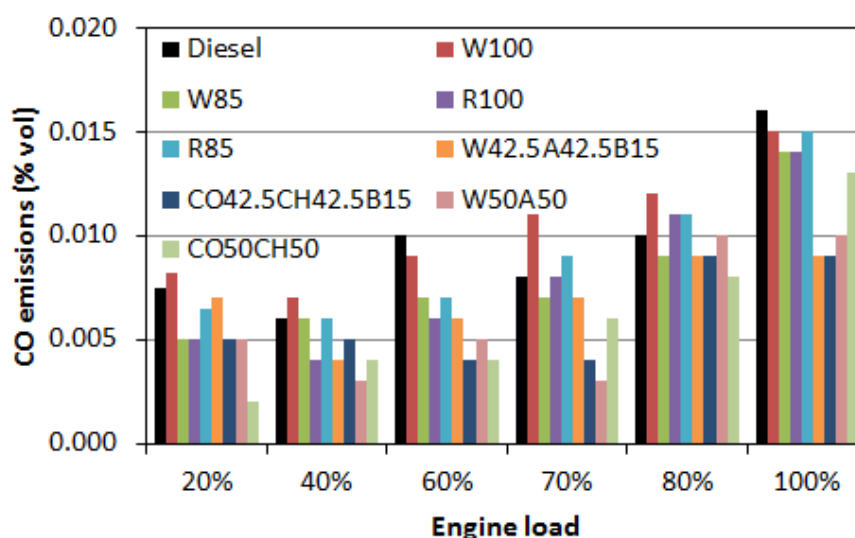
Figure 6.13: CO emissions of the test fuels at different engine loads.

Nitrogen oxide of all test fuels was measured at the different engine loads Figure 6.14. The 2-Butoxyethanol blends of biodiesels exhibited different behaviours at low, medium and high engine loads. The results at the low and medium loads were uneven such as W85, R85, W42.5A42.5B15 and CO42.5CH42.5B15 had around 15% increased NO emissions than neat biodiesels. Then, at the medium engine loads, NO emissions of W100 and R100 were comparable to W85 and R85, whereas W42.5A42.5B15 and CO42.5CH42.5B15 gave around 4.5% reduced NO emissions compared to W50A50 and CO50CH50 at the 60% load. Finally, after exceeding the 80% engine load, alcohol blends started to emit lower NO than the biodiesels without additive which reached to its maximum value at full load by 5.4%. Beside their neat biodiesel versions, they also emitted 3.5% lower NO emission than the diesel at the maximum load. This might be attributed to the higher enthalpy of vaporisation of the 2-butoxyethanol ($\Delta_{vap}H$= 51.20 kJ/mol at 372.5 K) which leads to better combustion of alcohol molecules at high engine loads (Yilmaz, 2012b). As a result of more alcohol fraction in the

combustion, it is believed that more cooling effect of the alcohol helped to reduce NO emissions at the high loads.
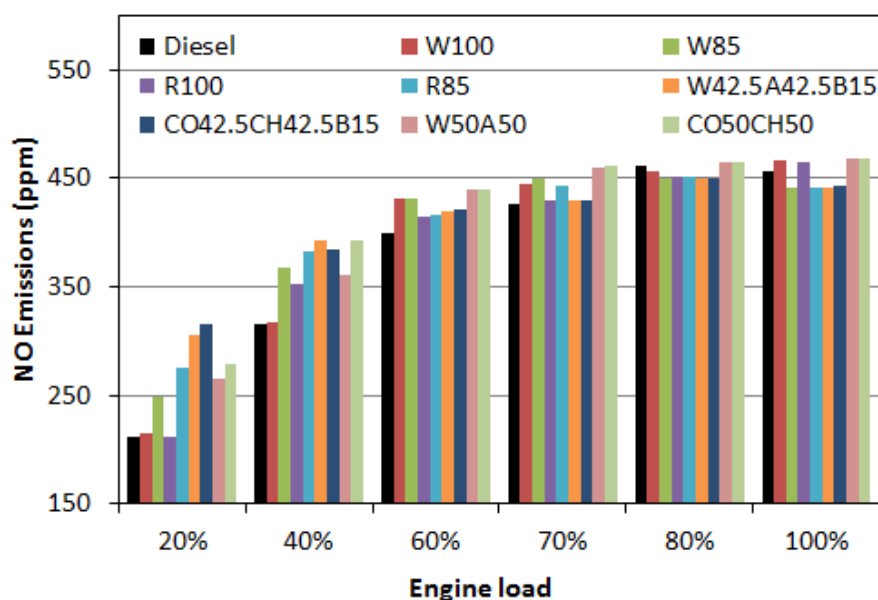
Figure 6.14: NO emissions of the test fuels at different engine loads.

Figure 6.15 presents trend of the smoke opacity with respect to the increasing engine load. It was clearly observed that smoke opacities of the all biofuels significantly reduced with the increasing engine loads. The maximum reductions on smoke opacities were recorded at full load as 73%, 79%, 66% and 71% for W100, W85, R100 and R85 respectively. Moreover, 97% reductions were observed for the W50A50, CO50CH50 biomixtures and their 2-Butoxyethanol blends again at the full load. Dramatic reductions in smoke opacities were due to the extra oxygen content in the biofuels content (Baskar and Senthilkumar, 2016). The additional oxygen molecules in the content of 2-butoxyethanol also caused further reduction compared to their neat versions at full load Figure 6.15.
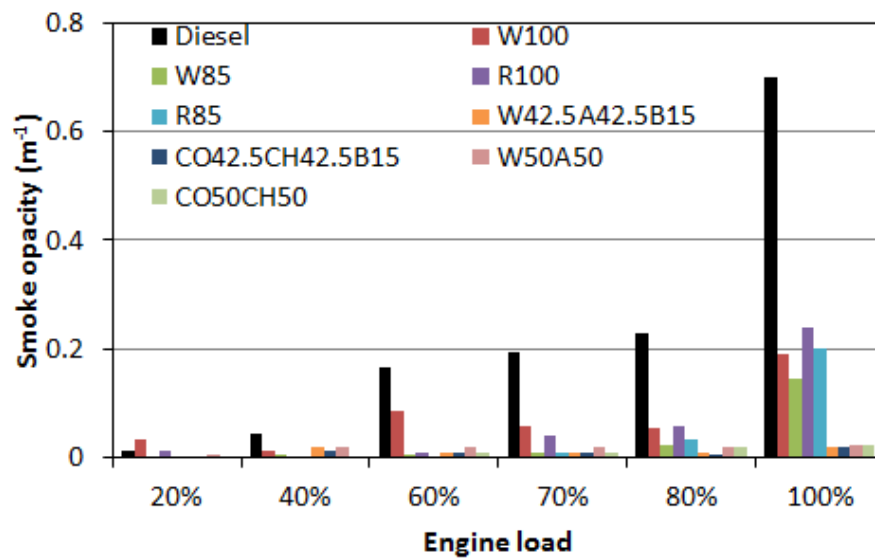
Figure 6.15: Smoke opacity of the test fuels at different engine loads.

The 2-Butoxyethanol additive gave 30%, 50%, 5.4% and 20% reductions in CO, HC, NO and smoke opacity compared to biodiesels without additive. However, at the same time 1-3% increase (in average) in CO_2 was also found for the 2-Butoxyethanol blends.

6.8. Conclusion

The 2-Butoxyethanol blends of the biodiesels with and without 2-Butoxyethanol additive were investigated in this chapter. According to in-cylinder pressure diagrams, there were no abnormalities found on combustion of the 2-Butoxyethanol additive. Hence, it could be concluded that the 2-Butoxyethanol (15% vol.) is a safe biodiesel additive for CI engine application. The major research outcomes are summarised below:

1. The 2-Butoxyethanol is an effective additive to reduce viscosity of a biodiesel. However, LHV of blended biodiesel also reduced with the additive. Therefore, optimum amount of 2-Butoxyethanol was found as 15% by volume.

2. BSFC of biodiesels was increased by approximately 5% when blended with the 2-Butoxyethanol (15% by volume). In addition, the additive decreased the BTE of the biodiesels by 2.6%. Nevertheless, BTE of the biodiesels were still comparable to diesel at full load.

3. Biomixtures with the 2-Butoxyethanol additive (W42.5A42.5B15 and CO42.5CH42.5B15) released around 5% higher peak pressure at full load. Comparable heat release rates were observed for the biofuels at the full load.

4. Total combustion duration of biodiesels was decreased around 1-2 ^0CA with the 2-Butoxyethanol additive due to improved cetane number.

5. The NO emissions of the biodiesels were successfully reduced approximately 5.4% with the 2-Butoxyethanol (15% vol.) Moreover, this value was around 3.5% lower than the diesel at full load. In addition, significant reductions in CO, HC and smoke emissions were observed by 30%, 50% and 20% with the 2-Butoxyethanol blends compared to the biodiesels without additive. However, CO_2 was slightly increased between 1-3% in average (maximum increase was observed with W42.5A42.5B15 by 10.8% at full load).

To sum up, this study concludes that the 2-Butoxyethanol is an effective and safe biodiesel additive. Compared to literature studies, it can be superior to other alcohols like methanol and ethanol especially in terms of BSFC, BTE and NO emission due to its fuel properties. Although, this chapter proved that 2-Butoxyethanol is a suitable biodiesel additive for the biodiesels including the W50A50 and CO50CH50 biomixtures, the biodiesel's NOx emissions can be reduced further with an after-treatment application. In this regard, the biomixtures will be tested with an after-treatment system with the purposes of (i) minimising the NOx penalty of biofuels and (ii) understanding the NOx mitigation capability of the biomixtures with the up to dated technology of urea injection.

Chapter 7

7. REDUCTION OF NO$_x$ EMISSION BY MODIFIED SELECTIVE NON CATALYTIC REDUCTION

This chapter reported the research work carried out on the modified Selective Non-Catalytic Reduction (SNCR) as an after-treatment system. The biomixtures introduced in the previous chapters W50A50 and CO50CH50 were tested in the presence of modified SNCR for the purpose of NOx mitigation. Commercially available urea-water solution (Adblue) was used as Diesel Exhaust Fluid (DEF) to react with the NOx emissions. Moreover, modified SNCR was also tested with neat distilled water injection. Research presented in Chapter 6 showed that 2-Butoxyethanol additive reduced the NO emission of the biomixtures by 5% at full load condition. Further reductions on NO emission were investigated by injection of urea-water solution and distilled water separately through modified SNCR aftertreatment system.

7.1. Introduction

Previous chapters proved that biomixtures obtained from waste resources like animal fats and waste cooking oil are good alternatives to replace fossil diesel. The biomixtures gave improved combustion characteristics compared to neat biodiesels. In addition, most of the exhaust gas emissions such as CO, CO_2, HC and smoke intensity were reduced with biomixtures compared to diesel. However, NOx emissions of biodiesels were comparable to neat biodiesels and diesel. Similarly, around 85% of the published studies reported an increase in NOx emission for biodiesel applications (Thangaraja *et al.,* 2016). The reason underlies on the increased combustion temperature as a result of the higher oxygen content of biofuels which provides improved combustion. Therefore, it was decided to cope with the NOx penalty at the exhaust system by a help of after-treatment system. In this regard, the latest technology found was ammonia injection after the combustion process i.e. at the exhaust system (Soleimanzadeh *et al.*, 2019). One application of this technique is Selective Non-Catalytic Reduction (SNCR) which generally used in relatively large engines, furnaces, incineration or boilers. SNCR system injects diesel exhaust fluid (DEF – ammonia) directly into the exhaust system without any catalyst. Another application is Selective Catalytic Reduction (SCR) which also involves catalytic to

upgrade the NOx reduction yield. Because of the cost of catalyst, it is mainly used in relatively small size applications such as the automotive sector.

7.2. Introduction Literature review – Selective Catalytic Reduction (SCR) and Selective Non-Catalytic Reduction (SNCR)

The SCR was first found in the 1970s and commercialised in Japan around 1957 (Javed *et al.,* 2007). The operational temperature of the system is above 350°C (Yim *et al.*, 2004). Up to 90% of NOx reductions were reported in the literature (Muzio *et al.,* 2002). However, these extreme NOx mitigations came up with well-developed designs providing reagent NH_3 to NOx ratio and uniform velocity through the catalyst (Muzio *et al.,* 2002). Even though SCR is a very effective technique, there are some drawbacks due to the presence of a catalyst such as erosion (because of dust or ammonium bisulphate), limited lifetime, expense and possibility of catalytic disintegration which cause an additional source of pollutant (Javed *et al.*, 2007). These problems can be avoided with SNCR system which is free of catalyst. However, SNCR systems have the operating temperature between 875°C and 1050°C, thus they are mainly used in large stationary sources like boilers, furnaces, incineration etc., (Hao *et al.*, 2015). This is mainly due to the lower reaction rate between ammonia and NOx below 800°C; hence the injected ammonia does not properly react with the exhaust gas. On the other hand, above 1200°C temperature, ammonia oxidises and starts forming NO which increases the emissions (Xu *et al.*, 2019). Mansha *et al.,* (2007) proved these conditions with a numerical study. They studied NOx reduction by utilising SNCR technique and predicted up to 96% reduction of thermal NOx under the conditions of; molar ratio of 1; the temperature at 800°C and residence time 2.5 seconds. However, the high-temperature window (i.e. operation range between 875°C and 1050°C) was considered as the biggest barrier for SNCR application for diesel engines (Muric *et al.*, 2018). To avoid this issue, studies have tried various solutions such as implementing an extra mixing chamber to enhance the turbulence (Thiyagarajan *et al.*, 2017), double compression expansion engines to increase the exhaust temperature (Muric *et al.*, 2018), various additives and/or injection agents (Krahl *et al.*, 2010) and injecting aqueous urea solution directly into the combustion chamber after the fuel injection (Yang *et al.*, 2015). For example, Thiyagarajan *et al.,* (2017) studied SNCR technique with an extra mixing chamber on a single cylinder CI engine on diesel operation. They have tested four different injection agents which were anhydrous ammonia, succinic acid, diethylamine and monoethanolamine at 1 kg/h flow rate. They reported maximum reductions of 10% and 15% for NO and CO_2 emissions with monoethanolamine injection at full load. Muric *et al.,* (2018)

used double compression expansion engine and reported 55% reduction on NOx emission at 1200 rpm and 1200 K temperature. However, the same study also provided 10-22% NOx reduction at 1000 K exhaust temperature. In another study, Krahl *et al.,* (2010) tested 1,2,3-tris-(diethylaminomethoxy)propane, 1,2-Bis-(diethylaminomethoxy)-3-ter/-butoxy propane and 2,2-dimethyl-(4-diethylaminomethoxy)-1,3-dioxolane additives with SNCR and obtained 22% NOx reduction for diesel and 47% NOx reduction for biodiesel. Yang *et al.,* (2015) used a separate injector to inject urea-water solution directly into the combustion chamber during the power stroke, they reported NOx reduction up to about 53%.

Based on the literature review, three parameters such as mixing (turbulence), exhaust temperature and residence time are critical for SNCR efficiency. This chapter will focus on a modified SNCR after-treatment system with a new design composed of two parts which are expansion and swirl chambers. Enhanced turbulence intensity and residence time are desired to improve NO reduction of biomixtures and diesel. The CFD analysis of design options was carried out to select the best design geometry in terms of turbulence intensity and injected particle residence time. Then, the selected design was manufactured and implemented on the test rig for experimental analysis.

7.3. Calculation of urea-water solution (32.5%) needed for injection

7.3.1.   NOx decomposition reaction mechanism

Ammonia is a well-known chemical that reacts with nitrogen oxides and forms nitrogen and water which are not harmful. However, ammonia itself is a dangerous chemical. Therefore, it is commonly stored and transferred in the form of urea $CO(NH_2)_2$. Typically, urea-water solution is used for injection through aftertreatment systems. Then the urea decomposes into ammonia in the presence of water as shown in equation 7.1 (Haridass and Jayaraman, 2018). This process takes place above 350°C with a residence time minimum of 0.1 s (Haridass and Jayaraman, 2018).

$$CO(NH_2)_2 + H_2O \rightarrow 2NH_3 + CO_2 \tag{7.1}$$

The three possible reaction mechanisms of NOx reduction in the presence of ammonia are illustrated in equations 7.2, 7.3 and 7.4 (Cho *et al.*, 2017; Haridass and Jayaraman, 2018; Mehregan and Moghiman, 2018; Sachuthananthan *et al.,* 2018).

$$4NH_3 + 4NO + O_2 \rightarrow 4N_2 + 6H_2O \tag{7.2}$$
$$4NH_3 + 2NO_2 + O_2 \rightarrow 3N_2 + 6H_2O \tag{7.3}$$
$$2NH_3 + NO_2 + NO \rightarrow 2N_2 + 3H_2O \tag{7.4}$$

The required amount of urea for an application can be calculated through the introduced equations. In this research, it was assumed that all NO will be converted through equation 7.2 and all NO_2 will be converted through equation 7.3. The equation 7.4 was not considered as it also requires the same molar ratio with the equations 7.2 and 7.3 (2 moles of NH_3 is required to convert 1 mole of NO_2 and 1 mole of NO). Ultimately, 1 mole of NH_3 is needed to decompose 1 mole of NO; and 2 moles of NH_3 is required for decomposing 1 mole of NO_2.

7.3.2.   Desired flow rate of the injection

Although the rated speed of the engine was 1500 rpm, the after-treatment system was tested at 2000 rpm and 80% engine load. This was simply because of the exhaust temperature limitations of the low power density engine. The exhaust temperature was around 380 °C at the mentioned condition. Exhaust heat wrap also applied to retain the heat at the exhaust pipe. The required injection amount was calculated in this section in accordance with the emissions of one of the promising biomixtures i.e. W50A50.

The NO and NO_2 emissions for the biomixture were previously measured as 1.408 g and 0.840 g through Horiba gas analyser. Table 7.1 shows the amount of NO and NO_2 release and required amount of NH_3 for full reduction of NOx for 1 second. Approximately 1.4 g of ammonia per second is required to be injected at the exhaust pipe. This corresponds to around 2.2 g of urea.

Table 7.1: The NO and NO_2 emissions of W50A50 biomixture for one second and NH_3 agent to be injected per second.

| | Emission released | | NH_3 needed | | $CO(NH_2)_2$ needed | |
	g	mole	mole	g	mole	g
NO	1.408	0.047	0.047	0.8	0.023	1.2
NO_2	0.840	0.018	0.037	0.6	0.018	1.0
NOx	2.248	0.065	0.084	1.4	0.041	2.2

The commercial Diesel Exhaust Fluids (DEF - AdBlue) are generally composed of %32.5 urea solution in deionised water. As a commercially available DEF was used in this study, the flow rate of the %32.5 urea solution in deionised water was calculated in equations 7.5 and 7.6.

$$Urea\ needed = \frac{2.2\ \left(\frac{g}{s}\right)}{1.32\ \left(\frac{g}{cm^3}\right)} = 1.67\ \left(\frac{cm^3}{s}\right) \tag{7.5}$$

$$32.5\%\ Urea\ solution\ needed = \frac{1.67\ \left(\frac{cm^3}{s}\right)\ x\ 100}{32.5} = 5.14\ \left(\frac{cm^3}{s}\right) = 308\ \left(\frac{ml}{min}\right) \tag{7.6}$$

7.4. Design and CFD simulation of the modified SNCR system

7.4.1. Design candidates

Three exhaust aftertreatment geometries were developed and modelled in ANSYS FLUENT software version 17.1 to figure out the best geometry Figure 7.1. The idea of the system was to inject the commercially available urea-water solution (AdBlue) but avoiding the catalytic; as the use of catalytic cannot be suitable for low power density engines which cannot cope with high back pressures. In this regard, it was planned to increase both turbulence intensity and particle residence time of the catalytic free system.
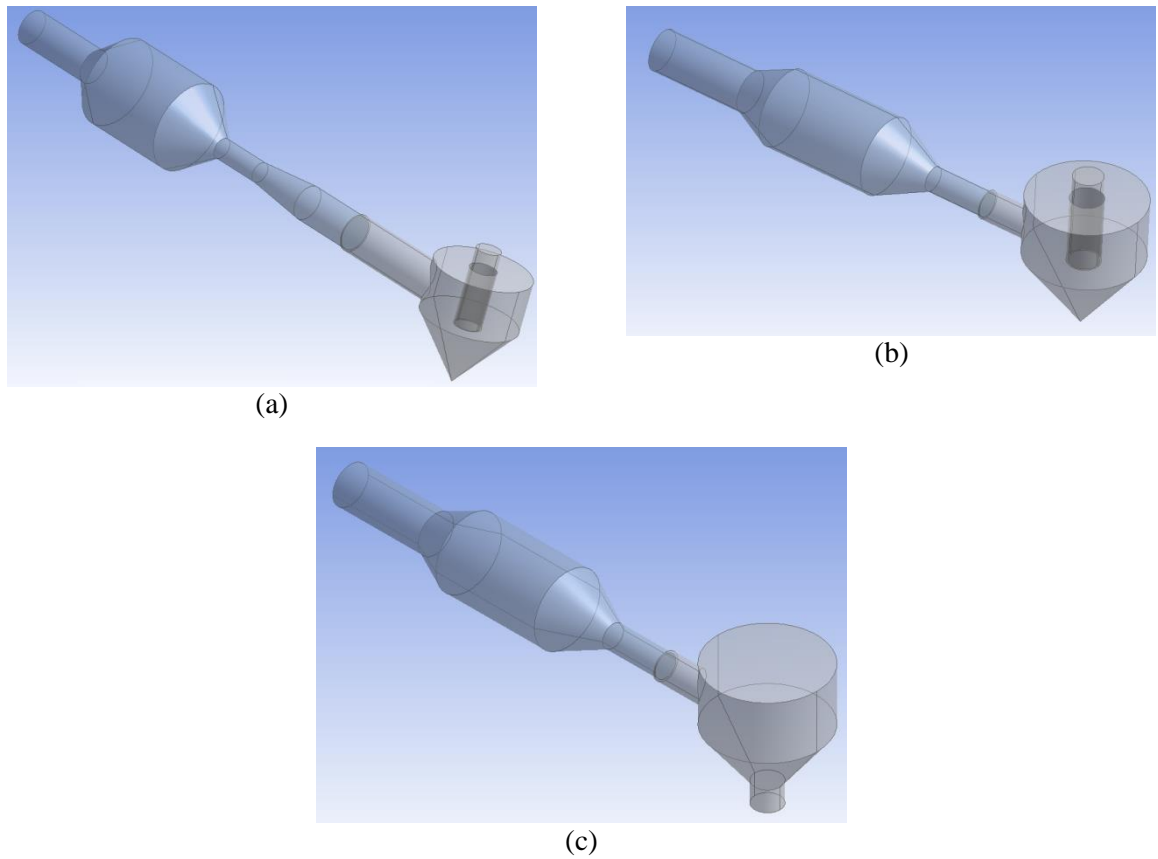
Figure 7.1: Design candidates tested in CFD simulation; (a) design A, (b) design B and (c) design C.

All three designs were composed of two parts which were named injection and expansion pipe and swirl chamber. The injection point was at the axis of the injection and expansion pipe and located just before the expansion section. In this regard, mixing between injected fluid and exhaust gas can be enhanced through the expansion pipe. More specifically, injection fluid molecules will enter the exhaust system whilst the diameter of the pipe is increasing, thus the gap between exhaust molecules also be enlarged and filled with the injected agent. Then, the diameter will again be reduced to increase the velocity before flowing into the swirl chamber, where the turbulence intensity was desired to increase.

The design A had larger expansion pipe diameter, compared to designs B and C. In addition, its exit diameter was the same as the inlet diameter. In contrast, designs B and C had the same injection and expansion pipe dimensions which has smaller exit diameter than exit diameter. The designs A and B had the same swirl chamber with an exit from the top of the chamber. Moreover, the exit pipe extends deep into the chamber, forces the entering exhaust fluid to rotate around it by flowing down (towards the conical part), then flowing towards upside through inside of the exit pipe. By this manner, not only

186

the turbulence intensity but also residence time was desired to improve. On the other hand, the swirl chamber of design C had an exit from the bottom (conical part) of the chamber.

7.4.2. Meshing

The maximum achievable mesh count was around 520,000 cells due to the limitations with the ANSYS (academic) software and computational cost. The numbers of cells were 492692, 505591 and 485258 for designs A, B and C, respectively. The numbers of nodes were 303136, 265173 and 278201 for designs A, B and C, respectively. Although more accurate results could be achieved with higher meshing size, the results obtained from a similar order of magnitude meshing size would be acceptable (Gomez, 2018). Because the design candidates will only be compared to each other (in terms of turbulence intensity and residence time) to select the best option rather than investigating the NOx reductions.
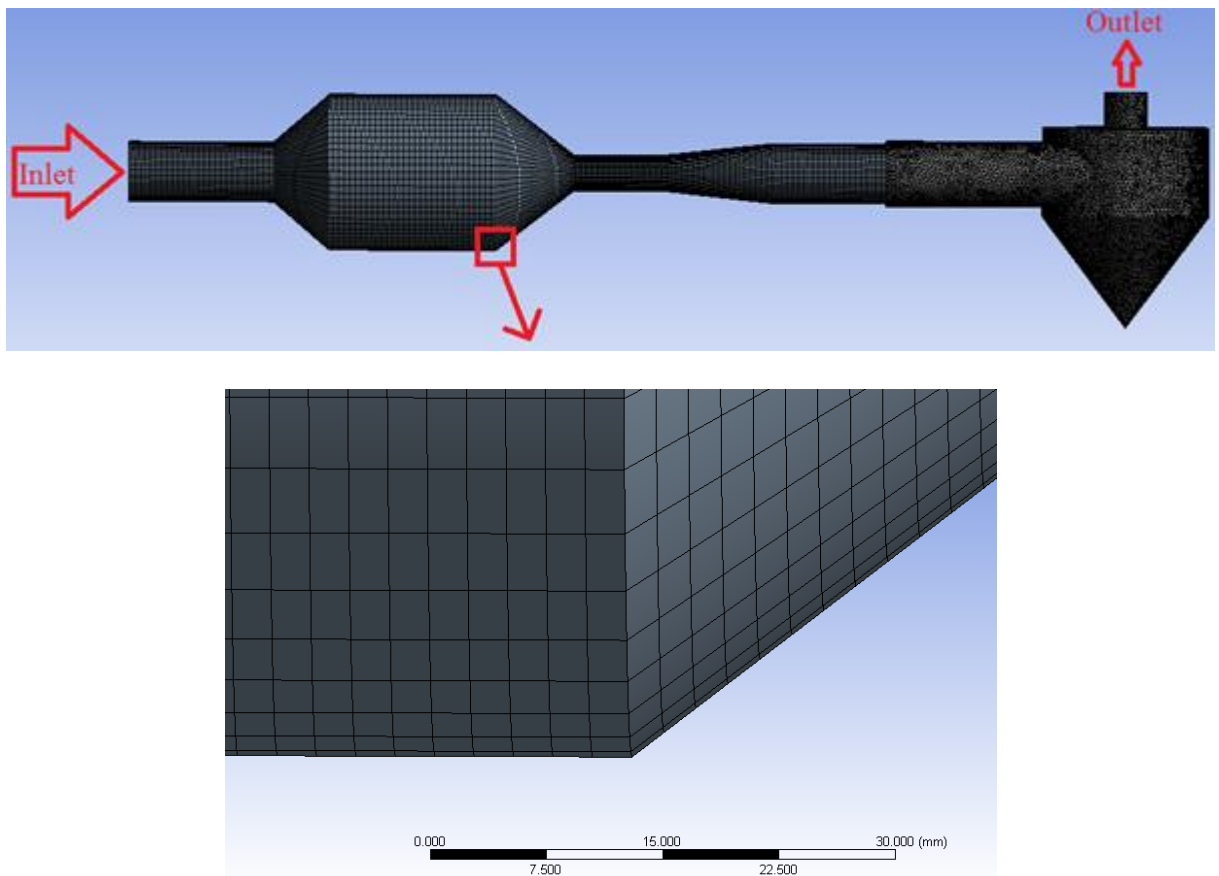
Figure 7.2: The meshing illustration of design A, which has a larger diameter expansion pipe and venturi between expansion pipe and swril chamber.
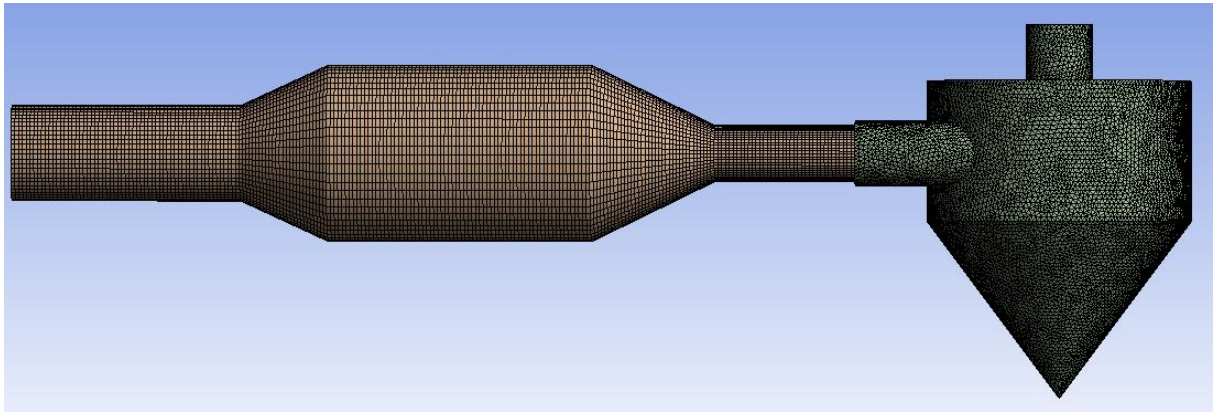
Figure 7.3: The meshing illustration of design B, which has no venturi between the expansion pipe and swril chamber and outlet is on top of the swril chamber.
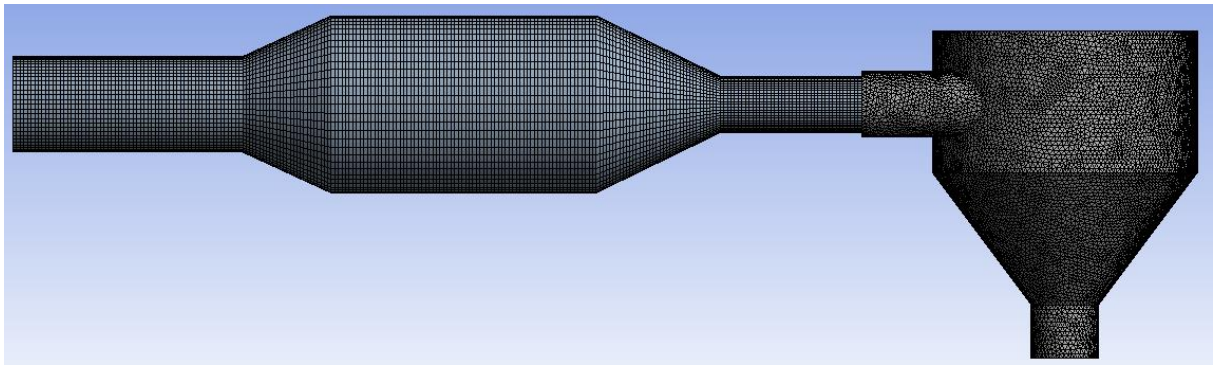
Figure 7.4: The meshing illustration of design C, which has no venturi between the expansion pipe and swril chamber and outlet is at the bottom of the swril chamber.

7.4.3.   CFD Model set up

This simulation was inspired from a CFD modelling for a study aimed for CO_2 emission reduction by magnesium hydroxide injection (Gomez, 2018). All three designs were modelled through the same calculation process, turbulence algorithms and boundary conditions. The viscous –RNG k-e, standard wall functions were selected to have the best monitoring on the turbulence motion (Yakhot *et al.*, 1992). In addition, swirl dominated flow option was selected as it was expected with the presence of the swirl chamber.

Three different species were selected for species model which were assumed as nitrogen oxide as a continuous phase (exhaust gas) and urea-water as a discrete phase. The other exhaust gases were neglected for the simplicity of the study. Nevertheless, the flow behaviour of the exhaust gas can be

considered a single-phase flow, hence neglecting other components was an acceptable assumption for the turbulence intensity and residence time analysis (Gomez, 2018).

The discrete phase model was selected for simulating the injection of urea-water solution (AdBlue) into the exhaust gas stream. Interaction with the continuous phase was activated to simulate The evaporation of injection agent and momentum change between the two phases (Gomez, 2018). Then, the injection conditions such as location, direction, nozzle type, temperature, flow rate, injection angle and diameter were introduced to the model. The urea-water option was selected as injection material.

Inlet boundary condition was entered in accordance with the previous experimental measurements (Chapter 4). On the other hand, the outlet boundary condition was set as out flow. To provide the interaction between the walls and injected fluid, wall-jet was property was activated. Gravity was also introduced to the model for realistic simulation.

According to Gomez Gomez (2018), SIMPLE scheme was used for the steady-state flow of pressure related equations; Least Squares Cell Based gradient was implemented for the selected mesh type and minimum false diffusion; PRESTO pressure for swirl flows involving pressure gradients; Second order upwind for more accurate results with Taylor series expansion of the cell-centred solution (Gomez, 2018).

7.5. Simulation outcomes and design selection

Initially exhaust gas flow was solved without any injection. Then, the injection was implemented too. The system was successfully converged.

As discussed earlier, the most important parameters are the turbulence intensity and particle residence time for this selection. The velocity magnitude and turbulence intensities for the design candidates were plotted through velocity vectors Table 7.2. The magnitude scales were arranged the same for the all three candidates, hence colour maps of velocity vectors indicate magnitudes of velocity and turbulence intensity. According to results, design A gave much lower velocity and turbulence than designs B and C, thus design A can be eliminated at this stage. However, no significant difference was spotted between designs B and C.
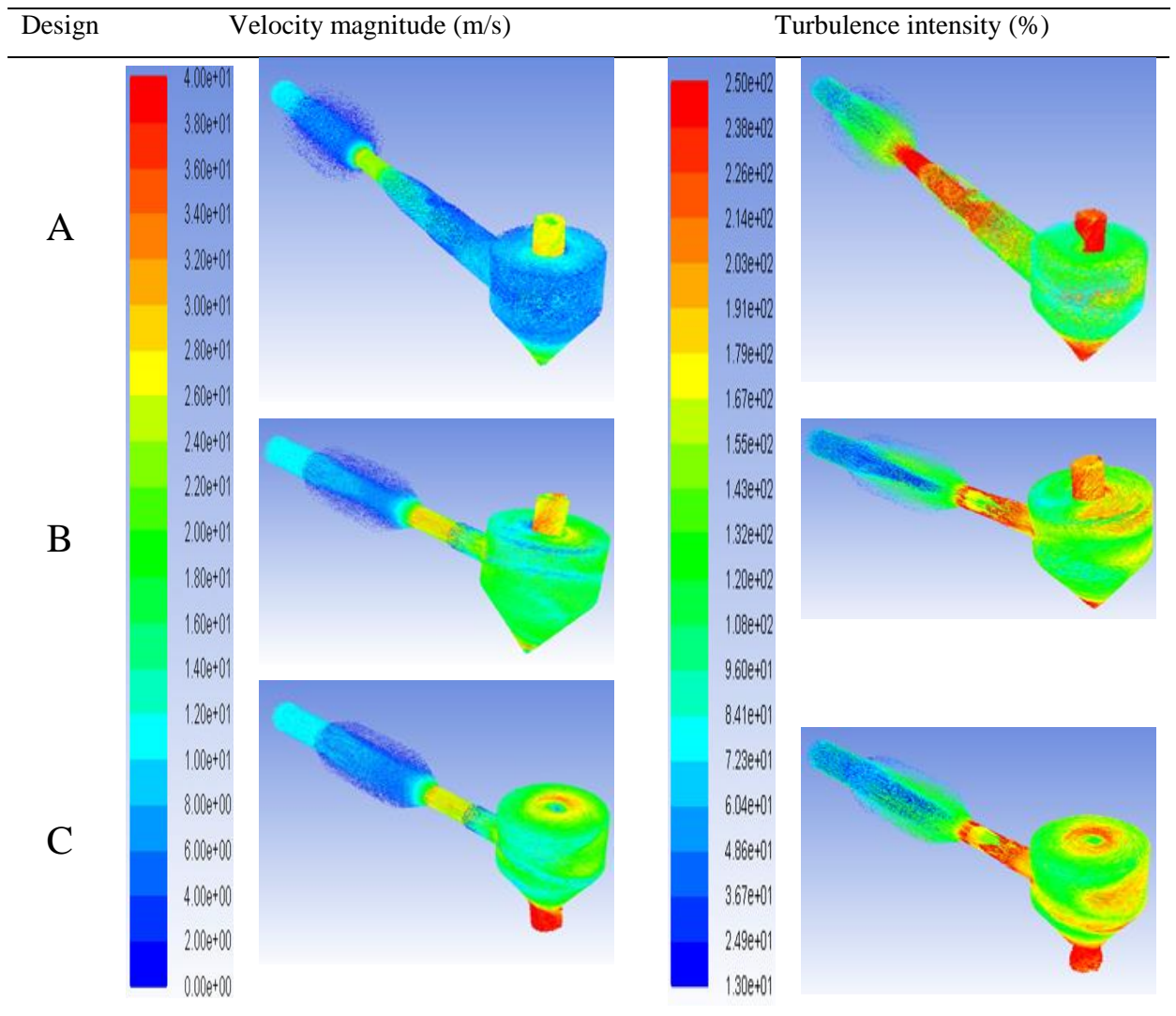
Figure 7.5: Comparison of design candidates A, B and C in terms of velocity magnitude and turbulence intensity.

Design A was eliminated for lower velocity and turbulence, thus designs B and C were compared in terms of particle residence time in Table 7.3. The residence time results of design B and C were again comparable at the expansion pipe. However, residence times of the design B and design C were recorded as 3 seconds and 1 second at the swirl chamber, respectively. Consequently, design B was superior to other candidates when all parameters were considered. Therefore, design B was selected to manufacture and conduct the experiment Figure 7.5. The mechanical drawings of the selected design were added in Appendix 1.

Design candidate	Particle residence time (s)	
A		
B		
C		
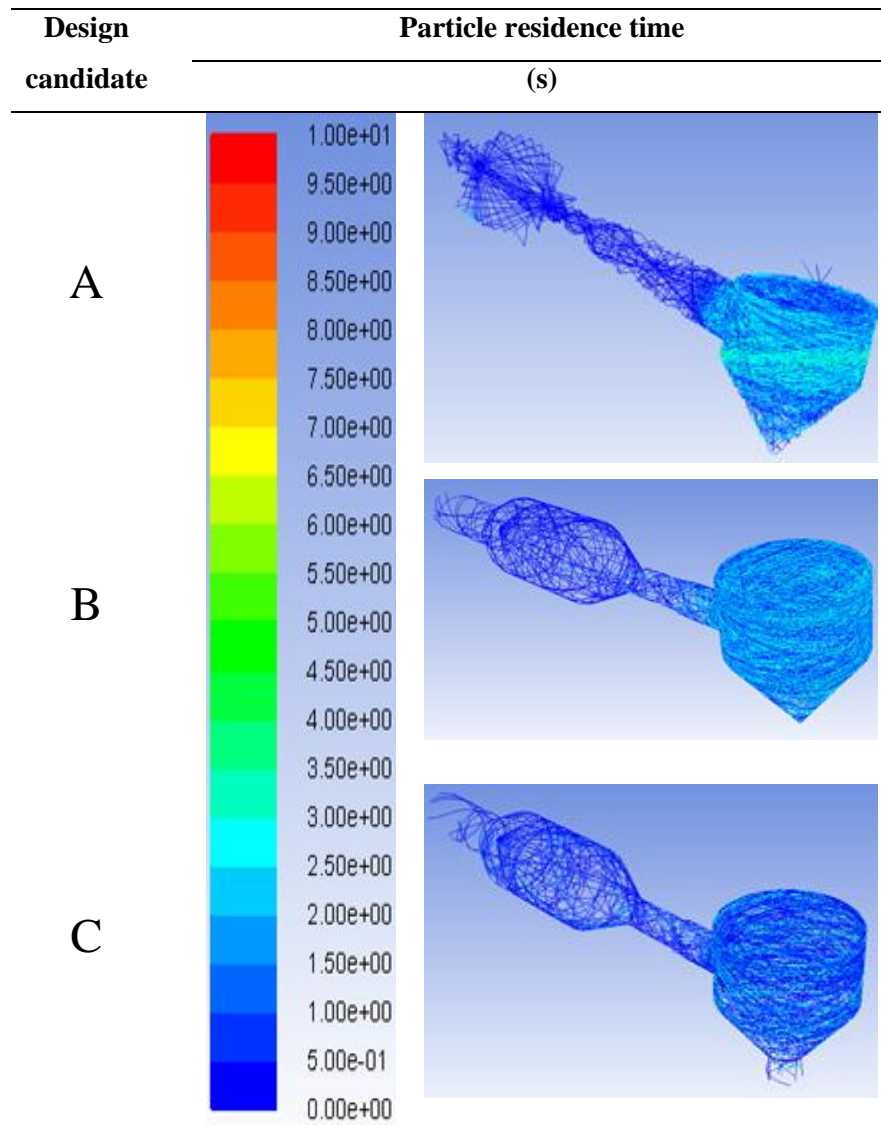
Figure 7.6: Comparison of design candidates A, B and C in terms of particle residence time.

7.6. Experimental investigation of the SNCR

The selected design was manufactured at the external metalwork company duRose Ltd in Birmingham. A small water pump and cone injector were used to develop an injection mechanism for the modified SNCR system Figure 7.5. The flow rate was measured by stopwatch-bucket method and the lowest flow rate of 375 ml/min was adjusted by providing 3 volts to the pump. Although this value was higher than the calculated value of 308 ml/min, it was used in the experiment as the NH_3 slip was out of the scope for this analysis.

(a)
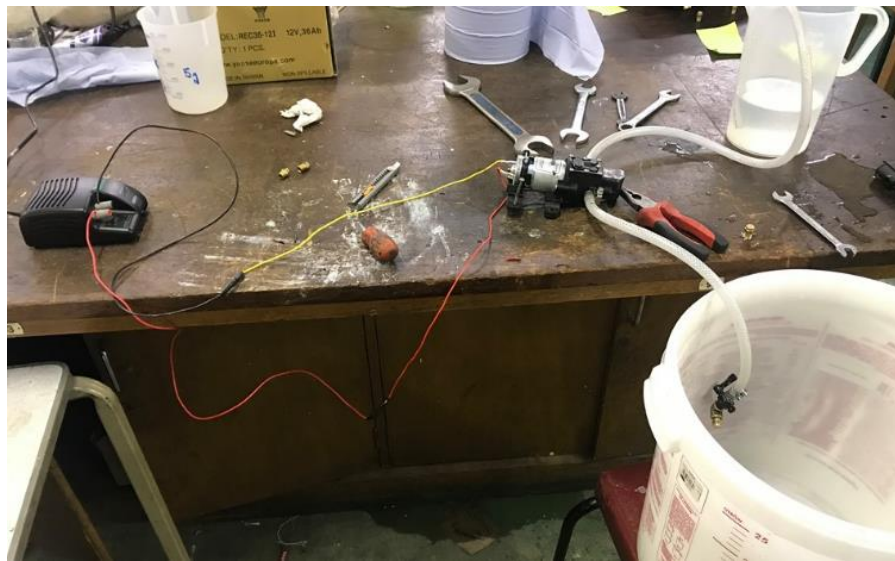
(b)

Figure 7.7: Components of the modified SNCR system (a) the injection mechanism of the after-treatment system and (b) system assembly.

Next, the injector was located into the injection pipe and the flow of the pattern was checked before installing the system on the test rig Figure 7.6.

Figure 7.8: Injection pattern starts just before the expansion pipe and expands along with the pipe.

The setup was installed on the exhaust system as shown in Figure 7.7. The national grid power converted into direct current and 3 volts supplied to the pump to obtain the desired flow rate. The expansion pipe was placed parallel to the ground and the exit of the swirl chamber was located vertically as simulated. The injection was controlled by the on-off switch of the power source (Figure 7.7). The system was commissioned by a leak test. Moreover, the in-cylinder pressure diagram was checked for any indication of abnormalities due to back pressure. Ultimately, the system was ready for the tests.
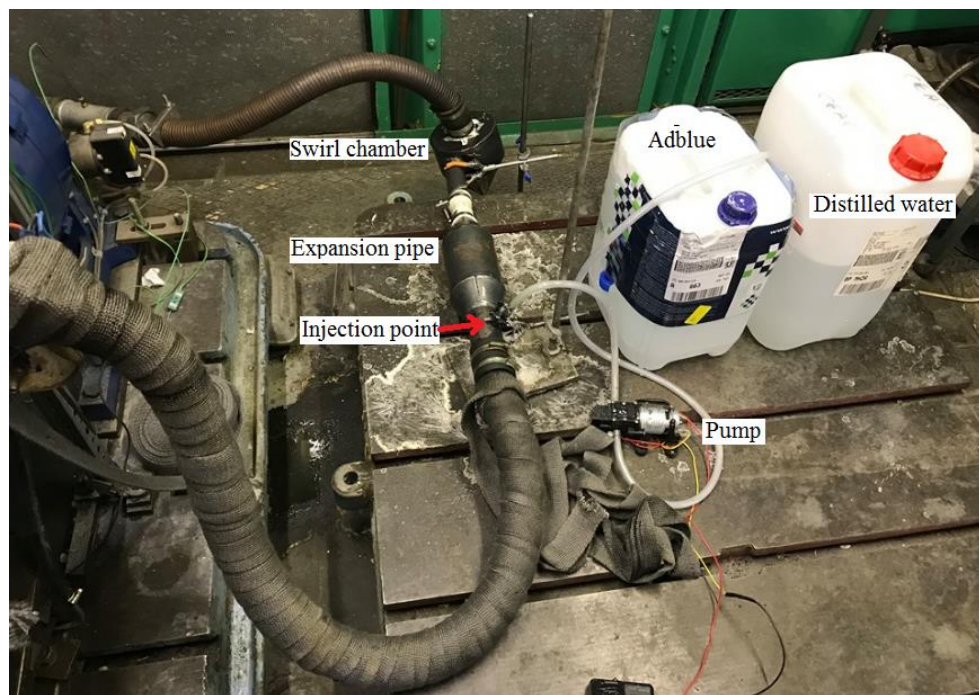
Figure 7.9: Engine test rig equipped with the modified SNCR aftertreatment system.

7.7. Results and discussions of SNCR aftertreatment

As mentioned earlier, exhaust emissions of the W50A50, CO50CH50 biomixtures and diesel were tested through modified SNCR aftertreatment at 2000 rpm and at 80% engine load. in-cylinder pressure diagrams are important to spot any abnormalities regarding the back pressure due to the implemented after-treatment system (Azimov *et al.,* 2018). Therefore, in-cylinder pressures of fossil diesel, W50A50 and CO50CH50 were measured at 2000 rpm and at 80% engine load with the modified SNCR system Figure 7.8. The results gave comparable results with each other such as 67 bars at 13°CA. Moreover, the trends before and after the application of the modified SNCR system were also the same with each other and no abnormal peak or jump was spotted.
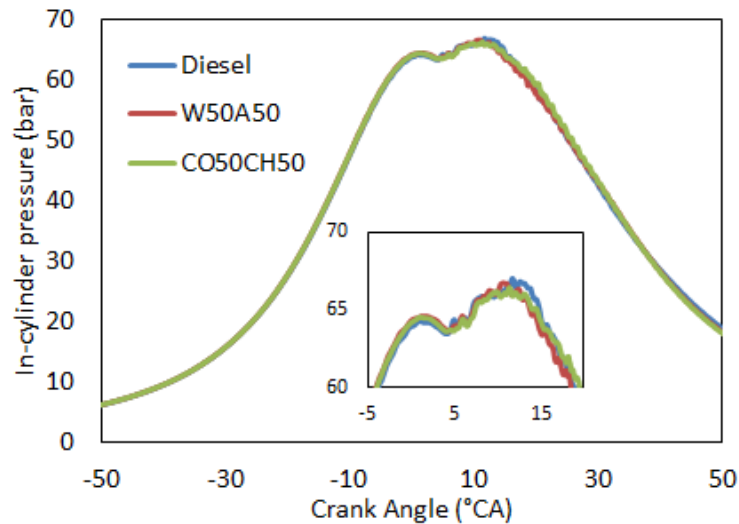
Figure 7.10: In-cylinder pressures for the test fuels with the modified SNCR aftertreatment system.

As the purpose of this chapter was the reduction of NO reduction, the main emphasis was on the emission results of the test fuels. Note that engine performance and combustion characteristics of the W50A50 and CO50CH50 biomixtures (including various other blend ratios) were analysed in detail in previous chapters. It was expected that similar engine performance and combustion characteristics would be observed with or without SNCR.

CO and CO_2 emissions under no injection, neat distilled water injection and urea-water (AdBlue) injection were given in Figure 7.9 and 7.10 respectively. It was clear that there was no significant effect of neither neat water injection nor urea-water injection on CO and CO_2 emissions. This was

because there was not any diesel oxidation catalyst (DOC) or diesel particular filter (DPF) facility on the test rig. However, CO emission was decreased slightly by around 0.006 volume %, 0.005 volume % and 0.003 volume % with the urea-water injection for the diesel, W50A50 and CO50CH50 respectively. CO reduction with urea-water injection was in good agreement with the literature. Praveen and Natarajan, (2014) also stated a 32% reduction with the urea injection for diesel-ethanol (90/10) blend and linked this reduction to oxidation of CO in the presence of excess oxygen. This also explains the slight increase in CO_2 with urea-water injection.
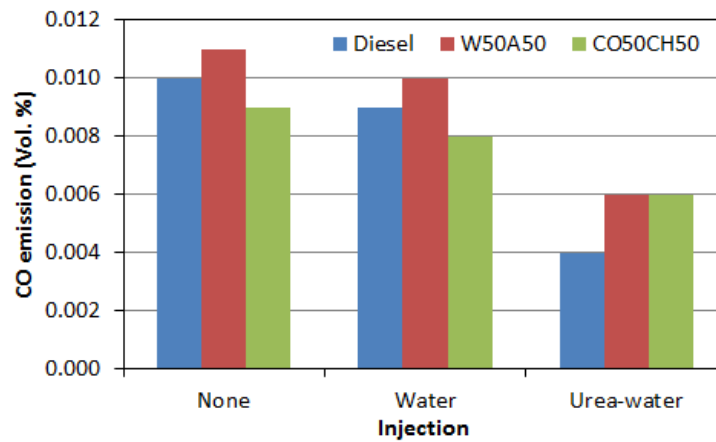
Figure 7.11: CO emissions of diesel, W50A50 and CO50CH50 with the modified SNCR application.
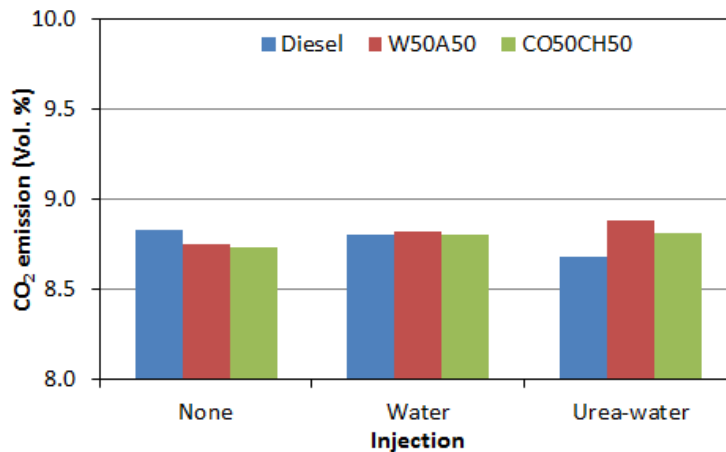
Figure 7.12: CO_2 emissions of diesel, W50A50 and CO50CH50 with the modified SNCR application.

The unburned hydrocarbons emissions were also measured with and without injections Figure 7.11. The results were the same in all scenarios; hence HC was not affected by the modified SNCR system. This finding agreed with the literature (Thiyagarajan *et al.*, 2017; Haridass and Jayaraman, 2018).
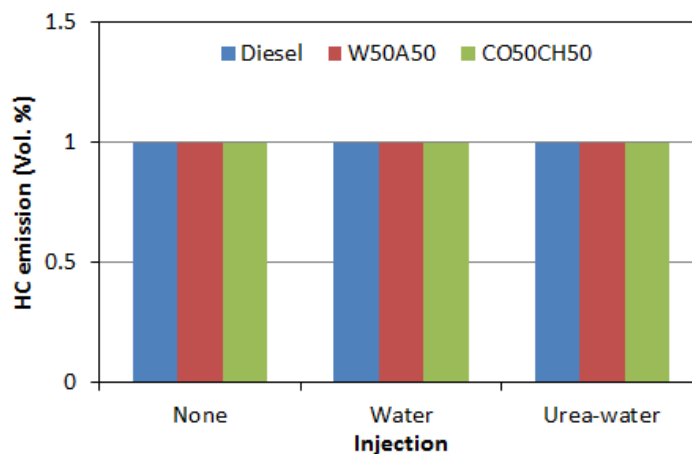
Figure 7.13: HC emissions of diesel, W50A50 and CO50CH50 with the modified SNCR application.

The most important emission in this chapter was the NO emission. Unfortunately, NO_2 emission could not be measured due to lack of equipment. Comparing the reductions of NO and NO_2 which are the main components of NOx emission, reduction of NO_2 is easier than NO emission as it reacts with water and forms nitric acid (Javed *et al.,* 2007). This fact should be highlighted as NOx reduction is expected to be higher than NO reduction. In other words, any promising results found for NO emission would be even better for the NOx emission.

Figure 7.12 studies the NO emissions of diesel, W50A50 and CO50CH50 with and without modified SNCR after-treatment system. Without any injection, the biomixtures of W50A50 and CO50CH50 gave similar NO emission (at 2000 rpm and 80% engine load) and it was around 1.5% higher than that of diesel. The neat distilled water injection through modified SNCR gave approximately 6% reduction for all three test fuels. Moreover, the urea-water injection reduced the NO emission by 13% and 15% lower than diesel and biomixtures. These emission reductions are likely to be increased for NOx emission, as NO_2 reductions will also contribute (Javed *et al.,* 2007).
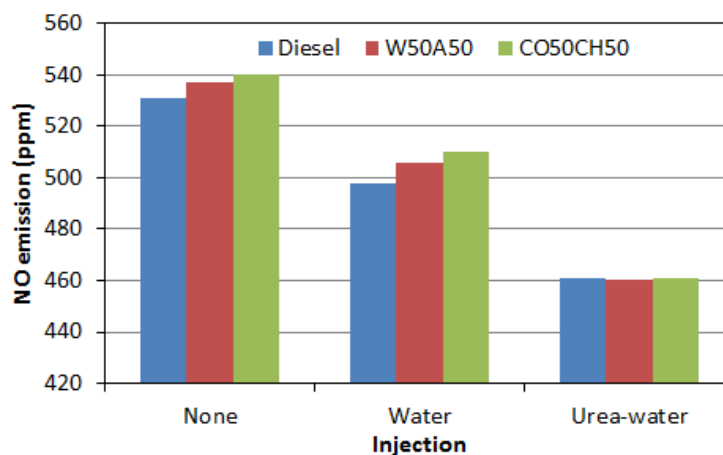
Figure 7.14: NO emissions of diesel, W50A50 and CO50CH50 with the modified SNCR application.

The modified SNCR aftertreatment system worked without any back pressure problem for low power density engine (11.2 kW at the engine speed of 2000 rpm). The exhaust temperature was observed as 378°C which was well below conventional SNCR temperature window (between 875°C and 1050°C) but above the lower limit of SCR (350°C). Nevertheless, the desired exhaust emission of NO was successfully reduced by 15%. These results proved that the idea of turbulence and residence time improvement through expansion pipe and swirl chamber was successful. Note that this value would be even higher for NOx emission if NO_2 emission could be measured. It is also believed that designed aftertreatment technique would yield further reductions under higher exhaust temperatures with medium or high energy density engines.

7.8. Conclusion

This chapter focused on NO emission reduction of the biomixtures of W50A50 and CO50CH50. The latest SCR and SNCR technologies found in literature were combined in a new design to enhance turbulence intensity and residence time. The main advantages of the new system were eliminating catalytic related problems such as weight, clogging, cost etc. The after-treatment system was tested in the engine at 80% load with two injection agents which were neat distilled water and commercially available urea-water solution also known as AdBlue. The NO emission of biomixtures and diesel was reduced by approximately 6% and 15% by neat water and urea-water solution injections at 375 ml/min flow rate and at 378°C exhaust temperature. On the other hand, no significant effect of catalyst free modified SNCR system on CO, CO_2 and HC was observed.

Chapter 8

8. CONCLUSIONS

This final chapter summarises the findings of the study by responding to aims and objectives given in Chapter 2. The research objectives were examined individually in order to demonstrate the extent to which they are achieved. In addition, recommendations for future work were made in the light of research outcomes.

8.1. Responses to objectives

Objective 1: To select feedstock for biodiesel-biodiesel blending by a detailed literature review in terms of biodiesels fuel properties, their combustion and emission characteristics results in the compression ignition engines.

This objective was met by an intensive literature review on possible feedstock candidates available in the literature. Biodiesel feedstock was grouped as animal fats, waste cooking oils and inedible vegetable oils. The biodiesels obtained from various sources were studied in terms of their fuel properties. The fuel properties were discussed and compared with in the BS EN 14214 biodiesel standard. According to differences in their fuel properties, the blending of animal fat based biodiesels with waste cooking oil was found to be an attractive option to upgrade the fuel properties. Particularly, animal fat biodiesels possesses promising heating value, cetane number and iodine number; but relatively poor viscosity compared to other biodiesels. On the other hand, waste cooking oil biodiesels have comparable viscosity, heating value, cetane number but relatively poor iodine value compared to other biodiesels and BS EN 14214 standard. The blending of these two different biodiesel agents was found to be a very promising technique in order to optimise fuel properties. The engine test results of the individual biodiesels were reviewed and summarised. The blending concept was also supported by the engine test results in terms of engine performance and exhaust emissions. In addition, published studies on biodiesel-biodiesel blending were reviewed to demonstrate the research gap.

The contribution to knowledge arising from the first objective was:

- Animal fat and waste cooking oil biodiesels very well matched for biodiesel-biodiesel blending with respect to viscosity, iodine value, degree of unsaturation and cetane number.

Objective 2: To produce biodiesel-biodiesel blends (biomixtures) in order to identify promising volume ratios which meets BS EN 14214 biodiesel standard. Moreover, to understand the effect of biodiesel degree of unsaturation on engine performance, combustion characteristics and exhaust emissions.

The first step to achieve this objective was to find an appropriate method for biodiesel production. The crucial parameters of the transesterification technique were reviewed from the literature. Next, the produced biodiesels were blended to perform various analyses such as (i) understanding the effect of biodiesel degree of unsaturation (DU) on engine results, (ii) optimising fuel properties to eliminate dependency on external additive agents to meet the BS EN 14214 standard (iii) making use of highly available waste biodiesel resources to meet the BS EN 14214 standard (iv) upgrading engine test results compared to neat biodiesels as a result of optimised fuel properties.

Firstly, waste sheep fat biodiesel was blended with the waste cooking biodiesel in order to understand the effect of biodiesel DU. As the biodiesles had an extreme difference on the DU, a wide range of biomixtures having various DU values was obtained. At the same time, other properties like densities, heating values, acid values, flash points and elemental concentrations were very close to each other. This study revealed that ignition delay and total combustion duration of the biomixtures was slightly shortened by reducing DU. Therefore, NOx emission increased with the decreased DU in accordance with the improved combustion characteristics. On the other hand, CO emission decreased with the decreased DU. No significant effect of changing DU was noticed on engine performance.

Secondly, biodiesel produced from waste cooking oil hardly satisfies the BS EN 14214 standard specifically because of higher iodine value as 145 g/100g; according to the standard, the upper limit of biodiesel iodine value is 120 g/100g. However, the WCO biodiesel-sheep fat biodiesel blends obtaining at least 40% volume fraction of animal biodiesel met the BS EN 14214 standard in terms of iodine value. This eliminates any requirement of an unsustainable agent like fossil diesel to meet the standard.

Thirdly, widely available chicken feedstock can be utilised as waste biodiesel source but chicken biodiesel has high viscosity problem. Although blending technique could help to reduce chicken biodiesel's viscosity within the acceptable range of BS EN 14214 standard (3.50-5.00 mm^2/s), it was quite challenging to find a waste driven biodiesel which has relatively low viscosity. However,

minimum 50% (by volume) cottonseed biodiesel blending of chicken biodiesel had successfully reduced the viscosity below 5.00 mm^2/s value at the 40$^\mathbf{o}$C.

The findings and contributions to knowledge arising from the second objective were:

- The decrease in the degree of unsaturation resulted in improved combustion of biodiesel which in turn reduced the CO emission but increased the NOx emission.

- The high iodine value challenge of waste cooking oil biodiesels was solved by animal fat biodiesel blending; hence any need for unsustainable additive was avoided.

- The high viscosity problem of animal fat biodiesels was eliminated by cottonseed biodiesel blending.

Objective 3: To assess the combustion and emission characteristics of the produced biomixtures in a CI engine and determine promising biodiesel-biodiesel blends (biomixtures) which improves combustion characteristics and reduces harmful exhaust emissions.

The biomixtures formed by waste cooking oil and sheep fat biodiesels blending were tested (presented in Chapter 4) at 60/40, 50/50 and 30/70 volume fractions. Similarly, biomixtures obtained by blending cottonseed biodiesel and chicken biodiesel with the same volume fractions and they were tested in the engine (presented in Chapter 5). The neat biodiesels along with diesel were also tested to be compared to biomixtures.

According to Chapter 4, the most promising volume fraction was 50/50. W50A50 gave 5.2% higher peak in-cylinder pressure than the neat biodiesels at 80% load. Similarly, the heat release rate of W50A50 was higher than the neat biodiesels. However, NOx emission of W50A50 was approximately 2.5% higher than the neat biodiesels as a result of improved combustion due to optimised fuel properties. In contrast, CO_2 emission of the W50A50 was 6% lower than the W100. Similarly, CO50CH50 was the best performing biomixture formed from blends of cottonseed and chicken biodiesels. Results given in Chapter 5 states that CO50CH50 had the highest in-cylinder pressure and heat release by 4.2% and 4.4% higher than the diesel. Moreover, CO_2 and CO emissions of the CO50CH50 were around 3% and 15% lower than diesel. The only disadvantage of CO50CH50 biomixture was the 6% increased NO emission compared to diesel. In contrast, CO60CH40 biomixture gave 6.5% reduced NO emission than diesel. All these improvements in the combustion characteristics were due to the optimised fuel properties such as viscosity, cetane number, iodine value and degree of unsaturation. Therefore, this thesis recommends the biodiesel-biodiesel blending

technique. However, fuel properties of neat biodiesels should be considered to find optimum blending matches in accordance with the desired properties to be optimised.

The contributions to knowledge arising from the third objective were:

- Biodiesel-biodiesel blending was improved the combustion characteristics such as in-cylinder pressure and heat release due to optimised fuel properties.

- Exhaust gas emissions such as CO_2 and CO were reduced by biodiesel-biodiesel blending as a result of improved combustion.

Objective 4: To assess the effectiveness of the 2-Butoxyethanol as biomixture and neat biodiesels additive in terms of fuel properties, engine performance, combustion characteristics and exhaust emissions characteristics.

The 2-Butoxyethanol was analysed as a biodiesel fuel additive in Chapter 6. The potential of the additive over fuel properties and engine test results of W50A50 and CO50CH50 were investigated. In addition, the additive was also tested with the two commonly used biodiesels in the UK which were waste cooking biodiesel and rapeseed biodiesel. Initially, the amount of the additive was determined by characterisation analysis. The 2-Butoxyethanol was doped into W50A50 at volume ratios of 10%, 15% and 20% to monitor the changes on fuel properties. Viscosity, heating value and flash point were observed as the most affected parameters by the presence of 2-Butoxyethanol. This was due to the alcohol properties of the additive. On the other hand, there was no insignificant change in cetane number, density and iodine value by the 2-Butoxyethanol addition. Therefore, neat versions of the mentioned test samples and 15% 2-Butoxyethanol blends were characterised and tested in the unmodified CI engine. Although BSFC and BTE of the biodiesels were reduced with the additive by around 5% and 2.5%, these values were still slightly higher than diesel at the medium engine loads. The additive improved the combustion characteristics of biodiesels. For example, peak in-cylinder pressure was recorded as 5% higher at the full load. This was attributed to lowered viscosity and improved volatility with the 2-Butoxyethanol additive. Biodiesels with 15% 2-Butoxyethanol additive emitted significantly reduced CO, HC and smoke emissions by 30%, 50% and 20%, respectively. Furthermore, the reduction in NO emission was also achieved by 5.4%. However, CO_2 emissions were slightly increased by 3% for neat biodiesels and 10% for the biomixtures.

The contributions to knowledge arising from the fourth objective were:

- The 2-Butoxyethanol is a safe additive for biodiesels and suitable for unmodified engine application.

- Combustion of biodiesels such as in-cylinder pressure was upgraded with the 2-Butoxyethanol additive as a result of improved viscosity and volatility.

- Harmful exhaust gas emissions such as CO, HC and smoke were further reduced with 2-Butoxyethanol additive up to 30%, 50% and 20%, respectively.

- NOx emission penalty of biodiesels was reduced by 5% NO share, solely with the 2-Butoxyethanol additive without any after-treatment or EGR application.

Objective 5: To design a new SNCR after-treatment system for minimising the NOx penalty of biofuels by injections of distilled water and urea-water solution separately at the exhaust system.

This objective was met (presented in Chapter 7). A combined version of SCR and SNCR after-treatment systems was used to avoid negative aspects of each technique. To illustrate, the modified SNCR system used in Chapter 7 was free of catalytic, hence catalytic related problems were prevented. Moreover, the high operating temperature window of the SNCR system was reduced down to suitable range for diesel engine operation by the design concept. The system was composed of two components which were namely injection and expansion pipe, and swirl chamber. The working principle to perform the injection whilst exhaust gas was expanding through the expansion pipe, thus injected agent can fill the created spaces between exhaust gas molecules at the lower velocity for better mixing. Then, increasing the velocity of the flowing medium by the Bernoulli principle before entering the swirl chamber where turbulence intensity and residence time were increased. The most promising biomixtures of W50A50 and CO50CH50 were tested through the novel design along with the diesel. After the implementation of the new SNCR system, safe engine operation of low power density engine was confirmed through in-cylinder pressure measurement. This proved that there was not any back pressure problem. Two different injection agents were tested which were distilled water and urea-water solution (commercially available AdBlue). Tests were conducted at 378°C which was well below the lower operation limit of conventional SNCR i.e. 800°C. Neither water nor urea-water injections had significant effect on CO_2, CO and HC emissions. However, NO emissions of diesel, W50A50 and CO50CH50 were all reduced by around 6% and 15% with the distilled water and urea-water injections. Note that NH_3 slip (unreacted ammonia release) and N_2O (potential new pollutant) were not considered. Moreover, NO_2 reduction could not be studied and it is believed that 15% reduction would be improved with the contribution of NO_2 reduction.

The contributions to knowledge arising from the fifth objective were:

- The new SNCR after-treatment design was provided a safe and smooth engine operation. No problem was observed in terms of back pressure in low power-density engine.

- The modified SNCR system prevents catalytic challenges.

- The high-temperature window of SNCR systems was reduced by increasing both residence time and turbulence intensity through design geometry.

- NO emission penalty of W50A50 and CO50CH50 biomixtures was reduced by 6% and 15% with distilled water and commercially available Adblue injections.

Objective 6: Recommendation on biodiesel-biodiesel mixture(s) for CI engine application with additive or with after-treatment system.

The both 50/50 blends, W50A50 and CO50CH50, revealed identical BTE and BSEC performances on the unmodified CI engine. They both had very similar fuel properties such as heating value. However, cetane number of CO50CH50 was around 4% higher than W50A50. In accordance with the CN difference, the in-cylinder pressure of CO50CH50 was recorded approximately 5% higher than W50A50 at full engine load. The exhaust gas emissions of CO_2, CO, HC and smoke opacity were comparable for both 50/50 blends. However, W50A50 had approximately 5% lower NO than CO50CH50 at full load. Consequently, the use of both 50/50 blends are suggested as they provided improved combustion and reduced emission characteristics than neat biodiesels and diesel. Comparing them among themselves, W50A50 is recommended as a first option as it had lower NO emission.

The NO emission of neat biodiesels and biomixtures were successfully reduced with the both 2-Butoxyethanol additive and new design SNCR after-treatment system by 5% and 15%, respectively. The use of both techniques together is recommended to minimise CO, HC, smoke and NO emissions with the combine effect. If the use of both additive and after-treatment together is not possible, application of at least one technique is strongly recommended to reduce NO emission below the level of fossil diesel.

8.2. Responses to the overall aim

The overall aim of this thesis is to blend two different biodiesels in accordance with their fuel properties for optimising the engine performance, combustion characteristics and exhaust emissions. Biodiesels should comply with the BS EN 14214 standard, and must reduce harmful exhaust gas emissions when compared to fossil diesel.

The overall aim of the thesis was achieved as the biodiesel-biodiesel blending successfully optimised fuel properties which in turn complied with BS EN 14214 standard. The thesis focused on two different biomixtures but in both cases, an animal fat biodiesel was blended with waste/inedible vegetable oil biodiesel. This was because of the complementary advantages of the mentioned biodiesel types, which compensate each other's weaknesses. This outcome was achieved in Chapter 2 as iodine value, heating value and cetane number of animal fats biodiesels were found to be better than other biodiesel types. In addition, they are considered as waste components and highly available. On the other hand, biodiesels of waste cooking oils or inedible vegetable oils had promising viscosity values. In the light of this issue, Chapter 4 studied the blending of sheep fat biodiesel with waste cooking oil biodiesel and successfully lowered the iodine value of WCO biodiesel within the BS EN 14214 standard. Moreover, the cetane number of WCO biodiesel was also upgraded and high viscosity of sheep fat biodiesel was optimised. The 50/50 blend which was named as W50A50 was found as the best-performing biodiesel. Chapter 5 investigated blends of cottonseed biodiesel with chicken fat biodiesel. Similarly, CO50CH50 was noticed as the best biomixture in terms of combustion characteristics and exhaust emissions. Both biomixtures (proved in Chapter 4 and 5) provided lower CO, CO_2, HC and smoke opacity compared to diesel. However, NO emissions were comparable with the diesel. Therefore, a new biodiesel additive 2-Butoxyethanol was introduced in Chapter 6, which slightly reduced the NO emissions of the biomixtures as well as neat biodiesels around 5%. NO emissions of the biodiesels further discussed in Chapter 7 with implementation of new SNCR after-treatment technique. The behaviour of the biomixtures with the latest idea of ammonia injection was studied through a new after-treatment design which was a combination of SCR and SNCR techniques. NO reduction up to 15% was achieved for the biomixtures and diesel with the SNCR technique. Consequently, this thesis proved that fuel properties of the biodiesels produced from waste resources can be upgraded by blending with another biodiesel. This can avoid dependency on any unsustainable agent such as fossil diesel or other additives to meet BS EN 14214 standard. In addition, biodiesel-biodiesel blends can reduce most of the exhaust gas emissions and provide comparable NO emission. It was also proved that NO emission was reduced with the 2-Butoxyethanol and SNCR after-treatment system.

Three peer-reviewed articles have been published on the basis of this PhD work by the time this thesis was written:

7. Masera, K., & Hossain, A. K. (2019). Combustion characteristics of cottonseed biodiesel and chicken fat biodiesel mixture in a multi-cylinder compression ignition engine. *SAE Technical Paper 2019-01-0015, 1*, pp. 1-14. doi: 10.4271/2019-01-0015.

8. Masera, K., & Hossain, A. K. (2019). Biofuels and thermal barrier: A review on compression ignition engine performance, combustion and exhaust gas emission. *Journal of the Energy Institute*. Elsevier Ltd, 92(3), pp. 783–801. doi: 10.1016/j.joei.2018.02.005.

9. Masera, K., & Hossain, A. K. (2017). Production, characterisation and assessment of biomixture fuels for compression ignition engine application. *International Journal of Mechanical, Aerospace, Industrial, Mechatronic and Manufacturing Engineering*, 11(12), pp. 1857 - 1863. doi: scholar.waset.org/1307-6892/10008317.

Papers regarding the 2-Butoxyethanol and modified SNCR after-treatment system have submitted/under preparation.

10. Masera, K., Hossain, A. K., Davies, P. A., & Doudin, K. (2019). Experimental investigation of the 2-butoxyethanol as a biodiesel additive. *Energy (submitted)*,

11. Masera, K., Hossain, A. K., Griffiths, G., & Safdar, S. (2019). Understanding the effect of degree of unsaturation by blending waste cooking oil biodiesel and sheep fat biodiesel. *Fuel (to be submitted)*,

12. Masera, K., & Hossain, A. K. (2020). Injection of urea-water solution through a modified selective non-catalytic reduction (SNCR) after-treatment system to reduce NOx emission. *4th South East European Conference on Sustainable Development of Energy, Water and Environment Systems,* Sarajevo, Bosnia and Herzegovina, *(abstract submitted)*,

8.3. Future work recommendations

Although this PhD work successfully provided upgraded combustion characteristics and reduced exhaust gas emissions using the biomixtures, there are further aspects that merit investigation.

One particular aspect recommended for future work is testing of the biomixtures at various engine conditions. For example, they could be examined in a direct injection diesel engine with a common rail injection system that complies with the latest emission standard. In addition, transient engine operations can be investigated with advanced emission analysers. Similarly, behaviours of the biomixtures with the commonly used modern technologies like turbocharge, supercharge, diesel particulate filter, diesel oxidation catalyst and exhaust gas recirculation facilities can be analysed.

Another aspect worth analysing further is oxidation stability and metal contents especially on aged biomixtures. Although no significant change in engine results of the one year aged biomixtures was spotted in Chapters 4 and 5, this was due to proper storage at the laboratory conditions such as perfectly sealed lid (minimum contact with the oxygen), dark and glass container. However, these conditions may not be found in some real life applications, thus further investigations on aged biomixtures and oxidation stability are recommended. Moreover, the best material for biomixture storage in terms of metal content should be studied.

Although the modified SNCR after-treatment system was successfully reduced the NO emission, its application may be upgraded by further improvements. To begin with, the, dimensions of the developed design can be investigated further in detail. Secondly, a novel concept may be developed for NH_3 slip recovery i.e. recirculation over exhaust piping. Thirdly, a smart control system can be produced that measures the upstream NOx emission and optimises the injection conditions like injection flow rate and pressure. Fourthly, potential new pollutants like N_2O as a result of ammonia-NOx reaction should be investigated with proper measurement techniques. This is a critical area to take precautions as N_2O is not a combustion product; hence neither emission regulations nor conventional gas analysers consider this pollutant. Finally, it is highly recommended to investigate the introduced after-treatment system with the TBC application.

Even though the biomixtures proved feasible and improved the CI engine operation without any need of fossil diesel, the biomixtures would likely be commercialised by blending with diesel at the maximum allowed biodiesel fraction set by the regulations, currently 7% in Europe. Therefore, biomixture-diesel blends should be investigated in accordance with this limit.

References

2-Butoxyethanol. (2018). National Center for Biotechnology Information. Retrieved July 16, 2018, from https://pubchem.ncbi.nlm.nih.gov/compound/2-Butoxyethanol#section=Top

Abu-Zaid, M. (2004). Performance of single cylinder, direct injection diesel engine using water fuel emulsions. *Energy Conversion and Management*, *45*(5), 697–705.

Adam, I. K., Heikal, M., Aziz, A. R. A., & Yusup, S. (2018). Mitigation of NOx emission using aromatic and phenolic antioxidant-treated biodiesel blends in a multi-cylinder diesel engine. *Environmental Science and Pollution Research*, *10*, 1–17. https://doi.org/doi.org/10.1007/s11356-018-2863-8

Adewale, P., Dumont, M. J., & Ngadi, M. (2015). Recent trends of biodiesel production from animal fat wastes and associated production techniques. *Renewable and Sustainable Energy Reviews*, *45*, 574–588. https://doi.org/10.1016/j.rser.2015.02.039

Adnan, R., Masjuki, H. H., & Mahlia, T. M. I. (2012). Performance and emission analysis of hydrogen fueled compression ignition engine with variable water injection timing. *Energy*, *43*(1), 416–426. https://doi.org/10.1016/j.energy.2012.03.073

Agarwal, A. K., Dhar, A., Gupta, J. G., Kim, W. Il, Choi, K., Lee, C. S., & Park, S. (2015). Effect of fuel injection pressure and injection timing of Karanja biodiesel blends on fuel spray, engine performance, emissions and combustion characteristics. *Energy Conversion and Management*, *91*, 302–314. https://doi.org/10.1016/j.enconman.2014.12.004

Alberici, S., & Toop, G. (2014). Overview of UK Biofuel Producers. *UK Department for Transport*.

Alhassan, Y., Kumar, N., Bugaje, I. M., Pali, H. S., & Kathkar, P. (2014). Co-solvents transesterification of cotton seed oil into biodiesel: Effects of reaction conditions on quality of fatty acids methyl esters. *Energy Conversion and Management*, *84*, 640–648. https://doi.org/10.1016/j.enconman.2014.04.080

Alkidas, A. C., & Cole, R. M. (1983). Gaseous and particulate emissions from a single-cylinder divided-chamber diesel engine. *SAE Technical Paper 831288*, 15. https://doi.org/10.4271/831288

Alptekin, E., & Canakci, M. (2009). Characterization of the key fuel properties of methyl ester-diesel fuel blends. *Fuel*, *88*(1), 75–80. https://doi.org/10.1016/j.fuel.2008.05.023

Alptekin, E., & Canakci, M. (2010). Optimization of pretreatment reaction for methyl ester production from chicken fat. *Fuel*, *89*(9), 4035–4039. https://doi.org/10.1016/j.fuel.2010.04.031

Alptekin, E., & Canakci, M. (2011). Optimization of transesterification for methyl ester production from chicken fat. *Fuel*, *90*(8), 2630–2638. https://doi.org/10.1016/j.fuel.2011.03.042

Altun, Ş. (2014). Effect of the degree of unsaturation of biodiesel fuels on the exhaust emissions of a diesel power generator. *Fuel*, *117*(PART A), 450–457. https://doi.org/10.1016/j.fuel.2013.09.028

Amini, Z., Ong, H. C., Harrison, M. D., Kusumo, F., Mazaheri, H., & Ilham, Z. (2017). Biodiesel production by lipase-catalyzed transesterification of Ocimum basilicum L. (sweet basil) seed oil. *Energy Conversion and Management*, *132*, 82–90. https://doi.org/10.1016/j.enconman.2016.11.017

An, H., Yang, W. M., Chou, S. K., & Chua, K. J. (2012). Combustion and emissions characteristics of diesel engine fueled by biodiesel at partial load conditions. *Applied Energy*, *99*, 363–371.

Anand, K., Sharma, R. P., & Mehta, P. S. (2011). Experimental investigations on combustion, performance and emissions characteristics of neat karanji biodiesel and its methanol blend in a diesel engine. *Biomass and Bioenergy*, *35*(1), 533–541. https://doi.org/https://doi.org/10.1016/j.biombioe.2010.10.005

Anderson, J. O., Thundiyil, J. G., & Stolbach, A. (2012). Clearing the air: a review of the effects of particulate matter air pollution on human health. *Journal of Medical Toxicology*, *8*(2), 166–175. https://doi.org/https://doi.org/10.1007/s13181-011-0203-1

Andrade, T. A., Errico, M., & Christensen, K. V. (2017). Influence of the reaction conditions on the enzyme catalyzed transesterification of castor oil: A possible step in biodiesel production. *Bioresource Technology*, *243*, 366–374. https://doi.org/10.1016/j.biortech.2017.06.118

Ang, G. T., Ooi, S. N., Tan, K. T., Lee, K. T., & Mohamed, A. R. (2015). Optimization and kinetic studies of sea mango (Cerbera odollam) oil for biodiesel production via supercritical reaction. *Energy Conversion and Management*, *99*, 242–251. https://doi.org/10.1016/j.enconman.2015.04.037

Annamalai, M., Dhinesh, B., Nanthagopal, K., SivaramaKrishnan, P., Lalvani, J. I. J., Parthasarathy, M., & Annamalai, K. (2016). An assessment on performance, combustion and emission behavior of a diesel engine powered by ceria nanoparticle blended emulsified biofuel. *Energy Conversion and Management*, *123*, 372–380.

Armas, O., García-Contreras, R., & Ramos, Á. (2012). Pollutant emissions from engine starting with ethanol and butanol diesel blends. *Fuel Processing Technology*, *100*, 63–73. https://doi.org/10.1016/j.fuproc.2012.03.003

Ashraf, S., Hussain, M., Mumtaz, M. W., & Shuaib, M. (2017). Biodiesel Production by Alkali Catalyzed Transesterification of Chicken and Beef Fats. *International Journal of Alternative Fuels and Energy*, *1*(1), 14–20.

Atabani, A. E., Silitonga, A. S., Badruddin, I. A., Mahlia, T. M. I., Masjuki, H. H., & Mekhilef, S. (2012). A comprehensive review on biodiesel as an alternative energy resource and its characteristics. *Renewable and Sustainable Energy Reviews*, *16*(4), 2070–2093. https://doi.org/10.1016/j.rser.2012.01.003

Atabani, A. E., Silitonga, A. S., Ong, H. C., Mahlia, T. M. I., Masjuki, H. H., Badruddin, I. A., & Fayaz, H. (2013). Non-edible vegetable oils: a critical evaluation of oil extraction, fatty acid compositions, biodiesel production, characteristics, engine performance and emissions production. *Renewable and Sustainable Energy Reviews*, *18*, 211–245.

Awad, S., Loubar, K., & Tazerout, M. (2014). Experimental investigation on the combustion, performance and pollutant emissions of biodiesel from animal fat residues on a direct injection diesel engine. *Energy*, *69*, 826–836. https://doi.org/10.1016/j.energy.2014.03.078

Aydin, H. (2013). Combined effects of thermal barrier coating and blending with diesel fuel on usability of vegetable oils in diesel engines. *Applied Thermal Engineering*, *51*(1), 623–629.

Aydin, H., & Bayindir, H. (2010). Performance and emission analysis of cottonseed oil methyl ester in a diesel engine. *Renewable Energy*, *35*(3), 588–592. https://doi.org/10.1016/j.renene.2009.08.009

Aydin, S., & Sayin, C. (2014). Impact of thermal barrier coating application on the combustion, performance and emissions of a diesel engine fueled with waste cooking oil biodiesel--diesel blends. *Fuel*, *136*, 334–340.

Azimov, U., Eiji, T., & Nobuyuki, K. (2018). Combustion and exhaust emission characteristics of diesel micro-pilot ignited dual-fuel engine. *Long-Haul Travel Motivation by International*

Tourist to Penang, *i*(tourism), 13.

Balakrishnan, A., Parthasarathy, R. N., & Gollahalli, S. R. (2016). Effects of degree of fuel unsaturation on NOx emission from petroleum and biofuel flames. *Fuel*, *182*, 798–806. https://doi.org/10.1016/j.fuel.2016.06.052

Bamgboye, A. I., Hansen, A. C., & others. (2008). Prediction of cetane number of biodiesel fuel from the fatty acid methyl ester (FAME) composition. *International Agrophysics*, *22*(1), 21.

Banković-Ilić, I. B., Stojković, I. J., Stamenković, O. S., Veljkovic, V. B., & Hung, Y. T. (2014). Waste animal fats as feedstocks for biodiesel production. *Renewable and Sustainable Energy Reviews*, *32*, 238–254. https://doi.org/10.1016/j.rser.2014.01.038

Barrios, C. C., Domínguez-Sáez, A., Martín, C., & Álvarez, P. (2014). Effects of animal fat based biodiesel on a TDI diesel engine performance, combustion characteristics and particle number and size distribution emissions. *Fuel*, *117*(PART A), 618–623. https://doi.org/10.1016/j.fuel.2013.09.037

Basha, J. S., & Anand, R. B. (2011). An experimental study in a CI engine using nanoadditive blended water--diesel emulsion fuel. *International Journal of Green Energy*, *8*(3), 332–348.

Baskar, P., & Senthilkumar, A. (2016). Effects of oxygen enriched combustion on pollution and performance characteristics of a diesel engine. *Engineering Science and Technology, an International Journal*, *19*(1), 438–443. https://doi.org/10.1016/j.jestch.2015.08.011

Behçet, R. (2011). Performance and emission study of waste anchovy fish biodiesel in a diesel engine. *Fuel Processing Technology*, *92*(6), 1187–1194.

Behçet, R., Oktay, H., Çakmak, A., & Aydin, H. (2015). Comparison of exhaust emissions of biodiesel--diesel fuel blends produced from animal fats. *Renewable and Sustainable Energy Reviews*, *46*, 157–165.

Benajes, J., Garcia, A., & Monsalve-Serrano, J. V. B. (2017). Achieving clean and efficient engine operation up to full load by combining optimized RCCI and dual-fuel diesel-gasoline combustion strategies. *Energy Conversion and Management*, *136*, 142–151. https://doi.org/10.1016/j.enconman.2017.01.010

Benjumea, P., Agudelo, J. R., & Agudelo, A. F. (2011). Effect of the degree of unsaturation of biodiesel fuels on engine performance, combustion characteristics, and emissions. *Energy and Fuels*, *25*(1), 77–85. https://doi.org/10.1021/ef101096x

Bessonette, P. W., Schleyer, C. H., Duffy, K. P., Hardy, W. L., & Liechty, M. P. (2007). Effects of Fuel Property Changes on Heavy-Duty HCCI Combustion. *SAE Technical Paper 2007-01-0191*, *2007*(724), 776–790. https://doi.org/10.4271/2007-01-0191

Bhale, P. V., Deshpande, N. V., & Thombre, S. B. (2009). Improving the low temperature properties of biodiesel fuel. *Renewable Energy*, *34*(3), 794–800. https://doi.org/10.1016/j.renene.2008.04.037

Bhatti, H. N., Hanif, M. A., Qasim, M., & Ata-ur-Rehman. (2008). Biodiesel production from waste tallow. *Fuel*, *87*(13–14), 2961–2966. https://doi.org/10.1016/j.fuel.2008.04.016

Boden, T. A., & Marland, R. J. A. (2015). Global, Regional, and National Fossil-Fuel CO2 Emissions. *Carbon Dioxide Information Analysis Center, Oak Ridge National Laboratory, U. s. Department of Energy, Oak Ridge, Tenn., U. S. A.* https://doi.org/10.3334/CDIAC/00001_V2015

Bowden, C. M., Samaga, B. S., & Lyn, W. (1969). Rate of heat release in high-speed indirect injection diesel engines. *Proceedings of the Institution of Mechanical Engineers*, *184*(310), 122–129.

https://doi.org/10.1243/PIME_CONF_1969_184_326_02

British Standard Institution. (2010). Bs En 14214:2008+a1:2009 Automotive fuels — Fatty acid methyl esters (FAME) for diesel engines — Requirements and test methods. *British Standard Institution*, 22. https://doi.org/ISBN 978 0 580 70781 0

Butyl-Alcohol. (2018). National Center for Biotechnology Information. Retrieved July 16, 2018, from https://pubchem.ncbi.nlm.nih.gov/compound/263#section=Top

Büyükkaya, E., Engin, T., & Cerit, M. (2006). Effects of thermal barrier coating on gas emissions and performance of a LHR engine with different injection timings and valve adjustments. *Energy Conversion and Management*, *47*(9), 1298–1310.

Campbell-Lendrum, D., & Prüss-Ustün, A. (2019). Climate change, air pollution and noncommunicable diseases. *Bulletin of the World Health Organization*, *97*(2), 160–161. https://doi.org/10.2471/blt.18.224295

Can, Ö. (2014). Combustion characteristics, performance and exhaust emissions of a diesel engine fueled with a waste cooking oil biodiesel mixture. *Energy Conversion and Management*, *87*(2014), 676–686. https://doi.org/10.1016/j.enconman.2014.07.066

Canakci, M., & Van Gerpen, J. H. (2003). Comparison of engine performance and emissions for petroleum diesel fuel, yellow grease biodiesel, and soybean oil biodiesel. *Transactions of the ASAE*, *46*(4), 937.

Cannon. (2012). Instrument Company. *Analytical Chemistry*, *34*(10), 150A-150A. https://doi.org/10.1021/ac60190a771

Carvalho, A. K. F., da Conceição, L. R. V., Silva, J. P. V., Perez, V. H., & de Castro, H. F. (2017). Biodiesel production from Mucor circinelloides using ethanol and heteropolyacid in one and two-step transesterification. *Fuel*, *202*, 503–511. https://doi.org/10.1016/j.fuel.2017.04.063

Chan, S. H., & Khor, K. A. (2000). The effect of thermal barrier coated piston crown on engine characteristics. *Journal of Materials Engineering and Performance*, *9*(1), 103–109.

Chauhan, B. S., Kumar, N., & Cho, H. M. (2011a). A study on the performance and emission of a diesel engine fueled with Jatropha biodiesel oil and its blends. *Energy*, *37*(1), 616–622. https://doi.org/10.1016/j.energy.2011.10.043

Chauhan, B. S., Kumar, N., & Cho, H. M. (2011b). A study on the performance and emission of a diesel engine fueled with Jatropha biodiesel oil and its blends. *Energy*, *37*(1), 616–622. https://doi.org/10.1016/j.energy.2011.10.043

Chen, L. C., & Lippmann, M. (2009). Effects of metals within ambient air particulate matter (PM) on human health. *Inhalation Toxicology*, *21*(1), 1–31. https://doi.org/https://doi.org/10.1080/08958370802105405

Cheruiyot, N. K., Wang, L.-C., Lin, S.-L., Yang, H.-H., & Chen, Y.-T. (2017). Effects of selective catalytic reduction on the emissions of persistent organic pollutants from a heavy-duty diesel engine. *Aerosol and Air Quality Research*, *17*(6), 1658–1665. https://doi.org/10.4209/aaqr.2017.04.0129

Chhabra, M., Sharma, A., & Dwivedi, G. (2017). Performance evaluation of diesel engine using rice bran biodiesel. *Egyptian Journal of Petroleum*, *26*(2), 511–518. https://doi.org/10.1016/j.ejpe.2016.07.002

Chintala, V., & Subramanian, K. A. (2014). Hydrogen energy share improvement along with NOx(oxides of nitrogen) emission reduction in a hydrogen dual-fuel compression ignition engine

using water injection. *Energy Conversion and Management*, *83*(x), 249–259. https://doi.org/10.1016/j.enconman.2014.03.075

Cho, C. P., Pyo, Y. D., Jang, J. Y., Kim, G. C., & Shin, Y. J. (2017). NOxreduction and N2O emissions in a diesel engine exhaust using Fe-zeolite and vanadium based SCR catalysts. *Applied Thermal Engineering*, *110*(2), 18–24. https://doi.org/10.1016/j.applthermaleng.2016.08.118

Chuang, S.-C., Chen, S.-J., Huang, K.-L., Wu, E. M.-Y., Chang-Chien, G.-P., & Wang, L.-C. (2010). Gas/particle partitioning of dioxins in exhaust gases from automobiles. *Aerosol and Air Quality Resarch*, *10*(5), 489–496. https://doi.org/doi: 10.4209/aaqr.2010.04.0028

Chung, K. H., Kim, J., & Lee, K. Y. (2009). Biodiesel production by transesterification of duck tallow with methanol on alkali catalysts. *Biomass and Bioenergy*, *33*(1), 155–158. https://doi.org/10.1016/j.biombioe.2008.04.014

Cinar, C., Uyumaz, A., Solmaz, H., & Topgul, T. (2015). Effects of valve lift on the combustion and emissions of a HCCI gasoline engine. *Energy Conversion and Management*, *94*(x), 159–168. https://doi.org/10.1016/j.enconman.2015.01.072

da Cunha, M. E., Krause, L. C., Moraes, M. S. A., Faccini, C. S., Jacques, R. A., Almeida, S. R., Rodrigues, M. R. A., & Caramão, E. B. (2009). Beef tallow biodiesel produced in a pilot scale. *Fuel Processing Technology*, *90*(4), 570–575. https://doi.org/10.1016/j.fuproc.2009.01.001

da Silva César, A., & Otávio Batalha, M. (2010). Biodiesel production from castor oil in Brazil: A difficult reality. *Energy Policy*, *38*(8), 4031–4039. https://doi.org/10.1016/j.enpol.2010.03.027

Datta, A., & Mandal, B. K. (2017). Engine performance, combustion and emission characteristics of a compression ignition engine operating on different biodiesel-alcohol blends. *Energy*, *125*, 470–483. https://doi.org/https://doi.org/10.1016/j.energy.2017.02.110

Davis, M., Ahiduzzaman, M., & Kumar, A. (2018). How will Canada's greenhouse gas emissions change by 2050? A disaggregated analysis of past and future greenhouse gas emissions using bottom-up energy modelling and Sankey diagrams. *Applied Energy*, *220*(April), 754–786. https://doi.org/10.1016/j.apenergy.2018.03.064

Day, C., & Day, G. (2017). Climate change, fossil fuel prices and depletion: The rationale for a falling export tax. *Economic Modelling*, *63*(January), 153–160. https://doi.org/10.1016/j.econmod.2017.01.006

Debnath, B. K., Saha, U. K., & Sahoo, N. (2015). A comprehensive review on the application of emulsions as an alternative fuel for diesel engines. *Renewable and Sustainable Energy Reviews*, *42*, 196–211.

Deep, A., Sandhu, S. S., & Chander, S. (2017). Experimental investigations on the influence of fuel injection timing and pressure on single cylinder C.I. engine fueled with 20% blend of castor biodiesel in diesel. *Fuel*, *210*(August), 15–22. https://doi.org/10.1016/j.fuel.2017.08.023

Deka, D. C., & Basumatary, S. (2011). High quality biodiesel from yellow oleander (Thevetia peruviana) seed oil. *Biomass and Bioenergy*, *35*(5), 1797–1803. https://doi.org/10.1016/j.biombioe.2011.01.007

Demirbas, A. (2009). Biodiesel from waste cooking oil via base-catalytic and supercritical methanol transesterification. *Energy Conversion and Management*, *50*(4), 923–927. https://doi.org/10.1016/j.enconman.2008.12.023

Department of Energy and Climate Change. (2012). *UK Bioenergy Strategy. Department for Transport*.

Dhamodaran, G., Krishnan, R., Pochareddy, Y. K., Pyarelal, H. M., Sivasubramanian, H., & Ganeshram, A. K. (2017). A comparative study of combustion, emission, and performance characteristics of rice-bran-, neem-, and cottonseed-oil biodiesels with varying degree of unsaturation. *Fuel*, *187*, 296–305. https://doi.org/10.1016/j.fuel.2016.09.062

Djerad, S., Crocoll, M., Kureti, S., Tifouti, L., & Weisweiler, W. (2006). Effect of oxygen concentration on the NOxreduction with ammonia over V2O5-WO3/TiO2catalyst. *Catalysis Today*, *113*(3–4), 208–214. https://doi.org/10.1016/j.cattod.2005.11.067

Dorado, M. P., Ballesteros, E., Arnal, J. M., Gomez, J., & Lopez, F. J. (2003). Exhaust emissions from a Diesel engine fueled with transesterified waste olive oil. *Fuel*, *82*(11), 1311–1315.

Dorado, M. P., Ballesteros, E., de Almeida, J. A., Schellert, C., Löhrlein, H. P., & Krause, R. (2002). An alkali–catalyzed transesterification process for high free fatty acid waste oils. *The American Society of Agricultural and Biological Engineers*, *45*(3), 525–529. https://doi.org/10.13031/2013.8849

dos Santos, V. H. J. M., Pestana, V. Z., de Freitas, J. S., & Rodrigues, L. F. (2018). A preliminary study on traceability of biodiesel mixtures based on the raw materials profiles from Brazilian regions and fourier transform infrared spectroscopy (FTIR). *Vibrational Spectroscopy*, *99*(April), 113–123. https://doi.org/10.1016/j.vibspec.2018.09.005

Eevera, T., Rajendran, K., & Saradha, S. (2009). Biodiesel production process optimization and characterization to assess the suitability of the product for varied environmental conditions. *Renewable Energy*, *34*(3), 762–765. https://doi.org/10.1016/j.renene.2008.04.006

Emiroğlu, A. O., Keskin, A., & Şen, M. (2018). Experimental investigation of the effects of turkey rendering fat biodiesel on combustion, performance and exhaust emissions of a diesel engine. *Fuel*, *216*(December 2017), 266–273. https://doi.org/10.1016/j.fuel.2017.12.026

Environment Agency. (2015). Biodiesel: quality protocol. Retrieved April 4, 2018, from https://www.gov.uk/government/publications/biodiesel-quality-protocol/biodiesel-quality-protocol#contents

Escobar, J. C., Lora, E. S., Venturini, O. J., Yáñez, E. E., Castillo, E. F., & Almazan, O. (2009). Biofuels: environment, technology and food security. *Renewable and Sustainable Energy Reviews*, *13*(6), 1275–1287.

Esso. (2019). Esso synergy diesels. Retrieved March 5, 2019, from https://www.esso.co.uk/diesel

Ethanol. (2018). National Center for Biotechnology Information. Retrieved July 16, 2018, from https://pubchem.ncbi.nlm.nih.gov/compound/702#section=Top

European Commision. (2014). A policy framework for climate and energy in the period from 2020 to 2030. *Https://Ec.Europa.Eu/Energy/En/Topics/Energy-Strategy/2030-Energy-Strategy*, Brussels. https://doi.org/10.1007/s13398-014-0173-7.2

European Parliament. (2009). Directive 2009/28/EC of the European Parliament and of the Council of 23 April 2009. *Official Journal of the European Union*, *140*(16), 16–62. https://doi.org/10.3000/17252555.L_2009.140.eng

European Parliament. (2015). Position of the European Parliament. *Consolidated Legislative Document*, *EP-PE_TC2*-(COD(2012)0288), 1–98.

European Standard EN 590:2013. (2009). Automotive fuels - Diesel - Requirements and test methods, 1–12.

Fadhil, A. B., Al-Tikrity, E. T. B., & Albadree, M. A. (2017). Biodiesel production from mixed non-

edible oils, castor seed oil and waste fish oil. *Fuel*, *210*(August), 721–728. https://doi.org/10.1016/j.fuel.2017.09.009

Fareez, M., Bin, E., Madzrol, N. B., Willa, R., & Patrick, A. (2016). Effects of Biodiesel Saturation Degrees on NOx Emission and FTIR Spectroscopy. *Journal of Applied Science & Process Engineering*, *3*(1), 24–33.

Felizardo, P., Baptista, P., Menezes, J. C., & Correia, M. J. N. (2007). Multivariate near infrared spectroscopy models for predicting methanol and water content in biodiesel. *Analytica Chimica Acta*, *595*(1), 107–113.

Felizardo, P., Correia, M. J. N., Raposo, I., Mendes, J. F., Berkemeier, R., & Bordado, J. M. (2006). Production of biodiesel from waste frying oils. *Waste Management*, *26*(5), 487–494.

Ferguson, C. R., & Kirkpatrick, A. T. (2015). *Internal combustion engines: applied thermosciences*. John Wiley & Sons.

Fisher Scientific. (2018). 2-Butoxyethanol, 99%, ACROS OrganicsTM. Retrieved June 26, 2018, from https://www.fishersci.com/shop/products/2-butoxyethanol-99-acros-organics-5/p-3735784

Forte, A., Zucaro, A., Faugno, S., Basosi, R., & Fierro, A. (2018). Carbon footprint and fossil energy consumption of bio-ethanol fuel production from Arundo donax L. crops on marginal lands of Southern Italy. *Energy*, *150*, 222–235. https://doi.org/10.1016/j.energy.2018.02.030

Ganapathy, T., Gakkhar, R. P., & Murugesan, K. (2011). Influence of injection timing on performance, combustion and emission characteristics of Jatropha biodiesel engine. *Applied Energy*, *88*(12), 4376–4386.

García-Martínez, N., Andreo-Martínez, P., Quesada-Medina, J., de los Ríos, A. P., Chica, A., Beneito-Ruiz, R., & Carratalá-Abril, J. (2017). Optimization of non-catalytic transesterification of tobacco (Nicotiana tabacum) seed oil using supercritical methanol to biodiesel production. *Energy Conversion and Management*, *131*, 99–108. https://doi.org/10.1016/j.enconman.2016.10.078

Geograph. (2009). Recycling of waste oil. Retrieved March 3, 2019, from https://www.geograph.ie/photo/1202969

Ghadge, S. V., & Raheman, H. (2005). Biodiesel production from mahua (Madhuca indica) oil having high free fatty acids. *Biomass and Bioenergy*, *28*(6), 601–605.

Gharehghani, A., Hosseini, R., Mirsalim, M., Jazayeri, S. A., & Yusaf, T. (2015). An experimental study on reactivity controlled compression ignition engine fueled with biodiesel/natural gas. *Energy*, *89*, 558–567. https://doi.org/10.1016/j.energy.2015.06.014

Ghojel, J., Honnery, D., & Al-Khaleefi, K. (2006). Performance, emissions and heat release characteristics of direct injection diesel engine operating on diesel oil emulsion. *Applied Thermal Engineering*, *26*(17), 2132–2141.

Giakoumis, E. G. (2013). A statistical investigation of biodiesel physical and chemical properties, and their correlation with the degree of unsaturation. *Renewable Energy*, *50*, 858–878. https://doi.org/10.1016/j.renene.2012.07.040

Gnanasekaran, S., Saravanan, N., & Ilangkumaran, M. (2016). Influence of injection timing on performance, emission and combustion characteristics of a DI diesel engine running on fish oil biodiesel. *Energy*, *116*, 1218–1229. https://doi.org/10.1016/j.energy.2016.10.039

Godiganur, S., Murthy, C. S., & Reddy, R. P. (2010). Performance and emission characteristics of a Kirloskar HA394 diesel engine operated on fish oil methyl esters. *Renewable Energy*, *35*(2),

355–359.

Gomez, M. F. (2018). *Aftertreatment system based on a magnesium hydroxide injection to reduce carbon dioxide emissions from an internal combustion engine*. Aston University.

Gray, J. I. (1978). Measurement of lipid oxidation: a review. *Journal of the American Oil Chemists' Society*, *55*(6), 539–546. https://doi.org/https://doi.org/10.1007/BF02668066

Grossale, A., Nova, I., & Tronconi, E. (2008). Study of a Fe-zeolite-based system as NH3-SCR catalyst for diesel exhaust aftertreatment. *Catalysis Today*, *136*(1–2), 18–27. https://doi.org/10.1016/j.cattod.2007.10.117

Guan, B., Zhan, R., Lin, H., & Huang, Z. (2014). Review of state of the art technologies of selective catalytic reduction of NOxfrom diesel engine exhaust. *Applied Thermal Engineering*, *66*(1–2), 395–414. https://doi.org/10.1016/j.applthermaleng.2014.02.021

Gumus, M., Sayin, C., & Canakci, M. (2012). The impact of fuel injection pressure on the exhaust emissions of a direct injection diesel engine fueled with biodiesel--diesel fuel blends. *Fuel*, *95*, 486–494.

Gürü, M., Koca, A., Can, Ö., Çinar, C., & Şahin, F. (2010). Biodiesel production from waste chicken fat based sources and evaluation with Mg based additive in a diesel engine. *Renewable Energy*, *35*(3), 637–643. https://doi.org/10.1016/j.renene.2009.08.011

Hajjari, M., Tabatabaei, M., Aghbashlo, M., & Ghanavati, H. (2017). A review on the prospects of sustainable biodiesel production: A global scenario with an emphasis on waste-oil biodiesel utilization. *Renewable and Sustainable Energy Reviews*, *72*(November 2016), 445–464. https://doi.org/10.1016/j.rser.2017.01.034

Ham, B., Shelton, R., Butler, B., & Thionville, P. (1998). Calculating the Iodine Value for marine oils from fatty acid profiles. *Journal of the American Oil …*, (20), 1445–1446. Retrieved from http://link.springer.com/article/10.1007/s11746-998-0197-2

Hamdan, S. H., Chong, W. W. F., Ng, J. H., Ghazali, M. J., & Wood, R. J. K. (2017). Influence of fatty acid methyl ester composition on tribological properties of vegetable oils and duck fat derived biodiesel. *Tribology International*, *113*(August 2016), 76–82. https://doi.org/10.1016/j.triboint.2016.12.008

Han L., Wenming Y., & Dezhi Zhou, W. Y. (2018). Numerical study of the effects of biodiesel unsaturation on combustion and emission characteristics in diesel engine. *Applied Thermal Engineering*, *137*(March), 310–318. https://doi.org/10.1016/j.applthermaleng.2018.03.066

Hannah, R., & Max, R. (2019a). Fossil Fuels. Retrieved June 7, 2019, from https://ourworldindata.org/fossil-fuels

Hao, J., Yu, W., Lu, P., Zhang, Y., & Zhu, X. (2015). The effects of Na/K additives and flyash on NO reduction in a SNCR process. *Chemosphere*, *122*(x), 213–218. https://doi.org/10.1016/j.chemosphere.2014.11.055

Haridass, M., & Jayaraman, M. (2018). Performance of multi-cylinder diesel engine fueled with mahua biodiesel using Selective Catalytic Reduction (SCR) technique. *Energy Sources, Part A: Recovery, Utilization, and Environmental Effects*, *40*(16), 1910–1918. https://doi.org/10.1080/15567036.2018.1487489

Hasimuglu, C., Ciniviz, M., Özsert, I., Içingür, Y., Parlak, A., & Salman, M. S. (2008). Performance characteristics of a low heat rejection diesel engine operating with biodiesel. *Renewable Energy*, *33*(7), 1709–1715.

Hazar, H. (2010). Cotton methyl ester usage in a diesel engine equipped with insulated combustion chamber. *Applied Energy*, *87*(1), 134–140.

Hazar, H., & Ozturk, U. (2010). The effects of Al 2 O 3--TiO 2 coating in a diesel engine on performance and emission of corn oil methyl ester. *Renewable Energy*, *35*(10), 2211–2216.

Heroor, S. H., & Bharadwaj, S. D. R. (2013). Production of bio-fuel from crude neem oil and its performance. *International Journal of Environmental Engineering and Management*, *4*, 425–432. article.

Hoekman, S. K., & Robbins, C. (2012). Review of the effects of biodiesel on NOx emissions. *Fuel Processing Technology*. https://doi.org/10.1016/j.fuproc.2011.12.036

Hossain, A. K., & Davies, P. A. (2013). Pyrolysis liquids and gases as alternative fuels in internal combustion engines - A review. *Renewable and Sustainable Energy Reviews*, *21*, 165–189. https://doi.org/10.1016/j.rser.2012.12.031

Hossain, A. K., Serrano, C., Brammer, J. B., Omran, A., Ahmed, F., Smith, D. I., & Davies, P. A. (2016). Combustion of fuel blends containing digestate pyrolysis oil in a multi-cylinder compression ignition engine. *Fuel*, *171*, 18–28. https://doi.org/10.1016/j.fuel.2015.12.012

Hossain, A. K, & Davies, P. A. (2012a). Combustion and emission characteristics of a typical biodiesel engine operated on waste cooking oil derived biodiesel. *SAE Technical Paper 2012-01-1624*, 8. https://doi.org/10.4271/2012-01-1624

Hossain, A. K, & Davies, P. A. (2012b). Performance, emission and combustion characteristics of an indirect injection (IDI) multi-cylinder compression ignition (CI) engine operating on neat jatropha and karanj oils preheated by jacket water. *Biomass and Bioenergy*, *46*, 332–342. https://doi.org/doi.10.1016/j.biombioe.2012.08.007

Hulwan, D. B., & Joshi, S. V. (2011). Performance, emission and combustion characteristic of a multicylinder DI diesel engine running on diesel--ethanol--biodiesel blends of high ethanol content. *Applied Energy*, *88*(12), 5042–5055.

Igobo, O. N. (2015). *Low-temperature Isothermal Rankine cycle for Desalination*. Aston University.

Imdadul, H. K., Masjuki, H. H., Kalam, M. A., Zulkifli, N. W. M., Alabdulkarem, A., Rashed, M. M., & Ashraful, A. M. (2016). Influences of ignition improver additive on ternary (diesel-biodiesel-higher alcohol) blends thermal stability and diesel engine performance. *Energy Conversion and Management*, *123*, 252–264.

Imdadul, H. K., Masjuki, H. H., Kalam, M. A., Zulkifli, N. W. M., Kamruzzaman, M., Shahin, M. M., & Rashed, M. M. (2017). Evaluation of oxygenated n-butanol-biodiesel blends along with ethyl hexyl nitrate as cetane improver on diesel engine attributes. *Journal of Cleaner Production*, *141*, 928–939. https://doi.org/https://doi.org/10.1016/j.jclepro.2016.09.140

Imtenan, S., Varman, M., Masjuki, H. H., Kalam, M. A., Sajjad, H., Arbab, M. I., & Rizwanul Fattah, I. M. (2014). Impact of low temperature combustion attaining strategies on diesel engine emissions for diesel and biodiesels: A review. *Energy Conversion and Management*, *80*(x), 329–356. https://doi.org/10.1016/j.enconman.2014.01.020

International Energy Agency. (2019). World Energy Outlook. Retrieved April 4, 2019, from https://www.iea.org/weo/

International Renewable Energy Agency. (2017). *Climate Policy Drives Shift To Renewable Energy*. Retrieved from https://www.irena.org/-/media/Files/IRENA/Agency/Topics/Climate-Change/IRENA_Climate_policy_2017.pdf

Iscan, B. (2016). Application of ceramic coating for improving the usage of cottonseed oil in a diesel engine. *Journal of the Energy Institute*, *89*(1), 150–157.

Jagadale, S. S., & Jugulkar, L. M. (2012). Production and Analysis of Chemical Properties of Chicken Fat Based Biodiesel and its various Blends. *International Journal of Engineering Research and Development*, *1*(7), 34–37.

Janardhan, N., Murali Krishna, M. V. S., Ushasri, P., & Murthy, P. V. K. (2013). Exhaust emissions and combustion characteristics of jatropha oil in crude form and biodiesel of low heat rejection diesel engine. *International Journal of Soft Computing and Engineering*, *3*(1), 91–95.

Jayaprabakar, J., Dawn, S. S., Ranjan, A., Priyadharsini, P., George, R. J., Sadaf, S., & Rajha, C. R. (2019). Process optimization for biodiesel production from sheep skin and its performance, emission and combustion characterization in CI engine. *Energy*, *174*, 54–68. https://doi.org/10.1016/j.energy.2019.02.140

Jesse Norman MP. (2018). New regulations to double the use of sustainable renewable fuels by 2020. Retrieved April 4, 2019, from https://www.gov.uk/government/news/new-regulations-to-double-the-use-of-sustainable-renewable-fuels-by-2020

John B. Heywood. (1988). *International Combustion Engine Fundamentals* (2nd ed.). USA.

Kamo, R., & Bryzik, W. (1978). Adiabatic turbocompound engine performance prediction. *SAE Technical Paper 780068*, 11. https://doi.org/10.4271/780068

Karabektas, M., Ergen, G., & Hosoz, M. (2008). The effects of preheated cottonseed oil methyl ester on the performance and exhaust emissions of a diesel engine. *Applied Thermal Engineering*, *28*(17–18), 2136–2143. https://doi.org/10.1016/j.applthermaleng.2007.12.016

Kettner, M., Dechent, S., Hofmann, M., Huber, E., Arruga, H., Mamat, R., & Najafi, G. (2016). Investigating the influence of water injection on the emissions of a diesel engine. *Journal of Mechanical Engineering and Sciences*, *10*(1), 1863–1881. https://doi.org/http://dx.doi.org/10.15282/jmes.10.1.2016.11.0179 Investigating

Khang, D. S., Tan, R. R., Uy, O. M., Promentilla, M. A. B., Tuan, P. D., Abe, N., & Razon, L. F. (2017). A design of experiments approach to the sensitivity analysis of the life cycle cost of biodiesel. *Clean Technologies and Environmental Policy*, *20*(3), 573–580. https://doi.org/10.1007/s10098-017-1384-3

Kirubakaran, M., & Arul Mozhi Selvan, V. (2018). A comprehensive review of low cost biodiesel production from waste chicken fat. *Renewable and Sustainable Energy Reviews*, *82*(September 2017), 390–401. https://doi.org/10.1016/j.rser.2017.09.039

Kistler Group. (2017). KiBox ® To Go Measurement and Evaluation System for Combustion. https://doi.org/2893A_000-724e-01.17

Knothe, G. (2006). Analyzing biodiesel: standards and other methods. *Journal of the American Oil Chemists' Society*, *83*(10), 823–833.

Knothe, G., Matheaus, A. C., & Ryan, T. W. (2003). Cetane numbers of branched and straight-chain fatty esters determined in an ignition quality tester. *Fuel*, *82*(8), 971–975. https://doi.org/10.1016/S0016-2361(02)00382-4

Komninos, N. P. (2009). Assessing the effect of mass transfer on the formation of HC and CO emissions in HCCI engines, using a multi-zone model. *Energy Conversion and Management*, *50*(5), 1192–1201. https://doi.org/10.1016/j.enconman.2009.01.026

Krahl, J., Tanugula, S., & Hopf, H. (2010). Diesel Fuel Additives to Reduce NOx Emissions from

Diesel Engines Operated on Diesel and Biodiesel Fuels by SNCR. *SAE Technical Paper 2010-01-2280*, *1*(x). https://doi.org/10.4271/2010-01-2280

Krishna, M. V. S. M., Prakash, T. O., Ushasri, P., Janardhan, N., & Murthy, P. V. K. (2016). Experimental investigations on direct injection diesel engine with ceramic coated combustion chamber with carbureted alcohols and crude jatropha oil. *Renewable and Sustainable Energy Reviews*, *53*, 606–628.

Krutof, A., & Hawboldt, K. (2016). Blends of pyrolysis oil, petroleum, and other bio-based fuels: A review. *Renewable and Sustainable Energy Reviews*, *59*, 406–419. https://doi.org/10.1016/j.rser.2015.12.304

Kumar, Ashok, & Subramanian, K. A. (2017). Control of greenhouse gas emissions (CO2, CH4and N2O) of a biodiesel (B100) fueled automotive diesel engine using increased compression ratio. *Applied Thermal Engineering*, *127*, 95–105. https://doi.org/10.1016/j.applthermaleng.2017.08.015

Kumar, Ashwani, & Sharma, S. (2011). Potential non-edible oil resources as biodiesel feedstock: An Indian perspective. *Renewable and Sustainable Energy Reviews*, *15*(4), 1791–1800. https://doi.org/10.1016/j.rser.2010.11.020

Kumar, D. V., Kumar, P. R., & Kumari, M. S. (2013). Prediction of performance and emissions of a biodiesel fueled Lanthanum Zirconate coated direct injection diesel engine using artificial neural networks. *Procedia Engineering*, *64*, 993–1002.

Kurtz, E., & Polonowski, C. J. (2017). The Influence of Fuel Cetane Number on Catalyst Light-Off Operation in a Modern Diesel Engine. *SAE International Journal of Fuels and Lubricants*, *10*(3), 664–671. https://doi.org/10.4271/2017-01-9378

Lam, M. K., Lee, K. T., & Mohamed, A. R. (2010). Homogeneous, heterogeneous and enzymatic catalysis for transesterification of high free fatty acid oil (waste cooking oil) to biodiesel: A review. *Biotechnology Advances*, *28*(4), 500–518. https://doi.org/10.1016/j.biotechadv.2010.03.002

Lambert, C., Dobson, D., Gierczak, C., Guo, G., Ura, J., & Warner, J. (2014). Nitrous oxide emissions from a medium-duty diesel truck exhaust system. *International Journal of Powertrains*, *3*(1), 4–25. https://doi.org/10.1504/IJPT.2014.059410

Lanjekar, R. D., & Deshmukh, D. (2016). A review of the effect of the composition of biodiesel on NOxemission, oxidative stability and cold flow properties. *Renewable and Sustainable Energy Reviews*, *54*, 1401–1411. https://doi.org/10.1016/j.rser.2015.10.034

Lapuerta, M., Armas, O., & Rodriguez-Fernandez, J. (2009). Effect of the Degree of Unsaturation of Biodiesel Fuels on NOx and Particulate Emissions. *SAE International Journal of Fuels and Lubricants*, *1*(1), 1150–1158.

Lawler, B., Splitter, D., Szybist, J., & Kaul, B. (2017). Thermally Stratified Compression Ignition: A new advanced low temperature combustion mode with load flexibility. *Applied Energy*, *189*, 122–132. https://doi.org/10.1016/j.apenergy.2016.11.034

Lee, R. A., & Lavoie, J.-M. (2013). From first- to third-generation biofuels: Challenges of producing a commodity from a biomass of increasing complexity. *Animal Frontiers*, *3*(2), 6–11. https://doi.org/10.2527/af.2013-0010

Leung, D. Y. C., & Guo, Y. (2006). Transesterification of neat and used frying oil: optimization for biodiesel production. *Fuel Processing Technology*, *87*(10), 883–890.

Li, L., Wang, J., Wang, Z., & Xiao, J. (2015). Combustion and emission characteristics of diesel engine fueled with diesel/biodiesel/pentanol fuel blends. *Fuel*, *156*, 211–218. https://doi.org/https://doi.org/10.1016/j.fuel.2015.04.048

Lin, C.-C., Chen, S.-J., Huang, K.-L., Hwang, W.-I., Chang-Chien, G.-P., & Lin, W.-Y. (2005). Characteristics of metals in nano/ultrafine/fine/coarse particles collected beside a heavily trafficked road. *Environmental Science & Technology*, *39*(21), 8113–8122. https://doi.org/DOI: 10.1021/es048182a

Lin, C.-C., Chen, S.-J., Huang, K.-L., Lee, W.-J., Lin, W.-Y., Tsai, J.-H., & Chaung, H.-C. (2008). PAHs, PAH-induced carcinogenic potency, and particle-extract-induced cytotoxicity of traffic-related nano/ultrafine particles. *Environmental Science & Technology*, *42*(11), 4229–4235. https://doi.org/DOI: 10.1021/es703107w

Lin, C.-Y., & Li, R.-J. (2009). Engine performance and emission characteristics of marine fish-oil biodiesel produced from the discarded parts of marine fish. *Fuel Processing Technology*, *90*(7), 883–888.

Lister-Petter Technical Publications. (2001). *Master Parts Manual for LPW , LPWT , LPWS Industrial Engines*.

Lloyd, A. C., & Cackette, T. A. (2001). Diesel engines: environmental impact and control. *Journal of the Air & Waste Management Association*, *51*(6), 809–847.

Ma, F., & Hanna, M. A. (1999). Biodiesel production: a review. *Bioresource Technology*, *70*(1), 1–15.

Mahla, S. K., Dhir, A., Gill, K. J. S., Cho, H. M., Lim, H. C., & Chauhan, B. S. (2018). Influence of EGR on the simultaneous reduction of NOx-smoke emissions trade-off under CNG-biodiesel dual fuel engine. *Energy*, *152*(x), 303–312. https://doi.org/10.1016/j.energy.2018.03.072

Mahrous, A. F. M., Potrzebowski, A., Wyszynski, M. L., Xu, H. M., Tsolakis, A., & Luszcz, P. (2009). A modelling study into the effects of variable valve timing on the gas exchange process and performance of a 4-valve DI homogeneous charge compression ignition (HCCI) engine. *Energy Conversion and Management*, *50*(2), 393–398. https://doi.org/10.1016/j.enconman.2008.09.018

Man, X. J., Cheung, C. S., Ning, Z., Wei, L., & Huang, Z. H. (2016). Influence of engine load and speed on regulated and unregulated emissions of a diesel engine fueled with diesel fuel blended with waste cooking oil biodiesel. *Fuel*, *180*, 41–49. https://doi.org/10.1016/j.fuel.2016.04.007

Mansha, M., Qureshi, A. H., & Shahid, E. M. (2007). Prediction of Optimum Parameters for NOx Reduction Utilizing Selective Non-Catalytic Reduction (SNCR) Technique (Thermal DeNOx Process). *Pakistan Journal of Engineering and Applied Sciences*, (x).

Mardhiah, H. H., Ong, H. C., Masjuki, H. H., Lim, S., & Lee, H. V. (2017). A review on latest developments and future prospects of heterogeneous catalyst in biodiesel production from non-edible oils. *Renewable and Sustainable Energy Reviews*, *67*, 1225–1236. https://doi.org/10.1016/j.rser.2016.09.036

Marinković, D. M., Avramović, J. M., Stanković, M. V., Stamenković, O. S., Jovanović, D. M., & Veljković, V. B. (2017). Synthesis and characterization of spherically-shaped CaO/Γ-Al2O3catalyst and its application in biodiesel production. *Energy Conversion and Management*, *144*, 399–413. https://doi.org/10.1016/j.enconman.2017.04.079

Marulanda, V. F., Anitescu, G., & Tavlarides, L. L. (2010). Investigations on supercritical transesterification of chicken fat for biodiesel production from low-cost lipid feedstocks. *Journal of Supercritical Fluids*, *54*(1), 53–60. https://doi.org/10.1016/j.supflu.2010.04.001

Marwaha, A., Rosha, P., Mohapatra, S. K., Mahla, S. K., & Dhir, A. (2018). Waste materials as potential catalysts for biodiesel production: Current state and future scope. *Fuel Processing Technology*, *181*(June), 175–186. https://doi.org/10.1016/j.fuproc.2018.09.011

Masada, Y. (1976). *Analysis of essential oils by gas chromatography and mass spectrometry*. United States. https://doi.org/OSTI ID: 5052228

Masera, K., & Hossain, A. K. (2017). Production , Characterisation and Assessment of Biomixture Fuels for Compression Ignition Engine Application. *International Journal of Mechanical and Mechatronics Engineering*, *11*(12), 1857–1863. https://doi.org/scholar.waset.org/1307-6892/10008317

Masera, K., & Hossain, A. K. (2019a). Biofuels and thermal barrier: A review on compression ignition engine performance, combustion and exhaust gas emission. *Journal of the Energy Institute*, *92*(3), 783–801. https://doi.org/10.1016/j.joei.2018.02.005

Masera, K., & Hossain, A. K. (2019b). Combustion Characteristics of Cottonseed Biodiesel and Chicken Fat Biodiesel Mixture in a Multi-Cylinder Compression Ignition Engine. *SAE Technical Paper 2019-01-0015*, *1*, 1–14. https://doi.org/10.4271/2019-01-0015

Masera, K., & Hossain, A. K. (2019c). Combustion Characteristics of Cottonseed Biodiesel and Chicken Fat Biodiesel Mixture in a Multi-Cylinder Compression Ignition Engine. *SAE Technical Papers*, *2019-Janua*(January). https://doi.org/10.4271/2019-01-0015

Mata, T. M., Cardoso, N., Ornelas, M., Neves, S., & Caetano, N. S. (2010). Sustainable production of biodiesel from tallow, lard and poultry fat and its quality evaluation. *Chemical Engineering Transactions*, *19*, 13–18. https://doi.org/10.3303/CET1019003

Mata, Teresa M., Cardoso, N., Ornelas, M., Neves, S., & Caetano, N. S. (2011). Evaluation of two purification methods of biodiesel from beef tallow, pork lard, and chicken fat. *Energy and Fuels*, *25*(10), 4756–4762. https://doi.org/10.1021/ef2010207

Mata, Teresa M., Mendes, A. M., Caetano, N. S., & Martins, A. A. (2014). Properties and sustainability of biodiesel from animal fats and fish oil. *Chemical Engineering Transactions*, *38*(October 2016), 175–180. https://doi.org/10.3303/CET1438030

Mazanov, S. V., Gabitova, A. R., Usmanov, R. A., Gumerov, F. M., Labidi, S., Amar, M. B., Passarello, L. P., Kanaev, A., Volle, F., & Neindre, B. L. (2016). Continuous production of biodiesel from rapeseed oil by ultrasonic assist transesterification in supercritical ethanol. *Journal of Supercritical Fluids*, *118*, 107–118. https://doi.org/10.1016/j.supflu.2016.07.009

McDougal, T. (2015). Millions of chickens go to landfill in UK each year. Retrieved July 2, 2018, from https://www.fwi.co.uk/news/environment/millions-chickens-go-landfill-uk-year

Meher, L. C., Dharmagadda, V. S. S., & Naik, S. N. (2006). Optimization of alkali-catalyzed transesterification of Pongamia pinnata oil for production of biodiesel. *Bioresource Technology*, *97*(12), 1392–1397. https://doi.org/10.1016/j.biortech.2005.07.003

Meher, L. C., Sagar, D. V., & Naik, S. N. (2006). Technical aspects of biodiesel production by transesterification—a review. *Renewable and Sustainable Energy Reviews*, *10*(3), 248–268.

Mehregan, M., & Moghiman, M. (2018). Effects of nano-additives on pollutants emission and engine performance in a urea-SCR equipped diesel engine fueled with blended-biodiesel. *Fuel*, *222*, 402–406. https://doi.org/10.1016/j.fuel.2018.02.172

Mehta, P. S., & Jeyaseelan, T. (2014). Controlling Nitric Oxide in C I Engine - Bio-Mix Approach. *SAE Technical Paper Series*, *1*. https://doi.org/10.4271/2014-01-2724

Melo-Espinosa, E. A., Piloto-Rodr\'\iguez, R., Goyos-Pérez, L., Sierens, R., & Verhelst, S. (2015). Emulsification of animal fats and vegetable oils for their use as a diesel engine fuel: An overview. *Renewable and Sustainable Energy Reviews*, *47*, 623–633.

Methyl-Alcohol. (2018). National Center for Biotechnology Information. Retrieved July 16, 2018, from https://pubchem.ncbi.nlm.nih.gov/compound/887#section=Top

Michael, J. M., Howard, N. S., & others. (2011). Fundamentals of engineering thermodynamics. *Fundamentals of Engineering Thermodynamics*.

Mingrui, W., Thanh Sa, N., Turkson, R. F., Jinping, L., & Guanlun, G. (2017). Water injection for higher engine performance and lower emissions. *Journal of the Energy Institute*, *90*(2), 285–299. https://doi.org/10.1016/j.joei.2015.12.003

Mittal, N., Athony, R. L., Bansal, R., & Kumar, C. R. (2013). Study of performance and emission characteristics of a partially coated LHR SI engine blended with n-butanol and gasoline. *Alexandria Engineering Journal*, *52*(3), 285–293.

Mofijur, M., Atabani, A. E., Masjuki, H. H., Kalam, M. A., & Masum, B. M. (2013). A study on the effects of promising edible and non-edible biodiesel feedstocks on engine performance and emissions production: A comparative evaluation. *Renewable and Sustainable Energy Reviews*. https://doi.org/10.1016/j.rser.2013.03.009

MohamedMusthafa, M., Sivapirakasam, S. P., & Udayakumar, M. (2011). Comparative studies on fly ash coated low heat rejection diesel engine on performance and emission characteristics fueled by rice bran and pongamia methyl ester and their blend with diesel. *Energy*, *36*(5), 2343–2351.

Mohammadshirazi, A., Akram, A., Rafiee, S., & Bagheri Kalhor, E. (2014). Energy and cost analyses of biodiesel production from waste cooking oil. *Renewable and Sustainable Energy Reviews*, *33*, 44–49. https://doi.org/10.1016/j.rser.2014.01.067

Moser, B. R. (2014). Impact of fatty ester composition on low temperature properties of biodiesel-petroleum diesel blends. *Fuel*, *115*, 500–506. https://doi.org/10.1016/j.fuel.2013.07.075

Muric, K., Andersson, A., Andersson, L., Oom, K., & Group, V. (2018). The Potential of SNCR Based NOx Reduction in a Double Compression Expansion Engine. *SAE Technical Paper 2018-01-1128*, (x), 1–14. https://doi.org/10.4271/2018-01-1128.Abstract

Murphy, M. J., Taylor, J. D., & Mccormick, R. L. (2004). Compendium of Experimental Cetane Number Data. *National Renewable Energy Laboratory*, (August), 1–48. https://doi.org/10.2172/1086353

Murthy, V. K. (2013). Improving of emissions and performance of rice brawn oil in medium grade low heat rejection diesel engine. *International Journal of Renewable Energy Research (IJRER)*, *3*(1), 98–108.

Muzio, L. J., Quartucy, G. C., & Cichanowiczy, J. E. (2002). Overview and status of post-combustion NOx control: SNCR, SCR and hybrid technologies. *International Journal of Environment and Pollution*, *17*(1–2), 4–30.

Nabi, M. N., Rahman, M. M., Islam, M. A., Hossain, F. M., Brooks, P., Rowlands, W. N., Tulloch, J., Ristovski, Z. D., & Brown, R. J. (2015). Fuel characterisation, engine performance, combustion and exhaust emissions with a new renewable Licella biofuel. *Energy Conversion and Management*, *96*, 588–598.

Nakamura, H., Kihara, N., Adachi, M., & Ishida, K. (2002). Development of a wetbased NDIR and its application to on-board emissions measurement system. In *SAE Technical Paper Series*.

https://doi.org/https://doi.org/10.4271/2002-01-0612

Nanthagopal, K., Ashok, B., Varatharajan, V., Anand, V., & Dinesh Kumar, R. (2017). Study on the effect of exhaust gas-based fuel preheating device on ethanol–diesel blends operation in a compression ignition engine. *Clean Technologies and Environmental Policy*, *19*(10), 2379–2392. https://doi.org/10.1007/s10098-017-1426-x

Nour, M., Kosaka, H., Bady, M., Sato, S., & Abdel-Rahman, A. K. (2017). Combustion and emission characteristics of DI diesel engine fuelled by ethanol injected into the exhaust manifold. *Fuel Processing Technology*, *164*, 33–50. https://doi.org/10.1016/j.fuproc.2017.04.018

Omari, A., Pischinger, S., Nuottimäki, J., & Honkanen, M. (2017). Improving Engine Efficiency and Emission Reduction Potential of HVO by Fuel-Specific Engine Calibration in Modern Passenger Car Diesel Applications Om Parkash Bhardwaj and Bastian Holderbaum. *SAE International Journal of Fuels and Lubricants*, *10*(3), 756–767. https://doi.org/10.4271/2017-01-2295

Öner, C., & Altun, S. (2009). Biodiesel production from inedible animal tallow and an experimental investigation of its use as alternative fuel in a direct injection diesel engine. *Applied Energy*, *86*(10), 2114–2120.

Ouachab, N., & Tsoutsos, T. (2013). Study of the acid pretreatment and biodiesel production from olive pomace oil. *Journal of Chemical Technology and Biotechnology*, *88*(6), 1175–1181.

Özener, O., Yüksek, L., Ergenç, A. T., & Özkan, M. (2014). Effects of soybean biodiesel on a DI diesel engine performance, emission and combustion characteristics. *Fuel*, *115*, 875–883. https://doi.org/10.1016/j.fuel.2012.10.081

Ozsezen, A. N., Canakci, M., Turkcan, A., & Sayin, C. (2009). Performance and combustion characteristics of a DI diesel engine fueled with waste palm oil and canola oil methyl esters. *Fuel*, *88*(4), 629–636.

Palaniswamy, E., & Manoharan, N. (2008). Ceramic coated combustion chamber for improving IC engine performance. *International Journal on Design and Manufacturing Technologies*, *2*(1).

Palash, S. M., Kalam, M. A., Masjuki, H. H., Arbab, M. I., Masum, B. M., & Sanjid, A. (2014). Impacts of NOxreducing antioxidant additive on performance and emissions of a multi-cylinder diesel engine fueled with Jatropha biodiesel blends. *Energy Conversion and Management*, *77*(x), 577–585. https://doi.org/10.1016/j.enconman.2013.10.016

Palash, S. M., Kalam, M. A., Masjuki, H. H., Masum, B. M., Rizwanul Fattah, I. M., & Mofijur, M. (2013). Impacts of biodiesel combustion on NOxemissions and their reduction approaches. *Renewable and Sustainable Energy Reviews*, *23*, 473–490. https://doi.org/10.1016/j.rser.2013.03.003

Parlak, A., Yasar, H., & Eldogan, O. (2005). The effect of thermal barrier coating on a turbo-charged Diesel engine performance and exergy potential of the exhaust gas. *Energy Conversion and Management*, *46*(3), 489–499.

Peja International. (2015). Rendering processes. Retrieved March 3, 2019, from https://peja.ru/en/catalog/rendering-processes/

Piaszyk, J. (2012). *Animal fat (tallow) as fuel for stationary internal combustion engines*. University of Birmingham.

Poorghasemi, K., Saray, R. K., Ansari, E., Irdmousa, B. K., Shahbakhti, M., & Naber, J. D. (2017). Effect of diesel injection strategies on natural gas/diesel RCCI combustion characteristics in a light duty diesel engine. *Applied Energy*, *199*, 430–446.

https://doi.org/10.1016/j.apenergy.2017.05.011

Prabhahar, M., & Rajan, K. (2013). Performance and combustion characteristics of a diesel engine with titanium oxide coated piston using Pongamia methyl ester. *Journal of Mechanical Science and Technology*, *27*(5), 1519–1526.

Prasath, B. R., Porai, P. T., & Shabir, M. F. (2010). Two-zone modeling of diesel/biodiesel blended fuel operated ceramic coated direct injection diesel engine. *International Journal of Energy and Environment*, *1*(6), 1039–1056.

Praveen, R., & Natarajan, S. (2014). Experimental study of selective catalytic reduction system on ci engine fuelled with diesel-ethanol blend for NOx reduction with injection of urea solutions. *International Journal of Engineering and Technology*, *6*(2), 895–904.

Predojević, Z. J. (2008). The production of biodiesel from waste frying oils: A comparison of different purification steps. *Fuel*, *87*(17–18), 3522–3528. https://doi.org/10.1016/j.fuel.2008.07.003

Qi, D. H., Chen, H., Matthews, R. D., & Bian, Y. Z. (2010). Combustion and emission characteristics of ethanol-biodiesel-water micro-emulsions used in a direct injection compression ignition engine. *Fuel*, *89*(5), 958–964. https://doi.org/10.1016/j.fuel.2009.06.029

Rao, P. V., Stephen, C., & Brown, R. (2010). Influence of Iodine Value on Combustion and NOx Emission Characteristics of a DI Diesel Engine. In *Chemeca 2010: The 40th Australasian Chemical Engineering Conference* (p. 12). Adelaide, South Australia.

Ragit, S. S., Mohapatra, S. K., & Kundu, K. (2010). Performance and emission evaluation of a diesel engine fueled with methyl ester of neem oil and filtered neem oil. *Journal of Scientific and Industrial Research*, *69*(1), 62–66.

Raheman, H., & Phadatare, A. G. (2004). Diesel engine emissions and performance from blends of karanja methyl ester and diesel. *Biomass and Bioenergy*, *27*(4), 393–397. https://doi.org/10.1016/j.biombioe.2004.03.002

Rajan, K., & Kumar, K. R. S. (2011). Combustion and emission characteristics of a biodiesel fuelled diesel engine with the effect of thermal barrier coated internal jet piston. In *Sustainable Energy and Intelligent Systems (SEISCON 2011), International Conference on* (pp. 184–189).

Rajkumar, S., & Thangaraja, J. (2019). Effect of biodiesel, biodiesel binary blends, hydrogenated biodiesel and injection parameters on NOx and soot emissions in a turbocharged diesel engine. *Fuel*, *240*(December 2018), 101–118. https://doi.org/10.1016/j.fuel.2018.11.141

Ramadhas, A. S., Jayaraj, S., & Muraleedharan, C. (2005). Biodiesel production from high FFA rubber seed oil. *Fuel*, *84*(4), 335–340. https://doi.org/10.1016/j.fuel.2004.09.016

Ramalingam, S., & Rajendran, S. (2017). NOx Emission Reduction in Annona Biodiesel Engine by Means of Antioxidant Additives. *SAE International Journal of Fuels and Lubricants*, *10*(3), 652–663. https://doi.org/10.4271/2017-01-9377

Ramírez-Verduzco, L. F., Rodríguez-Rodríguez, J. E., & Jaramillo-Jacob, A. D. R. (2012). Predicting cetane number, kinematic viscosity, density and higher heating value of biodiesel from its fatty acid methyl ester composition. *Fuel*, *91*(1), 102–111. https://doi.org/10.1016/j.fuel.2011.06.070

Ramos, M. J., Fernández, C. M., Casas, A., Rodriguez, L., & Pérez, Á. (2009). Influence of fatty acid composition of raw materials on biodiesel properties. *Bioresource Technology*, *100*(1), 261–268. https://doi.org/10.1016/j.biortech.2008.06.039

Ranjan, A., Dawn, S. S., Jayaprabakar, J., Nirmala, N., Saikiran, K., & Sai Sriram, S. (2018). Experimental investigation on effect of MgO nanoparticles on cold flow properties, performance,

emission and combustion characteristics of waste cooking oil biodiesel. *Fuel*, *220*(August 2017), 780–791. https://doi.org/10.1016/j.fuel.2018.02.057

Rao, G. L. N., Ramadhas, A. S., Nallusamy, N., & Sakthivel, P. (2010). Relationships among the physical properties of biodiesel and engine fuel system design requirement. *International Journal of Energy and Environment*, *1*(5), 919–926.

Rao, N. V., Krishna, M. V. S. M., & Murthy, P. V. K. (2013). Comparative studies on exhaust emissions and combustion characteristics of ceramic coated diesel engine with tobacco seed oil based biodiesel. *International Journal of Advanced Scientific & Technical Research*, *3*(5), 334–349.

Rao, S. M., & Anand, R. B. (2014). Working Characteristics of a DICI Engine by Using Water Emulsion Biodiesel Fuels. *Applied Mechanics and Materials*, *592–594*(x), 1847–1851. https://doi.org/10.4028/www.scientific.net/AMM.592-594.1847

Reddy, T. R., Krishna, M. V. S. M., Reddy, C. K., & Murthy, P. V. K. (2012). Comparative performance of ceramic coated diesel engine with mohr oil in crude and biodiesel form. *International Journal of Engineering and Advanced Technology*, *2*(3), 588–596.

Redel-Macías, M. D., Pinzi, S., Leiva-Candia, D. E., Cubero-Atienza, A. J., & Dorado, M. P. (2013). Influence of fatty acid unsaturation degree over exhaust and noise emissions through biodiesel combustion. *Fuel*, *109*, 248–255. https://doi.org/10.1016/j.fuel.2012.12.019

Refaat, A. A. (2009). Correlation between the chemical structure of biodiesel and its physical properties. *International Journal of Environmental Science & Technology*, *6*(4), 677–694. https://doi.org/10.1007/BF03326109

Ristovski, Z. D., Miljevic, B., Surawski, N. C., Morawska, L., Fong, K. M., Goh, F., & Yang, I. A. (2012). Respiratory health effects of diesel particulate matter. *Respirology*, *17*(2), 201–212. https://doi.org/https://doi.org/10.1111/j.1440-1843.2011.02109.x

Rizwanul Fattah, I. M., Hassan, M. H., Kalam, M. A., Atabani, A. E., & Abedin, M. J. (2014). Synthetic phenolic antioxidants to biodiesel: Path toward NOxreduction of an unmodified indirect injection diesel engine. *Journal of Cleaner Production*, *79*(x), 82–90. https://doi.org/10.1016/j.jclepro.2014.05.071

Rizwanul Fattah, I. M., Kalam, M. A., Masjuki, H. H., & Wakil, M. A. (2014). Biodiesel production, characterization, engine performance, and emission characteristics of Malaysian Alexandrian laurel oil. *RSC Advances*, *4*(34), 17787–17796. https://doi.org/10.1039/c3ra47954d

Robert, E. S., & Thomas J. W. (1981). Liquid hydrocarbon-soluble rare earth chelates prepared from the novelligand 2,2,7-trimethyl-3,5-octanedione and fuels containing same. US. https://doi.org/United States Patent Appl. No.: 17,459

Rogers, J. D., Burke, T. L., Osborn, S. G., & Ryan, J. N. (2015). A framework for identifying organic compounds of concern in hydraulic fracturing fluids based on their mobility and persistence in groundwater. *Environmental Science and Technology Letters*, *2*(6), 158–164. https://doi.org/10.1021/acs.estlett.5b00090

Rutz, D., & Janssen, R. (2006). *Overview and Recommendations on Biofuel Standards for Transport in the EU (Contribution to WP 3.2 and WP 5.5). Project: BiofuelMarketplace | WIP Renewable Energies*. Munchen, Germany. https://doi.org/(EIE/05/022/SI2.420009) Overview

Saba, T., Estephane, J., El Khoury, B., El Khoury, M., Khazma, M., El Zakhem, H., & Aouad, S. (2016). Biodiesel production from refined sunflower vegetable oil over KOH/ZSM5 catalysts. *Renewable Energy*, *90*, 301–306. https://doi.org/10.1016/j.renene.2016.01.009

Sachuthananthan, B., Balaji, G., & Krupakaran, R. L. (2018). Experimental exploration on NOxdiminution by the combined effect of antioxidant additives with SCR in a diesel engine powered by neem biodiesel. *International Journal of Ambient Energy*, 1–12. https://doi.org/10.1080/01430750.2018.1492443

Saint-Ramond, B. (2001). HITS-high insulation thermal barrier coating systems. *Air & Space Europe*, *3*(3), 174–177.

Sakthivel, G., Nagarajan, G., Ilangkumaran, M., & Gaikwad, A. B. (2014). Comparative analysis of performance, emission and combustion parameters of diesel engine fuelled with ethyl ester of fish oil and its diesel blends. *Fuel*, *132*, 116–124.

Sakthivel, R., Ramesh, K., Purnachandran, R., & Mohamed Shameer, P. (2018). A review on the properties, performance and emission aspects of the third generation biodiesels. *Renewable and Sustainable Energy Reviews*, *82*(5), 2970–2992. https://doi.org/10.1016/j.rser.2017.10.037

Salahi, M. M., Esfahanian, V., Gharehghani, A., & Mirsalim, M. (2017). Investigating the reactivity controlled compression ignition (RCCI) combustion strategy in a natural gas/diesel fueled engine with a pre-chamber. *Energy Conversion and Management*, *132*, 40–53. https://doi.org/10.1016/j.enconman.2016.11.019

Salamanca, M., Mondragon, F., Agudelo, J. R., Benjumea, P., & Santamaria, A. (2012). Variations in the chemical composition and morphology of soot induced by the unsaturation degree of biodiesel and a biodiesel blend. *Combustion and Flame*, *159*(3), 1100–1108. https://doi.org/10.1016/j.combustflame.2011.10.011

Samadi, H., & Coyle, T. W. (2009). Alternative thermal barrier coatings for diesel engines. In *5th Congress of Iran Ceramic Society, Iranian Ceramic Society* (pp. 1–8).

Sander, A., Antonije Košćak, M., Kosir, D., Milosavljević, N., Parlov Vuković, J., & Magić, L. (2018). The influence of animal fat type and purification conditions on biodiesel quality. *Renewable Energy*, *118*, 752–760. https://doi.org/10.1016/j.renene.2017.11.068

Sanders T. H. (2003). *Encyclopedia of Food Sciences and Nutrition (Second Edition)*. https://doi.org/https://doi.org/10.1016/B0-12-227055-X/01353-5

Sanjid, A., Kalam, M. A., Masjuki, H. H., Varman, M., Zulkifli, N. W. B. M., & Abedin, M. J. (2016). Performance and emission of multi-cylinder diesel engine using biodiesel blends obtained from mixed inedible feedstocks. *Journal of Cleaner Production*, *112*, 4114–4122. https://doi.org/10.1016/j.jclepro.2015.07.154

Sathiyagnnanam, A. P., Saravanan, C. G., & Dhandapani, S. (2010). Effect of thermal-barrier coating plus fuel additive for reducing emission from di diesel engine. In *Proceedings of the world Congress on Engineering* (Vol. 2).

Schober, S., & Mittelbach, M. (2007). Iodine value and biodiesel: Is limitation still appropriate? *Lipid Technology*, *19*(12), 281–284. https://doi.org/10.1002/lite.200700091

Schönborn, A. (2009). *Influence of the molecular structure of biofuels on combustion in a compression ignition engine*. University College London. Retrieved from http://discovery.ucl.ac.uk/18674/

Schönborn, A., Ladommatos, N., Williams, J., Allan, R., & Rogerson, J. (2009). The influence of molecular structure of fatty acid monoalkyl esters on diesel combustion. *Combustion and Flame*, *156*(7), 1396–1412. https://doi.org/10.1016/j.combustflame.2009.03.011

Şen, M., Emiroğlu, A. O., & Keskin, A. (2018). Production of Biodiesel from Broiler Chicken

Rendering Fat and Investigation of Its Effects on Combustion, Performance, and Emissions of a Diesel Engine. *Energy & Fuels*, acs.energyfuels.8b00278. https://doi.org/10.1021/acs.energyfuels.8b00278

Senthur Prabu, S., Asokan, M. A., Roy, R., Francis, S., & Sreelekh, M. K. (2017). Performance, combustion and emission characteristics of diesel engine fuelled with waste cooking oil bio-diesel/diesel blends with additives. *Energy*, *122*, 638–648. https://doi.org/10.1016/j.energy.2017.01.119

Shameer, P. M., & Ramesh, K. (2017a). Experimental evaluation on performance, combustion behavior and influence of in-cylinder temperature on NOx emission in a D.I diesel engine using thermal imager for various alternate fuel blends. *Energy*, *118*, 1334–1344. https://doi.org/10.1016/j.energy.2016.11.017

Shameer, P. M., & Ramesh, K. (2017b). Green technology and performance consequences of an eco-friendly substance on a 4-stroke diesel engine at standard injection timing and compression ratio. *Journal of Mechanical Science and Technology*, *31*(3), 1497–1507. https://doi.org/10.1007/s12206-017-0249-3

Sharma, V., & Ganesh, D. (2019). Combustion and emission characteristics of reformulated biodiesel fuel in a single-cylinder compression ignition engine. *International Journal of Environmental Science and Technology*, (0123456789). https://doi.org/10.1007/s13762-019-02285-8

Shu, Q., Tang, G., Lesmana, H., Zou, L., & Xiong, D. (2018). Preparation, characterization and application of a novel solid BrÖnsted acid catalyst SO42−/La3+/C for biodiesel production via esterification of oleic acid and methanol. *Renewable Energy*, *119*, 253–261. https://doi.org/10.1016/j.renene.2017.12.013

Silambarasan, R., Senthil, R., Manimaran, M., Pranesh, G., & Mebin S. P. (2015). Experimental Investigation of a Diesel Engine fueled by emulsified B20 biodiesel. *Journal of Chemical and Pharmaceutical Sciences*, (7), 26–28.

Sivaramakrishnan, K., & Ravikumar, P. (2012). Determination of cetane number of biodiesel and its influence on physical properties. *ARPN Journal of Engineering and Applied Sciences*, 7(2), 205–211.

Soares, S., Lima, M. J. A., & Rocha, F. R. P. (2017). A spot test for iodine value determination in biodiesel based on digital images exploiting a smartphone. *Microchemical Journal*, *133*, 195–199. https://doi.org/10.1016/j.microc.2017.03.029

Soleimanzadeh, H., Niaei, A., Salari, D., Tarjomannejad, A., Penner, S., Grünbacher, M., Hosseini, S. A., & Mousavi, S. M. (2019). Modeling and optimization of V2O5/TiO2 nanocatalysts for NH3-Selective catalytic reduction (SCR) of NOx by RSM and ANN techniques. *Journal of Environmental Management*, *238*(March), 360–367. https://doi.org/10.1016/j.jenvman.2019.03.018

Srikanth, D., Krishna, M. V. S. M., Ushasri, P., & Murthy, P. V. K. (2013). Performance exhaust emissions, and combustion characteristics of cotton seed oil based biodiesel in ceramic coated diesel engine. *International Journal of Mechanical Engineering*, 2(5), 67–82.

Srinivasan, G. R., Srinivasan, S. R., Venkatachalapathy, D., & Venkatachalapathy, N. (2017). Production, Performance, Combustion, Emission Characteristics of Biodiesel Synthesized from Mutton Suet. *International Journal of Engineering and Technology*, *9*(5), 3512–3518. https://doi.org/10.21817/ijet/2017/v9i5/170905038

Stanglmaier, R. H., Dingle, P. J., & Stewart, D. W. (2008). Cycle-Controlled Water Injection for Steady-State and Transient Emissions Reduction From a Heavy-Duty Diesel Engine. *Journal of*

Engineering for Gas Turbines and Power, *130*(3), 032801. https://doi.org/10.1115/1.2830856

Subramanian, K. A. (2011). A comparison of water-diesel emulsion and timed injection of water into the intake manifold of a diesel engine for simultaneous control of NO and smoke emissions. *Energy Conversion and Management*, *52*(2), 849–857. https://doi.org/10.1016/j.enconman.2010.08.010

Supriya B. Chavan, Meena Yadav, Reena Singh, Veena Singh, Rajendra R. Kumbhar, A., & Sharmab, Y. C. S. (2017). Production of Biodiesel from Three Indigenous Feedstock: Optimization of Process Parameters and Assessment of Various Fuel Properties. *Environmental Science & Technology*, *36*(3), 788–795. https://doi.org/10.1002/ep

Tadano, Y. S., Borillo, G. C., Godoi, A. F. L., Cichon, A., Silva, T. O. B., Valebona, F. B., Errera, M. R., Penteado Neto, R. A., Rampel, D., Martin, L., Yamamoto, C. I., & Godoi, R. H. M. (2014). Gaseous emissions from a heavy-duty engine equipped with SCR aftertreatment system and fuelled with diesel and biodiesel: Assessment of pollutant dispersion and health risk. *Science of the Total Environment*, *500–501*(x), 64–71. https://doi.org/10.1016/j.scitotenv.2014.08.100

Taher, H., & Al-Zuhair, S. (2016). The use of alternative solvents in enzymatic biodiesel production: a review. *Biofuels, Bioproducts and Biorefining*, *11*, 168–194. https://doi.org/10.1002/bbb.1727

Talebian-Kiakalaieh, A., Amin, N. A. S., & Mazaheri, H. (2013). A review on novel processes of biodiesel production from waste cooking oil. *Applied Energy*, *104*, 683–710. https://doi.org/10.1016/j.apenergy.2012.11.061

Tashtoush, G. M., Al-Widyan, M. I., & Al-Jarrah, M. M. (2004). Experimental study on evaluation and optimization of conversion of waste animal fat into biodiesel. *Energy Conversion and Management*, *45*(17), 2697–2711. https://doi.org/https://doi.org/10.1016/j.enconman.2003.12.009

Tauzia, X., Maiboom, A., & Shah, S. R. (2010). Experimental study of inlet manifold water injection on combustion and emissions of an automotive direct injection Diesel engine. *Energy*, *35*(9), 3628–3639. https://doi.org/10.1016/j.energy.2010.05.007

Taymaz, I., Cakir, K., Gur, M., & Mimaroglu, A. (2003). Experimental investigation of heat losses in a ceramic coated diesel engine. *Surface and Coatings Technology*, *169*, 168–170.

Tayyeb Javed, M., Irfan, N., & Gibbs, B. M. (2007). Control of combustion-generated nitrogen oxides by selective non-catalytic reduction. *Journal of Environmental Management*, *83*(3), 251–289. https://doi.org/10.1016/j.jenvman.2006.03.006

Tesfa, B., Mishra, R., Gu, F., & Ball, A. D. (2012). Water injection effects on the performance and emission characteristics of a CI engine operating with biodiesel. *Renewable Energy*, *37*(1), 333–344. https://doi.org/10.1016/j.renene.2011.06.035

Thangaraja, J., Anand, K., & Mehta, P. S. (2016). Biodiesel NOxpenalty and control measures - A review. *Renewable and Sustainable Energy Reviews*, *61*(x), 1–24. https://doi.org/10.1016/j.rser.2016.03.017

The UK Department for Business Energy & Industrial Strategy. (2017). Energy Trends March 2017. *National Statistics*.

The World Bank. (2017). Fossil fuel energy consumption. Retrieved April 23, 2017, from http://databank.worldbank.org/data/reports.aspx?source=2&series=EG.USE.COMM.FO.ZS&country=

Thiyagarajan, S., Geo, V. E., Martin, L. J., & Nagalingam, B. (2017). Selective Non-catalytic

Reduction (SNCR) of CO2 and NO Emissions from a Single-Cylinder CI Engine Using Chemical Absorbents. *Emission Control Science and Technology*, *3*(3), 233–242. https://doi.org/10.1007/s40825-017-0076-0

Thompson, E. M. (2008). amc technical briefs, *AMCTB No 2*(29). Retrieved from http://www.rsc.org/images/CHNS-elemental-analysers-technical-brief-29_tcm18-214833.pdf

Tiwari, A. K., Kumar, A., & Raheman, H. (2007). Biodiesel production from jatropha oil (Jatropha curcas) with high free fatty acids: an optimized process. *Biomass and Bioenergy*, *31*(8), 569–575.

Tong, D., Hu, C., Jiang, K., & Li, Y. (2011). Cetane number prediction of biodiesel from the composition of the fatty acid methyl esters. *Journal of the American Oil Chemists' Society*, *88*(3), 415–423. https://doi.org/10.1007/s11746-010-1672-0

Torres-Rodríguez, D. A., Romero-Ibarra, I. C., Ibarra, I. A., & Pfeiffer, H. (2016). Biodiesel production from soybean and Jatropha oils using cesium impregnated sodium zirconate as a heterogeneous base catalyst. *Renewable Energy*, *93*, 323–331. https://doi.org/10.1016/j.renene.2016.02.061

Tosun, E., Yilmaz, A. C., Ozcanli, M., & Aydin, K. (2014). Determination of effects of various alcohol additions into peanut methyl ester on performance and emission characteristics of a compression ignition engine. *Fuel*, *126*, 38–43. https://doi.org/https://doi.org/10.1016/j.fuel.2014.02.037

Tsai, J.-H., Chen, S.-J., Huang, K.-L., Lin, W.-Y., Lee, W.-J., Lin, C.-C., Hsieh, L., Chiu, J., & Kuo, W.-C. (2014). Emissions from a generator fueled by blends of diesel, biodiesel, acetone, and isopropyl alcohol: analyses of emitted PM, particulate carbon, and PAHs. *Science of the Total Environment*, *466*, 195–202. https://doi.org/https://doi.org/10.1016/j.scitotenv.2013.07.025

UK Department for Transport. (2018). Renewable Transport Fuel Obligation statistics: period 10 2017/18, report 3. Retrieved July 1, 2018, from https://assets.publishing.service.gov.uk/government/uploads/system/uploads/attachment_data/file/704390/rtfo-year-10-report-3.pdf

Ulusoy, Y., Arslan, R., Tekin, Y., Sürmen, A., Bolat, A., & Şahin, R. (2018). Investigation of performance and emission characteristics of waste cooking oil as biodiesel in a diesel engine. *Petroleum Science*, *15*(2), 396–404. https://doi.org/10.1007/s12182-018-0225-2

Usta, N., Öztürk, E., Can, Ö., Conkur, E. S., Nas, S., Çon, A. H., Can, A. C., & Topcu, M. (2005). Combustion of bioDiesel fuel produced from hazelnut soapstock/waste sunflower oil mixture in a Diesel engine. *Energy Conversion and Management*, *46*(5), 741–755. https://doi.org/10.1016/j.enconman.2004.05.001

Van Gerpen, J. (2005). Biodiesel processing and production. *Fuel Processing Technology*, *86*(10), 1097–1107. https://doi.org/10.1016/j.fuproc.2004.11.005

Varatharajan, K., & Cheralathan, M. (2012). Influence of fuel properties and composition on NO x emissions from biodiesel powered diesel engines: A review. *Renewable and Sustainable Energy Reviews*. https://doi.org/10.1016/j.rser.2012.03.056

Varatharajan, K., & Cheralathan, M. (2013). Effect of aromatic amine antioxidants on NOx emissions from a soybean biodiesel powered di diesel engine. *Fuel Processing Technology*, *106*(x), 526–532. https://doi.org/10.1016/j.fuproc.2012.09.023

Vardoulakis, S. and, & Heaviside, C. (2012). *Health Effects of Climate Change in the UK 2012 - Current evidence , recommendations and research gaps.*

Vedaraman, N., Puhan, S., Nagarajan, G., & Velappan, K. C. (2011). Preparation of palm oil biodiesel and effect of various additives on NOx emission reduction in B20: An experimental study. *International Journal of Green Energy*, *8*(3), 383–397. https://doi.org/https://doi.org/10.1080/15435075.2011.557847

Vellguth, G. (1983). Performance of vegetable oils and their monoesters as fuels for diesel engines. *SAE Transactions*, *92*, 1098–1107. https://doi.org/www.jstor.org/stable/44647674.

Venkatesan, H., John J., G., & Sivamani, S. (2017). Impact of oxygenated cottonseed biodiesel on combustion, performance and emission parameters in a direct injection CI engine. *International Journal of Ambient Energy*, *0750*, 1–12. https://doi.org/10.1080/01430750.2017.1381154

Verma, P., Sharma, M. P., & Dwivedi, G. (2016). Evaluation and enhancement of cold flow properties of palm oil and its biodiesel. *Energy Reports*, *2*, 8–13. https://doi.org/10.1016/j.egyr.2015.12.001

Wakode, V. R., & Kanase-Patil, A. B. (2017). Regression analysis and optimization of diesel engine performance for change in fuel injection pressure and compression ratio. *Applied Thermal Engineering*, *113*, 322–333. https://doi.org/10.1016/j.applthermaleng.2016.10.178

Wang, J., Feng, L., Tang, X., Bentley, Y., & Höök, M. (2017). The implications of fossil fuel supply constraints on climate change projections: A supply-side analysis. *Futures*, *86*, 58–72. https://doi.org/10.1016/j.futures.2016.04.007

Williams, P. T., Bartle, K. D., & Andrews, G. E. (1986). The relation between polycyclic aromatic compounds in diesel fuels and exhaust particulates. *Fuel*, *65*(8), 1150–1158. https://doi.org/10.1016/0016-2361(86)90184-5

Wyatt, V. T., Hess, M. A., Dunn, R. O., Foglia, T. A., Haas, M. J., & Marmer, W. N. (2005). Fuel properties and nitrogen oxide emission levels of biodiesel produced from animal fats. *JAOCS, Journal of the American Oil Chemists' Society*, *82*(8), 585–591. https://doi.org/10.1007/s11746-005-1113-2

Xie, H., Li, L., Chen, T., & Zhao, H. (2014). Investigation on gasoline homogeneous charge compression ignition (HCCI) combustion implemented by residual gas trapping combined with intake preheating through waste heat recovery. *Energy Conversion and Management*, *86*, 8–19. https://doi.org/10.1016/j.enconman.2014.05.022

Xu, M., Tu, Y., Zhou, A., Xu, H., Yu, W., Li, Z., & Yang, W. (2019). Numerical study of HCN and NH 3 reduction in a two-stage entrained flow gasifier by implementing MILD combustion. *Fuel*, *251*(March), 482–495. https://doi.org/10.1016/j.fuel.2019.03.135

Yakhot, V., Orszag, S. A., Thangam, S., Gatski, T. B., & Speziale, C. G. (1992). Development of turbulence models for shear flows by a double expansion technique. *Physics of Fluids A*, *4*(7), 1510–1520. https://doi.org/10.1063/1.858424

Yang, W., An, H., Li, J., Zhou, D., & Kraft, M. (2015). Impact of urea direct injection on nox emission formation of diesel engines fueled by biodiesel. In *Proceedings of the ASME 2015 Internal Combustion Engine Division Fall Technical Conference* (pp. 1–7). Retrieved from https://proceedings.asmedigitalcollection.asme.org

Yasin, M. H. M., Yusaf, T., Mamat, R., & Yusop, A. F. (2014). Characterization of a diesel engine operating with a small proportion of methanol as a fuel additive in biodiesel blend. *Applied Energy*, *114*, 865–873. https://doi.org/doi.10.1016/j.apenergy.2013.06.012

Yilmaz, I. T., Gumus, M., & Akcay, M. (2010). Thermal barrier coatings for diesel engines. In *International scientific conference* (pp. 19–20).

Yilmaz, N. (2012a). Comparative analysis of biodiesel--ethanol--diesel and biodiesel--methanol--diesel blends in a diesel engine. *Energy*, *40*(1), 210–213. https://doi.org/https://doi.org/10.1016/j.energy.2012.01.079

Yilmaz, N. (2012b). Performance and emission characteristics of a diesel engine fuelled with biodiesel--ethanol and biodiesel--methanol blends at elevated air temperatures. *Fuel*, *94*, 440–443. https://doi.org/https://doi.org/10.1016/j.fuel.2011.11.015

Yilmaz, N., & Atmanli, A. (2017). Experimental assessment of a diesel engine fueled with diesel-biodiesel-1-pentanol blends. *Fuel*, *191*, 190–197.

Yim, S. D., Kim, S. J., Baik, J. H., Nam, I., Mok, Y. S., Lee, J.-H., Cho, B. K., & Oh, S. H. (2004). Decomposition of Urea into NH3 for the SCR Process. *Industrial & Engineering Chemistry Research*, *43*(16), 4856–4863. https://doi.org/10.1021/ie034052j

Yousefi, A., Gharehghani, A., & Birouk, M. (2015). Comparison study on combustion characteristics and emissions of a homogeneous charge compression ignition (HCCI) engine with and without pre-combustion chamber. *Energy Conversion and Management*, *100*, 232–241. https://doi.org/10.1016/j.enconman.2015.05.024

Yucesu, H. S., & Ilkilic, C. (2006). Effect of cotton seed oil methyl ester on the performance and exhaust emission of a diesel engine. *Energy Sources Part A-Recovery Utilization and Environmental Effects*, *28*(4), 389–398. https://doi.org/10.1080/009083190927877

Zhang, Y., Lou, D., Tan, P., & Hu, Z. (2018). Experimental study on the durability of biodiesel-powered engine equipped with a diesel oxidation catalyst and a selective catalytic reduction system. *Energy*, *159*, 1024–1034. https://doi.org/10.1016/j.energy.2018.06.190

Zhen, X., Wang, Y., Xu, S., Zhu, Y., Tao, C., Xu, T., & Song, M. (2012). The engine knock analysis - An overview. *Applied Energy*, *92*, 628–636. https://doi.org/10.1016/j.apenergy.2011.11.079

Zhou, D. Z., Yang, W. M., An, H., Li, J., & Shu, C. (2015). A numerical study on RCCI engine fueled by biodiesel/methanol. *Energy Conversion and Management*, *89*, 798–807. https://doi.org/10.1016/j.enconman.2014.10.054

Zhu, L., Cheung, C. S., Zhang, W. G., & Huang, Z. (2010). Emissions characteristics of a diesel engine operating on biodiesel and biodiesel blended with ethanol and methanol. *Science of the Total Environment*, *408*(4), 914–921. https://doi.org/https://doi.org/10.1016/j.scitotenv.2009.10.078

Zhu, L., Cheung, C. S., Zhang, W. G., & Huang, Z. (2011). Combustion, performance and emission characteristics of a DI diesel engine fueled with ethanol--biodiesel blends. *Fuel*, *90*(5), 1743–1750.

Appendices

Appendix 1: Methanol content of the biodiesels

Methanol contents of the biodiesels were measured with Hydrogen Nuclear Magnetic Resonance technique at Aston University Chemical Engineering laboratories. Although around 2.4% methanol was detected for the freshly made crude biodiesel, one year old biodiesels and washed biodiesels gave 0% methanol in their contents as shown in Figure A.1. This result showed that if the biodiesel will be used right after the production, washing is crucial in terms of methanol content.
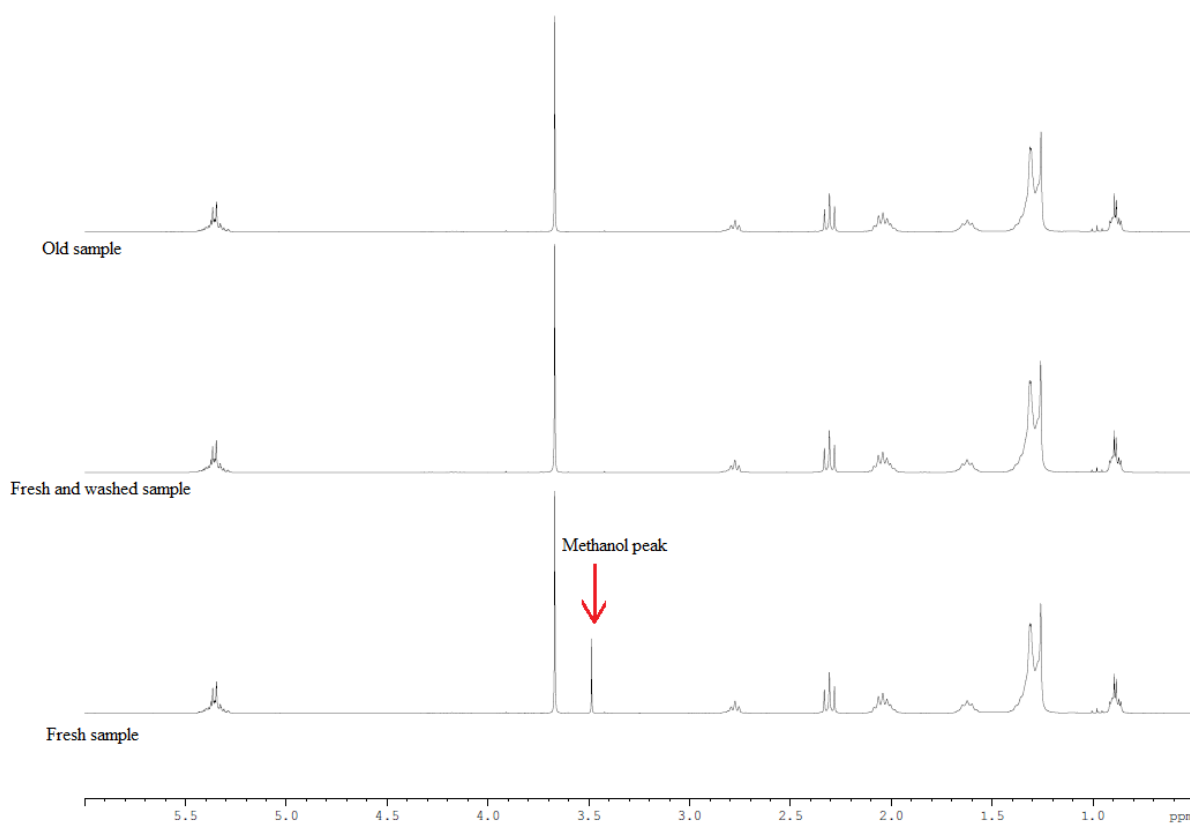

Figure A.1: Methanol contents of 1 year old biodiesel, freshly made and washed biodiesel and Fresh biodiesel.

Appendix 2: Calibration certificate of the BOSCH BEA 850 gas analyser

A.D.E. SYSTEMS LTD
84, Market Street, Adlington,
Lancashire. PR7 4HF.
Telephone: 01257 480999

CERTIFICATE OF CALIBRATION

APPROVED SIGNATORY	
Name	ᔆᔆᴉᴄᴋᴺᴇᴌᴌ
Signature	████

Certificate Number: 014008

Date of Issue: 22 november 2018

EQUIPMENT DETAILS
Manufacturer: Bosch
Model: BEA 850
Serial Number: 100
PEF: 0·530 006 220

LOCATION DETAILS
Contact: DR ABUL·HOSSAIN
Address: ASTON UNIVERSITY
ASTON ST. BIRMINGHAM
B4 7EI

INITIAL O_2 READING FOR AMBIENT AIR 20·66%

FINAL AMBIENT TEMPERATURE 16 °C

AMBIENT PRESSURE 1004 mbar

PRESSURE INDICATED BY ANALYSER 1004 mbar

CALIBRATION CHECK	Carbon monoxide (CO)	Hydrocarbons (HC)	Carbon dioxide (CO₂)	Oxygen (O₂)
Concentration of calibration gas	3·395 %	1945 ppm	13·99 %	0.0%
Concentration value X PEF		1030 ppm		
Initial analyser reading	3·416 %	1046 ppm	14·04 %	0·01 %
Final analyser reading	3·389 %	1030 ppm	13·88 %	0·00 %

FINAL O_2 READING 20·94%

The analyser has been calibrated to the manufacturer's specifications.

████

Signed: ████

Recalibration due before	01 JUNE 2021

Figure A.2: The calibration of the BOSCH BEA 850 gas analyser was carried out successfully.

Appendix 3: Technical drawings of the new Selective Non-Catalytic Reduction (SNCR) aftertreatment system
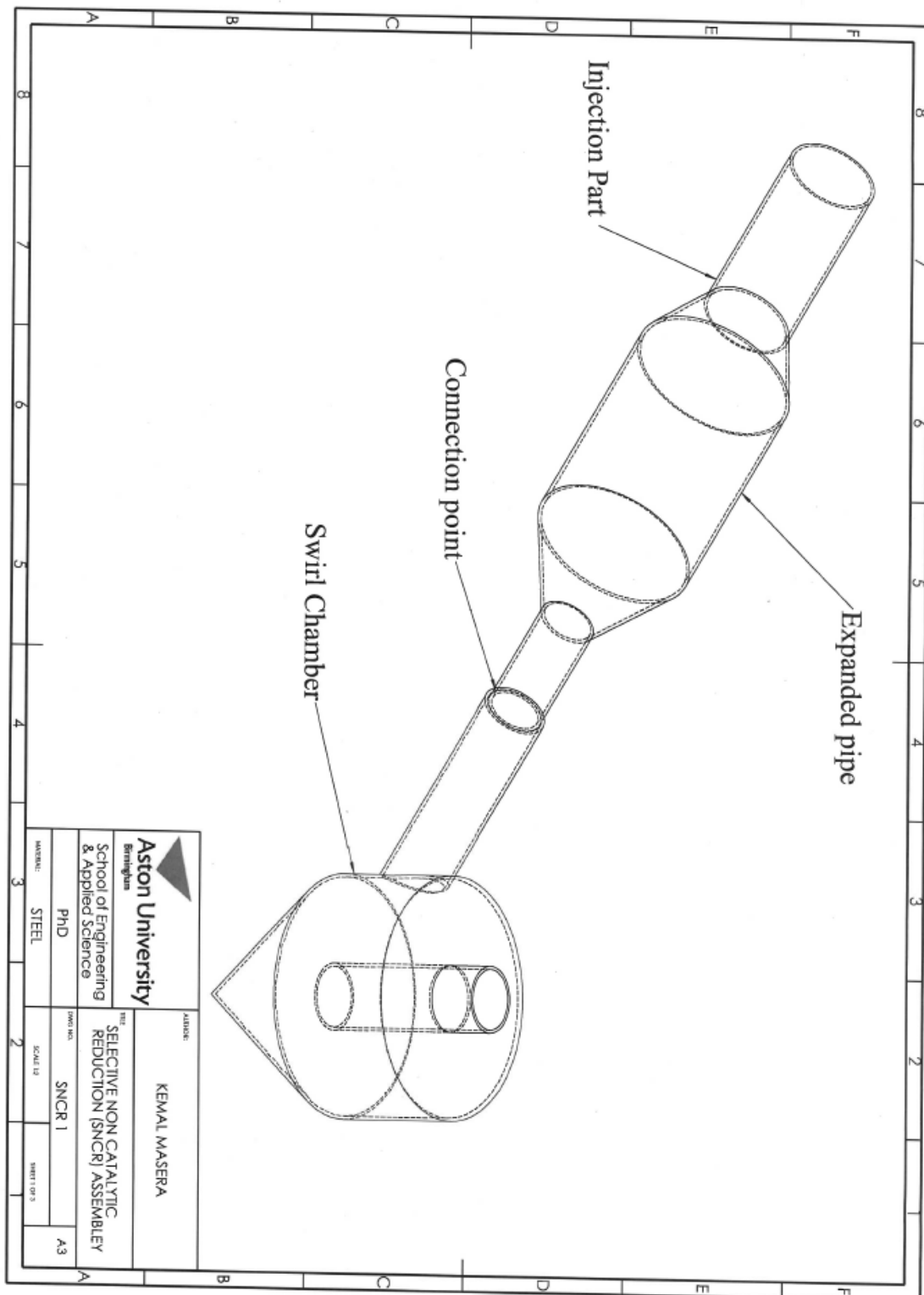

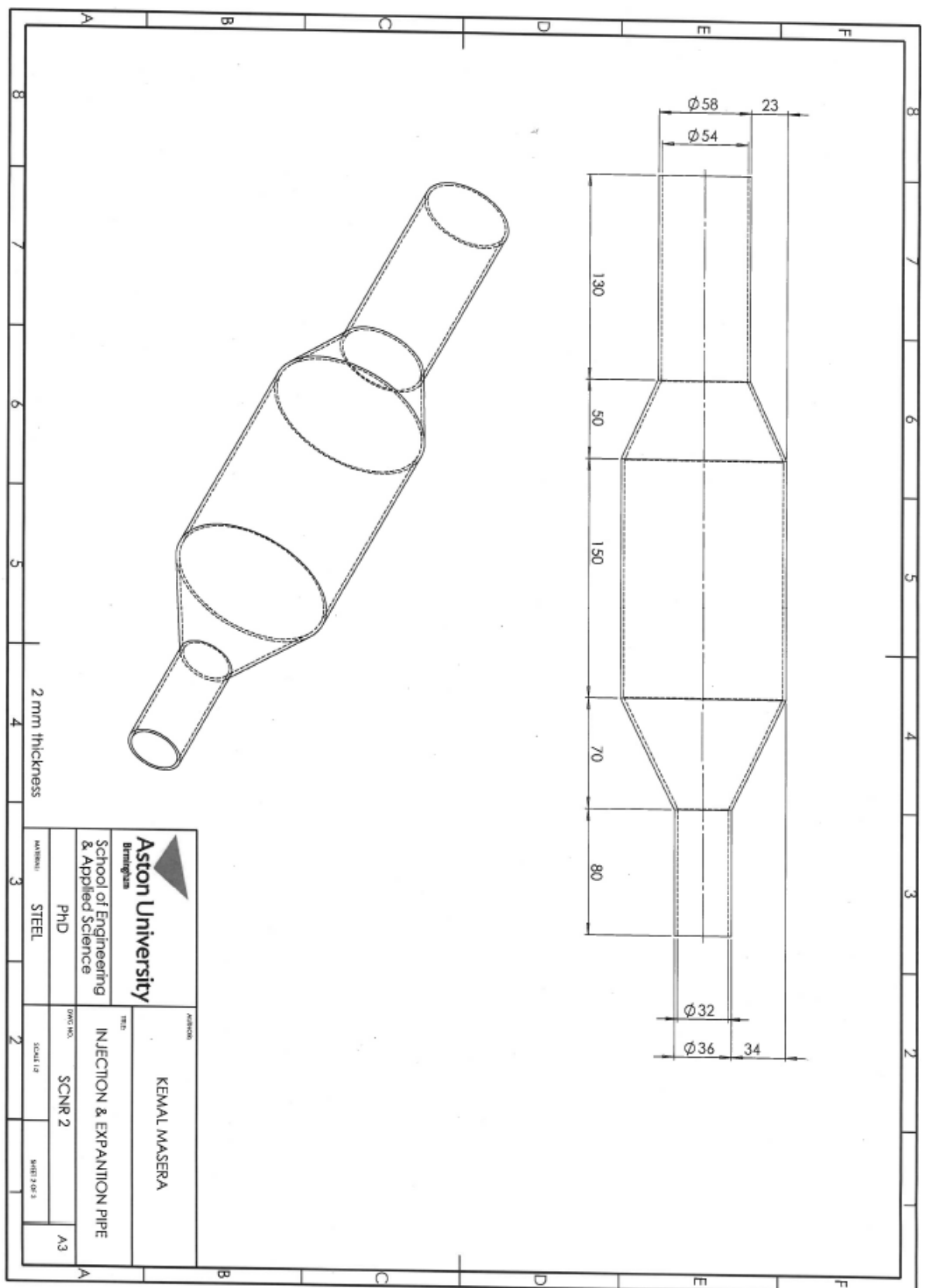Figure A.3: Technical drawing of the modified SNCR aftertreatment system.

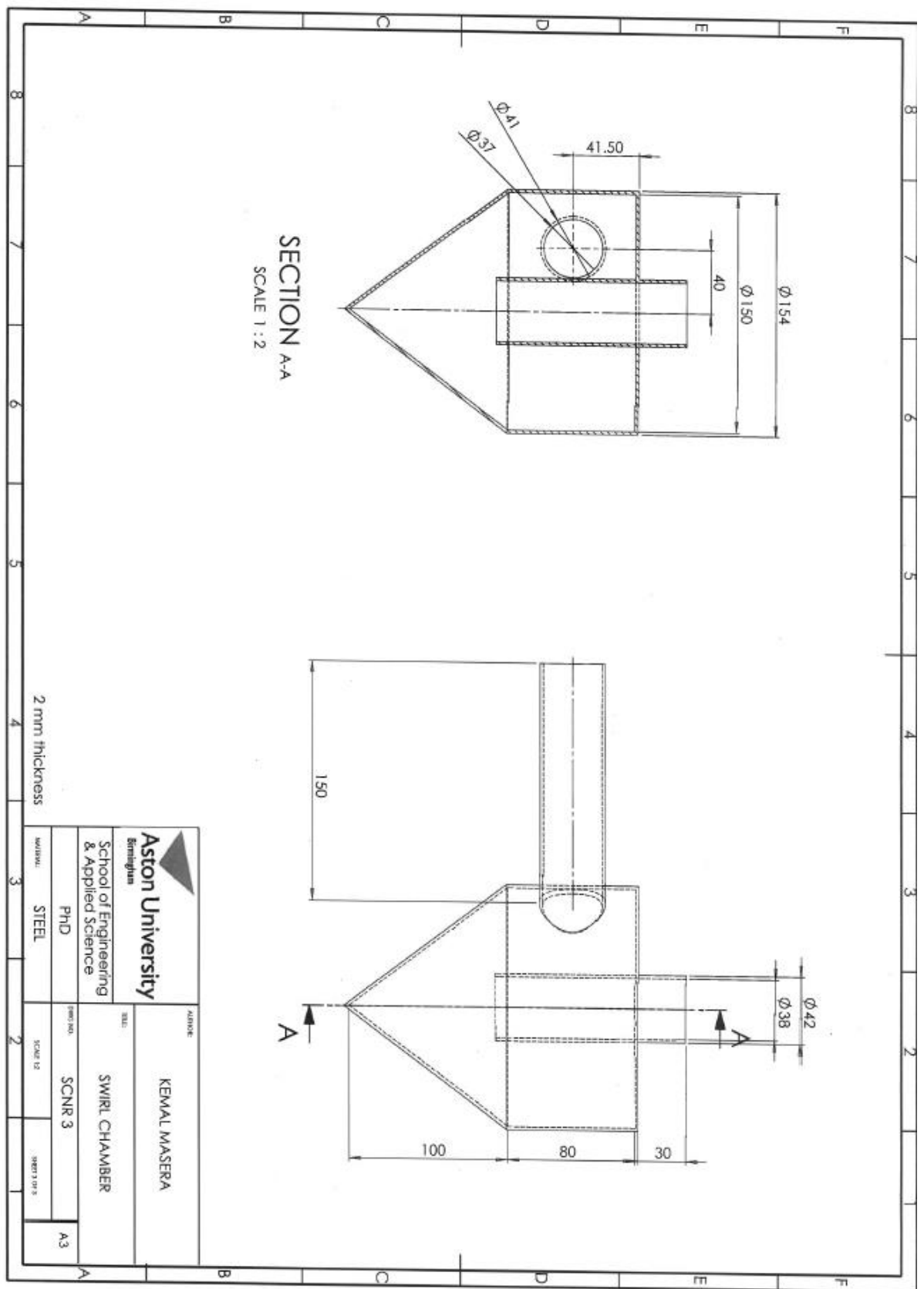Figure A.4: Technical drawing of the injection and expansion pipe.

Figure A.5: Technical drawing of the swirl chamber.

Appendix 4: Certificate of the Esso Diesel used as a reference fuel in this study.

Aston University

Illustration removed for copyright restrictions

Figure A.6: Certificate of reference fossil fuel purchased from Esso, UK.